G. S. Roslyakov and L. A. Chudov, Editors

# NUMERICAL METHODS IN GAS DYNAMICS



TRANSLATED FROM RUSSIAN



Published for the National Aeronautics and Space Administration, U.S.A.
and the National Science Foundation, Washington, D.C.
by the Israel Program for Scientific Translations

G. S. Roslyakov and L. A. Chudov, Editors

# NUMERICAL METHODS IN GAS DYNAMICS

(Chislennye metody v gazovoi dinamike)

A COLLECTION OF PAPERS OF THE
COMPUTATIONAL CENTER OF THE MOSCOW STATE UNIVERSITY
II

Izdalel'stvo Moskovskogo Universiteta
1963

Translated from Russian

Israel Program for Scientific Translations
Jerusalem 1966

NASA TT F-360
TT 65-50138

Published Pursuant to an Agreement with
THE NATIONAL AERONAUTICS AND SPACE ADMINISTRATION, U.S.A.
and
THE NATIONAL SCIENCE FOUNDATION, WASHINGTON, D.C.


IPST Cat. No. 1456

Translated by Z. Lerman

Printed in Jerusalem by S. Monson
Binding: K. Wiener

Price: $ 5.00

Available from the
U.S. DEPARTMENT OF COMMERCE
Clearinghouse for Federal Scientific and Technical Information
Springfield, Va. 22151

TABLE OF CONTENTS

## I. STEADY GAS FLOW



## II. BOUNDARY LAYER

## III. VISCOUS FLOW



## IV. SEEPAGE PROBLEMS

# I. STEADY GAS FLOW

*G.S. Roslyakov and G.F. Telenin*

## *SURVEY OF COMPUTATIONAL WORK ON STEADY AXISYMMETRIC GAS FLOW CARRIED OUT AT THE COMPUTATIONAL CENTER OF MOSCOW STATE UNIVERSITY*

This article reviews the computational work on steady axisymmetric gas flow carried out at the Computational Center of Moscow State University between 1957 and 1962. The work was undertaken by scientific workers of the Institute of Mechanics of Moscow State University, undergraduate and graduate students of the University, members of other organizations, and the regular staff of the Computational Center. The project was headed by Academician G. I. Petrov.

This article is of an informative nature and the results given are mostly those of completed works, some accounts of which are published in the present collection.

## I. NUMERICAL COMPUTATION OF SUPERSONIC GAS FLOW BY THE METHOD OF CHARACTERISTICS

### 1. Potential flow

The computation of exhaust nozzles of supersonic windtunnels is dealt with by V. K. Solodkin and G. S. Roslyakov /1/, who considered nozzles with plane transitional surface and uniform outlet flow (Figure 1). The radius of the critical section $OA$ is assumed to be known, as is the distribution of the Mach number $M$ over the nozzle axis (in the form of a monotonically increasing function $M=f(x)$ with a piecewise continuous derivative; $f(O)=1$, $f'(O)=0$; $f(C)=M_0$, $x$ being the coordinate along the nozzle axis). The computation is made by the method of characteristics from the straight characteristic $BC$ up to the critical section. Six series of nozzles have been tabulated:

| | | |
|---|---|---|
| Series I: | $M_0=1.506;\ 1.75;$ | |
| Series II: | $M_0=4.5;\ 5\,(1)\ 8;\ 10;$ | $\operatorname{tg}\theta_0=0.25;$ |
| Series III: | $M_0=4\,(0.5)\ 7;$ | $\operatorname{tg}\theta_0=0.1624;$ |
| Series IV: | $M_0=8,\ 9,\ 10;$ | $\operatorname{tg}\theta_0=0.229;$ |
| Series V: | $M_0=10\,(1)\ 20;$ | $\operatorname{tg}\theta_0=0.2553;$ |
| Series VI: | $M_0=10\,(5)\ 25;$ | $\operatorname{tg}\theta_0=0.1745$ |

The ratio of specific heats $\gamma$ was taken as 1.4 for series I - V, and $\frac{5}{3}$ for series VI. Nozzle contours in series III and IV are given both with and without allowance for the effect of the boundary layer. All nozzles of

series II - VI have a region of conical flow characterized by the angle $\theta_0$. The part of the nozzle contour from the sonic line to the conical region is common in all these series. Series II - V differ in their conical angle $\theta_0$.

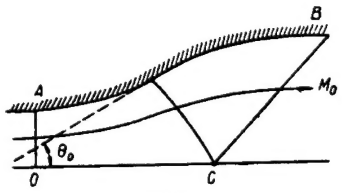

FIGURE 1

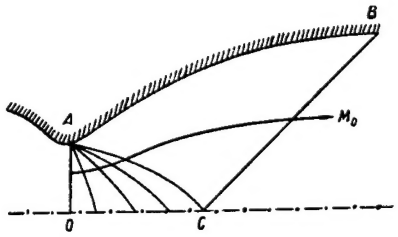

FIGURE 2

L. V. Pchelkina, V. A. Rubtsov, and V. M. Semichastnova /2/ give tables of conventional nozzles with an angular point, uniform outlet flow, and a plane transitional surface (Figure 2).

The fan of rarefaction waves arising at the angular point $A$ and the Goursat problem with boundary conditions for the extreme characteristic $AC$ of the fan and for the straight boundary characteristic $BC$ are computed by the method of characteristics. The computation of the sonic characteristic proceeds from a series expansion of the solution in terms of the characteristic coordinate*.

Reference /2/ is the first part of an atlas of conventional nozzles with an angular point, covering the following range of parameters:

$$M_0 = 1.4(0.4)3;\ 3\,(0.2)\,5;\ 5\,(0.1)\,7;$$
$$\gamma = 1.1\,(0.02)\,1.18.$$

The computational method and the programs have been described by L. V. Pchelkina and V. A. Rubtsov in /3/.

To facilitate the use of the atlas, tables have been compiled /4/ of the principal gas-dynamic functions $\lambda$, $q$, $\pi$, $\varepsilon$, $\tau$, $\theta$ for various Mach numbers $M$, $0 < M \leqslant 7$, for the following ratios of specific heats $\gamma$:

$$1.05;\ 1.1\ (0.01)\ 1.18;\ 1.20;\ 1.22;\ 1.25;\ 1.3;\ 1.4;\ 1.67.$$

L. V. Pchelkina and V. K. Solodkin /5/ tabulated conventional nozzles with an angular point and radial outlet flow. The computational procedure is similar to /2/, with the difference that the characteristic $BC$ (Figure 3) is a characteristic of sonic flow with the pole $O'$ on the axis of symmetry. Nozzle contours have been tabulated for

$$M_0 = 5,\ 6,\ 8,\ 10,\ 13,\ 15 \text{ and } \beta_0 = 0.01;\ 0.02;\ 0.04\ (\gamma = 1.4).$$

U. G. Pirumov and V. A. Rubtsov /6/ developed a method for computation of supersonic annular nozzles with two angular points and a straight sonic

* See Katskova O. N. and Yu. D. Shmyglevskii. Osesimmetrichnoe sverkhzvukovoe techenie svobodno rasshiryayushchegosya gaza s ploskoi poverkhnost'yu perekhoda (Axisymmetric Supersonic Flow of Freely Expanding Gas with Plane Transitional Surface). — Vychislitel'naya matematika, No. 2. 1957.

line. Nozzles with coplanar angular points (Figure 4), as well as nozzles with displaced angular points (Figures 5 and 6) are considered. Computations are made by the method of characteristics. It is shown that the annular nozzle is shorter than a conventional nozzle (Figure 2) with the same critical section area and the same $M_0$. It is also shown that displacement of the lower angular point (Figure 5) may increase the number $M_0$ at the nozzle outlet in comparison with the $M_0$ of an annular nozzle of the same critical section area which has coplanar angular points. Displacement of the upper angular point (Figure 6) lowers the $M_0$ at the nozzle outlet. The use of an annular nozzle with a displaced lower point enables the nozzle length to be reduced by a factor of close to 2 in comparison with the corresponding conventional nozzle. Tables of several annular nozzles are given by E. G. Mezhibovskaya, U. G. Pirumov, V. A. Rubtsov, and E. V. Sorokina /7/.

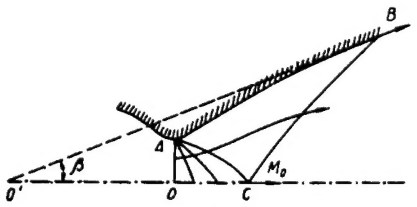

FIGURE 3

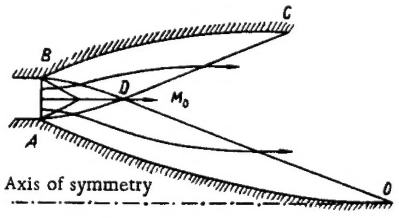

FIGURE 4

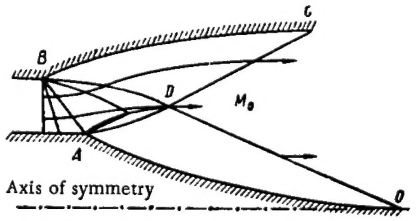

FIGURE 5

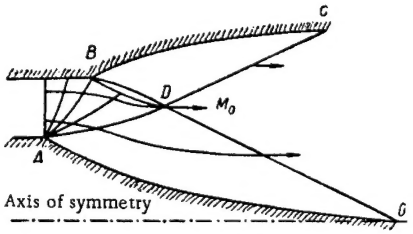

FIGURE 6

The sonic characteristics in /6/ and /7/ were assumed linear with constant $M = 1.001$ and velocity parallel to the axis, which introduces virtually no errors into the computational results.

An approximate method is also proposed in these works for computing the flow in an annular nozzle, which gives satisfactory agreement with the exact method in regions far from the axis of symmetry.

A large series of computations of intake nozzles was also carried out at the Computational Center.

## 2. Eddy flow

G. S. Roslyakov and N. V. Drozdova /8/ studied gas flow past a scalariform cone (Figure 7). The eddy region (beyond the curvilinear shock) is dealt with by the method of characteristics. To find a solution

near the turning point on the generatrix of the body, the solution is expanded in a Taylor series in terms of one of the unknown variables.

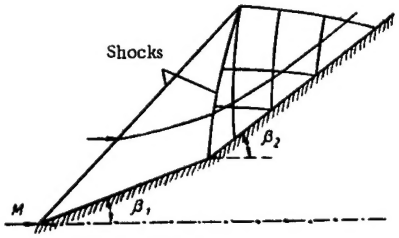


FIGURE 7

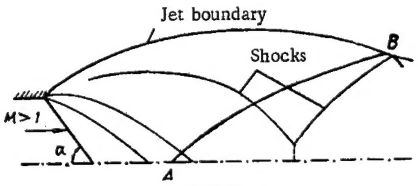


FIGURE 8

Computational results are given for a cone with $\beta_1 = 20°$, $\beta_2 = 35°$, for $M = 2.2$, 2.6, 3, 3.42, 4.098, 6.103, and for a cone with $\beta_1 = 15°$, $\beta_2 = 35°$, for $M = 2.594$, 4.097.

T. G. Volkonskaya /9/ applied the method of characteristics to the computation of a supersonic jet (Figure 8). The case considered is when the outlet pressure exceeds the pressure on the jet boundary, so that a "suspended" compression shock forms in the stream. A procedure is described for computing the "suspended" shock. It is shown that the errors in determining the shock point of origin have a negligible effect on the accuracy of the results. Some computational results are given. Computations are made only in the supersonic part of the flow up to some characteristic *AB*.

## 3. Computation of gas flow with an allowance for physicochemical reactions

U. G. Pirumov, V. A. Rubtsov, and V. N. Suvorova /10/ computed nozzles with an angular point (Figure 2) taking into consideration equilibrium physicochemical reactions. To compute the flow of an arbitray equilibrium mixture, it suffices to know the tabulated dependence of pressure on density (for constant entropy). This dependence is approximated in the computer and is then applied in the method of characteristics, which essentially does not differ from the method of characteristics for an ideal gas. Reference /10/ discusses the flow of real gases in nozzles of given contour and computations are made of nozzles with uniform and parallel outlet flow. For one given gas composition, the effect of real gas properties on the coefficient of momentum loss in the nozzle is studied, neglecting friction.

N. V. Dubinskaya, R. A. Gzhelyak and I. V. Igonina /11/ developed a procedure and compiled a program for computing, by the method of characteristics, supersonic flow of many-component (up to 32 components) gas mixtures with an allowance for nonequilibrium physicochemical reactions. The Prandtl-Mayer flow has been computed for nonequilibrium air flow.

## 4. Some procedural problems and organization of computational work

In view of the large volume of computational works applying the method of characteristics to steady axisymmetric gas flow, much attention is paid to the proper organization of the computational work.

During 1957, at the Computational Center of Moscow State University, G. S. Roslyakov, V. M. Paskonov, and A. A. Deeva /12/ developed a system of standard programs for the computation of axisymmetric potential flows of ideal gases on the STRELA computer. The subroutine library includes programs for computation of flow parameters at the inner nodes of the characteristic grid, at boundary points of various kinds, and also several service routines. One common part of the working memory has been allotted to all the subroutines. The programs have been written for an arbitrary ratio of specific heats $\gamma$. A provision is made for easy standard referencing of the subroutines from the main program. Any of the subroutines (and also the common part of the working memory) can be stored anywhere in the computer storage.

For each application the subroutines are adjusted in the computer memory by a special compiling program (SSP-2)*, which also ensures mutual referencing of the subroutines.

An analogous system of subroutines for computing turbulent gas flows on the STRELA computer was developed by V. M. Paskonov and L. V. Pchelkina /13/.

Standard programs for the computation of potential flow of ideal gases on the electronic computer of the Computational Center of Moscow State University were developed by R. A. Gzhelyak, E. G. Mezhibovskaya, L. V. Pchelkina, and V. A. Rubtsov /14/; for computation of equilibrium real-gas flow, by V. A. Rubtsov and V. N. Suvorova /15/; and for non-equilibrium flow, by N. V. Dubinskaya, R. A. Gzhelyak, and I. V. Igonina /16/. Besides the programs discussed in /12-16/ (programs for computation of typical points), programs for the solution of typical problems (Cauchy, Goursat, mixed problem, etc.) are also available at the Computational Center.

The experience gained in the solution of particular problems showed that the application of the library of standard subroutines shortens the time required for compilation and debugging of programs.

All of the preceding works employ a cylindrical system of coordinates. The unknown functions in /12, 13/ are the Mach angle $\alpha$ and the velocity argument $\theta$ (in /13/, also the entropy $s$). In /14/ more convenient variables are used, as proposed by Elers**: $\zeta = \operatorname{tg}\theta$ and $\beta = \sqrt{M^2 - 1}$; in /15/ the unknown variables are the density $\rho$ and $\zeta$, and in /16/ $\zeta$, $M$, pressure $p$ and concentrations $\alpha_i$ ($i \leqslant 32$).

In conclusion of this section we offer some remarks of a general nature.

* See Zhogolev, E.A. Sistema programmirovaniya s ispol'zovaniem biblioteki podprogramm (A Programming System with Utilization of a Subroutine Library).— In: "Sistema avtomatizatsii programmirovaniya", N. P. Trifonov and M.R. Shura-Bura, editors. Fizmatgiz, Moskva. 1961.

** See Elers, F.E. Method of Characteristics for Isoenergetic Supersonic Flows Adapted for High-Speed Digital Computers. [Russian translation. 1960.]

1°. To estimate the accuracy of the numerical solution, integral control is generally employed, i.e., the laws of conservation are checked. When solving problems of this particular class, it is most convenient to check the law of mass conservation. In computations using the method of characteristics, the flow rate $\psi$ is determined at every grid point. The flow rate along any streamline is conserved. Therefore, if the flow rate is known for some streamline, the (relative) deviation from this value at other points of the given streamline obtained in the computational procedure serves as an integral check of the accuracy of the numerical solution. Flow-rate control is used to some extent in the solution of all problems. Often the law of conservation of momentum is also checked. This momentum control is applied, for example, when computing nozzles with uniform outlet flow and plane transitional surface /1—7/. In this case, the momenta at the outlet and the inlet of the nozzle are easy to compute; the difference in the momenta should be equal to the projection on the $x$-axis of the pressure forces acting on the nozzle contour. An accuracy check on the computations is the difference between these values divided by the momentum at nozzle outlet.

Besides these control procedures, it is also advisable to compare the results obtained with different grid spacings. This, however, is generally practiced for one or two variations of the problem, mainly with the purpose of choosing the optimum characteristic grid spacing, while the production computations are controlled using flow rates or momenta.

2°. The unknown quantities are determined at characteristic grid points with an accuracy of second order with respect to the grid spacing. Correspondingly, all the interpolative and quadrature formulas used in computations are also of second order accuracy.

Some data on the accuracy of computations, the machine time required for the computation of one variation of a typical problem, etc., will be given for a particular case of work /2/ (see section 1). When computing the fan of rarefaction waves (region $OAC$, Figure 2), the computations are made along 2nd-family characteristics issuing from the angular point $A$. The intervals of the flow spreading angle at point $A$ and the position of points on the 2nd-family characteristics are chosen so as to maintain a uniform net (far from point $A$). The rarefaction of the points on the 2nd-family characteristic is made with an allowance for the variation of the various functions along it. The flow rate is computed along every characteristic. The difference from zero of the flow rate at the point of intersection of the characteristic with the axis, divided by the flow rate at point $A$, is used to check the computational accuracy. When computing the region $ABC$, the flow rate is used to determine the nozzle contour and therefore cannot be used for control purposes. To check the computations by means of conservation of momentum, we compute the projection of pressure forces along the nozzle contour on the $x$-axis. Here are some figures describing the computation of a certain variation ($M = 10$) on the electronic computer of the Computational Center. The number of points: 30 on the sonic characteristic, 160 on the boundary characteristic $AC$ of the fan; number of characteristics in region $OAC$, 200; number of points on characteristic $CB$, 120. Computer time for computation of region $OAC$ 30 minutes; flow-rate accuracy, 0.01 %. Computer time for region $ACB$, 20 minutes; momentum accuracy, 0.01 %.

In the region $OABC$ as well as the contour $AB$ several intermediate streamlines have been computed. Along these lines the forces of pressure, areas of the surfaces of revolution, and some quantities essential for taking friction into consideration were computed. The results along streamlines are tabulated at intervals suitable for quadratic interpolation.

## II. INVESTIGATION OF SUPERSONIC FLOW PAST BODIES WITH SEPARATED SHOCK WAVE

All the present methods for the computation of supersonic flow past bodies with separated shock wave for the construction of algorithms and successive approximations are based in a varying degree on the solution of the Cauchy problem in an elliptic domain. This is due to the relative simplicity of the ensuing numerical methods. It has been demonstrated that for linear elliptic equations the Cauchy problem is proper, provided some a priori restrictions are imposed on the class of solutions being considered*.

L. A. Chudov /17/ studied some problems connected with the application of difference schemes to the solution of the Cauchy problem for Laplace's equation, which is used as the model problem in gas dynamics. Stability has been demonstrated for one important class of explicit schemes, and convergence of the approximate solution to the exact solution has been proved.

Studies in this direction are being continued by L. A. Chudov and V. P. Kudryavtsev /18/. Using model examples, they obtained estimates of truncation and round-off errors and extended the results to a certain gas-dynamic system (taking dissociation into consideration). Let $l$ and $h$ be the intervals along the initial line and along the normal to it, respectively. It follows from the analysis of /17, 18/ that it is advisable to employ difference schemes of a high order of accuracy in $l$, so that $l$ can be made relatively large. $h$ may be reduced in a certain sense. For the limit, as $h \to 0$, we obtain the method of lines for the solution of partial differential equations.

G. F. Telenin and G. P. Tinyakov /19/ computed the subsonic and the transsonic regions beyond a shock wave for supersonic flow past blunt bodies whose generatrix has no angular points in this region. The method used is essentially the method of lines, adapted to the case when only a few strips need be taken. Systematic computations were made for flow past a sphere for Mach numbers of incident flow $M_1 = 2\ (1)\ 8,\ 10, \infty$, and a ratio of specific heats $\gamma = 1.405$. The problem was reduced to integration of a system of ordinary differential equations along three radial rays from the compression shock to the surface of the body. The generatrix of the compression shock was approximated by an even fourth-degree polynomial. The position of the shock on the three rays gave three free parameters, which were chosen so that the boundary conditions on the surface of the sphere were satisfied for the three rays simultaneously. The integration

* See, for example, Lavrent'ev, M. M. — Izvestiya AN SSSR, seriya matematicheskaya, Vol. 20, No. 6, 1956; DAN SSSR, Vol. 112, No. 2. 1957; also Pucci, C. — Rend. Acad. Naz. Lincei, Cl. Sci. Fis. Mat., Ser. VIII, Vol. 18, No. 5. 1955.

path chosen enabled the singularities arising with the Dorodnitsyn-Belotserkovskii method* to be avoided; this simplified the computational procedure and the program.

The three free parameters were automatically selected by the computer. The computations were made on the STRELA computer; machine time for one variation was on the average 1 minute. The integrals of the gas-dynamics equations not employed in actual computations and also the integral law of mass conservation, written for mass flow through the rays, were used to estimate the accuracy of the numerical solution. For the variations computed, the error in all the relationships used was less than 0.15%, which corresponds to the approximation accuracy of the partial differential equations in the program. The effect of ray position and the growth of error owing to distortion of the shock along the ray were studied (no essential growth of the error was observed). Figure 9 shows, as an example, the computed dependence of the separation of the shock wave on the number $M_1$.

G. F. Telenin and G. P. Tinyakov /20, 21/ computed and investigated the flow in subsonic and transsonic regions beyond a shock wave for supersonic flow past a sphere immersed in an equilibrium stream of air and carbon dioxide. The thermodynamic functions were approximated with the formulas of A. N. Kraiko (for air) and V. V. Mikhailov (for $CO_2$), which in the entire range of $p$ and $T$ ensure accuracies of 2% and 1% respectively. The method presented in /19/ was employed. Systematic computations of the flow past the sphere were made for a wide range of Mach numbers, temperature, and pressure of the incident flow: $M_1=4-50$, $T_1=250-1500$ °K, $p_1=10^{-5}-1$ atm for air and $M_1=2-35$, $T_1=250-500$ °K, $p_1=10^{-4}-1$ atm for carbon dioxide.

It was shown that when physicochemical reactions in the gas are taken into consideration, the separation of the shock wave and the entire geometric pattern of flow varies nonmonotonically as $M_1$ increases; the flow pattern depends little on $p_1$ and substantially more on $T_1$; the main parameter shaping the flow in the subsonic and the transsonic regions is the density increment in the direct shock. As an example, Figure 9 shows the separation of the shock wave as a function of $M_1$ in air for different values of $p_1$ and $T_1$

G. F. Telenin and S. M. Gilinskii /22/ investigated the applicability of the scheme described in /19/ to computation of flow past ellipsoids, and also to computation of low supersonic flow past a sphere.

G. S. Roslyakov and L. A. Chudov /23/ propose the method of steadying for the solution of the problem of flow past a blunt body. Applying the difference method they find the numerical stationary solution for the corresponding nonstationary problem (starting with arbitrary initial data).

The steadying of the solution is achieved by a special choice of difference ("viscous") schemes, and also by dissipation of energy on the shock wave.

The problem is solved in coordinates which reduce the domain of integration to a time-independent rectangle. The shock wave coincides with the coordinate line and serves as part of the boundary of the domain.

The numerical procedure is divided into two stages. In the first stage, using Lacks' scheme, which possesses considerable "viscosity", a "rough"

* See Belotserkovskii, O. M. — Vychislitel'naya matematika, No. 3. 1958; also PMM, Vol. 24, No. 3. 1960.

solution is computed. The application of the "viscous" scheme enables the computation to proceed from arbitrary (discontinuous) initial data (with arbitrary initial form of the shock wave). The shock waves arising inside the integration domain are smeared by "viscosity" and rapidly decay.

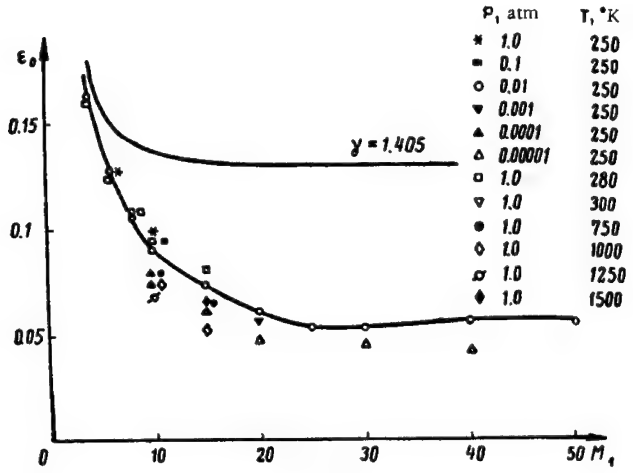


FIGURE 9

In the second stage the solution is rendered more accurate. Two-layer explicit difference schemes of second order accuracy are used. The second order of accuracy (and also stability) are achieved by introducing "half-integer" temporal layers, where the solution is obtained with Lacks' scheme and subsequent application of the "cross" scheme.

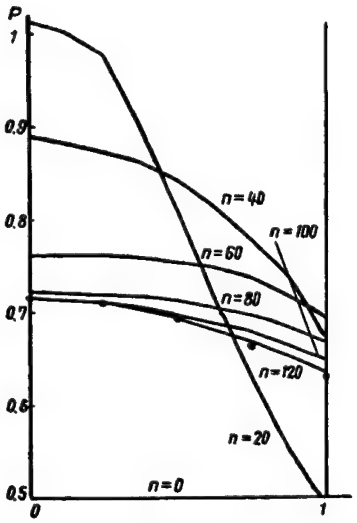


FIGURE 10

In systematic computations the first stage of the procedure may be omitted. Given a solution for a body of some known shape and for a certain Mach number $M$ of the incident flow, we may apply the scheme of second order of accuracy to find solutions for other values of $M$.

I. G. Belukhina /24/ considered various difference schemes for the solution by the method of steadying (presented in /23/) of the one-dimensional problem modelling the flow past a blunt body. The model problem was obtained from gas-dynamic equations (in spherical coordinates) by replacing the transverse velocity component and all the lateral derivatives along one of the rays with the corresponding values from a known solution. The effect of various factors on the rate of steadying of the solution was studied.

As an example, Figure 10 illustrates the process of steadying (in the first stage of the procedure) of pressure along the axis of symmetry.

BIBLIOGRAPHY


1. SOLODKIN, V.K. and G.S. ROSLYAKOV. Tablitsy sopel dlya aerodinamicheskikh trub sverkhzvukovykh skorostei (Tables of Nozzles for Supersonic Wind Tunnels). — Otchet VTs MGU. 1961.
2. PCHELKINA, L.V., V.A. RUBTSOV, and V.M. SEMICHASTNOV. Osesimmetrichnye sopla s uglovoi tochkoi (Axisymmetric Nozzles with an Angular Point). Tables. — Otchet VTs MGU. March 1963.
3. PCHELKINA, L.V. and V.A. RUBTSOV. Osesimmetrichnye sopla s uglovoi tochkoi. Opisanie metoda i programm (Axisymmetric Nozzles with an Angular Point. Description of Method and Programs). — Otchet VTs MGU. 1962.
4. Tablitsy gazodinamicheskikh funktsii dlya $\gamma$ ot 1.05 do 1.67 (Tables of Gas-Dynamic Functions for $\gamma$ from 1.05 to 1.67). — Otchet VTs MGU. March 1963.
5. PCHELKINA, L.V. and V.K. SOLODKIN. Osesimmetrichnye sopla s uglovoi tochkoi i radial'nym potokom na vykhode (Axisymmetric Nozzles with an Angular Point and Radial Outlet Flow). — Otchet VTs MGU. 1962.
6. PIRUMOV, U.G. and V.A. RUBTSOV. Raschet osesimmetrichnykh sverkhzvukovykh kol'tsevykh sopel (Computation of Axisymmetric Supersonic Annular Nozzles). — Izvestiya AN SSSR, seriya mekhaniki i mashinostroeniya, No. 6. 1961.
7. MEZHIBOVSKAYA, E.G., U.G. PIRUMOV, V.A. RUBTSOV, and E.V. SOROKINA. Raschet kol'tsevykh osesimmetrichnykh sopel (Computation of Annular Axisymmetric Nozzles). — Otchet VTs MGU. 1961.
8. ROSLYAKOV, G.S. and N.V. DROZDOVA. Numerical Computation of Flow Past a Scalariform Cone. — This volume.
9. VOLKONSKAYA, T.G. Calculation of Supersonic Axisymmetric Jets. — This volume.
10. PIRUMOV, U.G., V.A. RUBTSOV, and V.N.SUVOROVA. Calculation of Axisymmetric Exhaust Nozzles with an Allowance for Equilibrium Physicochemical Reactions. — This volume.
11. DUBINSKAYA, N.V., R.A. GZHELYAK, and I.V. IGONINA. Raschet obtekaniya tupogo ugla metodom kharakteristik s uchetom relaksatsii (Computation of Flow Past an Obtuse Angle by the Method of Characteristics with an Allowance for Relaxation). — Otchet VTs MGU. 1962.
12. DEEVA, A.A., V.M. PASKONOV, and G.S. ROSLYAKOV. Standartnye podprogrammy dlya resheniya zadach sverkhzvukovoi gazovoi dinamiki (Standard Subroutines for the Solution of Problems of Supersonic Gas Dynamics). — Otchet VTs MGU. 1958.
13. PASKONOV, V.M. and L.V. PCHELKINA. Standartnye podprogrammy dlya resheniya zadach, svyazannykh s raschetom neizentropicheskikh sverkhzvukovykh osesimmetrichnykh techenii ideal'nogo gaza (Standard Subroutines for the Solution of Problems Connected with Computation of Nonisentropic Supersonic Axisymmetric Flows of Ideal Gas). — Otchet VTs MGU. 1960.
14. GZHELYAK, R.A., E.G. MEZHIBOVSKAYA, L.V. PCHELKINA, and V.A. RUBTSOV. Standartnye podprogrammy dlya resheniya zadach sverkhzvukovoi gazovoi dinamiki dlya EVM VTs MGU (Standard Subroutines for the Solution of Problems of Supersonic Gas Dynamics for the Electronic Computer of the Computational Center of Moscow State University). — Otchet VTs MGU. 1961.
15. RUBTSOV, V.A. and V.N. SUVOROVA. Standartnye podprogrammy dlya rascheta ravnovesnykh techenii real'nogo gaza (Standard Subroutines for the Computation of Real Gas Equilibrium Flows). — Otchet VTs MGU. 1962.

16. DUBINSKAYA, N.V., R.A. GZHELYAK, and I.V. IGONINA. Standartnye podprogrammy dlya rascheta neravnovesnykh techenii real'nogo gaza (Standard Subroutines for the Computation of Real Gas Nonequilibrium Flows). — Otchet VTs MGU. 1962.
17. CHUDOV, L.A. Raznostnye metody resheniya ellipticheskoi zadachi Koshi (Difference Method for the Solution of the Elliptic Cauchy Problem). — DAN SSSR, Vol. 142, No. 5, 1962.
18. CHUDOV, L.A. and V.P. KUDRYAVTSEV. Round-Off Errors in Difference Solutions of Boundary-Value Problems For Elliptic Equations and Systems. — This volume.
19. TELENIN, G.F. and G.P. TINYAKOV. Metod rascheta sverkhzvukovogo obtekaniya tel s otoshedshei udarnoi volnoi (Method of Computation of Supersonic Flow Past Bodies with Separated Shock Wave). — Otchet NII mekhaniki MGU. December 1961.
20. TELENIN, G.F. and G.P. TINYAKOV. Raschet ravnovesnogo obtekaniya sfery sverkhzvukovym potokom vozdukha (Computation of Supersonic Air Flow Past a Sphere). — Otchet NII mekhaniki MGU. July 1962.
21. TELENIN, G.F. and G.P. TINYAKOV. Raschet sverkhzvukovogo obtekaniya sfery ravnovesnym potokom uglekislogo gaza (Computation of Supersonic Equilibrium Carbon-Dioxide Flow Past a Sphere). — Otchet NII mekhaniki MGU. December 1962.
22. TELENIN, G.F. and S.M. GILINSKII. K raschetu sverkhzvukovogo obtekaniya tel s otoshedshei udarnoi volnoi (The Computation of Supersonic Flow Past Bodies with Separated Shock Wave). — Otchet NII mekhaniki MGU. December 1962.
23. ROSLYAKOV, G.S. and L.A. CHUDOV. Raznostnyi metod resheniya zadachi ob otoshedshei udarnoi volne (Difference Method for the Solution of Problems with Separated Shock Wave). — Otchet VTs MGU. 1962.
24. BELUKHINA, I.G. Graduation thesis. — MGU. 1962.

*L. A. Chudov and V. P. Kudryavtsev*

# *ROUND-OFF ERRORS IN DIFFERENCE SOLUTIONS OF BOUNDARY-VALUE PROBLEMS FOR ELLIPTIC EQUATIONS AND SYSTEMS*

## § 1. Introduction

The calculation of ideal compressible gas flow past a blunt body by the so-called inverse method leads to a Cauchy problem for a nonlinear system of equations, which is elliptic in the subsonic range /1/. It is well known that the Cauchy problem for elliptic equations and systems of equations is "improper" in the sense that small perturbations in the initial conditions lead to large disturbances in the solution /2/. Since both truncation and round-off errors are inevitable in numerical solutions, the application of numerical methods to these improper problems should involve large practical difficulties.

Difference methods have been successfully applied in some recent works /1, 3, 4, 5/ to the solution of flow past a blunt body. Some of the difference methods were empirically proved unsuitable for this object, while other schemes yielded solutions whose accuracy is sufficient for all practical purposes.

A characteristic feature of the difference method used in the solution of these problems, as we see from the works cited, is the exceedingly rapid accumulation of round-off errors as the grid spacing is reduced. Clearly, only such grid spacings which give a round-off error not substantially greater than the truncation error should be used.

A correct evaluation of these errors is much more significant in the case of improper problems than in proper ones. The choice of difference schemes and the determination of lattice parameters for proper problems is now generally made by applying the theory of difference schemes to suitable model problems /6, 7/. This theory, however, does not apply to improper problems in its present form. To successfully apply difference schemes to more complex problems of gas dynamics (e. g., in inverse method of calculation of supersonic flow past a blunt body with separated shock wave allowing for physicochemical nonequilibrium of the gas /4/), we must at least devise some simple model to prove the convergence of the approximate solutions to the exact figure and to estimate the truncation and the round-off errors.

In /8/ the convergence of the difference method is discussed in its application to a certain model boundary-value problem for the Laplace equation. The study is based on the concept of properness in the sense of A. N. Tikhonov (uniqueness of solution and its continuity as a function of

the boundary values under a suitable a priori restriction of the class of solutions considered /9, 10/). This concept was found useful in defining a stable difference scheme for the model problem in question and in proving the convergence of approximate solutions to the exact solution for stable approximating difference schemes.

In the present article we investigate some problems bearing on the evaluation of round-off errors and rational choice of grid spacing for one important class of difference schemes. The theoretical analysis is given for the model problem discussed in /8/. Linearization and freezing of coefficients yield tentative estimates of round-off errors for one problem of gas dynamics (see /4/).

## § 2. The Model Problem. Stability and Convergence of Difference Schemes

Consider a boundary-value problem for a Cauchy-Riemann system of equations, i. e., the simplest elliptic system

$$\frac{\partial u}{\partial y} = -\frac{\partial v}{\partial x}; \quad \frac{\partial v}{\partial y} = \frac{\partial u}{\partial x}; \tag{1}$$

$$\left.\begin{aligned} u(0, y) = u(\pi, y) = 0; \\ v_x(0, y) = v_x(\pi, y) = 0; \end{aligned}\right\} \tag{2}$$

$$\left.\begin{aligned} u(x, 0) = \varphi(x); \\ v(x, 0) = \psi(x). \end{aligned}\right\} \tag{3}$$

Suppose that in the domain $0 \leqslant x \leqslant \pi$, $0 \leqslant y \leqslant Y$ this problem has a solution which satisfies the condition

$$\int_0^{\pi} u^2(x, y)\, dx \leqslant M^2, \quad (0 \leqslant y \leqslant Y). \tag{4}$$

This assumption will be called the basic a priori proposition. Using the Fourier method, we obtain the solution of boundary-value problem (1), (2), (3) in the form

$$\begin{aligned} u(x, y) &= \sqrt{\frac{2}{\pi}} \sum_{k=1}^{\infty} a_k e^{ky} \sin kx + \sqrt{\frac{2}{\pi}} \sum_{k=1}^{\infty} b_k e^{-ky} \sin kx, \\ v(x, y) &= \sqrt{\frac{2}{\pi}} \sum_{k=1}^{\infty} c_k e^{ky} \sin kx + \sqrt{\frac{2}{\pi}} \sum_{k=1}^{\infty} d_k e^{-ky} \sin kx, \end{aligned} \tag{5}$$

where $c_k = a_k$, $d_k = -b_k$, $k = 1, 2, \ldots$

In all that follows we shall take $b_k = 0, d_k = 0$, i. e., drop the second sum in the right-hand sides of the above equalities. Because of this proposition, $\varphi(x)$ and $\psi(x)$ can no longer be defined independently of each other. When studying the properness of boundary-value problem (1), (2), (3), we shall take the equality

$$u(x, 0) = \varphi(x)$$

as an independent initial condition and will seek the dependence of $u(x,y)$ on $\varphi(x)$. The second function $v(x,y)$ will thus only play an auxiliary role. It is easily seen that with $b_k = 0$, $d_k = 0$, we have $v = Tu$, where $T$ is an operator, isometric in $L_2(0,\pi)$, transforming the system of functions $\{\sin kx\}$, $(k = 1,2,...)$ into $\{\cos kx\}$, $(k=1,2,...)$.

For future reference we give here some results from /8/.

*Theorem 1. Boundary-value problem (1), (2), (3) is proper in the sense of Tikhonov under a priori proposition (4). The continuous dependence of the solution $u(x,y)$ on the initial function $\varphi(x) = u(x,0)$ follows from the estimate*

$$\int_0^\pi [u_1(x, y) - u_2(x, y)]^2 dx \leqslant$$

$$\leqslant (4M^2)^{\frac{y}{Y}} \left( \int_0^\pi [u_1(x, 0) - u_2(x, 0)]^2 dx \right)^{1-\frac{y}{Y}}. \qquad (6)$$

Estimate (6) is exact. It follows from this estimate that the operator transforming $u(x,0)$ into $u(x,y)$ does not constitute a continuous linear transformation, if the two functions $u(x,0)$ and $u(x,y)$ are regarded as elements of the space $L_2(0,\pi)$. Applying the a priori estimate (4) we may derive a stronger norm for the initial values:

$$\|\varphi\|_0 = \sqrt{\sum_{k=1}^{\infty} a_k^2 e^{2kY}}. \qquad (7)$$

Then, taking

$$\|u\| = \sup_{0<y<Y} \sqrt{\int_0^\pi u^2(x,y)\, dx}, \qquad (8)$$

we obtain from (5) an estimate which is uniform in the norms and does not contain explicitly the a priori propositions:

$$\|u\| \leqslant \|\varphi\|_0.$$

To evaluate the effectiveness of difference schemes and the influence of errors in the determination of initial values and of round-off errors, we should know to what degree a solution of problem (1), (2), (3) satisfying the basic a priori proposition (4) is specified by the approximate initial values $u(x,0) = \varphi(x)$ on the grid

$$x = x_m = mh; \quad m = 1, 2, \ldots, N-1; \quad h = \frac{\pi}{N}. \qquad (9)$$

We shall only be interested in the values of $u(x,y)$ on the rectilinear grid (9) for $0 \leqslant y \leqslant Y$, and we therefore introduce a suitable grid norm

$$\|u(y)\|_h = \sqrt{h \sum_{n=1}^{N-1} u^2(x_n, y)}.$$

*Theorem 2. Let $u(x,y)$ be a solution of problem (1), (2), (3) satisfying the a priori proposition (4) and meeting the additional requirement $b_k = 0$, $(k=1,2,\ldots)$. Construct the function*

$$\bar{u}(x, y) = \sqrt{\frac{2}{\pi}} \sum_{k=1}^{N-1} \bar{a}_k e^{ky} \sin kx,$$

*where the coefficients $\bar{a}_k$ are obtained from the conditions*

$$\bar{u}(x_m, 0) = u(x_m, 0) + \gamma_m, \qquad (m = 1, 2, \ldots, N-1)$$

*($\gamma_m$ are the initial-value errors).*

*Then*

$$\|\bar{u}(y) - u(y)\|_h \leqslant \sqrt{2}\, M \frac{e^{-(N+1)\eta}}{\sqrt{1 - e^{-4N\eta}}} + \gamma e^{(N-1)y}, \tag{10}$$

*where*

$$\eta = Y - y; \quad \gamma = \sqrt{h \sum_{m=1}^{N-1} \gamma_m^2}.$$

We now proceed with the discussion of the results which have bearing on the stability and convergence of difference schemes. We shall only consider two-layer schemes. The grid is assumed rectangular with constant spacings $\Delta x = h$, $\Delta y = \tau$, where $\tau = \tau(h)$ and $\tau(h) \to 0$ as $h \to 0$. For two-layer difference schemes, we define a norm of initial values by analogy with (7):

$$\|\varphi\|_{0h} = \sqrt{\sum_{k=1}^{N-1} \hat{a}_k^2 e^{2kY}},$$

where $\hat{a}_k$ are the coefficients in the expansion of the function $\varphi_m = \varphi(mh)$ defined on the grid in terms of the orthonormal grid functions

$$\left\{\sqrt{\frac{2}{\pi}} \sin kmh\right\}, \qquad (k = 1, 2, \ldots, N-1).$$

*Definition. A two-layer difference scheme is said to be stable in initial values if for $0 \leqslant y \leqslant Y$ and $0 < h \leqslant h_0$ we have*

$$\|u(y)\|_h \leqslant K \|\varphi\|_{0h}, \tag{11}$$

*where $K$ is a constant independent of $h$.*

For difference schemes having a solution of the form

$$u_m^n = u(mh, n\tau) = s^n(k;\ h)\sin kmh,$$
$$v_m^n = v(mh, n\tau) = s^n(k;\ h)\cos kmh, \tag{12}$$

we have directly from (11) the necessary condition of stability in initial values:

$$|s^n(k;\ h)| \leqslant Ke^{kY}; \qquad 0 \leqslant n\tau \leqslant Y.$$

The inequality

$$|s^n(k;\ h)| \leqslant Ke^{ky}; \qquad 0 \leqslant n\tau = y \leqslant Y \tag{13}$$

will be called the strong condition of stability in initial values. The stability of several difference schemes is investigated in /8/.

*Theorem 3. Let a two-layer difference scheme, for any integral* $N = \frac{\pi}{h}$, *have a system of solutions of the form (12) with* $k = 1, 2, \ldots, N-1$, *and let the strong condition of stability (13) be additionally satisfied. We further assume that the following condition of consistence is satisfied: for* $h \to 0$

$$\overline{k}(k;\ h) = \frac{1}{\tau}\ln s(k;\ h) \to k \tag{14}$$

*uniformly in every finite interval*

$$0 \leqslant k \leqslant k_0.$$

*Then an approximate solution* $u_h$ *converges to the exact solution* $u(x,y)$ *and the following estimate applies:*

$$\|u_h(y) - u(y)\|_h \leqslant M_1(h)\sup_k |1 - e^{(\overline{k}-k)y}|\, e^{-k\eta} + M\frac{e^{-(N+1)\eta}}{\sqrt{1-e^{-4N\eta}}},$$

*where*

$$\eta = Y - y, \quad M^2 = \sum_{k=1}^{\infty} a_k^2 e^{2kY} \text{ and } M_1(h) \to M \quad \text{for} \quad h \to 0;$$

*moreover,* $M_1(h)$ *is uniformly bounded on the class of solutions satisfying the basic inequality (4).*

## § 3. Many-Point Schemes

Inequality (10), which is the heart of the theorem, indicates the expediency of using schemes with a high order of accuracy relative to $h$. Indeed, two conclusions can be drawn from (10). First, setting $\gamma = 0$ we conclude that if the exact initial values $u(x,0)$ are known on grid (9), the function $u(x,y)$ is determined on this grid with exponential accuracy. The initial values thus carry a very large information content as regard the function $u(x,y)$, which should be utilized as thoroughly as possible in the construction of the difference scheme. Second, the form of the

second term in the right-hand side of (10) indicates that to reduce the effect of round-off and other analogous errors we should use grids with as large a spacing as is feasible. The so-called many-point schemes meet these requirements. A simplest scheme of this type has the form

$$\frac{u_m^{n+1}-u_m^n}{\tau}=-\frac{1}{h}\sum_{q=-p}^{p}a_q^{(p)}v_{m+q}^n;$$
$$\frac{v_m^{n+1}-v_m^n}{\tau}=\frac{1}{h}\sum_{q=-p}^{p}a_q^{(p)}u_{m+q}^n. \qquad (15)$$

The coefficients $a_q^{(p)}$ are defined as

$$a_q^{(p)}=(-1)^{q-1}\frac{(p!)^2}{(p-q)!\,q\,(p+q)!}\ ;\ a_0^{(p)}=0.$$

They can be obtained as follows.

Let $L(x_m+th)$ be a Stirling interpolation polynomial of degree $2p$ taking the values $f_{m+q}$ for $q=0,\pm1,\ldots,\pm p$. It is known (see /11/, p. 128) that

$$L(x_m+th)=f_0+tf_0^1+\frac{t^2}{2!}f_0^2+\ldots+$$
$$+\frac{t(t^2-1)(t^2-2^2)\ldots[t^2-(p-1)^2]}{(2p-1)!}f_0^{2p-1}+$$
$$+\frac{t^2(t^2-1)(t^2-2^2)\ldots[t^2-(p-1)^2]}{(2p)!}f_0^{2p}, \qquad (16)$$

where

$$f_0^{2p-1}=\frac{1}{2}[f_{1/2}^{2p-1}+f_{-1/2}^{2p-1}]$$

(for the definition and properties of the finite differences $f_0^k$, $f_{1/2}^{2p-1}$, $f_{-1/2}^{2p-1}$, see /11/, p. 113).

Differentiating (16) with respect to $\xi=th$ and setting $\xi=0$, we obtain an approximate expression for the derivative:

$$hf'(x_m)\approx f_0^1-\frac{1}{3!}f_0^3+\ldots+(-1)^{q-1}\frac{[(q-1)!]^2}{(2q-1)!}f_0^{2q-1}+\ldots$$
$$\ldots+(-1)^{p-1}\frac{[(p-1)!]^2}{(2p-1)!}f_0^{2p-1}. \qquad (17)$$

Expressing $f_0^{2q-1}$ in terms of $f_m$, we obtain the coefficients $a_q^{(p)}$. The table on the next page lists values of $a_q^{(p)}$ for some schemes

$$a_{-q}^{(p)}=-a_q^{(p)} \quad \text{and} \quad a_0^{(p)}=0.$$

We now investigate the stability of scheme (15). Let

$$\Delta f_m=f_{m+1}-f_m,\quad \nabla f_m=f_m-f_{m-1}.$$

| Scheme index $p$ | Symbolic notation | Coefficients $a_q^{(p)}$ | | | | | Truncation error |
|---|---|---|---|---|---|---|---|
| | | $a_1^{(p)}$ | $a_2^{(p)}$ | $a_3^{(p)}$ | $a_4^{(p)}$ | $a_5^{(p)}$ | |
| 1 | * *** | $\frac{1}{2}$ | — | — | — | — | $O(\tau)+O(h^2)$ |
| 2 | * ***** | $\frac{2}{3}$ | $-\frac{1}{12}$ | — | — | — | $O(\tau)+O(h^4)$ |
| 3 | * ******* | $\frac{3}{4}$ | $-\frac{3}{20}$ | $\frac{1}{60}$ | — | — | $O(\tau)+O(h^6)$ |
| 4 | * ********* | $\frac{4}{5}$ | $-\frac{1}{5}$ | $\frac{4}{105}$ | $-\frac{1}{280}$ | — | $O(\tau)+O(h^8)$ |
| 5 | * *********** | $\frac{5}{6}$ | $-\frac{5}{21}$ | $\frac{5}{84}$ | $-\frac{5}{504}$ | $\frac{1}{1260}$ | $O(\tau)+O(h^{10})$ |

It is easily seen that the following equalities apply:

$$f_0^{2r} = (\nabla\Delta)^r f_0,$$

$$f_0^{2r+1} = \frac{1}{2}(\Delta+\nabla) f_0^{2r}.$$

Formula (17) can thus be written in the following operational notation:

$$hf'(x_m) \approx \frac{1}{2}(\Delta+\nabla)\Big[1 - \frac{1}{3!}(\Delta\nabla) + \ldots +$$

$$+ (-1)^{q-1}\frac{[(q-1)!]^2}{(2q-1)!}(\Delta\nabla)^{q-1} + \ldots +$$

$$+ (-1)^{p-1}\frac{[(p-1)!]^2}{(2p-1)!}(\Delta\nabla)^{p-1}\Big] f_m = L_{(p)} f_m.$$

To investigate the stability of scheme (15), we write it in complex form, setting $f = u + iv$:

$$\frac{f_m^{n+1} - f_m^n}{\tau} = \frac{i}{h} L_{(p)} f_m^n.$$

(We return to our ordinary notation: $f_m^n = f(mh, n\tau.)$ Let $f_m^n = [s(k, h)]^n e^{-ikmh}$. It is easily seen that

$$\frac{1}{2}(\Delta+\nabla) e^{-ikmh} = -i \sin kh \; e^{-ikmh};$$

$$(\Delta\nabla) e^{-ikmh} = -2(1-\cos kh) e^{-ikmh};$$

$$(\Delta\nabla)^{q-1} e^{-ikmh} = (-2)^{q-1}(1-\cos kh)^{q-1} e^{-ikmh}.$$

Hence, setting $s(k, h) = s_p$, we have

$$s_p = 1 + \frac{\tau}{h}\sin kh \sum_{q=1}^{p} \frac{2^{q-1}[(q-1)!]^2}{(2q-1)!}(1-\cos kh)^{q-1} =$$

$$= 1 + \frac{\tau}{h}\sin kh \sum_{q=0}^{p-1} \frac{q!}{(2q+1)!!}(1-\cos kh)^q.$$

Clearly

$$s_p \leqslant s_\infty = 1 + \frac{\tau}{h} \sin kh \sum_{q=1}^{\infty} \frac{2^{q-1}[(q-1)!]^2}{(2q-1)!} (1 - \cos kh)^{q-1}.$$

Let us study in more detail the expression

$$H = \sin \alpha \sum_{q=0}^{\infty} \frac{q!}{(2q+1)!!} (1 - \cos \alpha)^q, \quad \text{where} \quad \alpha = kh. \tag{18}$$

Substituting $x = \sin \frac{\alpha}{2}$, we obtain from (18)

$$H = 2x\sqrt{1-x^2} \sum_{q=0}^{\infty} \frac{q!\, 2^q x^{2q}}{(2q+1)!!}.$$

It is known (see /12/; appendix to Chapter 8, § 5) that the series $\sum_{q=0}^{\infty} \frac{q!\, 2^q x^{2q+1}}{(2q+1)!!}$ converges for $|x| < 1$ (this follows directly from D'Alembert's criterion), its sum being

$$(1 - x^2)^{-\frac{1}{2}} \arcsin x.$$

Therefore $H = 2 \arcsin x$. This signifies that $S_\infty = 1 + \tau k$ and, consequently,

$$s^n = s^{Y/\tau} \leqslant (1 + \tau k)^{\tau} \leqslant e^{kY}.$$

This proves inequality (13).

Proceeding from these results we can easily calculate a simple implicit scheme, obtained from scheme (15):

$$\frac{\tilde{u}_m^{n+1} - u_m^n}{\tau} = -\frac{1}{h} \sum_{q=-p}^{p} a_q^{(p)} v_{m+q}^n; \quad \frac{\tilde{v}_m^{n+1} - v_m^n}{\tau} = \frac{1}{h} \sum_{q=-p}^{p} a_q^{(p)} u_{m+q}^n;$$

$$\frac{u_m^{n+1} - u_m^n}{\tau} = -\frac{1}{2h} \left[ \sum_{q=-p}^{p} a_q^{(p)} v_{m+q}^n + \sum_{q=-p}^{p} a_q^{(p)} \tilde{v}_{m+q}^{n+1} \right]; \tag{19}$$

$$\frac{v_m^{n+1} - v_m^n}{\tau} = \frac{1}{2h} \left[ \sum_{q=-p}^{p} a_q^{(p)} u_{m+q}^n + \sum_{q=-p}^{p} a_q^{(p)} \tilde{u}_{m+q}^{n+1} \right].$$

We shall prove that inequality (13) applies in this case, too. Indeed, for the implicit scheme (19)

$$s_p = 1 + \frac{\tau}{h} \sin kh \sum_{q=1}^{p} \frac{2^{q-1}[(q-1)!]^2}{(2q-1)!} (1 - \cos kh)^{q-1} +$$

$$+ \frac{1}{2} \frac{\tau^2}{h^2} \left[ \sum_{q=1}^{p} \frac{2^{q-1}[(q-1)!]^2}{(2q-1)!} (1 - \cos kh)^{q-1} \right]^2.$$

According to the preceding $s_p \leqslant s_\infty = 1 + k\tau + \frac{1}{2} k^2\tau^2$, and since the inequality

$$\left(1 + k\tau + \frac{1}{2} k^2\tau^2\right)^{\frac{y}{\tau}} \leqslant e^{ky}$$

is satisfied simultaneously with

$$1 + k\tau + \frac{1}{2} k^2\tau^2 \leqslant e^{k\tau},$$

the validity of the last inequality proves the strong condition of stability in initial values (13) if we set $K = 1$.

## § 4. Choosing the Grid Spacing with an Allowance for Round-Off Errors

In this section we shall derive comparative estimates of truncation and round-off errors for two difference schemes.

According to Theorem 3, the main part of the truncation error is equal in order of magnitude to

$$M \max_k e^{-k\eta} \left| 1 - e^{-(k-\bar{k})y} \right|.$$

Taking the ratio of this error to the maximum value of $\| u(y) \|_h$, whose order of magnitude is $M$, we obtain an estimate of the relative truncation error

$$R = \max_k e^{-k\eta} \left| 1 - e^{-(k-\bar{k})y} \right|.$$

We shall now estimate $R$ for scheme (15) with $p = 1$. We first set $\tau = 0$. Then $\bar{k} = \frac{\sin kh}{h}$ and consequently $k - \bar{k} > 0$. Further

$$1 - e^{-(k-\bar{k})y} = (k - \bar{k})\, y - \frac{(k-\bar{k})^2}{2!} y^2 + \frac{(k-\bar{k})^3}{3!} y^3 - \dots$$

Suppose that at point $k$, where $R$ is maximized, $(k - \bar{k})y \leqslant 2$. Applying Leibnitz's theorem on alternating decreasing series we obtain

$$R < (k - \bar{k})\, y e^{-k\eta}.$$

We further have

$$k - \bar{k} = k - \frac{\sin kh}{h} = \frac{1}{h} \left[ \frac{k^3h^3}{3!} - \frac{k^5h^5}{5!} + \dots \right].$$

Let $k^2h^2 < 20$; from Leibnitz's theorem $k - \bar{k} < \frac{k^3h^2}{6}$ and $R < \tilde{R}_3 = e^{-k\eta} \frac{k^3h^2}{6} y$.

$\tilde{R}_3$ is maximized at $k = \frac{3}{\eta}$, so that

$$R < \tilde{R}_3 \leqslant \frac{9}{2} e^{-3} \frac{h^2 y}{\eta^3}. \qquad (20)$$

We now estimate the errors due to inaccuracies in initial values (round-off errors or errors of measurements). All calculations will be assumed to

be made without rounding off. Let $\delta_0$ be the root-mean-square norm of the initial error divided by $M$. Then the relative error $\delta(y,h)$ due to this initial error is estimated as

$$\delta_0 \max_k e^{\frac{\sin kh}{h} y} = \delta_0 e^{\frac{y}{h}}.$$

For a given $y$, the optimal grid spacing $h$ ensures that the truncation error and the error $\delta(y, h)$ both have the same order of magnitude. This choice of optimal spacing gives the maximum accuracy attainable with the particular scheme in question for a given $\delta_0$.

Let us consider a particular example. Suppose that the initial error $\delta_0 = 10^{-8}$; it is stipulated that the relative error produced by this inaccuracy should not exceed $\varepsilon = 10^{-2}$. Hence

$$e^{\frac{y}{h}} \leqslant 10^6 \text{ and } \frac{y}{h} \leqslant 6 \ln 10 \approx 13.8.$$

Taking the truncation error from (20), we obtain

$$\varepsilon = 10^{-2} \approx \frac{9}{2} e^{-3} \frac{1}{(13.8)^2} \frac{y^3}{\eta^3}. \tag{21}$$

Setting $\vartheta = \frac{y}{Y}$, we have $\eta = (1 - \vartheta) Y$, and then from (21)

$$\frac{\vartheta}{1-\vartheta} \approx \sqrt[3]{\frac{2}{9} e^3 (13.8)^2 10^{-2}} \approx 2.042.$$

Hence

$$\vartheta \approx 0.67 \text{ and } h = \frac{Y}{21}.$$

This result can be summed up as follows. When using scheme (15) with $p = 1$ and a sufficiently small $\tau$, a relative error of the order of $10^{-2}$ for $\delta_0 = 10^{-8}$ can be obtained only up to $\vartheta = 0.67$; correspondingly, $h \approx \frac{Y}{21}$.

We now consider scheme (15) with $p = 2$. For this scheme

$$s_2 = 1 + c\left(\frac{4}{3}\sin kh - \frac{1}{6}\sin 2kh\right), \left(c = \frac{\tau}{h}\right)$$
$$\bar{k} = \frac{1}{\tau} \ln\left[1 + c\left(\frac{4}{3}\sin kh - \frac{1}{6}\sin 2kh\right)\right].$$

With $\tau = 0$ we have

$$\bar{k} = \frac{1}{h}\left(\frac{4}{3}\sin kh - \frac{1}{6}\sin 2kh\right).$$

Estimating $R$ as we have done before, we find that, for $k^2h^2 < 42$:

$$R < R_5 = e^{-k\eta} \frac{k^5 h^4}{30} y \leqslant \frac{625}{6} e^{-5} \frac{h^4}{\eta^5} y. \tag{22}$$

The maximum growth of the initial error is

$$\max_k \exp \frac{y}{h}\left(\frac{4}{3}\sin kh - \frac{1}{6}\sin 2kh\right) \approx \exp\ 1.372222\ \frac{y}{h}.$$

Equating $\delta(y,h)$ with $\tilde{R}_5$ for $\delta_0 = 10^{-8}$, $\varepsilon = 10^{-2}$, we obtain, after simple calculations, $\vartheta = 0.73$, $h = \frac{Y}{14}$. With this scheme the required accuracy ($\varepsilon \sim 10^{-2}$) can thus be obtained for higher values of $\vartheta$ than in scheme (15) with $p = 1$; the corresponding $x$-interval is about 1.5 times as large as in scheme (15) with $p = 1$. This example hints at the advantages of the high-precision schemes discussed in § 3.

For these schemes we have calculated the quantity

$$e^{-k\eta}(1 - e^{-(k-\bar{k})y}),$$

as the estimate of the relative truncation error for different $y$. The results of calculations given in the Appendix confirm the validity of the assumption made in the derivation of estimates (20) and (22) and enable the conclusion to be made that these estimates are fairly accurate for the values of $h$ in question and for $y \leqslant \vartheta Y$ (the maximum permissible values of $\vartheta$ are given above).

Let us briefly consider the problem with $\tau \neq 0; \frac{\tau}{h} = c \leqslant 1$. For scheme (15) with $p = 1$ we have, provided $(k - \bar{k})y$ and $kh$ are sufficiently small,

$$1 - e^{-(k-\bar{k})y} \leqslant (k - \kappa)\, y = y\left[k - \frac{1}{ch}\ln(1 + c\sin kh)\right] \leqslant$$

$$\leqslant y\left(k - \frac{\sin kh}{h} + \frac{c}{2}\frac{\sin^2 kh}{h}\right) \leqslant \frac{k^2h^2}{2}\left(\frac{kh}{3} + c\right)y.$$

Thus

$$R \leqslant \tilde{R}_3(c) = e^{-k\eta}\frac{k^2h}{2}\left(\frac{kh}{3} + c\right).$$

We shall not attempt to derive an accurate estimate of $\tilde{R}_3(c)$. Instead we shall determine $c$ from the condition that at the point of maximum $\tilde{R}_3$ (see derivation of estimate (20)) $c = \frac{kh}{3}$. Then, for the given frequency $k = \frac{3}{\eta}$, both $\tau$ and $h$ take equal parts in the truncation error. We find $c = \frac{h}{\eta}$. For the preceding case ($\varepsilon = 10^{-2}$, $\delta_0 = 10^{-8}$) we have $c \approx \frac{1}{7}$. Then $\tau \sim \frac{Y}{150}$ and the number of layers for $\vartheta = 0.67\,Y$ will be of the order of 100.

The error of scheme (15) with other values of $p$ can be estimated analogously. When choosing the spacing $h$, the following table of $f^{(p)}_{\max}$ and $\alpha_{\max}$ will be useful; in this table

$$f^{(p)}_{\max} = \max_{\alpha} \sin\alpha \sum_{q=1}^{p} \frac{2^{q-1}[(q-1)!]^2}{(2q-1)!}(1 - \cos\alpha)^{q-1} =$$

$$= \max_{\alpha} 2\sum_{q=1}^{p} a_q^{(p)} \sin\alpha q,$$

and $\alpha_{\max}$ is the value of $\alpha$ at which maximum is reached.

| Difference scheme index | $f_{\max}^{(p)}$ | $\alpha_{\max}$ |
|---|---|---|
| | | $\frac{\pi}{2}$ |
| 1 | 1 | |
| 2 | 1.372222 | 1.797477 |
| 3 | 1.585978 | 1.936074 |
| 4 | 1.730598 | 2.033371 |
| 5 | 1.837438 | 2.107086 |
| 6 | 1.920846 | 2.165720 |
| 7 | 1.988481 | 2.213967 |
| 8 | 2.044869 | 2.254671 |

In the preceding examples, neglecting the round-off errors, we could have two correct significant figures only. The growth of round-off errors in these many-layered cases may result in a situation where the approximate solution will not contain a single correct significant figure. Hence the advisability of employing schemes with truncation error $O(\tau^2)$ is clear. For the particular purposes of equations of gas dynamics, which are all highly complex, it is best to use implicit schemes.

## § 5. Estimating Grid Spacing for a Certain Problem of Gas Dynamics

Let us consider the problem of supersonic flow past a blunt axisymmetric body making due allowance for physicochemical nonequilibrium of the gas.

The inverse method for the solution of this problem amounts to a determination of flow parameters and shape of the body from the boundary conditions at the shock wave. The problem is described by a system of partial differential equations, which are elliptic in the subsonic range.

We shall not dwell here on the derivation of the equations and the general statement of the problem. These questions are discussed in detail in /4/. Let $(r,z)$ be an orthogonal system of coordinates centered on the shock wave, with the $z$-axis pointing along the axis of symmetry of the body. Let the equation of the shock wave have the form $r = f(z)$; $(x,y)$ is a new system of coordinates chosen /4/ so that $x$ is the distance along the shock wave and the $y$- axis is parallel to the normal shock wave.

As in /4/ we denote by $\alpha_j$ $(j = 1, 2, ..., J)$ the concentrations of the different components; by $u$, $v$ the component velocities along $x$ and $y$, respectively; by $\rho$ the density; $p$ the pressure; and $T$ the temperature.

The flow equations then have the form

$$\frac{\partial \alpha_j}{\partial y} = A_j - \frac{u}{v(1+Ky)} \cdot \frac{\partial \alpha_j}{\partial x}; \qquad (j = 1, 2, \ldots, J) \tag{23}$$

$$\frac{\partial u}{\partial y} = \frac{1}{v(1+Ky)}\left[-\frac{1}{\rho} - Kuv - u\frac{\partial u}{\partial x}\right]; \tag{24}$$

$$\frac{\partial v}{\partial y} = \Phi\left(x, y, \frac{\partial u}{\partial x}, \ldots, \frac{\partial \alpha_1}{\partial x}, \ldots, \frac{\partial \alpha_J}{\partial x}, u, v, \ldots, \alpha_1, \ldots, \alpha_J\right); \tag{25}$$

$$\frac{\partial p}{\partial y} = -\frac{\rho}{1+Ky}\left[u\frac{\partial v}{\partial x} + (1+Ky)v\frac{\partial v}{\partial y} - Ku^2\right]; \tag{26}$$

$$\frac{\partial \rho}{\partial y} = -\frac{\rho}{v(1+Ky)}\left[(1+Ky)\frac{\partial v}{\partial y} + \frac{\partial u}{\partial x} + \frac{u}{\rho}\cdot\frac{\partial \rho}{\partial x} + \right.$$

$$\left. + (1+Ky)\frac{v}{r}\cdot\frac{\partial r}{\partial y} + vK + \frac{u}{r}\cdot\frac{\partial r}{\partial y}\right]; \qquad (27)$$

$$p = \rho\frac{T}{M}. \qquad (28)$$

Here $\frac{1}{M} = \sum_{j=1}^{J}\frac{\alpha_j}{M_j}$, where $M_j$ is the molecular weight of the respective gas component; $A_j$ is a function of flow parameters $u$, $v$, $\rho$, $p$, $T$, $\alpha_1, \ldots, \alpha_J$ characterizing the reaction rate for the $j$-th mixture component; and $\Phi$ is a function of the parameters $u$, $v$, $\rho$, $p$, $T$, $\alpha_1, \ldots, \alpha_J$ linear in the derivatives of these parameters.

When solving this problem by the difference method, the author of /4/ approximated all the equations by difference schemes (15) and (19) discussed for the model problem. However, although system (23)-(28) is elliptic on the whole, the application of these schemes to equations (23), which are clearly hyperbolic, is inexpedient, since these schemes are unstable (in the ordinary sense of the word) and, moreover, the functions $\alpha_j$ lack the smoothness required for the application of high-order difference schemes. System (23), which describes dissociation processes, is therefore solved using a stable (with weight $\lambda \geqslant 0.5$) implicit scheme

$$(\alpha_j)_{m+1}^{n+1} = \omega(\alpha_j)_m^n + (1-\omega)(\alpha_j)_{m+1}^n +$$

$$+ (1-2\omega\lambda)[(\alpha_j)_m^n - (\alpha_j)_m^{n+1}] + (A_j)_{m+1/2}^{n+1/2}, \qquad (23^*)$$

where

$$\omega = \frac{\gamma}{1+\gamma\lambda}, \quad \lambda = \text{const}, \quad \gamma = 2B_{m+1/2}^{n+1/2}\frac{\tau^*}{h^*},$$

$$B = \frac{u}{v(1+Ky)}.$$

In some problems, allowing for the particular nature of the functions $\alpha_j$, it is expedient to calculate these functions using a fine auxiliary grid with $\Delta y = \tau^*$ and $\Delta x = h^*$. Seeing that scheme (23*) is stable, we can concentrate on the partial differential equations of gas dynamics proper, i. e., (24)-(28). In what follows we propose a method for determining a tentative estimate of $h$ which makes use of the boundary conditions given on the shock wave.

Let us consider a specific case. Let the shock wave be described by the equation $r = \text{arc cosh}(z+1)$. In the new coordinate system $(x, y)$ linked with the shock wave, functions $K = K(x)$ and $r = r(x, y)$ depending on the shape of the shock wave appear in the equations of our gas-dynamics problem. In our particular example

$$K = K(x) = \frac{-1}{1+x^2}; \quad r(x, y) = \ln[x + (1+x^2)^{1/2}] - (1+x^2)^{-\frac{1}{2}}xy.$$

Let the incident flow be made of carbon dioxide $CO_2$; $\alpha_1$, $\alpha_2$, $\alpha_3$, $\alpha_4$ are the concentrations of the reacting mixture components $CO_2$, CO, $O_2$, O, respectively.

Equation (25) then takes the form

$$\frac{\partial v}{\partial y}\left[\frac{v}{T}+\sum_{j=1}^{4}\alpha_j\frac{dh_j}{dT}\left(\frac{1}{v}-\frac{Mv}{T}\right)\right]=-\frac{u}{T}\cdot\frac{\partial u}{\partial y}-$$
$$-\sum_{j=1}^{4}\left[\frac{h_j}{T}-\frac{M}{M_j}\sum_{j=1}^{4}\alpha_j\frac{dh_j}{dT}\right]\frac{\partial\alpha_j}{\partial x}+$$
$$+\frac{\sum_{j=1}^{4}\alpha_j\frac{dh_j}{dT}}{1+Ky}\left[\frac{M}{T}\left(u\frac{\partial v}{\partial x}-Ku^2\right)-\right.$$
$$\left.-\frac{1}{v}\left(\frac{\partial u}{\partial x}+\frac{u}{\rho}\cdot\frac{\partial\rho}{\partial x}+\frac{u}{z}\cdot\frac{\partial z}{\partial x}+vK+(1+Ky)\frac{v}{z}\cdot\frac{\partial z}{\partial y}\right)\right].$$

The enthalpy $h_i = h_i(T)$ is a known function of temperature. Fixing the coefficients of the derivatives, we can calculate their values at some point of the shock wave. We thus reduce (23)-(28) to a system of linear equations with constant coefficients:

$$\frac{\partial u}{\partial y}=-a_1\frac{\partial p}{\partial x}-a_2-a_3\frac{\partial u}{\partial x};\tag{29}$$

$$\frac{\partial v}{\partial y}=-b_1\frac{\partial u}{\partial y}+b_2\frac{\partial v}{\partial x}-b_3\frac{\partial u}{\partial x}-b_4\frac{\partial\rho}{\partial x}-b_5;\tag{30}$$

$$\frac{\partial p}{\partial y}=-c_1\frac{\partial v}{\partial x}-c_2\frac{\partial v}{\partial y}+c_3;\tag{31}$$

$$\frac{\partial\rho}{\partial y}=-d_1\frac{\partial v}{\partial y}-d_2\frac{\partial u}{\partial x}-d_3\frac{\partial\rho}{\partial x}-d_4.\tag{32}$$

To these equations we now apply the many-point difference schemes (15), previously considered for the model problem. For each component of the solution $w(x, y)$ we write

$$\left(\frac{\partial w}{\partial y}\right)_m^n\approx\frac{w_m^{n+1}-w_m^n}{\tau};$$
$$\left(\frac{\partial w}{\partial x}\right)_m^n\approx\frac{1}{h}\sum_{q=-p}^{p}a_q^{(p)}w_{m+q}^n.\tag{33}$$

Substituting expressions (33) for the derivatives, we obtain a system of difference equations. Without writing it out, we shall refer to it as system (A). This system, after certain transformations, has a solution

$$w_m^n=s(k,h)\,e^{im\alpha}\tilde{w}.\tag{34}$$

Here $w_m^n = w(mh, n\tau)$, and $\alpha = kh$.
Then

$$\left(\frac{\partial w}{\partial y}\right)_m^n\approx e^{im\alpha}\,\frac{s^n(s-1)}{\tau}\,\tilde{w},$$
$$\left(\frac{\partial w}{\partial x}\right)_m^n\approx e^{im\alpha}\,s^n\,\frac{i}{h}\left(\sum_{q=1}^{p}2a_q^{(p)}\sin\alpha q\right)\tilde{w}.\tag{35}$$

In the following we shall use the abbreviated notation

$$\sum = \sum_{q=1}^{p} 2a_q^{(p)} \sin aq.$$

In conjunction with system (A), we shall also investigate a simple system obtained by eliminating $p$ (see /3/) and keeping $\rho$ constant. We shall later justify our assumption that $\rho$ changes very little along the $y$-axis.

The quantity $\frac{\partial p}{\partial x}$ can thus be regarded as a coefficient. Rewriting the terms $a_2$, $b_5$, $c_3$, $d_4$, etc., in equations (29)-(32) to bring out the desired functions sought for (e.g., $b_4 \frac{\partial p}{\partial x} + b_5 = b_4^* v$; $c_3 = c_3^* u$), we reduce the system (29)-(31) to the set

$$\begin{aligned} &\frac{\partial^2 u}{\partial y^2} + a_3 \frac{i}{h} \sum \frac{\partial u}{\partial y} - c_1 a_1 \frac{i}{h} \sum \frac{\partial v}{\partial x} - c_2 a_1 \frac{i}{h} \sum \frac{\partial v}{\partial y} + \\ &\qquad + c_3^* a_1 \frac{i}{h} \sum = 0, \\ &\frac{\partial v}{\partial y} + b_1 \frac{\partial u}{\partial y} - b_2 \frac{\partial v}{\partial x} + b_3 \frac{\partial u}{\partial x} + b_4^* v = 0. \end{aligned} \tag{36}$$

Applying the Fourier method, we can investigate the system of difference equations corresponding to system (36), substituting (34) and (35) in the difference equations. We thus obtain

$$\begin{aligned} &\tilde{u}\left[(s-1)^2 + a_3 \frac{i\tau}{h} \sum (s-1) + c_3^* a_1 \tau \frac{i\tau}{h} \sum\right] + \\ &\quad + \tilde{v}\left[c_1 a_1 \frac{\tau^2}{h^2} \sum^2 - c_2 a_1 \frac{i\tau}{h} \sum (s-1)\right] = 0, \\ &\tilde{u}\left[(s-1) b_1 + b_3 \frac{i\tau}{h} \sum\right] + \tilde{v}\left[(s-1) - b_2 \frac{i\tau}{h} \sum + b_4^* \tau\right] = 0. \end{aligned} \tag{37}$$

For system (37) to have a nontrivial solution $\tilde{u}$, $\tilde{v}$, it is necessary and sufficient that its determinant vanishes. Expanding the determinant, we have

$$\begin{aligned} &(s-1)^3 + \left[b_4^* \tau + (a_3 - b_3 + c_3 a_1 b_1) \frac{i\tau}{h} \sum\right](s-1)^2 + \\ &+ \left[\tau (c_3^* a_1 + b_4^* a_3) \frac{i\tau}{h} \sum + (a_3 b_2 - b_1 c_1 a_1 - b_3 c_2 a_1) \frac{\tau^2}{h^2} \sum^2\right](s-1) + \\ &+ \left[\tau^2 c_3^* a_1 b_4^* \frac{i\tau}{h} \sum + \tau c_3^* a_1 b_2 \frac{\tau^2}{h^2} \sum^2 - b_3 c_1 a_1 \frac{i\tau^3}{h^3} \sum^3\right] = 0. \end{aligned}$$

Seeing that $\tau = ch$, $c = \text{const}$, we neglect all quantities which, beside $\tau/h = \text{const}$, also contain a factor $\tau$; then for a small $h$ we have

$$\begin{aligned} &(s-1)^3 + (a_3 - b_3 + c_3 a_1 b_1) \frac{i\tau}{h} \sum (s-1)^2 + \\ &+ (a_3 b_2 - b_1 c_1 a_1 - b_3 c_2 a_1) \frac{\tau^2}{h^2} \sum^2 (s-1) - \\ &\qquad - b_3 c_1 a_1 \frac{i\tau^3}{h^3} \sum^3 = O(\tau). \end{aligned} \tag{38}$$

In dropping the right-hand side of (38), we neglect an expression of the form

$$\tau\left[b_4^*(s-1)^2+(c_3^*a_1+b_4^*a_3)\frac{i\tau}{h}\sum(s-1)+\right.$$
$$\left.+c_3^*a_1b_4^*\tau\frac{\tau}{h}\sum+c_3^*a_1b_2\frac{\tau^2}{h^2}\sum^2\right]. \tag{39}$$

Since

$$\sum=\sum_{q=1}^{p}2a_q^{(p)}\sin khq \text{ and } s-1=\frac{\tau}{h}\sum_{q=1}^{p}2a_q^{(p)}\sin khq$$

is bounded (this follows from our analysis of the model problem), expression (39) can be estimated as $G\tau$, where $G$ is uniformly bounded in $h, \tau$, and $k$.

Thus making the left-hand side of (38) zero and setting

$$z=\frac{s-1}{\frac{i\tau}{h}\sum_{q=1}^{p}2a_q^{(p)}\sin\alpha q},$$

we obtain

$$z^3+(a_3-b_3+c_3a_1b_1)z^2-(a_3b_3-b_1c_1a_1-b_3c_2a_1)z+$$
$$+b_3c_1a_1=0. \tag{40}$$

For the system corresponding to equations (29)-(32) we similarly obtain

$$z^4+(a_3d_3-b_2-d_1b_4+b_1c_2a_1)z^3+$$
$$+[a_3(d_3-b_2-d_1b_4)+b_1c_1a_1+c_2a_1(b_3+d_3b_1)-d_3b_2]z^2-$$
$$-[a_3d_3b_2+c_2a_1(d_2b_4-d_3b_3)-c_1a_1(b_3-d_3b_1)]z-$$
$$-c_1a_1(d_2b_4-d_3b_3)=0. \tag{41}$$

We shall now give some results obtained by numerical solution of these equations. The coefficients of equations (40) and (41) are calculated from the boundary values on a shock wave at points $x = 0.02,\ 0.035,\ 0.05,\ 0.1$.

For cubics and quartics with complex coefficients (when the truncated terms are taken into consideration), with $\tau = 0.007$, $h = 0.015$, we obtain for $x = 0.02$, $y = 0$,

| | |
|---|---|
| $z_1 = 0.01237 + i \cdot 1.04488$<br>$z_2 = 0.0075 - i \cdot 0.8856$<br>$z_3 = -0.9311 - i \cdot 0.0145$ | $z_{1,2} = 0.0131 \pm i \cdot 1.0429$ |

Among the numbers of this table, we should concentrate on the negative imaginary part of the roots which has the greatest modulus. In this sense the investigation of the four equations (29)-(32), as in fact expected, did not yield essentially new information in comparison with the results

obtained from the three equations (29)-(31). Examining the roots of the equation written for $\tau \neq 0$ with an allowance for the previously omitted terms (39), we come to the same conclusion.

| Cubic (40) | Quartic (41) |
|---|---|
| $z_{1,2} = 0.0102 \pm i \cdot 1.0393$ | $z_{1,2} = 0.0192 \pm i \cdot 1.0417$ |
| $z_3 = -0.2538$ | $z_3 = -0.2514$ |
| | $z_4 = 0.309 \cdot 10^{-9}$ |
| $z_{1,2} = 0.0178 \pm i \cdot 1.0392$ | $z_{1,2} = 0.0299 \pm i \cdot 1.0448$ |
| $z_3 = -0.4442$ | $z_3 = -0.4327$ |
| | $z_4 = 0.258 \cdot 10^{-9}$ |
| $z_{1,2} = 0.0254 \pm i \cdot 1.0390$ | $z_{1,2} = 0.0367 \pm i \cdot 1.0468$ |
| $z_3 = -0.6344$ | $z_3 = -0.606$ |
| | $z_4 = 0.202 \cdot 10^{-9}$ |
| $z_{1,2} = 0.0381 \pm i \cdot 1.0382$ | $z_{1,2} = 0.0613 \pm i \cdot 1.0501$ |
| $z_3 = -0.9971$ | $z_3 = -0.910$ |
| | $z_4 = 0.112 \cdot 10^{-9}$ |

We now can estimate $h$ from below.

We have

$$z = a \pm ib = \frac{s-1}{\frac{i\tau}{h}\sum_{q=1}^{p} 2a_q^{(p)} \sin \alpha q}.$$

Since

$$|s(k,h)|^n = \left|1 \mp b\frac{\tau}{h}\sum_{q=1}^{p} 2a_q^{(p)} \sin \alpha q + ia\frac{\tau}{h}\sum_{q=1}^{p} 2a_q^{(p)} \sin \alpha q\right|^n \leqslant$$

$$\leqslant \exp \frac{y}{h}\, b \sum_{q=1}^{p} 2a_q^{(p)} \sin \alpha q,$$

we should pick out from among the roots of equations (40), (41) the root $z$ whose negative imaginary part has the greatest modulus, $b_{\max}$. In our case $b_{\max} \sim 1.05$. We shall determine $Y/h$ so that the round-off error does not grow by more than a factor of $10^6$.

According to § 4 of the present paper,

$$\sum_{q=1}^{p} 2a_q^{(p)} \sin \alpha q = \sin \alpha \sum_{q=1}^{p} \frac{2^{q-1}[(q-1)!]^2}{(2q-1)!}(1-\cos\alpha)^{q-1} \leqslant 1.8374$$

for $p = 5$.

Further

$$\exp\left(\frac{y}{h} 1.8374 \cdot 1.05\right) \leqslant 10^6,$$

so

$$\frac{y}{h} \leqslant 7.2, \quad \text{or} \quad h \geqslant \frac{y}{7.2}.$$

Results of numerical solution of these problems show /3/ that with $M_\infty = 14$, the blunt edge of the body is $Y \approx 0.09 - 0.11$ from the shock wave. For $y = \vartheta, Y \approx 0.8\,Y$, we have $h \approx 0.01$.

## APPENDIX*

1°. First let $c = 0$ ($\tau = 0$). We consider the behavior of the relative truncation error $R_3 = R_3(0)$ as a function of $\alpha = kh$. We have shown in § 4 that, under the conditions specified, an effective grid spacing for scheme (15) with $p = 1$ is $h = \frac{Y}{21}$. Then, if $\bar{k} = \frac{\sin kh}{h}$,

$$y = \vartheta Y, \quad \eta = Y - y = (1 - \vartheta) Y,$$

we have

$$R_3(0) = e^{-k\eta}[1 - e^{(\bar{k}-k)y}] = e^{-\kappa(1-\vartheta)Y}[1 - e^{\frac{y}{h}(\sin kh - kh)}],$$

so

$$R_3(0) = e^{-\alpha(1-\vartheta)21}\,[1 - e^{21\vartheta(\sin\alpha - \alpha)}].$$

Analogously, in calculations with a five-point scheme (15) with $p = 2$ and grid size $h = \frac{Y}{14}$, we have

$$R_5(0) = e^{-\alpha(1-\vartheta)14}[1 - e^{14\vartheta\left(\frac{4}{3}\sin\alpha - \frac{1}{6}\sin 2\alpha - \alpha\right)}].$$

These errors were calculated as function of $\alpha$ for various values of $\vartheta = \frac{y}{Y}$. For $\vartheta = \vartheta_2 = 0.429$ and $\vartheta = \vartheta_3 = 0.667$ the results are plotted in Figure 1. The dashed lines give the maximum values of $\tilde{R}_3(0)$ and $\tilde{R}_5(0)$.

The values of $\max\limits_{\alpha} R_3(0)$ and $\max\limits_{\alpha} R_5(0)$ and also the maximum values of $\tilde{R}_3(0)$ and $\tilde{R}_5(0)$ are given in Table 1 for various $\nu$. This table also gives $\alpha_{max}$ (the points where $R_3(0)$ and $R_5(0)$ are maximized)**.

The numbers in the table justify the assumption imposed on $kh = \alpha$ in the derivation of $\tilde{R}$ for three- and five-point schemes and show that the estimates obtained with the aid of $\tilde{R}$ are fairly accurate.

2°. We now let $c \neq 0$ ($\tau \neq 0$). For the case discussed in § 4 we give in Table 2 the maximum values of $\tilde{R}_3(c)$ calculated for $c = \frac{1}{7}$. Thus, if $h \approx \frac{Y}{21}, \tau \sim \frac{Y}{150}$ and $k \approx \frac{3}{\eta}$, we have

$$\tilde{R}_3(c) = e^{-k\eta}\frac{k^2h}{2}\left(\frac{kh}{3} + c\right)y \approx e^{-3}\frac{3\vartheta}{98(1-\vartheta)^2}\left[\frac{1}{3(1-\vartheta)} + 1\right].$$

* See §4.

** In columns for max $\tilde{R}_i$, and max $R_i (i=3,5)$, each group of four digits gives the mantissa of a decimal number, followed by the signed exponent.

TABLE 1

| $\vartheta = \frac{y}{Y}$ | max $\widetilde{R}_3$ | $\tilde{\alpha}^{(3)}_{max}$ | max $R_3$ | $\alpha^{(3)}_{max}$ | max $\widetilde{R}_5$ | $\tilde{\alpha}^{(5)}_{max}$ | max $R_5$ | $\alpha^{(5)}_{max}$ |
|---|---|---|---|---|---|---|---|---|
| 0.048 | 2801 —04 | 0.150 | 2797 —04 | 0.15 | 1110 —05 | 0.375 | 1092 —05 | 0.37 |
| 0.095 | 6533 —04 | 0.158 | 6518 —04 | 0.16 | 2870 —05 | 395 | 2817 —05 | 0.39 |
| 0.143 | 1152 —03 | 0.167 | 1487 —03 | 0.17 | 5641 —05 | 0.417 | 5524 —05 | 0.41 |
| 0.190 | 1824 —03 | 0.176 | 1817 —03 | 0.18 | 1001 —04 | 0.441 | 9775 —04 | 0.44 |
| 0.238 | 2735 —03 | 0.188 | 2721 —03 | 0.19 | 1694 —04 | 0.469 | 1649 —04 | 0.45 |
| 0.286 | 3983 —03 | 0.200 | 3959 —03 | 0.20 | 2807 —04 | 0.500 | 2721 —04 | 0.49 |
| 0.333 | 5715 —03 | 0.214 | 5669 —03 | 0.21 | 4625 —04 | 0.536 | 4457 —04 | 0.53 |
| 0.381 | 8158 —03 | 0.231 | 8071 —03 | 0.23 | 7656 —04 | 0.577 | 7325 —04 | 0.57 |
| 0.429 | 1167 —02 | 0.250 | 1150 —02 | 0.25 | 1285 —03 | 0.625 | 1218 —03 | 0.61 |
| 0.476 | 1683 —02 | 0.273 | 1650 —02 | 0.27 | 2206 —03 | 0.682 | 2062 —03 | 0.66 |
| 0.524 | 2464 —02 | 0.300 | 2396 —02 | 0.29 | 3909 —03 | 0.750 | 3579 —03 | 0.72 |
| 0.571 | 3688 —02 | 0.333 | 3543 —02 | 0.32 | 7221 —03 | 0.833 | 6412 —03 | 0.78 |
| 0.619 | 5689 —02 | 0.375 | 5364 —02 | 0.36 | 1410 —02 | 0.938 | 1192 —02 | 0.85 |
| 0.667 | 9145 —02 | 0.429 | 8373 —02 | 0.40 | 2960 —02 | 1.071 | 2312 —02 | 0.93 |
| 0.952 | 4481 +01 | 3.000 | 3683 —00 | 0.87 | 7106 +02 | 7.500 | 3401 —00 | .49 |

TABLE 2

$$c=\frac{\tau}{h}=\frac{1}{7}$$

| $\vartheta$ | max $\tilde{R}_3(c)$ | $\vartheta$ | max $\tilde{R}_3(c)$ |
|---|---|---|---|
| 0.048 | 1080 —03 | 0.429 | 3167 —02 |
| 0.095 | 2426 —03 | 0.476 | 4328 —02 |
| 0.143 | 4116 —03 | 0.524 | 5985 —02 |
| 0.190 | 6254 —03 | 0.571 | 8430 —02 |
| 0.238 | 8986 —03 | 0.619 | 1219 —01 |
| 0.286 | 1252 —02 | 0.667 | 1829 —01 |
| 0.333 | 1715 —02 | 0.952 | 5121 —01 |
| 0.381 | 2331 —02 | | |

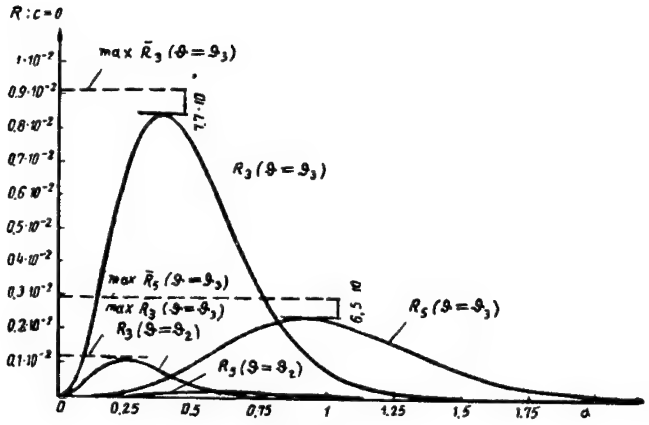


FIGURE 1

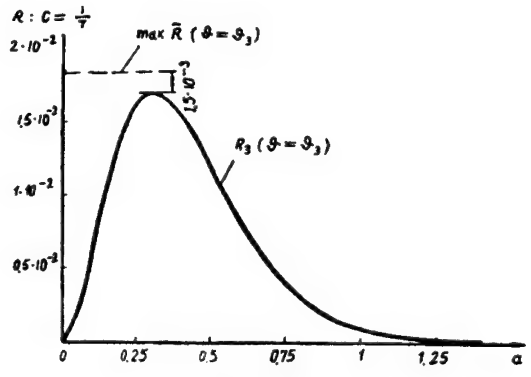


FIGURE 2

Owing to the particular choice of $c=\frac{h}{\eta}$, for $y=0.667Y$ we have for $\tilde{R}$ at the point of maximum $\tilde{R}_3(0)$

$$\tilde{R}_3(c)=2\tilde{R}_3(0).$$

The relative truncation error $R_3(c)$ in calculations by scheme (15) with $p = 1$ and grid size $h = \frac{Y}{21}$ has the form

$$R_3(c) = e^{-k\eta}\left[1 - e^{\frac{y}{\tau}[\ln(1+c\sin\alpha)-k\tau]}\right].$$

Seeing that $\tau = ch$, $y = \vartheta Y$, $\tau \approx \frac{Y}{150}$, we have

$$R_3(c) = e^{-\alpha(1-\vartheta)21}\left[1 - e^{150\vartheta[\ln(1+c\sin\alpha)-c\alpha]}\right].$$

Figure 2 shows a graph of this error for $\vartheta = 0.667$. Note that

$$\max_{\alpha} R_3(c) = 0.01681 \approx 2 \max_{\alpha} R_3(0) = 0.01675,$$

as expected. The abscissa of the $R_3(c)$ and $R_3(0)$ maxima are comparatively close.

BIBLIOGRAPHY


1. VAN DYKE, M. The Problem of Supersonic Flow Past a Blunt Body. [Russian translation. 1958.]
2. PETROVSKII, I.G. Lektsii ob uravneniyakh s chastnymi proizvodnymi (Lectures on Partial Differential Equations). — Fizmatgiz, Moskva. 1961. [Translated into English, Interscience. 1955.]
3. MILTON, D., M. VAN DYKE, and HELEN GORDON. Supersonic Flow Past a Family of Blunt Axisymmetric Bodies. — National Aeronautics and Space Administration, American Research Center, Technical Report R — 1, Moffet Field, California. 1959.
4. LICK, W. Inviscid Flow of a Reacting Mixture of Gases around a Blunt Body. — Journal of Fluid Mechanics, Vol. 7, No. 1. 1960.
5. VALIO LAURIN, R. and A. FERRI. A Theoretical Study of Flow Past Blunt Bodies in Supersonic Flight [Russian translation. 1959.]
6. RICHTMEYER, R.D. Difference Methods for the Solution of Boundary-Value Problems. — (Interscience) Wiley. 1958.
7. RYABEN'KII, V.S. and A.F. FILIPPOV. Ob ustoichivosti raznostnykh uravnenii (The Stability of Difference Equations). — GITTL, Moskva. 1956.
8. CHUDOV, L.A. Raznostnye metody resheniya zadachi Koshi dlya uravneniya Laplasa (Difference Methods for the Solution of the Cauchy Problem for the Laplace Equation). — DAN SSSR, Vol. 143, No. 4. 1962.
9. TIKHONOV, A.N. Ob ustoichivosti obratnykh zadach (The Stability of Inverse Problems). — DAN SSSR, Vol. 39, No. 5. 1943.
10. LAVRENT'EV, M.M. Doctorate dissertation. Novosibirsk. 1961.
11. BEREZIN, I.S. and N.P. ZHIDKOV. Metody vychislenii (Numerical Methods), Vol. I. — Fizmatgiz, Moskva. 1959.
12. COURANT, R. Course of Differential and Integral Calculus, Part I. Blackie and Son Ltd. London.

*U. G. Pirumov, V. A. Rubtsov, and V. N. Suvorova*

# *CALCULATION OF AXISYMMETRIC EXHAUST NOZZLES WITH AN ALLOWANCE FOR EQUILIBRIUM PHYSICOCHEMICAL REACTIONS*

Several works on the calculation of equilibrium gas flows by the method of characteristics have been recently published /1—3/. In /1, 2/ the method is adapted to the flow of real gases, and results are given on nozzle contours with uniform and parallel flow at the nozzle exit plane. In /3/ a calculation is given of a flow of real gas with a given axial distribution of velocity. However, these works do not consider the problem of the flow of different gases in a nozzle of given contour and hardly touch on the effect of the real gas properties on the coefficient of momentum losses in the exhaust nozzle. To study these problems, the Computational Center of Moscow State University undertook calculations of equilibrium gas flows in a nozzle of given contour and calculation of nozzle contours ensuring uniform and parallel exit flow. Axisymmetric nozzles with an angular point (Figure 1) were considered and the effects of viscosity and heat conduction were neglected.

Before proceeding with the analysis of the computational results, we shall briefly describe the method of calculation of equilibrium gas flows by the method of characteristics. Since the flow is assumed in equilibrium and no shock waves are allowed in the nozzle, then for every particular composition of gas with given stagnation parameters we can find an isentropic line, $S = \text{const}$ and a function giving the variation of pressure with density along this line, $p = p(\rho)$. These functions can be obtained by thermodynamic calculations of the equilibrium gas state, making due allowance for dissociation and recombination processes. Many tables of thermodynamic functions are now available (e.g., for air, see /4/). For some compositions even $\tau$—$s$ diagrams have been published /5/, which enable the function $p = p(\rho)$ to be calculated without difficulty along the line $s = \text{const}$ for given stagnation parameters. Therefore, for most gas compositions of practical interest, the variation of $p$ with $\rho$ along the isentropic lines can be tabulated without difficulty.


FIGURE 1. Axisymmetric nozzle with an angular point

Given a tabulation of $\bar{p}$ vs $\bar{\rho}$ ($\bar{p} = \frac{p}{p_0}$, $\bar{\rho} = \frac{\rho}{\rho_0}$, where $p_0$ and $\rho_0$ are the stagnation parameters), we piecewise approximate this function by the expression $\bar{p} = \bar{\rho}^{k_{av}} + a_0 + a_1\bar{\rho} + a_2\bar{\rho}^2$, where $k_{av} = \frac{\ln \bar{p}_a}{\ln \bar{\rho}_a}$, $\bar{p}_a$ is the tabulated density

close to the presumed minimum density in the flow, and $\bar{p}_a$ is the corresponding pressure. The coefficients $a_0$, $a_1$ and $a_2$, differing in different regions, were chosen so that the approximating curve passes through the tabulated points and that the derivative $\frac{d\bar{p}}{d\bar{\rho}}$ is continuous at all points.

The dependence of $\bar{p}$ on $\bar{\rho}$ was further used in the method of characteristics which, in the case of equilibrium gas flow, does not differ in principle from the method of characteristics for isentropic ideal gas flow.

As the dependent variables we used $\rho$ and $\zeta = \mathrm{tg}\theta$.

The equations of the characteristics of the system of differential equations describing isentropic gas flow of a gas in a state of thermodynamic equilibrium are written in the form

$$\frac{dr}{dx} = \frac{\beta\zeta \pm 1}{\beta \mp \zeta}.$$

Consistence equations along the characteristics have the form

$$d\zeta \pm \frac{\beta d\bar{\rho}}{\bar{\rho}(\beta^2 + 1)} \pm \frac{\zeta(1 + \zeta^2)}{r(\zeta\beta \pm 1)} dr = 0.$$

Here $x$, $r$ are Cartesian coordinates in the meridional flow plane; $\theta$ is the angle of inclination of the velocity vector to the $x$-axis;

$$\beta = \sqrt{M^2 - 1}; \quad M = \sqrt{-\frac{2}{f(\bar{\rho})} \int_1^{\bar{\rho}} \frac{f(\bar{\rho})}{\bar{\rho}} d\bar{\rho}}; \quad f(\bar{\rho}) = \frac{d\bar{p}}{d\bar{\rho}}.$$

The variables $\beta$ and $\zeta$ were first used by Elers in /10/.

Let us first consider the flow of real gas in a nozzle of given contour. First the parameters $p^*$ and $\rho^*$ in the critical nozzle section are calculated from $\bar{p} = \bar{p}(\bar{\rho})$ with $M = 1$. Then, taking the velocity in the critical section to be parallel to the $x$-axis, the fan of expansion waves arising at the angular point $A$ (Figure 1) is calculated. When calculating the expansion wave fan, the sonic characteristic is determined by expanding the solution in a series in terms of the characteristic coordinate /6/. It is assumed that the ratio of specific heats of the flow near the sonic line is constant, being equal to

$$k_{av} = \left(\frac{d \ln \bar{p}}{d \ln \bar{\rho}}\right)_{\bar{p} = \bar{p}^*}.$$

Having calculated the expansion wave fan, we calculate the flow between the characteristic $AO$ and the nozzle contour. The equations $x$, $r$, $\theta$, $\alpha$ and $\bar{p}$ ($\alpha = \arcsin\frac{1}{M}$), are calculated on the characteristics of the expansion wave fan. The lateral surface $S$, the flow rate $\psi$ and $P = \int \bar{p} r dr$ (the $x$ projection of the pressure forces acting on the streamline) are determined on the streamlines and at the nozzle contour. In the present work we considered a gas whose function $\bar{p} = \bar{p}(\bar{\rho})$ is shown in Figure 2. The $k_{av}$ for this composition is 1.207. In the following we shall refer to this gas as composition I. The formulas for $\bar{p} = \bar{p}(\bar{\rho})$ used in the calculations approximate the tabulated values to within 1% in pressure and 0.3% in velocity, which is well within the margin of error in calculation of thermodynamic data. Flow in two exhaust nozzles was calculated. The first nozzle (No. 1 contour)

was calculated by approximate formulas for ideal gas with $k=1.14$. The second nozzle (No. 2 contour) was calculated exactly (by the method of characteristics) and has uniform and parallel outlet flow for an ideal gas with $k=1.25$. The flow of real gas of composition I was calculated for both nozzles. We also calculated the flow of an ideal gas with $k=1.114$, 1.14, 1.185, and 1.33 in the first nozzle, and with $k=1.14$, 1.25, 1.33, and 1.4 in the second nozzle.

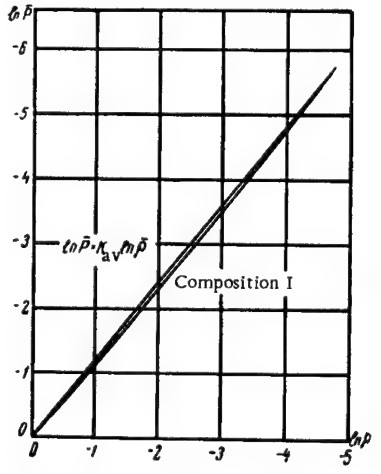


FIGURE 2. $\ln \bar{p}$ vs $\bar{\rho}$ for composition I

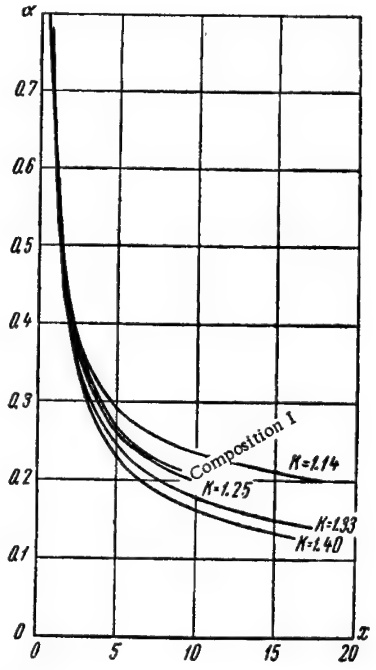


FIGURE 3. Variation of the angle $\alpha$ along the nozzle axis for various gases

The solution of the mixed problem (flow between the characteristic and the nozzle contour) in the second nozzle, was obtained by the method of characteristics applied to the Goursat problem and calculated to ensure uniform and axisymmetric exit flow of an ideal gas with ratio of specific heats $k=1.25$. To evaluate its accuracy we calculated the flow of ideal gas with $k=1.25$. The results of this calculation gave virtually identical parameters in both cases. For example, the difference in the integral $P$ in the two calculations was 0.05%. When calculating the flow of ideal gas with $k=1.14$ in the first nozzle, the characteristics intersected near the axis (see Figure 1). We nevertheless succeeded in calculating the parameters at the contour, because this intersection occurred below the characteristic $DC$. No such intersection was observed in the second nozzle. The intersection of characteristics can be attributed to the solution of the first nozzle by approximate calculations, while the second nozzle was calculated exactly.

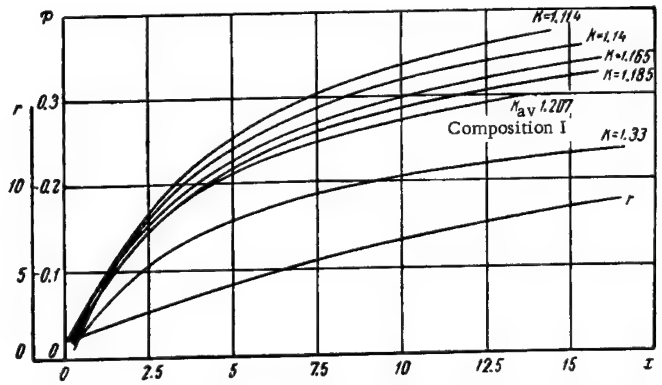


FIGURE 4. Pressure integral $P$ on No. 1 contour for various gases. Lower curve —No. 1 contour

We now proceed to analyze the results. It is interesting to compare the variation of $\alpha$ along the nozzle axis for different gases. Figure 3 shows that the variation of angle $\alpha$ for composition I is closest to the variation for an ideal gas with $k = 1.25$ (for composition I, $k_{av} = 1.207$). The distribution of the integral over No. 1 contour plotted in Figure 4 shows that, as expected, the nozzle momentum increases with decreasing ratio of specific heats and that the pressure integral for composition I is closest to the pressure integral of ideal gas with $k = 1.185$, although the difference in momentum of the two gases is substantial, and may reach 3—4%.

The question of the loss of momentum as a function of the specific heat ratio is of considerable interest. We first consider the effect of the specific heat ratio on momentum losses in a nozzle of given contour. We shall only consider momentum losses due to nonuniformity and imperfect parallel alignment of the outlet flow. The coefficient of momentum losses $\xi$ is then calculated from the formula

$$\xi = 1 - \frac{\left(\overline{p}^* + \frac{\overline{p}^*}{A}\right) + 2P}{\overline{F}\left(\overline{p} + \frac{1}{A}\overline{\rho}\overline{w}^2\right)},$$

where $\overline{F}$ is the area of the given nozzle section divided by the area of the critical section, $\overline{w}$ the velocity divided by the velocity in the critical section, and $A = \frac{p_0}{\rho_0 w^{*2}}$, $w^*$ being the velocity in the critical section. For gases with constant specific heat ratios, this formula takes the form

$$\xi_f = \frac{\varepsilon(1)[z(\lambda_r) - 2] - 2P}{\varepsilon(1) z(\lambda_r)},$$

where

$$\varepsilon(1) = \left(\frac{2}{k+1}\right)^{\frac{1}{k-1}}, \quad z(\lambda_r) = \lambda_r + \frac{1}{\lambda_r},$$

and $\lambda_r$ is the velocity coefficient calculated from the ratio of areas. When calculating the losses, we compared the momentum at a given nozzle section with the momentum at the exit plane of an ideal nozzle with uniform and

parallel flow whose critical-section area and flow rate are equal to those of the given nozzle and whose exit plane area is equal to the area of the section being considered. An analogous coefficient was introduced in /7/.

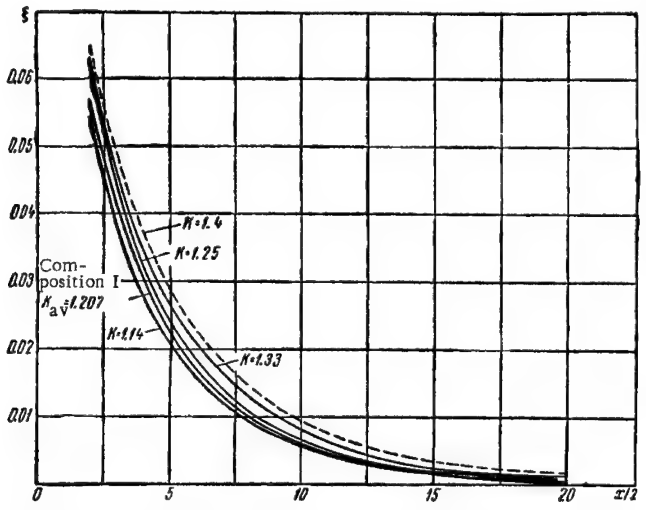


FIGURE 5. Coefficient of momentum loss ξ on No. 2 contour for various gases

Figure 5 shows the variation of ξ along the contour for the flow of various gases in the second nozzle. Examination of this figure reveals that ξ decreases noticeably with the decrease of the specific heat ratio. The difference in this coefficient for gases with $k = 1.33$ and $k = 1.14$ is as high as 1% for values of ξ of 3—5%. For smaller ξ the difference is from 0.2 to 0.6%. On the other hand, the difference in losses between a gas of composition I and an ideal gas with $k = 1.25$, for ξ-values not exceeding 3%, is a mere 0.1%. The difference in ξ in the range of high losses is somewhat greater, about 0.4%, and is due to the fact that in this range $k = \frac{d \ln \bar{p}}{d \ln \bar{\rho}}$ differs from $k_{aw}$, being equal to 1.14-1.17. Correspondingly (see Figure 5) the coefficient ξ for composition I in the range of high losses is closer to the curve with $k = 1.14$ than to the curve with $k = 1.25$. On the whole, ξ does not decrease with decreasing $k$. However, in the No. 2 contour with $k = 1.25$, the outlet flow becomes uniform and parallel and therefore on an untruncated contour, ξ drops to zero at the last point for $k = 1.25$. A gas with other $k$ will not give a uniform and parallel flow at the nozzle outlet, and therefore the curve for $k = 1.14$, which at first is below the curve for $k = 1.25$, intersects it at a certain point, so that the losses for $k = 1.14$ become greater than for $k = 1.25$ from this point on (see Figure 5).

It is also interesting to compare the coefficient ξ for two contours reaching the same point, which have been calculated for different $k$, but which carry the same gas. These contours are plotted in Figure 6 for valves of $k = 1.14$ and $k = 1.25$. The coordinates of these contours differ but slightly. This fact was also emphasized in /7/. Calculations made for several such contours and for different $k$ show that ξ of these contours differ at most by 0.3%. Note that ξ can be calculated at least to within 0.03%.

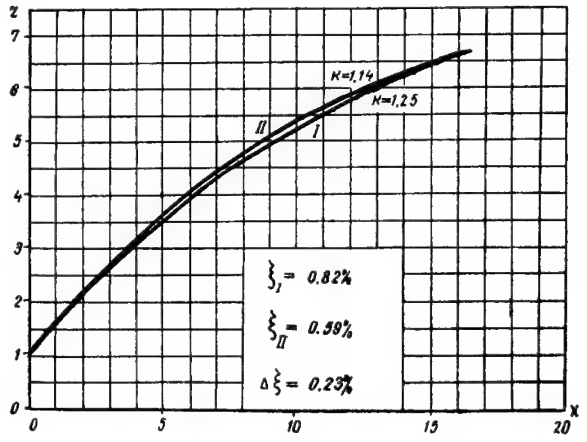


FIGURE 6. Comparison of coordinates and momentum losses for two contours reaching the same point

Besides calculating the flow of a real gas in nozzles of given contour, we also calculated nozzle contours ensuring uniform and parallel outlet flow for composition I. Five nozzles were calculated with outlet $\alpha$ equal to 0.270, 0.256, 0.236, 0.231, and 0.212. The contours of these nozzles and the contours of nozzles with uniform and parallel outlet flow of ideal gas with $k = 1.25$ and outlet $\alpha$ equal to 0.297, 0.268, 0.229, and 0.208 are plotted in Figure 7. The same figure shows the contour end lines for composition I and for ideal gas with $k = 1.25$. An examination of these lines shows that the difference between the coordinates of contour end lines for composition I and for an ideal gas with $k = 1.25$ does not exceed 5—10%. This difference will be even smaller when we compare composition I with an ideal gas having $k = 1.207$.

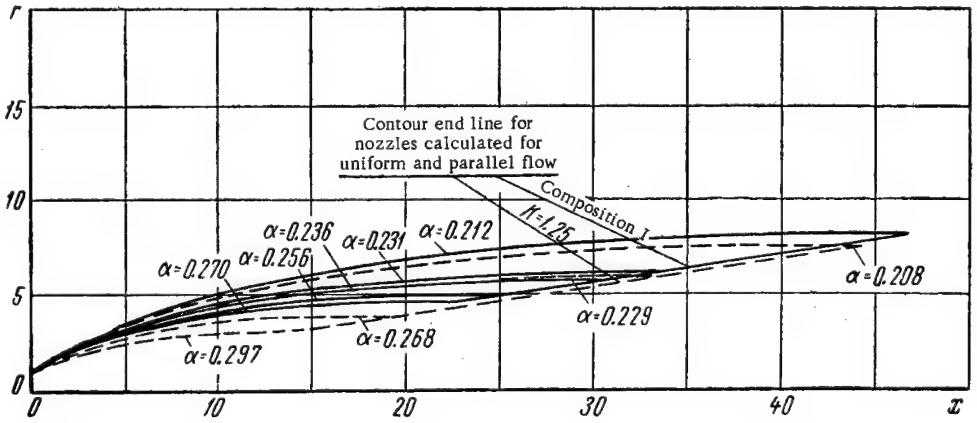


FIGURE 7. Nozzle contours calculated for uniform and parallel flow of ideal gas ($\kappa = 1.25$) and real gas (composition I)

——— real gas (composition I); — — — ideal gas ($\kappa = 1.25$).

We have considered the effect of real gas properties on the loss of momentum in the nozzle for a pre-established nozzle size. Given calculations of nozzles for real gas with uniform and parallel flow, we can evaluate the effect of real gas properties on the choice of nozzle size in various problems. Consider the choice of a nozzle ensuring maximum momentum for given area or given length. In /8, 9/ variational methods have been developed for designing nozzles which ensure maximum exit velocity for given length and given outlet area. These methods can easily be generalized to the case of equilibrium flow of a real gas. In the present work, however, the basic comparison is made for a family of nozzles constructed using uniform characteristics. It can nevertheless be expected that the estimates of losses due to incorrect choice of nozzle size by failing to allow for the real gas properties obtained in the above case will also apply to nozzles constructed with the aid of variational characteristics. If we neglect friction, then among nozzles of given exit plane area maximum exit velocity is found in the nozzle with uniform and parallel flow. Insofar as the contour end lines of nozzles with uniform flow for composition I and for ideal gas with $k = 1.25$ are similar, and the losses of contours reaching one point are also similar, it is sufficiently accurate to solve problems of given outlet area by solving for a family of nozzles with uniform flow calculated for some constant $k$.

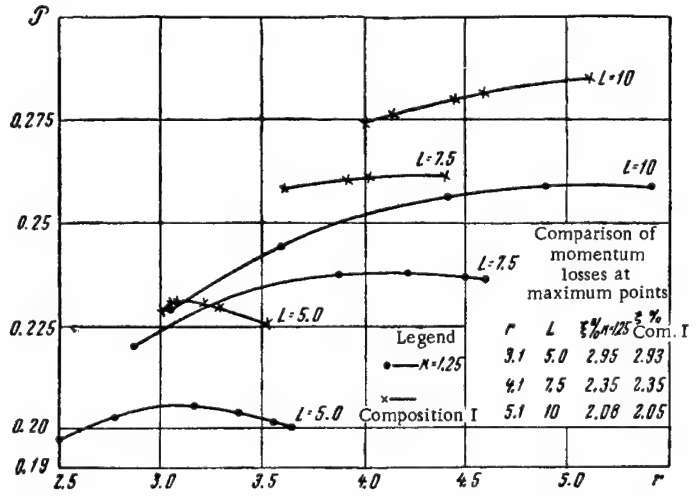


FIGURE 8. Comparison of coefficients of momentum loss $\xi$ at maximum points

Consider the problem of determining the size of the nozzle with maximum momentum for a given length. The choice of this nozzle from the family of nozzles with uniform characteristics is made from Figure 8. It follows from this figure that the maximum momentum $P_{max}$ of a real gas and that of a gas with $k = 1.25$ may differ to a considerable extent. The difference sometimes reaches 10%. However, there is very little difference in the position of the maxima of the $L = \text{const}$ curves and in the values of the momentum-loss coefficients $\xi$. In this case the choice of nozzle size and

the evaluation of the losses can be made with fair accuracy by proceeding from the family of nozzles with constant $k = k_{av}$. Analogous results can be expected to apply to the choice of a nozzle ensuring maximum exit velocity for given surface area.

In conclusion we observe that our results on the effect of the real gas properties on the coefficient of momentum loss $\xi$ were obtained for one particular gas composition. Qualitatively, these results apparently will not change for other gas compositions, but this proposition requires further substantiation.

BIBLIOGRAPHY


1. KATSKOVA, O.N. Ob osesimmetrichnom svobodnom rasshirenii real'nogo gaza (Axisymmetric Free Expansion of a Real Gas).— Zhurnal Vychislitel'noi Matematiki i Matematicheskoi Fiziki, Vol. 1, No. 2. 1961.
2. KATSKOVA, O.N. and A.N. KRAIKO. Raschet osesimmetrichnykh izentropicheskikh techenii real'nogo gaza (Calculation of Axisymmetric Isentropic Real-Gas Flows). — Zhurnal Vychislitel'noi Matematiki i Matematicheskoi Fiziki, Vol. 2, No. 1. 1962.
3. GUENTERT, E.C. and H.E. NEUMANN. Design of Axisymmetric Exhaust Nozzles by the Method of Characteristics Incorporating a Variable Isentropic Exponent. — NASA, TR, R — 53. 1938.
4. PREDVODITELEV, A.S., E.V. STUPOCHENKO, A.S. PLESHANOV, E.V. SAMUILOV, and I.B. ROZHDESTVENSKII. Tablitsy termodinamicheskikh funktsii vozdukha (Tables of Thermodynamic Functions of Air). —Izdatel'stvo AN SSSR, Moskva. 1959.
5. SINYAREV, G.B. and M.V. DOBROVOL'SKII. Zhidkostnye raketnye dvigateli (Liquid-Fuel Rocket Engines). —Oborongiz, Moskva. 1955.
6. KATSKOVA, O.N. and Yu.D. SHMYGLEVSKII. Osesimmetrichnoe sverkhzvukovoe techenie svobodno rasshiryayushchegosya gaza s ploskoi poverkhnost'yu perekhoda (Axisymmetric Supersonic Flow of Freely Expanding Gas with Plane Interface). — Vychislitel'naya Matematika, No.2. 1957.
7. RAO, G.V.R. Recent Developments in Pocket Nozzle Configurations. —ARS Journal, No. 11. 1961.
8. SHMYGLEVSKII, Yu. D. Nekotorye variatsionnye zadachi gazovoi dinamiki osesimmetrichnykh sverkhzvukovykh techenii (Some Variational Problems in Gas Dynamics of Axisymmetric Supersonic Flows). — PMM, Vol. 21, No. 2. 1957.
9. HUDERLEY, G. and B. HUNTCH. Best Configurations of Supersonic Axisymmetric Jet Nozzles. [Russian translation. 1956.]
10. ELERS, H.E. Method of Characteristics for Isoenergetic Supersonic Flows Adapted to Digital Computers. [Russian translation. 1960.]

*G. S. Roslyakov and N. V. Drozdova*

# *NUMERICAL COMPUTATION OF FLOW PAST A SCALARIFORM CONE*

1. In this article a numerical computation is made of the flow past a scalariform circular cone (Figure 1) immersed in a supersonic stream of ideal gas. It is assumed that the flow is uniform, the velocity vector of the incident flow is parallel to the axis of the body, while the flow velocity and the cone angles are such that the flow is supersonic at all points. It is also assumed that the angle of the second cone is larger than that of the first cone, so that a curvilinear compression shock is formed issuing from the jointing line on the surface of the body, as well as the conical shock in the frontal needle.

In the region enclosed by the shocks the flow is self-adjusted; conical flows are tabulated in /1/. Beyond the second curvilinear shock the flow becomes turbulent, and its computation is very difficult. The turbulent region, with the exception of the jointing line, is computed by the method of characteristics. To determine the flow parameters near the jointing line, the results of an approximate theory were applied.

2. Because of the axial symmetry of the flow, we shall use a cylindrical system of coordinates, placing the origin at the needle point of the body (Figure 1).

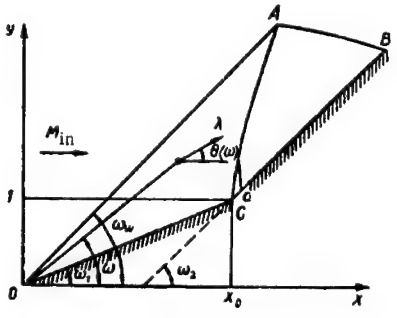


FIGURE 1

In the following we confine the discussion to one meridional plane only. The conical half-angles $\omega_1$, $\omega_2$ and the Mach number of the incident flow $M_{in}$ are assumed known. The $y$ coordinate of the point $C$ is taken equal to 1.

We shall compute the flow in the region $OABC$ limited by the conical (linear) shock $OA$, the generatrix of the body, and the characteristic $AB$ of the 2nd family passing through the intersection point of the compression

shocks. This should be adequate for most practical applications. In the following we use the notation: $M$, the Mach number; $\alpha$, the Mach angle; $p$, $\rho$, the pressure and density divided by the pressure and the density of the incident flow; $\theta$, the angle of inclination of the velocity vector to the $x$-axis; $s$, entropy; $\psi$, flow rate and $\varkappa$, specific heat ratio. In addition to the cylindrical coordinates $x$, $y$, we shall also use polar coordinates $r$, $\omega$ centered at $O$. By $\lambda_r$, $\lambda_\omega$ we denote the radial and the normal (to the radius) components of the dimensionless velocity $\lambda$; $\lambda$ is related to $M$ by the equality*

$$M^2 = \frac{\frac{2}{\varkappa+1}\lambda^2}{1-\frac{\varkappa-1}{\varkappa+1}\lambda^2}.$$

The parameters beyond the first shock will have the subscript $w$, and beyond the second shock, 2.

3. The parameters of conical flow remain constant along any ray passed from the apex of the cone, i.e., they only depend on the polar angle $\omega$. The velocity components $\lambda_r$, $\lambda_\omega$ satisfy the following system of ordinary differential equations:

$$\frac{d\lambda_r}{d\omega} = \lambda_\omega,$$

$$\frac{d\lambda_\omega}{d\omega} = -\lambda_r - \frac{\lambda_r + \lambda_\omega \operatorname{ctg}\omega}{1-\frac{\frac{2}{\varkappa+1}\lambda_\omega^2}{1-\frac{\varkappa-1}{\varkappa+1}\lambda^2}}. \tag{1}$$

System (1) will be integrated for the following boundary conditions:

$$\omega = \omega_1, \quad \lambda_\omega = 0; \tag{2}$$

at the second (unknown) end point $\omega = \omega_w$, the solution must satisfy the equations

$$\lambda_{in}\cos\omega_w = \lambda_r, \tag{3}$$

$$\lambda_r\lambda_\omega \operatorname{tg}\omega_w - \frac{\varkappa-1}{\varkappa+1}\lambda_r^2 + 1 = 0. \tag{4}$$

Given $\lambda_r$ and $\lambda_\omega$ from the solution of system (1)—(4), we can determine

$$\lambda(\omega) \text{ and } \theta(\omega) = \omega + \operatorname{arctg}\frac{\lambda_\omega}{\lambda_r}.$$

Pressure and density are found from

$$p(\omega) = p_w \frac{\pi[\lambda(\omega)]}{\pi(\lambda_w)}, \quad \rho(\omega) = \rho_w \frac{\varepsilon[\lambda(\omega)]}{\varepsilon(\lambda_w)}, \tag{5}$$

where

$$\pi(\lambda) = \left(1-\frac{\varkappa-1}{\varkappa+1}\lambda^2\right)^{\frac{\varkappa}{\varkappa-1}}, \quad \varepsilon(\lambda) = \left(1-\frac{\varkappa-1}{\varkappa+1}\lambda^2\right)^{\frac{1}{\varkappa-1}},$$

and $p_w$ and $\rho_w$ are determined from the conditions on the conical shock:

* All unreferenced formulas in the text can be found, e. g., in /2/ or are easily derived.

$$p_w = \frac{2\varkappa}{\varkappa+1} M_{in}^2 \sin^2 \omega_w - \frac{\varkappa-1}{\varkappa+1}, \qquad (6)$$

$$\rho_w = \frac{\frac{\varkappa+1}{\varkappa-1} M_{in}^2 \sin^2 \omega_w}{\frac{2}{\varkappa-1} + M_{in}^2 \sin^2 \omega_w}.$$

4. As we have already observed, the flow beyond the curvilinear shock is determined by the method of characteristics.

The gas-dynamic system of equations written in characteristics has the form

$$\frac{dy}{dx} = \operatorname{tg}(\theta \pm \alpha),$$

$$\Phi_\pm \equiv d\theta \pm \frac{1+\cos 2\alpha}{\varkappa - \cos 2\alpha} d\alpha \pm \frac{\sin\theta \sin\alpha}{y \cos(\theta \pm \alpha)} dx \mp \frac{\sin 2\alpha}{2\varkappa(\varkappa-1)} ds = 0 \qquad (7)$$

(characteristics of 1st and 2nd families),

$$\frac{dy}{dx} = \operatorname{tg}\theta, \quad ds = 0$$

(characteristics of 3rd family — streamlines). We shall not dwell on the practical application of the method of characteristics (the interested reader will find ample material, e.g., in /3/), and will only give formulas for computation of the shock.

Using the ordinary conditions on the oblique shock, it is easy to derive the following formulas for the various parameters beyond the curvilinear compression shock:

$$\alpha_2 = \frac{1}{2} \arccos\left(\varkappa - \frac{\varkappa+1}{\lambda_2^2}\right),$$

$$\theta_2 = \theta(\omega) + \delta, \qquad (8)$$

$$s_2 = \ln \frac{p_2}{\rho_2^{\varkappa}},$$

where

$$p_2 = p(\omega)\left[\frac{2\varkappa}{\varkappa+1} M^2(\omega)\sin^2\varepsilon - \frac{\varkappa-1}{\varkappa+1}\right],$$

$$\rho_2 = \rho(\omega) \frac{\frac{\varkappa+1}{\varkappa-1} M^2(\omega)\sin^2\varepsilon}{\frac{2}{\varkappa-1} + M^2(\omega)\sin^2\varepsilon},$$

$$\lambda_2^2 = \lambda^2(\omega)\cdot\left[1 + \left(\frac{\rho^2(\omega)}{\rho_2^2} - 1\right)\sin^2\varepsilon\right],$$

$$\delta = \operatorname{arctg}\left[\operatorname{ctg}\varepsilon \frac{M^2(\omega)\sin^2\varepsilon - 1}{1 + M^2(\omega)\left[\frac{\varkappa+1}{2} - \sin^2\varepsilon\right]}\right],$$

$$\varepsilon = \sigma - \theta(\omega).$$

Here $\delta$ is the deflection angle of the flow, and $\sigma$ the inclination angle of the shock to the $x$-axis.

These relations should be supplemented with a condition which is satisfied along the 1st family characteristics.

A special computational procedure is applied near the jointing point. At the jointing point the deflection angle $\delta$ is known: $\delta = \omega_2 - \omega_1$; $\varepsilon$ is determined from the cubic

$$\operatorname{tg}^3 \varepsilon + A \operatorname{tg}^2 \varepsilon + B \operatorname{tg} \varepsilon + C = 0,$$

where

$$C = \frac{\frac{2}{\varkappa - 1}}{\operatorname{tg} \delta \left[ M^2(\omega_1) + \frac{2}{\varkappa - 1} \right]},$$

$$B = \frac{\frac{\varkappa + 1}{\varkappa - 1} M^2(\omega_1) + \frac{2}{\varkappa - 1}}{M^2(\omega_1) + \frac{2}{\varkappa - 1}},$$

$$A = C[1 - M^2(\omega_1)],$$

after which all the unknown quantities are determined from finite relations (8). A certain difficulty is encountered in the computation of the first point on the shock. As the characteristic of the 1st family issuing from this point meets the wall, the solution cannot be found by the method of characteristics.

Let the characteristic meet the generatrix of the second cone at point $a$ with $y = 1 + \Delta y$ (Figure 1). To determine the required parameters at point $a$ we proceed as follows.

We first find the pressure at point $a$, using the expansion

$$p_a \approx p_2 + \left( \frac{dp}{dy} \right)_2 \Delta y,$$

where

$$\left( \frac{dp}{dy} \right)_2 = -2\varkappa p_2 M_2^2 \sin \omega_2 \left[ K_1 - \frac{\sin \omega_1}{\sin \omega_2} K_2 \right],$$

$$K_1 = \frac{1}{A_1} \operatorname{tg} (\varepsilon - \delta),$$

$$K_2 = \frac{1}{A_1} [\sin \delta + \operatorname{tg} (\varepsilon - \delta) \cos \delta],$$

$$A_1 = 2 \sqrt{1 + M_2^2} \left[ \frac{b}{a} + \operatorname{tg} (\varepsilon - \delta) \sqrt{1 + M_2^2} \right],$$

$$a = 2 \operatorname{tg} (\varepsilon - \delta) \sqrt{1 + M_2^2} \left[ 1 + \frac{\varkappa - 1}{2} B_1 \right],$$

$$b = 1 + \operatorname{tg} \varepsilon \operatorname{tg} (\varepsilon - \delta)(1 + M_2^2) - \varkappa B_1,$$

$$B_1 = M_2^2 \sin^2 (\varepsilon - \delta) [\operatorname{tg} \varepsilon \operatorname{tg} (\varepsilon - \delta) - 1]$$

(here $p_2$, $M_2$, $\varepsilon$, and $\delta$ are taken at the jointing point, beyond the shock). Formulas in this form were obtained by Mel'nikov by a method analogous to

that employed in /4, Chapter IV/. We can now easily determine all the other quantities at point $a$:

$$\theta_a = \omega_2,\ \alpha_a = \arcsin\frac{1}{M_a},\ s_a = s_2,$$

where

$$\rho_a = (p_a e^{-s_2})^{\frac{1}{\varkappa}},$$

$$M_a^2 = \frac{2}{\varkappa - 1}\left[\frac{\rho_a}{p_a}\left(1 + \frac{\varkappa - 1}{2}M_{\text{in}}^2\right) - 1\right].$$

Given the flow parameters at point $a$, we can compute the shock point from (8) (applying the condition along the characteristics of the 1st family).

5. We now offer some remarks concerning the computational scheme.

1°. The system of equations of conical flow (1) was integrated by the Runge-Kutta method.

To solve the boundary-value problem (1)—(4) at the left end point, with $\omega = \omega_1$, the value of $\lambda_r$ was varied so that for some $\omega = \omega_w$ equations (3) and (4) were satisfied simultaneously (with pre-established accuracy). $\omega_w$ was assumed to be the conical-shock angle. In practice, since $\lambda_r(\omega_1)$ is approximately known (from the tables in /1/), the conical-flow parameters could be determined with the required accuracy by solving 2-3 initial-value problems. As the result of these calculations, $\lambda^2(\omega)$ and $\theta(\omega)$ were tabulated as functions of the angle $\omega$.

2°. Computations beyond the curvilinear shock are made along the characteristics of the 2nd family from the shock to the body. The following scheme was chosen for computing a point on the shock.

System (8) should be solved simultaneously with the equation $\Phi_+ = \theta$, (see (7)). Let the solution be known at point $P$ on the shock and at points of the characteristic of the 2nd family passing through point $P$ (Figure 2). We find the intersection point $Q$ of the line passing through point $P$ at an angle of $\sigma_P + \Delta\sigma$, with the line $x = x_P + \Delta x$. We now determine the polar angle $\omega_Q$ of this point and, by quadratic interpolation from the table of conic flow parameters, find $\lambda^2(\omega_Q)$ and $\theta(\omega_Q)$. From (5) we compute $p(\omega_Q)$ and $\rho(\omega_Q)$. Now from (8) we find the parameters beyond the shock at points $Q$ (for $\sigma = \sigma_P + \Delta\sigma$). We compute the value of $\Phi_+$ by replacing the differentials with corresponding difference expressions at points $Q$ and $q$ and approximating the coefficients with half the sum of their values at points $Q$ and $q$. Drawing straight lines through $P$ at angles $\sigma_P + \Delta\sigma - \bar{\Delta}\sigma$ and $\sigma = \sigma_P + \Delta\sigma - 2\bar{\Delta}\sigma$ we find the required quantities beyond the shock at points $L$ and $M$ (for $\sigma = \sigma_P + \Delta\sigma - \bar{\Delta}\sigma$ and $\sigma = \sigma_P + \Delta\sigma - 2\bar{\Delta}\sigma$, respectively) and compute $\Phi_+$ at these points. Now the true position of the point $N$ of the shock (with $\Phi_+ = 0$) and the value of the required quantities at this point (beyond the shock) are found by quadratic interpolation of all the quantities as functions of $\Phi_+$. $\Delta\sigma$ and $\bar{\Delta}\sigma$ are chosen so that $\Phi_+$ has different signs at points $Q$ and $M$, i.e., so that the shock passes within the angle $QPM$.

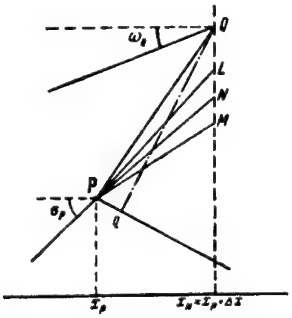

FIGURE 2

Having determined the shock point, we compute the flow rate at this point:

$$\psi_N = e^{-\frac{s_\omega}{\varkappa-1}\varepsilon[\lambda(\omega_N)]\lambda(\omega_N)\sin(\omega_N-\theta(\omega_N))} \frac{}{\varepsilon(\lambda_{in})\lambda_{in}\sin\omega_N} y_N^2 \qquad (9)$$

and compute, up to the body, the characteristic of the 2nd family issuing from point $N$. At every point of the characteristic we compute $x$, $y$, $\theta$, $\alpha$, $s$, $\psi$. To determine $x$, $y$, $\theta$, $\alpha$, $s$ we apply the characteristic equations (7). The flow rate $\psi$ between any two points $(x_1, y_1)$, $(x_2, y_2)$ on the characteristic is given by the integral

$$\sqrt{2(\varkappa+1)}\frac{1}{\lambda_{in}\varepsilon(\lambda_{in})}\int_{x_1}^{x_2} e^{-\frac{s}{\varkappa-1}}\left(\frac{1-\cos 2\alpha}{\varkappa-\cos 2\alpha}\right)^{\frac{\varkappa+1}{2(\varkappa-1)}}\frac{y\,dx}{\cos(\theta-\alpha)}, \qquad (10)$$

which is computed by the trapezoid formula.

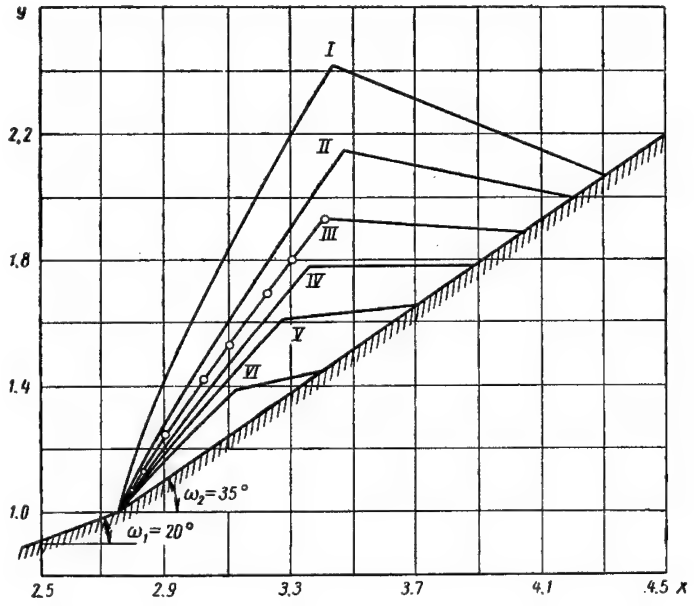


FIGURE 3. Compression shock and boundary characteristic for various $M_{in}$ (see Table 2); $\omega_1=20°$; $\omega_2=35°$. Circles mark experimental data

In this computational scheme the unknown quantities $x$, $y$, $\theta$, $\alpha$, $s$ are independent of the flow rate; the flow rate is computed only for control purposes. For example, the flow rate $\psi_N$ computed from (9) should coincide with integral (10), where one of the points is $N$ and the other is a point on the body. In practice, since we compute from the shock to the body, an integral accuracy check will be that the flow rate does not vanish on the generatrix of the body.

6. Computations were made on the STRELA computer at the Computational Center of Moscow State University. The results are shown in Figures 3—6 and in Tables 1, 2. The specific heat ratio $\varkappa$ for all the alternatives was taken as 1.4. Figures 3 and 4 give graphs of the curvilinear shock and the boundary characteristic for different values of $M_{in}$ of the incident flow for

bodies with $\omega_1 = 20°$, $\omega_2 = 35°$ and $\omega_1 = 15°$, $\omega_2 = 35°$. Experimental points obtained by V. I. Goryachev are plotted in Figure 3 for the case $M_{in} = 3$ (alternative III).

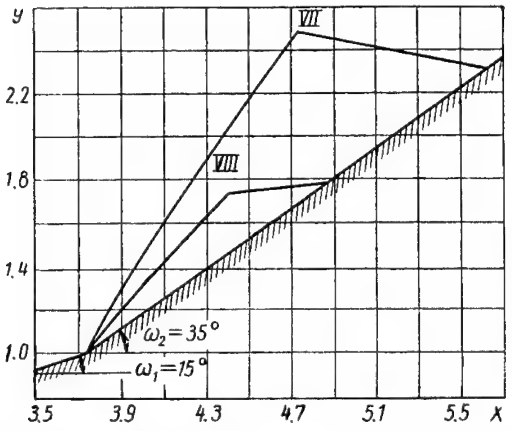


FIGURE 4. Compression shock and boundary characteristic for $M_{in} = 2.594$ (VII) and $M_{in} = 4.097$ (VIII); $\omega_1 = 15°$, $\omega_2 = 35°$

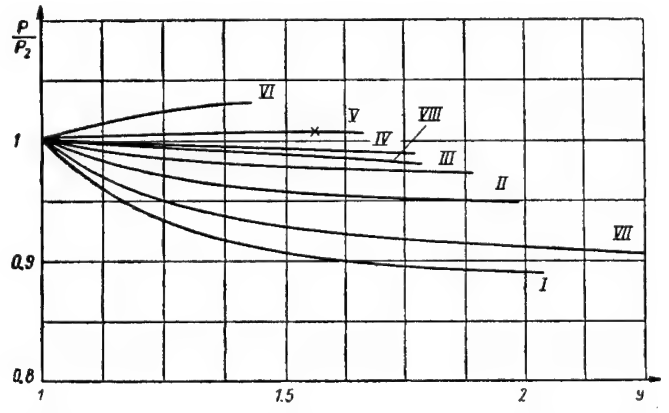


FIGURE 5. Distribution of dimensionless pressure over the generatrix of the second cone ($p_2$ is the pressure at the jointing point; see Table 2)

Figure 5 shows the pressure (divided by the pressure at the jointing point, beyond the shock) along the generatrix of the second cone. Note that pressure varies sharply with $M_{in}$ (see Table 2). It should be noted that at high $M_{in}$ a stagnation region forms near the jointing point. As $M_{in}$ increases, the pressure along the generatrix becomes more intense. Unfortunately, as computations were made for a comparatively small flow region beyond the shock, the point of maximum pressure for $M_{in} = 6.1$ does not appear on the graph. The point of maximum for $M_{in} = 4.098$ is marked by a cross.

Figure 6 shows the variation of flow rate $\psi$ along the shock as a function of $y$.

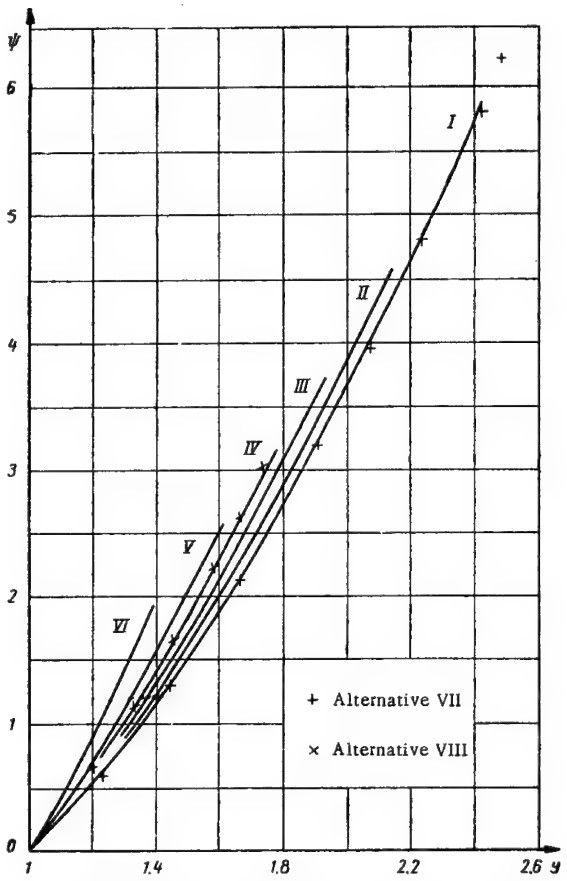


FIGURE 6. Flow rate along the shock as a function of $y$

Table 1 gives the variation of entropy $s$ as a function of $\psi$. Note the trend of entropy for various $M_{in}$. For small $M_{in}$ the entropy (as a function of $\psi$) has a minimum point, while for high $M_{in}$ $s$ becomes a monotonically increasing function of $\psi$.

In Table 2, $\bar{x}$, $\bar{y}$ are the coordinates of the intersection point of the two shocks. $p_\infty$ is the pressure on the second cone for $y \to \infty$ divided by the pressure of the incident flow ($p_\infty$ was computed from the data of /1/). The last column of Table 2 give the maximum flow rate $\psi_{max}$ on the second cone divided by the flow rate at the corresponding shock point. As we have already observed, $\psi_{max}$ characterizes to a certain extent the accuracy of computations.

All the alternatives were computed with $\Delta x = 0.01$ ($\Delta x$ the interval along the shock, see Section 5). Since the pressure at point $a$ was computed using a linear relation, $\Delta x$ was reduced near the jointing point.

Alternative IV was also computed with $\Delta x = 0.005$. Comparison of the two sets of results for this alternative shows that the error in flow rate $\psi$ does not exceed 0.1%, and the error in all other parameters is less than 0.05%. The error of all other alternatives apparently does not exceed $\psi_{max}$.

Finally we should comment on the method used. The method described for the computation of the first point on the shock is somewhat cumbersome. On the other hand, if $\Delta x$ is substantially reduced (near the jointing point), a much simpler scheme can be proposed in which the first point on the wave is computed from (8) using $\sigma$ equal to the angle of inclination of the shock at the jointing point of the generatrix. Below we give the values of the parameters at two points on the shock in cases when the first point was computed using this simplified scheme (right column) and the scheme described in Section 4. $\Delta x$ was taken as 0.001 for both calculations.

| | | |
|---|---|---|
| $x$ | 2.748477 | 2.748477 |
| $y$ | 1.001498 | 1.001499 |
| $\theta$ | 0.610495 | 0.610834 |
| $\alpha$ | 0.548388 | 0.548663 |
| $s$ | 0.076099 | 0.076206 |
| $\psi$ | 0.004316 | 0.004324 |

| | | |
|---|---|---|
| $x$ | 2.758477 | 2.758477 |
| $y$ | 1.016410 | 1.016413 |
| $\theta$ | 0.606883 | 0.606882 |
| $\alpha$ | 0.548323 | 0.548323 |
| $s$ | 0.076086 | 0.076085 |
| $\psi$ | 0.047742 | 0.047752 |

We see that the divergence in numerical results is slight and quickly smoothes off.

TABLE 1

Entropy $s$ as a function of flow rate $\psi$ (along the shock)

| $\psi$ | $s \cdot 10^2$ | | | | | | | |
|---|---|---|---|---|---|---|---|---|
| | I | II | III | IV | V | VI | VII | VIII |
| 0.000 | 2.42 | 3.41 | 5.14 | 7.61 | 12.9 | 35.0 | 5.31 | 14.08 |
| 0.300 | 2.30 | 3.36 | 5.12 | 7.62 | 12.9 | 35.2 | 5.10 | 14.10 |
| 0.600 | 2.22 | 3.33 | 5.12 | 7.65 | 13.0 | 35.4 | 4.97 | 14.21 |
| 0.900 | 2.17 | 3.32 | 5.15 | 7.70 | 13.1 | 35.6 | 4.88 | 14.37 |
| 1.200 | 2.13 | 3.32 | 5.18 | 7.77 | 13.2 | 35.9 | 4.84 | 14.56 |
| 1.500 | 2.11 | 3.34 | 5.22 | 7.85 | 13.3 | 36.2 | 4.81 | 14.79 |
| 1.800 | 2.10 | 3.36 | 5.27 | 7.94 | 13.5 | 36.6 | 4.80 | 15.13 |
| 1.932 | — | — | — | — | — | 36.7 | — | — |
| 2.100 | 2.09 | 3.39 | 5.32 | 8.03 | 13.7 | — | 4.81 | 15.32 |
| 2.400 | 2.08 | 3.42 | 5.39 | 8.14 | 13.9 | — | 4.83 | 15.66 |
| 2.545 | — | — | — | — | 14.0 | — | — | — |
| 2.700 | 2.09 | 3.45 | 5.46 | 8.25 | — | — | 4.85 | 16.00 |
| 3.000 | 2.10 | 3.49 | 5.54 | 8.38 | — | — | 4.87 | 16.42 |
| 3.022 | — | — | — | — | — | — | — | 16.43 |
| 3.300 | 2.11 | 3.53 | 5.63 | — | — | — | 4.91 | — |
| 3.600 | 2.12 | 3.58 | 5.72 | — | — | — | 4.96 | — |
| 3.714 | — | — | 5.75 | — | — | — | — | — |
| 3.900 | 2.14 | 3.63 | — | — | — | — | 5.02 | — |
| 4.200 | 2.16 | 3.69 | — | — | — | — | 5.07 | — |
| 4.500 | 2.18 | 3.75 | — | — | — | — | 5.12 | — |
| 4.597 | — | 3.77 | — | — | — | — | — | — |
| 4.800 | 2.20 | — | — | — | — | — | 5.20 | — |
| 5.100 | 2.23 | — | — | — | — | — | 5.27 | — |
| 5.400 | 2.26 | — | — | — | — | — | 5.35 | — |
| 5.700 | 2.30 | — | — | — | — | — | 5.46 | — |
| 5.726 | 2.30 | — | — | — | — | — | — | — |
| 6.000 | — | — | — | — | — | — | 5.55 | — |
| 6.216 | — | — | — | — | — | — | 5.62 | — |

In conclusion we express our thanks to V. I. Goryachev for his experimental data, and also some computational results of approximate theories.

TABLE 2 *

| Alternative | $M_{in}$ | $\omega_1$ | $\omega_w$ | $\bar{x}$ | $\bar{y}$ | $p_2$ | $\left(\frac{dp}{dy}\right)_2$ | $p_\infty$ | $\psi_{max}$ |
|---|---|---|---|---|---|---|---|---|---|
| I | 2.200 | 20° | 35° 18′ | 3.423 | 2.424 | 4.413 | —0.255 | 3.74 | 0.001 |
| II | 2.600 | 20° | 31° 52′ | 3.450 | 2.144 | 5.281 | —0.0910 | 4.65 | 0.001 |
| III | 3.000 | 20° | 29° 37′ | 3.405 | 1.935 | 6.529 | —0.0432 | 5.72 | 0.001 |
| IV | 3.420 | 20° | 27° 59′ | 3.347 | 1.779 | 8.125 | —0.0120 | 7.01 | 0.001 |
| V | 4.098 | 20° | 26° 17′ | 3.265 | 1.613 | 11.504 | 0.0232 | 9.48 | 0.001 |
| VI | 6.103 | 20° | 24° 00′ | 3.122 | 1.390 | 26.856 | 0.0852 | 19.5 | 0.002 |
| VII | 2.594 | 15° | 27° 44′ | 4.743 | 2.493 | 5.463 | —0.1665 | 4.65 | 0.002 |
| VIII | 4.097 | 15° | 21° 34′ | 4.397 | 1.737 | 11.906 | —0.0112 | 9.48 | 0.002 |

* For all alternatives, $\omega_2 = 35°$.

BIBLIOGRAPHY

1. KOPAL, Z. Tables of Supersonic Flows around Cones. — Mass. Inst. Techn., Center of Analysis., Rep. 1. 1947.
2. FERRY, A. Aerodynamics of Supersonic Flow. [Russian translation. 1953.]
3. KATSKOVA, O.N., I.N. NAUMOVA, Yu.D. SHMYGLEVSKII, and N.P. SHULISHNINA. Opyt rascheta ploskikh i osesimmetrichnykh techenii gaza metodom kharakteristik (A Computation of Plane and Axisymmetric Gas Flows by the Method of Characteristics). — Vychislitel'nyi Tsentr AN SSSR, Moskva. 1961.
4. CHERNYI, G.G. Techeniya gaza s bol'shoi sverkhzvukovoi skorost'yu (Gas Flows of High Supersonic Velocities). — Fizmatgiz, Moskva. 1959.

*T. G. Volkonskaya*

# *CALCULATION OF SUPERSONIC AXISYMMETRIC JETS*

1. The application of the method of characteristics to the calculation of an axisymmetric jet emerging from a nozzle are considered in /1, 2/. In /1/ finite-difference formulas are given for calculating the typical points and a general calculational procedure is described. No scheme for calculating the flow parameters on the compression shock are given. Paper /2/ mainly deals with the effect of nozzle and jet parameters on jet structure, initial wavelength, and shape and curvature of the jet boundary based on experimental data and numerical calculations. This work is mostly concerned with subsonic jets or supersonic jets where the compression shock forms far downstream, i.e., cases where the shock need not be calculated. The authors maintain that the method of determination of the shock with allowance for the transient conditions across the shock front are exceedingly complicated. They therefore determine the position of the shock as the envelope of the intersection points of characteristics of one type. Correspondingly the calculational procedure ignores the intersection of characteristics of one type.

The present work also deals with the numerical calculation of supersonic jets. The main attention is focused on the procedure for calculating the compression shock.

2. Consider an axisymmetric jet emerging with supersonic velocity from a nozzle into a stationary gas (Figure 1). We shall assume the flow at the nozzle outlet to be uniform, having its velocity vector parallel to the nozzle axis. We shall also assume that the pressure of the surrounding medium is less than the pressure at the nozzle outlet. In this case a "suspended" compression shock may form in the jet, whose intensity increases with the coordinate $x$. Near the nozzle axis, the dropping compression shock is reflected forming a direct shock on the axis, and the flow changes from supersonic to subsonic (upstream from the direct shock). The compression shock reflected from the axis and the free boundary again forms a direct shock on the axis, etc. The complete problem of jet calculation is highly complicated owing to the presence of subsonic regions in the jet. The purpose of this work is to obtain a numerical solution only in the range of supersonic flow limited on its right by the first direct shock. The calculation will be made by the method of characteristics in the region bounded by the initial linear characteristic $AB$, the segment $BC$ of the axis of symmetry, the free boundary $AD$, and some characteristic $CD$. The following notation is employed throughout: $x$, $r$, cylindrical coordinates; $\theta$, the inclination angle of the velocity vector to the $x$-axis; $\alpha$, the Mach angle; $S$, the entropy; $M$, the Mach number;

$M_0$, the Mach number at nozzle outlet; $M_b$, the Mach number at jet boundary; $\sigma$ the inclination angle of the compression shock to the $x$-axis; $\varkappa$ specific heat ratio.

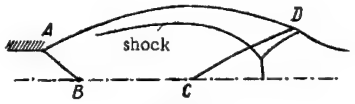


FIGURE 1

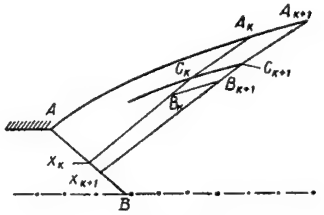


FIGURE 2

3. Let us consider a general scheme of computation. The calculation is made along characteristics of the 1st family starting from the initial (given) characteristic $AB$ or axis $BC$ to the free jet boundary (Figure 2). At the angular point $A$, the well-known Prandtl-Mayer equations are used. When a shock is observed, the sequence of computations is as follows. Let $X_k B_k$ be a part of previously calculated characteristic $X_k A_k$ lying in region I.* $C_k$ is the point at which the characteristic $X_k A_k$ meets the shock. Starting with characteristic $X_k B_k$ we construct in region I the characteristic $X_{k+1} B_{k+1}$. Then applying the formulas for transition across the shock, we find the point $C_{k+1}$ on the shock. From point $C_{k+1}$ we then construct in region II a 1st-family characteristic $C_{k+1} A_{k+1}$.

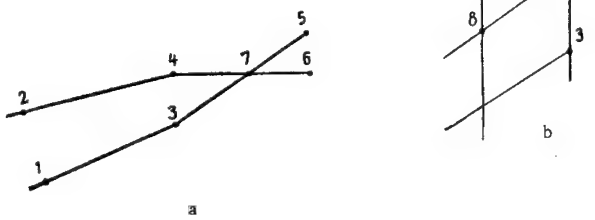


FIGURE 3

4. Let us now consider a scheme for calculating a point on the compression shock. Primed quantities will refer to a point on the shock facing region I, and double-primed quantities to a point on the side of region II. The beginning of the shock, point 7 (Figure 3a), lies at the intersection of the last characteristic of the rarefaction-wave fan, with

* Region I is located upstream from the compression shock, and region II downstream from it.

flow parameters given at points 1, 3, 5 of this characteristic, and the characteristic reflected from the free boundary (known points — 2, 4, 6). The flow parameters at point 7 on the side of region I are found by quadratic interpolation for points 1, 3, 5; quadratic interpolation for points 2, 4, 6 gives the flow parameters at point 7 on the side of region II. To determine the inclination $\sigma_7$ of the shock, we apply one of the conditions of transition across the shock:

$$\theta_7^{\cdot\cdot} - \theta_7^{\cdot} + \operatorname{arctg}\left\{\frac{\sin^2(\theta_7^{\cdot}-\sigma_7) - \sin^2\alpha_7^{\cdot}}{\operatorname{tg}(\theta_7^{\cdot}-\sigma_7)\left[\frac{\varkappa+1}{2} - \sin^2(\theta_7^{\cdot}-\sigma_7) + \sin^2\alpha_7^{\cdot}\right]}\right\} = 0.$$

Suppose that point 0 of the shock (Figure 3b) has already been computed and that the solution is known at points 5, 6, 8 of the 1st-family characteristic passing through this point. The required point of the shock, 2, lies at the intersection of the shock line with the neighboring 1st-family characteristic, at points 1 and 3 of which the flow parameters are known. The algorithm for the determination of the parameters at point 2 on the side of region I is analogous to that described in /3/, and it amounts to the following. We continue the characteristic 3—1 into region II ignoring the discontinuity at the shock front. From point 0 (assuming the parameters which apply on the side of region I) we draw a 2nd-family characteristic to its intersection (at point 4) with the 1st-family characteristic issuing from point 1. The parameters at point 2 on the side of region I are then found by quadratic interpolation for points 3, 1, 4. To determine the required quantities at point 2 on the side of region II, we apply the following conditions of transition across the shock:

$$\theta_2^{\cdot\cdot} = \theta_2^{\cdot} - \operatorname{arctg}\left\{\frac{\sin^2(\theta_2^{\cdot}-\sigma_2) - \sin^2\alpha_2^{\cdot}}{\operatorname{tg}(\theta_2^{\cdot}-\sigma_2)\left[\frac{\varkappa+1}{2} - \sin^2(\theta_2^{\cdot}-\sigma_2) + \sin^2\alpha_2^{\cdot}\right]}\right\},$$

$$\alpha_2^{\cdot\cdot} = \arcsin\left\{\sin(\theta_2^{\cdot\cdot}-\sigma_2)\left[\frac{\varkappa+1}{2}\operatorname{tg}(\theta_2^{\cdot}-\sigma_2)\cos(\theta_2^{\cdot\cdot}-\sigma_2) - \frac{\varkappa-1}{2}\sin(\theta_2^{\cdot\cdot}-\sigma_2)\right]\right\}^{\frac{1}{2}}, \qquad (1)$$

$$S_2^{\cdot\cdot} = S_2^{\cdot} + \ln\left[\frac{2\varkappa}{\varkappa+1}\cdot\frac{\sin^2(\theta_2^{\cdot}-\sigma_2)}{\sin^2\alpha_2^{\cdot}} - \frac{\varkappa-1}{\varkappa+1}\right] + \varkappa\ln\left[\frac{2}{\varkappa+1}\cdot\frac{\sin^2\alpha_2^{\cdot}}{\sin^2(\theta_2^{\cdot}-\sigma_2)} + \frac{\varkappa-1}{\varkappa+1}\right].$$

We supplement this system with a differential relationship holding on the 2nd-family characteristic 2—7. Writing it in a finite-difference form*, we obtain

$$\Phi \equiv \theta_2^{\cdot\cdot} - \theta_7 - K(\alpha_2^{\cdot\cdot} - \alpha_7) - L(x_2 - x_7) + l(S_2^{\cdot\cdot} - S_7) = 0, \qquad (2)$$

* The parameters at point 7 are found by quadratic interpolation for points 0, 5, 6.

where

$$K = \frac{1}{2}\left(\frac{1+\cos 2\alpha_7}{\varkappa - \cos 2\alpha_7} + \frac{1+\cos 2\alpha_2''}{\varkappa - \cos 2\alpha_2''}\right),$$

$$L = \frac{1}{2}\left[\frac{\sin\theta_7 \sin\alpha_7}{r_7 \cos(\theta_7 - \alpha_7)} + \frac{\sin\theta_2'' \sin\alpha_2''}{r_2 \cos(\theta_2'' - \alpha_2'')}\right],$$

$$l = \frac{1}{4\varkappa(\varkappa - 1)}(\sin 2\alpha_7 + \sin 2\alpha_2'').$$

Regarding $\theta''_2$, $\alpha''_2$, $S''_2$ in (2) as functions of $\sigma_2$, we in fact reduce the solution of system (1) and (2) to the solution of the equation $\Phi(\sigma_2) = 0$ on the segment $\left[\sigma_0, -\frac{\pi}{2}\right]$. We should first seek the segment $[\sigma_2^i, \sigma_2^{i+1}]$ on which $\Phi(\sigma_2) = 0$ has a root ($\sigma_0^i = \sigma_0 - i\Delta\sigma_2$, $i = 1, 2, \ldots$, $\Delta\sigma_2$ being the difference between the values of $\sigma$ at two preceding points on the shock), and then on this segment find by quadratic interpolation a new value of $\sigma$ so that $\Phi(\sigma_2)$ vanishes.

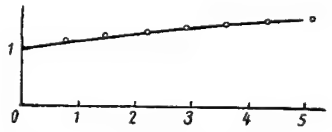


FIGURE 4. Jet boundary for $M_0 = 2.5$, $M_b = 3.0$ No shock formed in the region in question

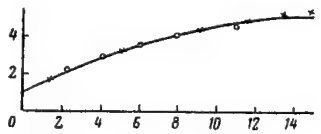


FIGURE 5. Jet boundary for $M_0 = 3.0$, $M_b = 5.2867$. Intersection of similar characteristics was ignored

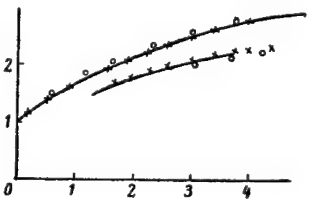


FIGURE 6. Jet boundary and the shock for $M_0 = 1.5$, $M_b = 2.9996$

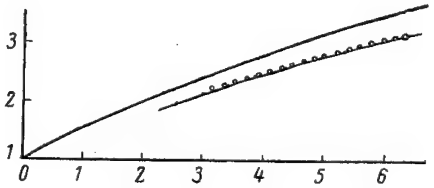


FIGURE 7. Jet boundary and shock for $M_0 = 3.0$, $M_b = 5.2867$. The dash-dot line gives a shock whose origin is defined as the intersection point of the boundary characteristic of the fan with the first characteristic reflected from the jet boundary; circles mark the results obtained with the intersection of the fifth reflected characteristic

5. The numerical calculations were carried out on the STRELA computer at the Computational Center of the Moscow State University. The results of calculations were plotted graphically. In all cases, $\varkappa$ was taken as 1.4. Figures 4—6 give the results of calculations carried out with the object of checking both the accuracy of our work and the accuracy of the results in /2/. Figure 4 gives the shape of the jet boundary for $M_0 = 2.5$, $M_b = 3.0$. No shock formed in the calculated region of the jet. The results

published in /2/ are shown as circles. We see from the graph that the two sets of calculations are closely identical in the isentropic case. Figure 5 gives the shape of the jet boundary for $M_0 = 3.0$, $M_b = 5.2867$. The solid line marks the jet boundary obtained in calculations in which intersections of similar boundaries were ignored. The crosses mark the boundary obtained in exact calculation (also see Figure 10). A divergence in the results becomes noticeable only at a comparatively large distance from the nozzle outlet, when the shock is fairly intense. The results from /2/ (marked by circles) show a higher discrepancy, which is apparently due to the inaccuracy of the method of shock calculation used in this work. This is also shown in the analysis of the data plotted in Figure 6. The solid lines in this figure mark the jet boundary and the shock for $M_0 = 1.5$, $M_b = 2.9996$ obtained by exact calculation. The results of calculation in a finer grid (halved spacing) are indicated by crosses. The divergence between these two sets of data is insignificant. On the other hand, the results of /2/, shown by circles, show a greater discrepancy.

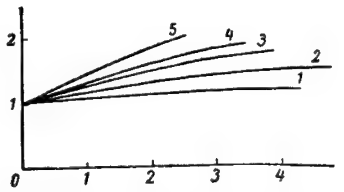


FIGURE 8. Jet boundary for $M_0 = 2.5$, $M_b = 2.7$ (curve 1); 3.0 (curve 2); 3.3 (curve 3); 3.5 (curve 4); 4.0 (curve 5)

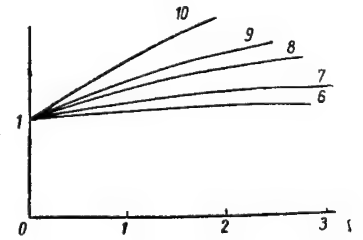


FIGURE 9. Jet boundary for $M_0 = 1.6$, $M_b = 1.8$ (curve 6); 2.0 (curve 7); 2.3 (curve 8); 2.5 (curve 9); 3.0 (curve 10)

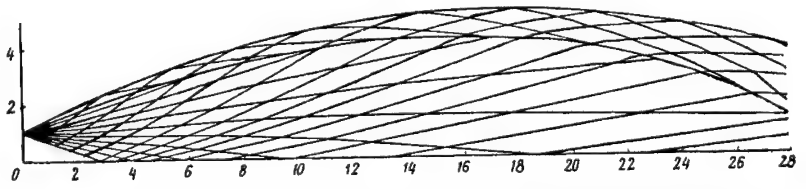


FIGURE 10. Characteristic grid for $M_0 = 3.0$, $M_b = 5.2867$. The free boundary and the shock are marked by thick lines

Calculations were made to determine the effect of an error in the position of the point of origin of the shock on the accuracy of the results. Examination of Figure 7 shows that the point of origin of the shock can be determined very roughly*. The dash-dot line gives the shock whose origin is determined as the intersection point of the boundary characteristic of the fan with the first characteristic reflected from the jet boundary; the circles plot the results obtained when the fifth reflected characteristic is

* A similar conclusion was reached in /3/ in calculation of "suspended" shock waves in one-dimensional problems of gas dynamics.

substituted. The difference in the coordinates of the "points of origin" of the shocks (especially as regards the abscissa) is fairly large. This, however, has virtually no effect on the shape of the jet boundary, and both shocks merge at a certain distance.

Figures 8 and 9 show how the jet boundary varies with $M_b$, $M_0$ remaining constant. In all the cases no shock formed in the region in question.

Figure 10 gives the characteristic grid for $M_0 = 3.0$, $M_b = 5.2867$. The free boundary and the shock are marked by thick lines.

BIBLIOGRAPHY


1. WAND and PETERSON. Spreading of Supersonic Jets from Axially Symmetric Nozzles. — Jet Propulsion, May 1958.
2. LOVE, E.S., C.E. GRIGSBY, L.P. LEE, and M.J. WOODLING. Experimental and Theoretical Studies of Axisymmetric Free Jets. — NASA, Technical Report R—6. 1959.
3. ZHUKOV, A.I. Primenenie metoda kharakteristik k chislennomu resheniyu odnomernykh zadach gazovoi dinamiki (Application of the Method of Characteristics to the Numerical Solution of One-Dimensional Problems in Gas Dynamics). — Trudy Matematicheskogo Instituta im. V.A. Steklova, Vol. 58. 1960.

## *II. BOUNDARY LAYER*

*L. A. Chudov*

# *REVIEW OF BOUNDARY-LAYER STUDIES CARRIED OUT AT THE COMPUTATIONAL CENTER OF MOSCOW STATE UNIVERSITY**

During 1959 – 1962 some 30 numerical investigations of boundary-layer problems were carried out at the Computational Center of Moscow State University under the general guidance of Academician G. I. Petrov with the participation of workers from some other organizations, as well as graduate and undergraduate students of the Moscow University. These studies cover a very wide range, and besides their theoretical and methodical value most of them also have direct applied interest. The problems were solved by a variety of numerical methods (reduction to a system of ordinary equations, series expansions, difference methods, etc.).

The reviewed solutions are grouped according to the computational procedures employed. Some points concerning the physical statement of the problems are occasionally discussed, but the practical conclusions not at all.

## I. SELF-SIMILAR PROBLEMS. ANALYTICAL METHODS

V. S. Avduevskii and E. I. Obroskova /1/ considered the boundary layer in a compressible gas flow over a plane permeable plate with gas inblow (without dissociation and chemical reactions); the inblown gas (hydrogen or argon) strongly differs in its physical properties from the embient gas (air). The binary-mixture approximation was used to compute the diffusion. An exact numerical solution of the problem was obtained for self-similar boundary conditions on the plate (constant surface temperature; inblow velocity proportional to $x^{-1/2}$, where $x$ is the downstream coordinate along the plate). The profiles obtained in the solution of this self-similar problem were used in the same work in numerical computations with the method of integral relations for non-self-similar boundary conditions (in particular, with constant inblow).

E. I. Obroskova and E. N. Starova /13/, considered the same physical statement of the problem with regard to the critical point, when the problem is also self-similar, and the solution is reduced to that of a boundary-value problem for a system of ordinary differential equations. As in some other works, this boundary-value problem was solved by the method of iterations, applying the forcing function method for the solution of every particular

* Lecture delivered at the Conference on Numerical Methods in Gas Dynamics, Moscow, March 1962.

equations. (Third order equations in the stream function can also be conveniently solved by the forcing function method.)

The next four works are of particular interest in elucidating certain questions pertaining to the physical statement of boundary-value problems in many-component gases.

A. B. Karasev /2/ computed the boundary layer near the critical point in a ternary mixture (atomic oxygen, molecular nitrogen, and silicon oxide), which forms on the wall and is entirely inblown into the boundary layer. The reactions are "frozen" in the boundary layer. The main methodic purpose of the work was to compare the results obtained with different representations of the diffusive fluxes. Three alternatives were considered: Wilke's formula, averaged Wilke's formula, and simple binary formula. The solutions obtained in the first and the second alternatives differed insignificantly; the third alternative showed considerable divergence from the results of the previous two, which indicates the inapplicability of the binary formula for the computation of ternary mixtures of this kind.

N. A. Anfimov /3/ considered the boundary-layer near the critical point in a many-component gas. Computations were made for the case of five components. The gas was assumed to be in equilibrium at the wall and the outer limit of the boundary layer, while in the boundary layer the reactions were "frozen". Diffuse fluxes were computed using Wilke's formula. The main methodic problem was to establish the effect of various physical assumptions adopted in the computation of the transport properties of the individual components on the various profiles and the heat conduction. Two interaction models were considered (rigid sphere model, and Lennard-Jones potential). It was found that the results of computations substantially depend on the procedure used in the computation of the properties of the atomic components. The same work also dealt with another methodic problem, namely the degree of reliability of Wilke's formula. It was shown that this formula may give noticeable deviations from the principle of mass conservation (up to 3%). An approximate method was proposed for correcting this.

In /4/ N. A. Anfimov considered the boundary-layer on a chemically active surface near the critical point. The main physical premises were as in /3/, but computationally the problem was much more complicated. The number of components was 8; the boundary conditions on the wall are mixed, i. e., as a rule every unknown function (and its normal derivatives) enters in every boundary condition. The method proposed by the author, reducing the mixed boundary conditions to simplest conditions in every iteration, ensures satisfactory convergence of the iterative process. The main attention was focused on the rate of combustion under various physical assumptions discussed by the author in /3/.

The two works of V. I. Stulov /5, 6/ investigate the boundary layer on a plate with an allowance for nonequilibrium dissociation. Diatomic gas is considered under conditions close to those of equilibrium dissociation. Small variations are introduced, characterizing the departure from equilibrium, and equations of zero and first approximation are considered, which are reduced to ordinary equations. To determine the concentration of the atomic components, it is necessary to construct an additional "boundary-layer" solution, i. e., a rapidly varying function which converges to zero at infinity.

B. M. Budak, T. F. Bulatskaya, and F. P. Vasil'ev /7/ made a numerical computation of a certain self-similar case of the boundary layer on an axisymmetric body in a compressible heat-conducting gas. This case was outlined by V. V. Lunev*. The problem was reduced to the solution of a system of two nonlinear integro-differential equations with a parameter, which was determined by solving a cubic, one of whose coefficients depended on the solution. The iterative process was devised so that at every step only a boundary-value problem for a linear differential equation of second order had to be solved. This problem was solved by the forcing function method.

We now pass to the treatments by analytical methods (series expansions). I. P. Soprunenko /8/ considered the boundary-layer flow of an incopressible fluid on a slightly wavy wall. The waviness of the wall was described by sinusoidal perturbations with small amplitude $\varepsilon$. The solution was represented as a series in powers of $x$. The procedure involves simultaneous linearization with respect to $\varepsilon$. To investigate the solution over two waves of the sinusoidal disturbance, up to 40 terms must be retained in the expansion. The expansion coefficients are determined by successively solving boundary-value problems of linear differential equations. These boundary-value problems were numerically solved by the ranging method. The method used in this work can be extended to the case of compressible gas, but, as the author observed, the resulting recurring system of ordinary equations is fairly cumbersome.

V. Ya. Shkadov /9/ obtained, for the case of incompressible fluid, an expansion of the stream function in terms of some dimensionless combinations containing the velocity $U_\infty(x)$ and its derivatives. Analogous, but more complicated, expansions were constructed, under certain restrictions, for the case of compressible gas. It is noteworthy that the practical use of this method on electronic computers involves considerable difficulties owing to the complexity of the right-hand sides of the differential equations defining the expansion coefficients.

Series expansion of the solution in complicated problems seems to lead invariably to cumbersome and non-standard computations which are not suitable for electronic computers.

## II. DIFFERENCE METHODS

Application of difference schemes to the solution of particular problems of the boundary layer was preceded by works mainly of methodic significance. The system of equations describing the boundary layer in a

* See Lunev, V. V. Avtomodel'nyi sluchai giperzvukovogo obtekaniya osesimmetrichnogo tela vyazkim teploprovodnym gazom (Self-Similar Hypersonic Flow of Viscous Heat-Conducting Gas Past an Axisymmetric Body). — PMM, Vol. 24 (3): 554 - 550. 1960.

compressible many-component gas can be represented by the following scheme:

$$a_i \frac{\partial u_i}{\partial x} + b_i \frac{\partial u_i}{\partial y} = \frac{\partial}{\partial y}\left(\mu_i \frac{\partial u_i}{\partial y}\right) + F_i; \qquad (A)$$

$$(i = 1, 2, \ldots, p);$$

$$\frac{\partial}{\partial x}(\rho u) + \frac{\partial}{\partial y}(\rho v) = 0. \qquad (B)$$

The coefficients of equations in group (A), i.e., $a_i$, $b_i$, $\mu_i$, depend on the unknown functions $u_i$, which include the horizontal velocity component $u$ and the concentrations of the various components, and also on the vertical velocity component $v$. The free term $F_i$ depends, in the general case, on the unknown functions $u_i$ and their first derivatives with respect to $y$. Since the coefficients $a_i$ vanish at the wall, it is natural to approximate equations (A) by an implicit six-point difference scheme which is stable as $a_i \to 0$. The continuity equation (B), from which $v$ is determined, is essentially an ordinary equation (in $y$), and therefore (B) can be approximated by any stable difference scheme. The nonlinearity of system (A), (B) makes it necessary to iterate on every $x$-layer, to ensure second-order accuracy in $\Delta x$.

In /10, 11, 12/, L. A. Chudov, I. Yu. Brailovskaya, and I. I. Gezenko studied in detail the various methodic problems arising when this scheme is used (choice of mesh size, iteration convergence, special features of computation near the wall and the outer limit of the boundary layer, accuracy estimates). The study was carried out by varying the mesh size and the number of iterations, and also by comparing the results of difference computations with the solutions obtained by other methods. Similar methodic problems were later considered by T. S. Varzhanskaya and E. I. Obroskova /13/.

The Moscow University undergraduate students Ma Yen-wen /14/ and Kuo Ching-tang /15/ and the graduate student Hsü Chiu-yuan /16/ considered some problems related to the application of difference schemes to the computation of the boundary layer near the separation point. In /14/ it was shown that the basic difference scheme described in /10/ can be used to approach the separation point very closely. This, however, calls for many more iterations to compute $v$, owing to the unbounded increase of the derivative $\frac{\partial u}{\partial x}$. In /15, 16/ some procedures of accelerating the convergence of iterations were studied. It was shown in /14/ that the results of numerical computations confirm the asymptotic formulas of L. D. Landau for $u$, $v$ near the separation point*.

In /16/ these formulas were used to improve the numerical computation by suitable transformation of the unknown functions.

The expediency of using schemes of 4-th order in $y$ is discussed in /15/. It is shown that these schemes approximate equations of the type (A) with very few grid points, without essentially complicating the computational procedure. However, this sparse grid turns out to be insufficient for the integration of the continuity equation (B), and it is therefore advisable to replace $v$ by some other, smoother function.

* See Landau, L. D. and E. M. Lifshitz. Mekhanika sploshnykh sred (Mechanics of Continuous Media), 2nd ed, Ch. IV, §40. — GITTL, Moskva, 1953.

The methodic investigations, and also the experience gained in the solution of boundary-value problems in two-component gas /10, 11/ helped in progressing toward the solution of various particular problems.

V. M. Paskonov /17/ developed for the STRELA-4 computer a standard program for the solution of the system of equations (A), (B) according to the difference scheme described in /10, 11/. This standard program can be conveniently used in the compilation of specific programs for the solution of various boundary-layer problems reducible to system (A), (B).

We shall now briefly describe some particular projects. The problem of the two-component boundary layer in the statement proposed by /1/ was considered in /10, 11/ for the case of a plane plate and constant inblow, and in /13/, near the critical point. The self-similar solution is determined in /13/ by the method of steadying. The solution of partial differential equations determined by more or less arbitrary conditions at $x = 0$ will, in suitable variables, converge to the self-similar solution as $x \to \infty$.

M. G. Merzlyakova and G. A. Beda /18/ computed a liquid boundary layer on the surface of a truncated cone. The coordinate system used the limit of the liquid boundary layer as a coordinate line. In this system of coordinates the thickness of the boundary layer is constant.

E. I. Obroskova and V. M. Paskonov /19/ studied a many-component compressible boundary layer with combustion at the wall and radiation. The problem is stated as follows. A porous plane plate is immersed in a stream of oxygen. Hydrogen is fed through the plate, which burns entirely on its surface. Inside the boundary layer there is a mixture of water vapor and oxygen which at certain temperatures is capable of emitting and absorbing radiant energy.

I. M. Soprunenko and V. M. Paskonov /20/ studied the boundary layer in an incompressible fluid on a wavy surface. The problem was posed as in /8/, but solved directly, using a difference scheme. The main attention was devoted here to establishing a relationship between the magnitude of waviness and the separation.

In /21/ T. F. Bulatskaya, for the physical problem of /4/, computed the boundary layer on the lateral surface of a blunt body immersed in a high-temperature flow of dissociated air. A comparison is given of the results obtained with rates of diffusion computed by two different methods: Wilke's formula and Hirschfelder's formula.

V. M. Paskonov and Yu. V. Polezhaev /22/ considered unsteady melting of a viscous material near the critical point. The system of equations in this problem reduces to (A), which is then solved by the standard program. Interesting results were obtained concerning the time required to reach steady melting.

T. S. Varzhanskaya and E. I. Obroskova /23/ computed a two-component boundary-layer with inblow, which was described by a discontinuous (piecewise-constant) function. It was shown that the standard difference scheme is adequate also in the presence of such discontinuous boundary conditions. This work raised an interesting theoretical question regarding the conditions for applicability of the boundary-layer equations in similar problems (see Section III).

The standard program for the solution of boundary-layer equations can also be applied to a nonstationary two-dimensional boundary layer. In

/24/, V. M. Paskonov and S. I. Serdyukova considered the problem of propagation of disturbances in an incompressible boundary layer on a plate. The disturbances are set up by periodic variations in the normal velocity component, confined to a small interval on the leading edge of the plate.

In conclusion of this section, we should mention two studies employing different difference approximations. V. G. Gromov /25/ considered the boundary layer on a plate in a many-component mixture of gases (oxygen, nitrogen, hydrogen, water vapor) with combustion in the flame front. A coordinate system moving with the flame front was used. The derivatives in directions perpendicular to the wall were approximated using many-point formulas (separate approximations for the regions separated by the flame front, employing all the points in the respective regions).

The system of ordinary equations (in the second independent variable) was solved by the Runge-Kutta method. Kh. S. Kestenboim /26/ applied a similar method to the problem of a two-component boundary layer (hydrogen-air) with constant inblow.

## III. SOME PROBLEMS OF BOUNDARY-LAYER THEORY

The solution of some of the problems discussed in the previous section raised certain theoretical questions. For example, in /10/ it was shown that the depth of the diffusive and the temperature boundary layers can be several times greater than the thickness of the dynamic boundary layer. This means that computations must be made in the region where the horizontal velocity component $u$ virtually coincides with the given velocity of inviscid flow $u_\infty(x)$. If the vertical component $v$ is determined, as is usually done, from the continuity equation, then with $u_\infty(x) \neq$ const, an absurd result is obtained: as $y \to \infty, v$ boundlessly increases in absolute value. When the temperature and the diffusive layers are fairly thick, i. e., when $y$ is large, this circumstance can have considerable influence on concentration and temperature profiles far from the wall.

The classical boundary layer theory, with its conception of the asymptotic boundary layer, neglects the problem of construction of a "global" approximation, i.e., a solution applying near the boundary as well as in the region of main flow. It is easily seen that the asymptotic solution cannot be matched continuously with the solution of inviscid flow past a wall. For some problems of modern aerodynamics, the classical conception of the boundary layer is inadequate, and more complete allowances must be made for the effects of viscosity, and in particular its influence on the main flow. The problem arises of obtaining better approximations with regard to viscosity both near the body and far from it. The methods available in the literature for matching the boundary layer with the inviscid flow solution are also inadequate, since in the best case a continuous solution (without continuous derivatives) is obtained for $u(x,y)$ only, while $v(x, y)$ remains discontinuous at the limit of the boundary layer.

L. A. Chudov, applying the procedure developed by M. I. Vishik and L. A. Lyusternik, constructed zero and first approximations in the parameter $\varepsilon = \sqrt{\nu}$ for the case of two-dimensional steady incompressible flow past

a flat plate /27/. These approximations are represented by functions which are continuous and smooth in the entire flow domain. Residuals of zero and first approximations were computed. It was shown that higher approximations in $\varepsilon$ can be analogously obtained. A comparison of the zero approximation with the asymptotic solution of Prandtl's equations furnished an explanation for the previously mentioned paradoxical behavior of $v$.

Of considerable practical significance is the problem of stabilization of the solution in $x$. In many problems the initial profiles of all the quantities (for $x = 0$) are only known in a rough approximation. However, seeing that the boundary-layer equations are parabolic, we can assume that the difference of two solutions for different initial conditions will rapidly decrease as $x$ increases. Numerical tests of the rate of stabilization of solutions were carried out by V. M. Paskonov and L. G. Isaeva /28/.

BIBLIOGRAPHY


1. AVDUEVSKII, V.S. and E.I.OBROSKOVA. Issledovanie laminarnogo pogranichnogo sloya na poristoi plastine s uchetom teplo- i massoobmena (A Study of Laminar Boundary Layer of a Porous Plate with Heat and Mass Transfer). — Izv. AN SSSR, Seriya mekhaniki i mashinostroeniya, No.4. 1960.

2. KARASEV, A.B. Reshenie uravnenii pogranichnogo sloya v perednei kriticheskoi tochke troinoi smesi (Solution of Boundary Layer Equations at the Frontal Critical Point of a Ternary Mixture). — Izv. AN SSSR, Seriya mekhaniki i mashinostroeniya, No.6. 1961.

3. ANFIMOV, N.A. Laminarnyi pogranichnyi sloi v mnogokomponentnoi smesi gazov v okrestnosti kriticheskoi tochki (Laminar Boundary Layer in a Many-Component Gas Mixture Near the Critical Point). — Izv.AN SSSR, Seriya mekhaniki i mashinostroeniya, No.1. 1962.

4. ANFIMOV, N.A. Laminarnyi pogranichnyi sloi na khimicheski aktivnoi poverkhnosti (Laminar Boundary Layer on Chemically Active Surface). — Izv.AN SSSR, Seriya mekhaniki i mashinostroeniya, No.3. 1962.

5. STULOV, V.N. Pogranichnyi sloi na plastine s uchetom neravnovesnoi dissotsiatsii (Boundary Layer on a Plate with Nonequilibrium Dissociation). — Izv. AN SSSR, Seriya mekhaniki i mashinostroeniya, No.3. 1962.

6. STULOV, V.N. Teploperedacha v laminarnom pogranichnom sloe na plastine s uchetom khimicheskoi neravnovesnosti (Heat Transfer in Laminar Boundary Layer on a Plate with Chemical Nonequilibrium). — Izv.AN SSSR, Seriya mekhaniki i mashinostroeniya, No.6. 1961.

7. BUDAK, B.M., T.F.BULATSKAYA, and F.P.VASIL'EV. Numerical Solution of a Boundary-Value Problem for the System of Nonlinear Integro-Differential Equations of a Hypersonic Boundary Layer. — This volume.

8. SOPRUNENKO, I.P. Pogranichnyi sloi na volnistoi stenke (Boundary Layer on a Wavy Wall). — Izv.AN SSSR, Seriya mekhaniki i mashinostroeniya, No.2. 1962.

9. SHKADOV, V.Ya. Ob integrirovanii uravnenii pogranichnogo sloya (On Integration of Boundary-Layer Equations). — DAN SSSR, Vol.126, No.4. 1959.

10. BRAILOVSKAYA, I.Yu. and L.A.CHUDOV. Reshenie uravnenii pogranichnogo sloya metodom setok (Solution of Boundary-Layer Equations by Difference Methods). — Otchet VTs MGU. 1960.

11. BRAILOVSKAYA, I.Yu. and L.A.CHUDOV. Reshenie uravnenii pogranichnogo sloya raznostnym metodom (Solution of Boundary-Layer Equations by Difference Methods). — In: "Vychislitel'nye metody i programmirovanie", Izdatel'stvo MGU. 1962.

12. GEZENKO, I.I. M.Sc. thesis. — MGU. 1960.

13. VARZHANSKAYA, T.S., E.I.OBROSKOVA, and E.N.STAROVA. Boundary Layer Near the Critical Point. — This volume.

14. MA YEN-WEN. M.Sc. Thesis. — MGU. 1961.

15. KUO CHING-TANG. M.Sc. Thesis — MGU. 1961.

16. HSÜ CHIU-YUAN. Unpublished work. — MGU. 1961.

17. PASKONOV, V.M. Standard Program for the Solution of Boundary-Layer Problems. — This volume (see also Otchet VTs MGU. 1961).

18. MERZLYAKOVA, M.G. and G.A.BEDA. Raschet zhidkogo pogranichnogo sloya na bokovoi poverkhnosti prituplennogo konusa (Computation of a Liquid Boundary Layer on the Lateral Surface of a Truncated Cone). — Otchet VTs MGU. 1960.

19. OBROSKOVA, E.I. and V.M.PASKONOV. Raschet szhimaemogo pogranichnogo sloya s goreniem i izlucheniem (Computation of a Compressible Boundary Layer with Combustion and Radiation). — Otchet VTs MGU. 1962.

20. PASKONOV, V.M. and I.P.SOPRUNENKO. Boundary Layer on a Slightly Wavy Wall. — This volume.

21. BULATSKAYA, T.F. Laminarnyi Pogranichnyi sloi v mnogokomponentnoi smesi gazov na bokovoi poverkhnosti tela (Laminar Boundary Layer in a Many-Component Gas Mixture on the Lateral Surface of a Body). — Otchet VTs MGU. 1962.

22. PASKONOV, V.M. and Yu.V.POLEZHAEV. Unsteady Melting of a Viscous Material near Stagnation Point. — This volume.

23. VARZHANSKAYA, T.S. and E.I.OBROSKOVA. Raschet pogranichnogo sloya pri nalichii vduva, opisaemogo razryvnoi funktsiei (Computation of Boundary Layer with Gas Inblow Described by a Discontinuous Function).—Otchet VTs MGU. 1962.

24. PASKONOV, V.M. and S.I.SERDYUKOVA. Dvumernyi pogranichnyi sloi s nestatsionarnym vduvom (Two-Dimensional Boundary Layer with Nonstationary Inblow). — Otchet VTs MGU. 1961.

25. GROMOV, V.G. M.Sc. thesis. — MGU. 1961.

26. KESTENBOIM, Kh.S. M.Sc. thesis. — MGU. 1961.

27. CHUDOV, L.A. Some Shortcomings of Classical Boundary-Layer Theory. — This volume.

28. PASKONOV, V.M. and L.G.ISAEVA. Vliyanie nachal'nykh profilei na razvitie pogranichnogo sloya (The Effect of Initial Profiles on the Development of Boundary Layer). — Otchet VTs MGU. 1962.

*L. A. Chudov*

# *SOME SHORTCOMINGS OF CLASSICAL BOUNDARY-LAYER THEORY*

1. The classical theory of the boundary layer is concerned with the flow of viscous fluid which, as the viscosity $\nu$ approaches zero, tends to some "limiting" ideal-fluid flow in the entire subdomain which excludes boundary points of the flow domain. It is assumed that for small $\nu$ the entire flow domain can be divided into the "main domain", where the flow differs little from the limiting flow, and the so-called boundary layer — narrow regions situated along various parts of the boundary, where the viscous flow differs greatly from the limiting one and is described by the appropriate boundary-layer equations.

A fairly rigourous and convincing derivation of equations describing boundary-layer flow was given by Prandtl for the case of a boundary layer on an impermeable boundary. The extension of these equations to some other cases of boundary layers was purely formal. For example, in the case of a permeable boundary, one of the basic premises of Prandtl — that the normal velocity component vanishes at the wall — is not valid. We are thus faced with the question of applicability of Prandtl equations already in this simple and practically very common case*.

Similar questions arise in connection with other applied problems. No analysis has been made for boundary layers whose structure is substantially different from that of the boundary layer on an impermeable wall. As an example we can mention the boundary layer forming at the outlet of a rectangular channel under certain natural boundary conditions. Unlike the Prandtl boundary layer, its thickness is of the order of $\nu$ and it is described by ordinary differential equations.

The investigation of the conditions of applicability of the classical boundary-layer equations and study of other types of boundary layers, especially in cases of compressible gases, becomes more urgent as the problems of boundary-layer theory grow in complexity.

Very little has been done on the problem of boundary conditions consistent with the equations of the boundary layer. We shall not dwell here on the question of determination of initial conditions on the line $x = x_0$ (in the following we use the conventional designations of boundary-layer theory). We shall only discuss the conditions specified on the "outer face" of the boundary layer.

* It can be shown that the Prandtl equations apply if the normal velocity component at the wall is of the order of $\sqrt{\nu}$.

In practice, the asymptotic Prandtl boundary conditions are often used, which in the simplest case of viscous incompressible flow near a plane wall have the following form: as $y \to \infty, u(x, y) \to U(x)$, where $U(x)$ is the tangential component of the "limiting" flow at the wall. It is well known that if $U(x) \neq$ const, these conditions lead to a paradoxical result: as we move away from the wall, the normal velocity component $v$ increases indefinitely. In some cases (computation of a many-component boundary layer), this physically meaningless behavior of $v$ may seriously distort the results (see /1/, p. 94).

Some papers and text books also consider boundary conditions based on the introduction of a certain spurious "interface" of the boundary-layer. The conditions specifying the position of this "interface" are physically unsound in our opinion. Some alternatives of these conditions cannot be realized altogether at finite distances from the wall owing to the simple properties of the solution of the boundary-layer equations. (Such, for example, are the conditions $u(x, \delta) = U(x)$, $\frac{\partial u(x, \delta)}{\partial y} = 0$, advanced in /2/). The construction of a "global" approximate solution, i. e., a solution applying throughout the flow domain, is hardly touched in the classical treatments. The description is mostly confined to a general sketch of the structure of the solution for small $\nu$. It is easily seen that in the general case it is impossible to construct a continuous and smooth (in all components) approximate solution by matching the "limiting" flow and the solution of the classical boundary-layer equations.

In some problems of aerodynamics, the "feedback" reaction of the boundary layer on the main flow is by no means negligible (see, e.g., /3/). Investigations of this problem are in fact mainly concerned with the construction, in the "main domain", of the next approximation in the parameter $\varepsilon = \sqrt{\nu}$. Applied problems thus mainly require higher approximations in $\varepsilon$.

Physical considerations and some mathematical analogies with linear differential equations with small coefficients of the leading derivatives indicate that we may regard as an approximation of order $n$ any system of sufficiently smooth functions $(u, v, p)$ defined in the entire flow domain and satisfying the Navier-Stokes equations and the boundary conditions of viscous flow with residuals of the order of $\varepsilon^{n+1}$ *. Known methods for matching the boundary layer on a plane wall with the "limiting flow", as we have already observed, do not ensure continuity and smoothness of the approximate solution. The residual arising when this solution is substituted into the Navier-Stokes equation contains singular terms of the type of the $\delta$-function or its derivatives. This is clearly not something inherent, but due to an imperfection of the method. It is now natural to ask how in general may sufficiently smooth approximations of any order in $\varepsilon$ be constructed throughout the flow domain in the above sense. The main object of this article is to demonstrate that all these questions can be resolved by the procedure developed in the familiar work of M. I. Vishik and L. A. Lyusternik (see, e.g., /4, 5/). Formally, the main difference between this procedure and the approach of classical boundary-layer theory

* The present mathematical theory of viscous incompressible flow is unable to bear this out by providing estimates of the difference between the exact and the approximate solutions. Our definition of the approximate solution of order $n$ is thus incomplete, giving no indication as to the norms for measuring the residuals.

consists in that, in Vishik and Lyusternik's method, the equations are written not for the approximate solution, but for the "corrections" to smooth solutions obtained from the Navier-Stokes equations by formal expansion in terms of the small parameter $\varepsilon$ with an allowance for the boundary conditions of the "limiting" flow. The "corrections" are introduced for every section of the boundary separately, to ensure that the boundary conditions of viscous flow are satisfied. These are smooth functions which rapidly fall off to zero as we move away from the corresponding part of the boundary. The approximation is therefore automatically continuous and smooth.

In this paper we consider the simplest case of viscous incompressible flow near a plane impermeable wall. The zero approximation is constructed using the Vishik-Lyusternik method. A relationship is established between the equations obtained and the Prandtl equations, the paradoxical behavior of $v$ as $y \to \infty$ in the asymptotic Prandtl solution is explained, and a simple procedure is indicated for the construction, from this solution, of a continuous and smooth approximate solution valid in the entire flow domain. Equations and boundary conditions are derived, specifying the first approximation in the "main domain".

2. Consider plane-parallel viscous incompressible flow near a flat surface. Let the $x$-axis be directed downstream along the plane, and the $y$-axis perpendicular to the surface. The surface will be regarded as impermeable. We write the Navier-Stokes equations, setting $\nu = \varepsilon^2$, and the boundary conditions for the corresponding part of the boundary:

$$N_1(u, v, p, \varepsilon) \equiv u\frac{\partial u}{\partial x} + v\frac{\partial u}{\partial y} + \frac{1}{\rho}\cdot\frac{\partial p}{\partial x} - \varepsilon^2\Delta u = 0; \tag{1}$$

$$N_2(u, v, p, \varepsilon) \equiv u\frac{\partial v}{\partial x} + v\frac{\partial v}{\partial y} + \frac{1}{\rho}\cdot\frac{\partial p}{\partial y} - \varepsilon^2\Delta v = 0; \tag{2}$$

$$N_3(u, v) \equiv \frac{\partial u}{\partial x} + \frac{\partial v}{\partial y} = 0; \tag{3}$$

$$u|_{y=0} = 0; \tag{4}$$

$$v|_{y=0} = 0. \tag{5}$$

Following Vishik and Lyusternik's procedure, we shall seek an approximate solution of the problem as a sum of two series in terms of $\varepsilon$. The first series, called the smooth part of the approximation, is constructed using functions independent of $\varepsilon$. Recurrence relations defining these functions in $n$-th order approximation are chosen so that the smooth part satisfies equations (1), (2), (3) with a residual of the order of $\varepsilon^{n+1}$. On the relevant stretch of the boundary the smooth part of the approximation corresponds to the boundary condition of inviscid flow, i. e., $v = 0$. However, the smooth part of the approximation does not satisfy the boundary condition (5). This is remedied by the second series, which comprises local functions, i. e., functions depending on $x$ and $\eta = \frac{y}{\varepsilon}$ and rapidly converging to zero, with any derivatives with respect to $x$ and $\eta$, as $\eta \to \infty$. This series is called the local part of the approximation. Recurrence relations for the successive terms of the local part of the approximation are constructed so that the local part of the residual,

obtaining when the sum of the smooth and the local parts of the approximation is substituted in equations (1), (2), (3), also has the order of $\varepsilon^{n+1}$.

3. As the smooth part of the zero approximation we take the corresponding "limiting" solution. Let the velocity components and the pressure for this solution be $u_0(x,y)$, $v_0(x,y)$, $p_0(x,y)$. To satisfy boundary condition (4), we set in the zero approximation $u = u_0 + \tilde{u}_0$, where $\tilde{u}_0$ is a local function. Inserting this equation for $u$ in the continuity equation (3) and applying condition (5), we find

$$v = v_0(x, y) - \int_0^y \frac{\partial \tilde{u}_0}{\partial x} dy = v_0(x, y) - \varepsilon \int_0^\eta \frac{\partial \tilde{u}_0}{\partial x} d\eta, \tag{6}$$

where $\eta = \frac{y}{\varepsilon}$. Let

$$\bar{v}_0(x) = -\int_0^\infty \frac{\partial \tilde{u}_0}{\partial x} d\eta, \tag{7}$$

$$\tilde{v}_0(x, \eta) = \int_\eta^\infty \frac{\partial \tilde{u}_0}{\partial x} d\eta. \tag{8}$$

From (6) we have

$$v = v_0(x, y) + \varepsilon \tilde{v}_0(x, \eta) + \varepsilon \bar{v}_0(x). \tag{9}$$

If $\tilde{u}_0$ is a local function, then from (8) $\tilde{v}_0(x,\eta)$ is also a local function. Inserting $u = u_0 + \tilde{u}_0$, $v = v_0 + \varepsilon\tilde{v}_0 + \varepsilon\bar{v}_0$, $p = p_0$ in the left-hand side of (1), we obtain three groups of terms:

$$u_0 \frac{\partial u_0}{\partial x} + v_0 \frac{\partial u_0}{\partial y} + \frac{1}{\rho} \cdot \frac{\partial p_0}{\partial x}, \tag{10}$$

$$(u_0 + \tilde{u}_0) \frac{\partial \tilde{u}_0}{\partial x} + (v_0 + \varepsilon\tilde{v}_0 + \varepsilon\bar{v}_0) \frac{\partial \tilde{u}_0}{\partial y} + \tilde{u}_0 \frac{\partial u_0}{\partial x} - \varepsilon^2 \frac{\partial^2 \tilde{u}_0}{\partial y^2}, \tag{11}$$

$$(\varepsilon\tilde{v}_0 + \varepsilon\bar{v}_0(x)) \frac{\partial u_0}{\partial y} - \varepsilon^2 \frac{\partial^2 u_0}{\partial x^2} - \varepsilon^2 \frac{\partial^2 u_0}{\partial y^2} - \varepsilon^2 \frac{\partial^2 \tilde{u}_0}{\partial x^2}. \tag{12}$$

Sum (10) vanishes by the definition of $u_0$, $v_0$, $p_0$. The terms in (12) will be regarded as the residual of the zero approximation and considered in detail later on. The second group, (11), is transformed by substituting $\eta = \frac{y}{\varepsilon}$:

$$[u_0(x, \varepsilon\eta) + \tilde{u}_0(x, \eta)] \frac{\partial \tilde{u}_0}{\partial x} + \frac{1}{\varepsilon} [v_0(x, \varepsilon\eta) + \varepsilon\tilde{v}_0(x, \eta) + \varepsilon\bar{v}_0(x)] \frac{\partial \tilde{u}_0}{\partial \eta} +$$

$$+ \tilde{u}_0(x, \eta) \frac{\partial u_0}{\partial x} - \frac{\partial^2 \tilde{u}_0(x, \eta)}{\partial \eta^2} = S_0 + S_1,$$

where

$$S_0 = [u_0(x,0) + \tilde{u}_0(x,\eta)]\frac{\partial \tilde{u}_0(x,\eta)}{\partial x} + \left[\eta\frac{\partial v_0(x,0)}{\partial y} + \tilde{v}_0(x,\eta) + \right.$$

$$\left. + \bar{v}_0(x)\right]\frac{\partial \tilde{u}_0(x,\eta)}{\partial \eta} + \tilde{u}_0(x,\eta)\frac{\partial u_0(x,0)}{\partial x} - \frac{\partial^2 \tilde{u}_0}{\partial \eta^2}; \tag{13}$$

$$S_1 = [u_0(x,\varepsilon\eta) - u_0(x,0)]\frac{\partial \tilde{u}_0(x,\eta)}{\partial x} +$$

$$+ \frac{1}{\varepsilon}\left[v_0(x,\varepsilon\eta) - \varepsilon\eta\frac{\partial v_0(x,0)}{\partial y}\right]\frac{\partial \tilde{u}_0(x,\eta)}{\partial \eta} +$$

$$+ \left[\frac{\partial u_0(x,\varepsilon\eta)}{\partial x} - \frac{\partial u_0(x,0)}{\partial x}\right]\tilde{u}_0(x,\eta). \tag{14}$$

The terms entering $S_1$ will be combined with residual of zero approximation. Setting $S_0$ equal to zero and combining this equation with (7), (8), and the continuity equation (3), we arrive at a system of equations of zero approximation. We write this system in terms of the original variable $y$, and set $\varepsilon w_0 = \varepsilon\tilde{v}_0 + \varepsilon\bar{v}_0(x)$:

$$[u_0(x,0) + \tilde{u}_0]\frac{\partial \tilde{u}_0}{\partial x} + \left[y\frac{\partial v_0(x,0)}{\partial y} + \varepsilon w_0\right]\frac{\partial \tilde{u}_0}{\partial y} +$$

$$+ \tilde{u}_0\frac{\partial u_0(x,0)}{\partial x} - \varepsilon^2\frac{\partial^2 \tilde{u}_0}{\partial y^2} = 0, \tag{15}$$

$$\frac{\partial \tilde{u}_0}{\partial x} + \frac{\partial}{\partial y}(\varepsilon w_0) = 0. \tag{16}$$

The boundary conditions are

$$(u_0 + \tilde{u}_0)_{y=0} = 0, \tag{17}$$

$$(v_0 + \varepsilon w_0)_{y=0} = 0, \tag{18}$$

$$\tilde{u}_0 \to 0 \text{ as } y \to \infty. \tag{19}$$

It is easily seen that equations (15), (16) with boundary conditions (17), (18), (19) do not determine $\tilde{u}_0$, $w_0$ uniquely. We shall moreover assume that for some $x = x_0$ the function $\tilde{u}_0$ is known:

$$\tilde{u}_0|_{x=x_0} = \tilde{\varphi}_0(\eta). \tag{20}$$

where $\tilde{\varphi}_0$ is a local function*.

4. Let us compare the zero approximation with Prandtl's asymptotic solution of the classical boundary-layer equations. This solution satisfies the following equations and boundary conditions:

$$u_{Pr}\frac{\partial u_{Pr}}{\partial x} + v_{Pr}\frac{\partial u_{Pr}}{\partial y} + \frac{1}{\rho}\cdot\frac{\partial p_0(x,0)}{\partial x} - \varepsilon^2\frac{\partial^2 u_{Pr}}{\partial y^2} = 0; \tag{21}$$

* We shall assume that boundary-value problem (15)-(20) has a unique solution $\tilde{u}_0$ in some interval $x_0 < x < x_1$, this solution being a local function. With some additional restrictions, this assumption can be proved following O.A.Oleinik /6/.

$$\frac{\partial u_{Pr}}{\partial x} + \frac{\partial v_{Pr}}{\partial y} = 0; \tag{22}$$

$$u_{Pr}(x, 0) = 0; \tag{23}$$

$$v_{Pr}(x, 0) = 0; \tag{24}$$

$$u_{Pr}(x, \infty) = u_0(x, 0) \tag{25}$$

($u_0(x,y)$, $v_0(x,y)$, $p_0(x,y)$, as before, denote the components of the corresponding limiting solution of the equation of inviscid flow).

We introduce "increments" $\tilde{u}_{Pr}$, $\varepsilon w_{Pr}$ defined by

$$u_{Pr} = u_0(x, 0) + \tilde{u}_{Pr}, \tag{26}$$

$$v_{Pr} = y\frac{\partial v_0(x, 0)}{\partial y} + \varepsilon w_{Pr}. \tag{27}$$

Inserting (26), (27) in (21) and (22), and also in (23), (24), (25), and applying the equations of inviscid flow relating $u_0$, $v_0$, $p_0$, we obtain for $\tilde{u}_{Pr}$, $w_{Pr}$ the equations (15), (17) with boundary conditions (17), (18), (19), originally written for the functions of zero approximation $\tilde{u}_0$, $\varepsilon w_0$. Let the functions $\tilde{u}_{Pr}$ and $\tilde{u}_0$ coincide for $x = x_0$. Then, if the corresponding uniqueness theorem applies, $\tilde{u}_{Pr} \equiv \tilde{u}_0$, $\varepsilon w_{Pr} = \varepsilon w_0$. Comparing $u_{Pr}$, $v_{Pr}$ with the zero approximation $u^{(0)} = u_0 + \tilde{u}_0$, $v^{(0)} = v_0 + \varepsilon w_0$, we find

$$u^{(0)} = u_{Pr} + (u_0(x, y) - u_0(x, 0)), \tag{28}$$

$$v^{(0)} = v_{Pr} + \left(v_0(x, y) - y\frac{\partial v_0(x, 0)}{\partial y}\right). \tag{29}$$

It follows from (28) and (29) that the asymptotic solution ($u_{Pr}$, $v_{Pr}$) will describe a solution of the problem of viscous flow with errors of the order $\varepsilon$ only for those $y$ for which the differences $u_0(x, y) - u_0(x, 0)$ and $v_0(x, y) - y\frac{\partial v_0(x, 0)}{\partial y}$ do not exceed $\varepsilon$ in order of magnitude.

We now also have an explanation of the paradox of $v_{Pr}$ increasing boundlessly in absolute value as $y \to \infty$ if

$$\frac{\partial v_0(x, 0)}{\partial y} = -\frac{\partial u_0(x, 0)}{\partial x} \neq 0.$$

The zero approximation constructed in the preceding section is free from the restriction imposed on $y$ when the asymptotic solution is used. It is noteworthy that owing to (28) and (29) the zero approximation can be constructed from the asymptotic solution, so that the numerical computations can be made with the aid of the various approximate methods developed for the classical Prandtl equations (21), (22) with boundary conditions (23), (24), (25).

5. We shall now show that the residual of the zero approximation is of the order of $\varepsilon$. The residual of the zero approximation for equation (1) consists of the terms written out in (12) and (14).

We write separately the smooth and the local parts of the residual, and in the process isolate the terms which are of first order relative to $\varepsilon$. The smooth part of the residual of order $\varepsilon$ is

$$\varepsilon A_1(x, y) = \varepsilon \bar{v}_0(x) \frac{\partial u_0}{\partial y}. \tag{30}$$

The smooth part of the residual of order $\varepsilon^2$ is

$$\varepsilon^2 B_1(x, y) = -\varepsilon^2 \frac{\partial^2 u_0}{\partial x^2} - \varepsilon^2 \frac{\partial^2 u_0}{\partial y^2}. \tag{31}$$

The local part of the residual of order $\varepsilon$ is

$$\begin{aligned} \varepsilon \tilde{C}_1 = \varepsilon \tilde{v}_0 \frac{\partial u_0(x, 0)}{\partial y} + \varepsilon\eta \frac{\partial u_0(x; 0)}{\partial y} \frac{\partial \tilde{u}_0}{\partial x} + \\ + \frac{1}{2} \varepsilon\eta^2 \frac{\partial^2 v_0(x, 0)}{\partial y^2} \cdot \frac{\partial \tilde{u}_0}{\partial \eta} + \varepsilon\eta \frac{\partial^2 u_0(x, 0)}{\partial x \partial y} \tilde{u}_0. \end{aligned} \tag{32}$$

The local part of the residual of order $\varepsilon^2$ is

$$\begin{aligned} \varepsilon^2 \tilde{D}_1(x, \eta; \varepsilon) = -\varepsilon^2 \frac{\partial^2 \tilde{u}_0}{\partial x^2} + [u_0(x, \varepsilon\eta) - u_0(x, 0) - \\ - \varepsilon\eta \frac{\partial u_0(x, 0)}{\partial y}] \frac{\partial \tilde{u}_0}{\partial x} + \frac{1}{\varepsilon}\Big[v_0(x, \varepsilon\eta) - \varepsilon\eta \frac{\partial v_0(x, 0)}{\partial y} - \\ - \frac{1}{2} \varepsilon^2\eta^2 \frac{\partial^2 v_0(x, 0)}{\partial y^2}\Big] \frac{\partial \tilde{u}_0}{\partial \eta} + \Big[\frac{\partial u_0(x, \varepsilon\eta)}{\partial x} - \frac{\partial u_0(x, 0)}{\partial x} - \\ - \varepsilon\eta \frac{\partial^2 u_0(x, 0)}{\partial x \partial y}\Big] \tilde{u}_0 + \varepsilon \tilde{v}_0 \Big[\frac{\partial u_0(x, \varepsilon\eta)}{\partial y} - \frac{\partial u_0(x, 0)}{\partial y}\Big]. \end{aligned} \tag{33}$$

Let us now compute the residual for equation (2). This equation was used with $\varepsilon = 0$ to construct the functions $u_0$, $v_0$, $p_0$, , i. e. , the smooth part of the zero approximation. The smooth part of the residual therefore contains no terms of zero order in $\varepsilon$. As regards the local part of the residual, it contains the terms

$$\tilde{u}_0 \frac{\partial}{\partial x}(v_0(x, \varepsilon\eta)) + v_0(x, \varepsilon\eta) \frac{\partial}{\partial \eta} \tilde{v}_0, \tag{34}$$

which are formally of zero order in $\varepsilon$. This is so because equation (2) has not been used in the construction of the local part of the zero approximation. However, it is easily seen that in fact these terms are of first order of smallness relative to $\varepsilon$: we apply condition (5) and rewrite them in the form

$$\begin{aligned} \varepsilon\eta \frac{\partial^2 v_0(x, 0)}{\partial x \partial y} \tilde{u}_0 + \varepsilon\eta \frac{\partial v_0(x, 0)}{\partial y} \cdot \frac{\partial}{\partial \eta} \tilde{v}_0 + \Big[\frac{\partial v_0(x, \varepsilon\eta)}{\partial x} - \varepsilon\eta \frac{\partial^2 v_0(x, 0)}{\partial x \partial y}\Big] \tilde{u}_0 + \\ + \Big[v_0(x, \varepsilon\eta) - \varepsilon\eta \frac{\partial v_0(x, 0)}{\partial y}\Big] \frac{\partial}{\partial \eta} \tilde{v}_0. \end{aligned}$$

We now treat the residual of equation (2) as we have done for equation (1).

The smooth part of the residual of order $\varepsilon$ is

$$\varepsilon A_2(x, y) = u_0 \frac{\partial}{\partial x}(\varepsilon \bar{v}_0(x)) + \varepsilon \bar{v}_0(x) \frac{\partial v_0}{\partial y}.$$

The smooth part of the residual of order $\varepsilon^2$ (and higher) is

$$\varepsilon^2 B_2(x, y, \varepsilon) = -\varepsilon^2 \frac{\partial^2 v_0}{\partial x^2} - \varepsilon^2 \frac{\partial^2 v_0}{\partial y^2} - \varepsilon^3 \frac{\partial^2 \bar{v}_0(x)}{\partial x^2}.$$

The local part of the residual of order $\varepsilon$ is

$$\varepsilon \tilde{C}_2(x, \eta) = u_0(x, 0) \frac{\partial}{\partial x}(\varepsilon \tilde{v}_0) + \tilde{u}_0 \frac{\partial}{\partial x}\left[\varepsilon\eta \frac{\partial v_0(x, 0)}{\partial y} + \varepsilon \bar{v}_0(x) + \varepsilon \tilde{v}_0\right] +$$
$$+ \left[\varepsilon\eta \frac{\partial v_0(x, 0)}{\partial y} + \varepsilon \tilde{v}_0 + \varepsilon \bar{v}_0(x)\right] \frac{\partial}{\partial \eta} \tilde{v}_0 + \varepsilon \tilde{v}_0 \frac{\partial v_0(x, 0)}{\partial y} - \varepsilon \frac{\partial^2 \tilde{v}_0}{\partial \eta^2}. \qquad (35)$$

The local part of the residual of order $\varepsilon^2$ (and higher) is

$$\varepsilon^2 \tilde{D}_2(x, \eta; \varepsilon) = [u_0(x, \varepsilon\eta) - u_0(x, 0)] \frac{\partial}{\partial x}(\varepsilon \tilde{v}_0) +$$
$$+ \tilde{u}_0 \frac{\partial}{\partial x}\left[v_0(x, \varepsilon\eta) - \varepsilon\eta \frac{\partial v_0(x, 0)}{\partial y}\right] + \left[v_0(x, \varepsilon\eta) - \varepsilon\eta \frac{\partial v_0(x, 0)}{\partial y}\right] \frac{\partial}{\partial \eta} \tilde{v}_0 +$$
$$+ \varepsilon \tilde{v}_0 \left[\frac{\partial v_0(x, \varepsilon\eta)}{\partial y} - \frac{\partial v_0(x, 0)}{\partial y}\right] - \varepsilon^3 \frac{\partial^2 \tilde{v}_0}{\partial x^2}. \qquad (36)$$

Equation (3) satisfies the zero approximation exactly, i. e., its residual vanishes.

6. The zero approximation satisfies the boundary conditions for $y = 0$ exactly. On other parts of the boundary, the increments $\tilde{u}_0$, $\varepsilon \tilde{v}_0 + \varepsilon \bar{v}_0(x)$ introduce an additional residual into the boundary conditions. The increment $\tilde{u}_0$, according to our assumptions, converges to zero for $\varepsilon \to 0$ faster than any power of $\varepsilon$, while the increment $\varepsilon \tilde{v}_0 + \varepsilon \bar{v}_0(x)$ is of the first order relative to $\varepsilon$. Following the Vishik-Lyusternik procedure, we could have "truncated" the increments $\tilde{u}_0$, $\varepsilon \tilde{v}_0 + \varepsilon \bar{v}_0(x)$ using a smooth "truncating" function independent of $\varepsilon$. The smooth parts of the residuals of equations (1), (2) would change, but nevertheless retain the previous orders relative to $\varepsilon$, and a residual of the order of $\varepsilon$ would appear in equation (3). We shall not follow this course, since our approach is fully consistent with the possibility of a residual of the order of $\varepsilon$ in the boundary conditions, too. In what follows, in the first approximation this residual can be eliminated by replacing it with a residual of the order of $\varepsilon^2$.

The smooth part of the first approximation is sought in the form $u = u_0 + \varepsilon u_1$, $v = v_0 + \varepsilon v_1$, $p = p_0 + \varepsilon p_1$. Inserting these expressions in (1), (2), (3), applying the definitions of $u_0$, $v_0$, $p_0$, and dropping all terms of second order relative to $\varepsilon$, we obtain equations of the first approximation for the smooth part:

$$u_0 \frac{\partial}{\partial x}(\varepsilon u_1) + v_0 \frac{\partial}{\partial y}(\varepsilon u_1) + \varepsilon u_1 \frac{\partial u_0}{\partial x} + \varepsilon v_1 \frac{\partial u_0}{\partial y} + \frac{\partial}{\partial x}(\varepsilon p_1) = 0;$$

$$u_0 \frac{\partial}{\partial x}(\varepsilon v_1) + v_0 \frac{\partial}{\partial y}(\varepsilon v_1) + \varepsilon u_1 \frac{\partial v_0}{\partial x} + \varepsilon v_1 \frac{\partial v_0}{\partial y} + \frac{\partial}{\partial y}(\varepsilon p_1) = 0; \qquad (37)$$

$$\frac{\partial}{\partial x}(\varepsilon u_1) + \frac{\partial}{\partial y}(\varepsilon v_1) = 0.$$

We demand that the normal velocity component vanish at $y = 0$ for the sum of the smooth part of the first approximation and the local part of the zero approximation. We then obtain

$$v_0 + \varepsilon v_1 + \varepsilon \tilde{v}_0 = 0 \quad \text{for} \quad y = 0.$$

Since $\varepsilon \tilde{v}_0 + \varepsilon \bar{v}_0(x) = 0$ for $y = 0$ according to (18), then for the smooth part of the first approximation we have the boundary condition

$$v_0 + \varepsilon v_1 = \varepsilon \bar{v}_0(x) \quad \text{for} \quad y = 0. \tag{38}$$

Condition (38) indicates that when constructing the smooth part of the first approximation the normal velocity component is taken equal to the increment acquired by this component in the zero approximation "at the limit of the boundary layer", or, more precisely, sufficiently far from the wall, where the local part $\varepsilon \tilde{v}_0$ can be neglected.

Note that in some treatments of the effect of the boundary layer on the main flow a boundary condition analogous to (38) is given, not at the wall, but on a certain line away from the wall a distance of the order of the "thickness" of the boundary layer, i. e., a distance of the order of $\varepsilon$. It is easily seen that the difference in the definition of the boundary conditions introduces an effect of the order of $\varepsilon^2$, which is insignificant as far as the first approximation is concerned.

BIBLIOGRAPHY


1. CHUDOV, L.A. Review of Boundary Layer Studies Carried out at the Computational Center of Moscow State University. — This volume.

2. SLEZKIN, N.A. Dinamika vyazkoi neszhimaemoi zhidkosti (Dynamics of Viscous Incompressible Fluids).— GITTL, Moskva. 1955.

3. LEASE, L. Modern State of the Aerodynamics of Hypersonic Flows. — Russian translation in: "Problemy dvizheniya golovnoi chasti raket dal'nogo deistviya", IL, Moskva. 1959.

4. VISHIK, M.I. and L.A.LYUSTERNIK Regulyarnoe vyrozhdenie i pogranichnyi sloi dlya lineinykh differentsial'nykh uravnenii s malym parametrom (Regular Degeneracy and Boundary-Layers for Linear Differential Equations with a Small Coefficient). — UMN, Vol.12, No.5 (77). 1957.

5. VISHIK, M.I. and L.A.LYUSTERNIK. Ob asimptotike resheniya kraevykh zadach dlya kvazilineinykh differentsialnykh uravnenii (The Asymptotic Behavior of the Solution of Boundary-Value Problems for Quasilinear Differential Equations). — DAN SSSR, Vol. 121 , No.5. 1958.

6. OLEINIK, O.A. O sisteme uravnenii pogranichnogo sloya (On the Boundary-Layer Equations). — Zhurnal Vychislitel'noi Matematiki i Matematicheskoi Fiziki, Vol.3, No.3. 1963.

*V. M. Paskonov*

## *A STANDARD PROGRAM FOR THE SOLUTION OF BOUNDARY-LAYER PROBLEMS*

The system of equations describing the flow of a viscous compressible gas in the boundary layer, with all the unknown functions depending on two space coordinates $x, y$, can formally be reduced to the following form (see /1/):

$$a_i \frac{\partial f_i}{\partial x} + b_i \frac{\partial f_i}{\partial y} = \frac{\partial}{\partial y}\left(c_i \frac{\partial f_i}{\partial y}\right) + d_i + e_i f_i, \qquad (1)$$

$$\frac{\partial \rho u}{\partial x} + \frac{\partial \rho v}{\partial y} = 0, \ (i = 1,2,\ldots, k). \qquad (2)$$

(I)

Equation (2) is the ordinary continuity equation where $u$ and $v$ are, respectively, the longitudinal and the transverse velocity component, $\rho$ the density. System (I) contains $k+1$ unknowns, namely $v$ and $f_i$ $(i = 1,2,\ldots k)$. Note that one of the $f_i$ should identically coincide with $u$, since the equation of motion can always be brought to form (1). It is assumed that the coefficients $a_i$, $b_i$, $c_i$, $d_i$, $e_i$ may depend on $v$, $f_i$ and various combinations of their derivatives. The standard form (1) suits not only the equation of motion, but also the energy equation (the equation of the temperature boundary layer), the diffusion equations for each component (equations of continuity for every individual component) when we are concerned with a flow of a multicomponent gas mixture in the boundary layer, and the radiative balance equation when we are concerned with radiative transfer in the boundary layer. System (I) also describes the boundary layer behavior for the oblique flow of a compressible gas past a cylinder or, with some approximation, for the gliding of a wing of finite span under conditions of zero lift. The flow in a wake is also described by system (I). The class of problems considerably increases if the diverse boundary conditions which can be imposed on system (I) are taken into consideration. For purposes of numerical solution of this extensive class of problems it is desirable to have a standard program which would enable the entire system (I) or at least the system (1) to be integrated for various boundary conditions, various coefficients $a_i$, $b_i$, $c_i$, $d_i$, $e_i$, and various dependence of $\rho$ on the unknown functions or their derivatives. This standard program was evolved at the Computational Center of the Moscow State University for the STRELA computer. The standard program is so written that it even permits the application of certain difference schemes for the solution of nonstationary boundary layer problems.

As in /2/, the system (I) is solved by a difference method. Equation (1) is approximated by a two-layer implicit six-point scheme. A rectangular grid is chosen on the $(x, y)$ plane

$$x = x_0 + n\Delta x, \qquad y = m\Delta y, \qquad (m, n = 0, 1, 2, \ldots),$$

and an auxiliary net

$$\begin{aligned} &x = x_0 + n\Delta x, && y = (m + {}^1/_2)\,\Delta y, \\ &x = x_0 + (n + {}^1/_2)\,\Delta x, && y = m\Delta y, \end{aligned} \qquad (m,\ n = 0, 1, 2, \ldots).$$

Note that the mesh spacings $\Delta x$ and $\Delta y$ may vary, depending on the behavior of the solutions of system (I).

The coefficients $a_i$, $b_i$, $c_i$, $d_i$, $e_i$ are computed at the auxiliary grid points (the "half-integral" or "central" points).

Setting

$$f_{im}^n = f_i(x_0 + n\Delta x, \quad m\Delta y),$$

we write the finite-difference approximation of equation (1) in the form

$$\begin{aligned} a_{im}^{n-1/2}\frac{f_{im}^n - f_{im}^{n-1}}{\Delta x} + b_{im}^{n-1/2}\frac{s_i(f_{im+1}^n - f_{im-1}^n) + (1-s_i)(f_{im+1}^{n-1} - f_{im-1}^{n-1})}{2\Delta y} = \\ = \frac{1}{\Delta y^2}\{[(1-s_i)(f_{im+1}^{n-1} - f_{im}^{n-1}) + s_i(f_{im+1}^n - f_{im}^n)]\ c_{im+1/2}^{n-1/2} - \\ - [(1-s_i)(f_{im}^{n-1} - f_{im-1}^{n-1}) + s_i(f_{im}^n - f_{im-1}^n)]\ c_{im+1/2}^{n-1/2}\} + \\ + d_{im}^{n-1/2} + e_{im}^{n-1/2}[(1-s_i)f_{im}^{n-1} + s_i f_{im}^n], \end{aligned} \qquad (3)$$

where the averaging parameter $s_i$ can be chosen differently for each equation $\left(\frac{1}{2} \leqslant s_i \leqslant 1\right)$. Note that (3) can be written in the form

$$\alpha_{im} f_{im-1}^n + \beta_{im} f_{im}^n + \gamma_{im} f_{im+1}^n = \delta_{im},$$

where

$$\begin{aligned} \alpha_{im} &= -\frac{1}{2\Delta y}\, s_i\left[b_{im}^{n-1/2} + \frac{1}{\Delta y}(c_{im}^{n-1/2} + c_{im-1}^{n-1/2})\right], \\ \beta_{im} &= \frac{1}{\Delta x}\, a_{im}^{n-1/2} + s_i\left[\frac{1}{2\Delta y^2}(c_{im+1}^{n-1/2} + 2c_{im}^{n-1/2} + c_{im-1}^{n-1/2}) - e_{im}^{n-1/2}\right], \\ \gamma_{im} &= \frac{1}{2\Delta y}\, s_i\left[b_{im}^{n-1/2} - \frac{1}{\Delta y}(c_{im+1}^{n-1/2} + c_{im}^{n-1/2})\right], \\ \delta_{im} &= \frac{1}{2\Delta y}(1-s_i)\left[b_{im}^{n-1/2} + \frac{1}{\Delta y}(c_{im}^{n-1/2} + c_{im-1}^{n-1/2})\right] f_{im-1}^{n-1} + \\ &+ \left\{\frac{1}{\Delta x}\, a_{im}^{n-1/2} - (1-s_i)\left[\frac{1}{2\Delta y^2}(c_{im+1}^{n-1/2} + 2c_{im}^{n-1/2} + c_{im-1}^{n-1/2}) - e_{im}^{n-1/2}\right]\right\} f_{im}^{n-1} - \\ &- \frac{1}{2\Delta y}(1-s_i)\left[b_{im}^{n-1/2} - \frac{1}{\Delta y}(c_{im+1}^{n-1/2} + c_{im}^{n-1/2})\right] f_{im+1}^n + d_{im}^{n-1/2}. \end{aligned} \qquad (4)$$

System (3), together with finite-difference approximation of the boundary conditions, specifies the values of $f_i$ on layer $n$, if the values of $f_i$ on the preceding $(n-1)$-th layer and the values of $a_i$, $b_i$, $c_i$, $d_i$, $e_i$ at the

corresponding points are known. This system is solved by the forcing method*.

The solution of system (I) is thus found successively on every layer. To find $f_i$ on the $n$-th layer, we first calculate the forcing coefficients in the recursion formula

$$f_{im}^{n} = A_{im} f_{im+1}^{n} + B_{im} \tag{5}$$

from the equalities

$$A_{im} = -\frac{\gamma_{im}}{\alpha_{im} A_{im} + \beta_{im}}, \qquad B_{im} = \frac{\delta_{im} - \alpha_{im} B_{im-1}}{\alpha_{im} A_{im-1} + \beta_{im}}. \tag{6}$$

$A_{i0}$ and $B_{i0}$ are found from finite-difference approximation of the boundary conditions at $y = 0$. Integration of particular systems of the type (I) may prove the necessity of increasing or decreasing $\Delta y$. The program allows doubling or halving of the mesh size $\Delta y$. To maintain the recursion formula (5) at points where $\Delta y$ is replaced by $2\Delta y$ or $\frac{1}{2}\Delta y$, the forcing coefficients are computed from equalities which somewhat differ from (6). If the mesh spacing between the $(m-2)$-th and the $(m-1)$-th points and between the $(m-1)$-th and the $m$-th points is $\Delta y$, while the spacing between the $m$-th and the $(m+1)$-th points is $2\Delta y$, the derivatives with respect to $y$ in equation (1) are approximated at the $m$-th point using the $(m-2)$-th, $m$-th, and $(m+1)$-th points, and the coefficients are computed from the formulas

$$A_{im} = -\frac{\bar{\gamma}_{im}}{A_{im-1} A_{im-2} \bar{\alpha}_{im} + \bar{\beta}_{im}}, \qquad B_{im} = \frac{\bar{\delta}_{im} - \bar{\alpha}_{im} (B_{im-1} A_{im-2} + B_{im-2})}{A_{im-1} A_{im-2} \bar{\alpha}_{im} + \bar{\beta}_{im}},$$

where $\bar{\alpha}_{im}$, $\bar{\beta}_{im}$, $\bar{\gamma}_{im}$, $\bar{\delta}_{im}$ are determined from (4) with $m-2$ substituted for $m-1$ and $2\Delta y$ for $\Delta y$.

When the mesh size changes at the $m$-th point from $\Delta y$ to $\frac{1}{2}\Delta y$, i.e., when the spacing between the $(m-1)$-th and the $m$-th points is $\Delta y$ and between the $m$-th, $(m+1)$-th, and $(m+2)$-th points it is $\frac{1}{2}\Delta y$, the derivatives with respect to $y$ in (1) are approximated at the $m$-th point using the $(m-1)$-th, $m$-th, and $(m+2)$-th points, and the coefficients are computed from

$$A_{im} = \frac{\bar{\gamma}_{im} \bar{\beta}_{im+1}}{\bar{\gamma}_{im+1} (\bar{\alpha}_{im+1} A_{im-1} + \bar{\beta}_{im}) - \bar{\gamma}_{im} \bar{\alpha}_{im+1}}, \qquad B_{im} = \frac{\bar{\gamma}_{im+1} (\bar{\delta}_{im} - \bar{\alpha}_{im} B_{im-1}) - \bar{\gamma}_{im} \bar{\delta}_{im+1}}{\bar{\gamma}_{im+1} (\bar{\alpha}_{im+1} A_{im-1} + \bar{\beta}_{im}) - \bar{\gamma}_{im} \bar{\alpha}_{im+1}}.$$

The quantities $\bar{\alpha}_{im}$, $\bar{\beta}_{im}$, $\bar{\gamma}_{im}$, $\bar{\delta}_{im}$ should be determined from (4) with $m+2$ substituted for $m+1$ and $\frac{1}{2}\Delta y$ for $\Delta y$; $\bar{\alpha}_{im+1}$, $\bar{\beta}_{im+1}$, $\bar{\gamma}_{im+1}$, $\bar{\delta}_{im+1}$ are also determined from (4) when $m$ is substituted for $m-1$, $m+1$ for $m$, $m+2$ for $m+1$, and

*[Cf., e.g., I.S. Berezin and N.P. Zhidkov, Metody vychisleniya (Numerical Methods), Vol. II. Fizmatgiz, Moskva, 1959, and later editions.]

$\frac{1}{2}\Delta y$ for $\Delta y$. The program allows 5 regions with different $\Delta y_j\,(j=1, 2, \ldots 5)$ in one layer: $m_1$ intervals of length $\Delta y_1$, $m_2$ intervals of length $\Delta y_2 = \frac{1}{2}\Delta y_1$ (or $\Delta y_2 = 2\Delta y_1$), ...., $m_5$ intervals of length $\Delta y_5 = \frac{1}{2}\Delta y_4$ (or $\Delta y_5 = 2\Delta y_4$).

Given the forcing coefficients $A_{im}$, $B_{im}$ ($i=1, 2, \ldots k$; $m=0,1, \ldots, M-1$; $M+1$ being the number of points in the ($n-1$)-th layer) on the $n$-th layer and applying the boundary conditions at the outer face of the boundary layer (for $m=M$), we can find $f_i$ at the $n$-th layer. However, seeing that as $x$ increases the boundary layer may become thicker, we should before solving (5) for $f_i$ at all the grid points, check for one of the functions $f_i$ for the matching condition

$$||f^n_{i'M}|-|f^n_{i'M-1}||<\varepsilon, \tag{7}$$

where $\varepsilon$ is a small positive number. If this condition is not satisfied on the $n$-th layer, a point with $\Delta y = y_M - y_{M-1}$ is added and the coefficients $A_{iM}$, $B_{iM}$ are found; in computing these coefficients, the limit values of $f_i$ are used at all unknown points. We thus add in the $n$-th layer as many points as necessary to ensure smooth matching for the two last points of the layer. Addition of many points in the $n$-th layer generally shows that $\Delta x$ is too large. $f_i$ in condition (7) is the function with the maximum thickness of the asymptotic boundary layer. This choice of the test function should be verified in every particular problem by numerical computations.

The continuity equation (2) is approximated by the difference equation

$$\frac{1}{2\Delta x}[(\rho u)^n_m - (\rho u)^{n-1}_m] + \frac{1}{2\Delta x}[(\rho u)^n_{m+1} - (\rho u)^{n-1}_{m+1}] + \\ + \frac{1}{\Delta y}[\rho v)^{n-1/2}_{m+1} - (\rho v)^{n-1/2}_m] = 0. \tag{8}$$

If the functions $f_i$, $\rho$ are known at all grid points on the $n$-th layer and $v_0^{n-1/2}$ can be found from the lower boundary condition for the transverse velocity component, equation (8) enables $v_m^{n-1/2}$ to be found for $m=1, 2, \ldots, M'$, where $M'$ is the number of intervals in the $n$-th layer ($M' \geqslant M$).

The coefficients $a_i$, $b_i$, $c_i$, $d_i$, $e_i$ in system (I), as indicated above, can depend on $v$, $f_i$, and various combinations of their derivatives. They are found at auxiliary points using linear interpolation over $v$ and $f_i$ and the principal points. We thus have to compute $a_i$, $b_i$, $c_i$, $d_i$, $e_i$ on the $n$-th layer as functions of unknown functions. This is carried out by iteration in the usual way. In the first approximation the values of a function on the ($n-1$) -th layer are assumed for the corresponding points of the $n$-th layer.

Systems (I) of different particular problems differ in their coefficients $a_i$, $b_i$, $c_i$, $d_i$, $e_i$, in definitions of density $\rho$, in boundary conditions at $y=0$ for $f_i$ (different formulas for $A_{io}$, $B_{io}$) and for $v$, and in upper boundary conditions for $f_i$. All these calculations should be performed using special subroutines, which can be incorporated in the main program. These subroutines, as a rule, perform simple arithmetic operations and are compiled for every particular problem anew. The core addresses of these subroutines are given by referencing the standard program according to 77 SP /3/:

| | | | | | |
|---|---|---|---|---|---|
| x | x | 4004 | $a_{csa}$ | 0 | 77 |
| x+1 | $\alpha_{csa}$ | $v_{csa}$ | $M_{max}$ | $j'$ | $m_1$ |
| x+2 | $\beta_{csa}$ | $\rho_{csa}$ | $k$ | $j_2$ | $m_2$ |
| x+3 | $\gamma_{csa}$ | $\xi_{csa}$ | $N$ | $j_3$ | $m_3$ |
| x+4 | $\delta_{csa}$ | $\zeta_{csa}$ | $i'$ | $j_4$ | $m_4$ |
| x+5 | $<\Delta y_1>$ | $<\Delta x>$ | $<\varepsilon>$ | $j_5$ | $m_5$ |

Here $\alpha_{csa}, \beta_{csa}, \gamma_{csa}, \delta_{csa}, v_{csa}, \rho_{csa}$, are the core starting addresses of the subroutines for the calculation of the following functions: 1) $A_{io}$, $B_{io}$ (initial conditions for $y=0$); 2) $a_{im}^{n-1/2}$, $b_{im}^{n-1/2}$, $d_{im}^{n-1/2}$, $e_{im}^{n-1/2}$; 3) $c_{im}^{n-1/2}$; 4) $f_{iM'}$ (upper boundary conditions); 5) $v_0^{n-1/2}$; 6) $\rho_{m-1}^{n-1}$, $\rho_m^{n-1}$, $\rho_{m-1}^n$, $\rho_m^n$.

$\xi_{csa}$ is the core starting address of the subroutine which is referenced after every iteration. This subroutine can be compiled, for example, so that it would control the convergence of iterations and suitably adjust the interval $\Delta x$, etc.

$\zeta_{csa}$ is the core starting address of a subroutine which is referenced after a required number of iterations (this number is specified in the subroutine described before) or after a pre-determined number $N$ of iterations included in referencing the program. This subroutine is generally used for controlling the computations, for finding the unknown functions from the solution obtained on the $n$-th layer, for modifying the intervals $\Delta x$ and $\Delta y$, printing out results, etc.

The initial data fed into the computer include the number of equations (1), $k$; the number of the equation for which condition (7) should be checked, $i'$; the core address of the word where the $\varepsilon$ of condition (7) is stored, $<\varepsilon>$; the core addresses of the words where $\Delta y_1$ and $\Delta x$ are stored, $<\Delta y_1>$, $<\Delta x>$; the maximum permissible number of points in a layer, $M_{max}$; the number of $\Delta y_j$ intervals in the initial layer, $m_j$ ($j=1, 2, \ldots, 5$; $m_k = 0$, if $m_l = 0$ and $k \geqslant l$, $k, l = 1, 2, \ldots, 5$).

$$j' = \begin{cases} 1, \text{ if } \Delta y \text{ is constant; then } M = \sum_{j=1}^{5} m_j. \\ 0, \text{ otherwise.} \end{cases}$$

$$j_q = \begin{cases} 0, \text{ if } \Delta y_q = 2\Delta y_{q-1}. \\ 1, \text{ if } \Delta y_q = \frac{1}{2}\Delta y_{q-1}. \end{cases} \quad (q = 2, 3, 4, 5)$$

The standard program occupies 1146 words of memory. When using the program, memory space should be allocated to the working program (0424 words), to the $(n-1)$-th layer ($kM_{max}+14$ words), to the $n$-th layer ($2k(M_{max}+1)+k+1$ words), to the storage of $s_i$ ($kl$ words, where $l$ is the number of intervals with different $\Delta y_j$ in the layer). When SSP-2 /3/ is used the program can be loaded anywhere in the computer memory.

The standard program can also be used to solve systems of type (1); a possibility is provided of bypassing the part of the program where equation (2) is integrated.

BIBLIOGRAPHY

1. SCHLICHTING, H. Grenzschichttheorie. [Russian translation. 1956.]
2. BRAILOVSKAYA, I. Yu. and L. A. CHUDOV. Reshenie uravnenii pogranichnogo sloya raznostnymi metodami (Solution of Boundary-Layer Equations by Difference Methods). — In: "Vychislitel'nye metody i programmirovanie". Izdatel'stvo MGU. 1962.
3. ZHOGOLEV, E.A. Sistema programmirovaniya s ispol'zovaniem biblioteki podprogramm (Programming with a Subroutine Library). —In: "Sistema avtomatizatsii programmirovaniya," N.P. TRIFONOV and M.R.SHURA-BURA, Editors. Fizmatgiz, Moskva. 1961.

*V. M. Paskonov and I. P. Soprunenko*

## *BOUNDARY LAYER ON SLIGHTLY WAVY WALL*

In formulating problems of boundary-layer flow it is sometimes necessary to make allowance for the waviness of the contact surface. Even slight waviness will produce periodic fluctuation of pressure. This has a considerable effect on boundary-layer flow, may lead to separation of the boundary layer, and to onset of turbulence.

A solution of the problem of potential flow on a wavy wall with sinusoidal profile $y=a_0\sin\frac{2\pi x}{\lambda}$ is given in /1/ ($x$, $y$ define Cartesian coordinates with $x$-axis parallel to the incident flow). Assuming the wave amplitude $a_0$ to be small in comparison with the wavelength $\lambda$, the expression for the downstream velocity component of the incompressible gas flow can be written

$$u = V_\infty + 2\pi a V_\infty \sin\frac{2\pi x}{\lambda} e^{-\frac{2\pi y}{\lambda}}, \tag{1}$$

and the expression for the pressure on the wall as

$$p = p_\infty - 2\pi a \rho_\infty V_\infty^2 \sin\frac{2\pi x}{\lambda}, \tag{2}$$

where $a=\frac{a_0}{\lambda}$ is the dimensional amplitude, $p_\infty, \rho_\infty, V_\infty$ are the pressure, density, and velocity at infinity.

The problem of boundary-layer flow on a slightly wavy wall was solved in /2/ assuming linearity in $a$ and expanding the stream function in powers of $x$; the expansion coefficients were taken as functions of the characteristic variable $\eta = y\sqrt{\frac{V_\infty}{\nu}}$ ($\nu=\frac{\mu}{\rho}$ is the kinematic viscosity, $\mu$ viscosity, $\rho$ density). It was found that, depending on the amplitude $a$, the boundary layer will separate at the first, second, etc., ridge. For each wave there exists an amplitude $a=a_*$ such that for all $a<a_*$ no separation occurs, while for all $a \geqslant a_*$ the boundary layer will separate at this ridge. The value of $a_*$ for the first ridge was found equal to 0.011, and separation occurred at $\frac{x}{\lambda}=0.6125$; for the second ridge, $a_*=0.0055$, with separation at $\frac{x}{\lambda}=1.6$.

In /3/ the following criterion is given for the separation of a laminar boundary layer:

$$\frac{\partial p}{\partial x}\cdot\frac{\partial^2}{u_\infty \mu} = 2, \tag{3}$$

where $u_\delta$ is the velocity at the outer face of the boundary layer. Assuming a pressure distribution (2), and boundary-layer thickness on the plate $\delta = 5.5 \cdot \frac{x}{\sqrt{Re_x}} \left( Re_x = \frac{\rho V_\infty x}{\mu} \right)$, we find that according to criterion (3) separation should first occur at $a_* = 0.0032$ at the point $\frac{x}{\lambda} = 0.52$ of the first ridge, and at $a_* = 0.0011$ at the point $\frac{x}{\lambda} = 1.515$ of the second ridge.

The present work was carried out with the purpose of establishing, by the difference method, the values of $a_*$ at which separation occurs at the first and second ridges. All the calculations were made with the standard program for solution of boundary-layer equations /4/.

Consider incompressible gas flow in the boundary layer on a wavy wall with the $x$-axis directed downstream and the $y$-axis normally. The pressure distribution (2) is assumed. In the variables $x$, $y$ the problem reduces to the following system of equations:

$$u \frac{\partial u}{\partial x} + v \frac{\partial u}{\partial y} = \frac{V_\infty^2}{\lambda} (2\pi)^2 a \cos \frac{2\pi x}{\lambda} + \nu \frac{\partial^2 u}{\partial y^2}, \qquad (4)$$

$$\frac{\partial u}{\partial x} + \frac{\partial v}{\partial y} = 0.$$

Here $u$ and $v$ are the components of the velocity vector along the $x$ and $y$ axes. System (4) should be integrated with zero boundary conditions at $y=0$ ($u=0$, $v=0$), while at the upper face of the boundary-layer $u$ is taken equal to the longitudinal component of the potential flow velocity at $y=0$:

$$u = V_\infty + V_\infty 2\pi a \sin \frac{2\pi x}{\lambda}.$$

Introducing the dimensionless quantities

$$x' = \frac{x}{\lambda}, \quad y' = \frac{y\sqrt{Re}}{\lambda}, \quad u' = \frac{u}{V_\infty}, \quad v' = \frac{v\sqrt{Re}}{V_\infty},$$

$$p' = \frac{p}{\rho V_\infty^2}, \quad \left( Re = \frac{\rho V_\infty \lambda}{\mu} \right),$$

and omitting the primes, we obtain the system of equations

$$u \frac{\partial u}{\partial x} + v \frac{\partial u}{\partial y} = (2\pi)^2 a \cos 2\pi x + \frac{\partial^2 u}{\partial y^2}, \qquad (5)$$

$$\frac{\partial u}{\partial x} + \frac{\partial v}{\partial y} = 0$$

with boundary conditions

$$u = 0, \quad v = 0$$

with $y = 0$,

$$u = 1 + 2\pi a \sin 2\pi x \qquad (6)$$

at the upper face of the boundary layer.

To determine the values of $a_*$ at the first, second, etc., ridge, system (5), (6) was integrated for various values of $a$. As the initial velocity profile, we assumed the values of $u$ and $v$ for $x = 0.01$ from the Blasius solution for a plane plate.

An analysis of the effect of mesh spacing $\Delta x$, $\Delta y$ and of the number of iterations on the accuracy with which the point of separation is determined was made for $a = 0.01$. The number of points on the initial profile was 21, $\Delta y = 0.04$. We first made calculations with a constant interval $\Delta x = 0.01$ and 6 iterations. The point of separation was found to lie between $x = 0.53$ and $x = 0.54$. When approaching the separation point, a sharp increase in the number of points in a layer was observed on passing from layer to layer, clearly a result of a poor choice of the $\Delta x$ interval. We therefore made another calculation with $\Delta x = 0.005$, starting at $x = 0.41$ and using the profile obtained with $\Delta x = 0.01$, but $\Delta y = 0.08$. The number of iterations was again 6. Up to $x = 0.46$ the results of computations with $\Delta x = 0.01$ and $\Delta x = 0.005$ were fairly close, but further on the divergence increased. The point of separation for $\Delta x = 0.005$ was found to lie between $x = 0.480$ and $x = 0.485$. Starting with the same velocity profiles for $x = 0.41$, we made another computation with $\Delta x = 0.001$. The number of iterations was increased to 12. The new velocity profile closely followed the preceding results up to $x = 0.46$. The point of separation shifted again: $0.479 < x_{sep} < 0.480$.

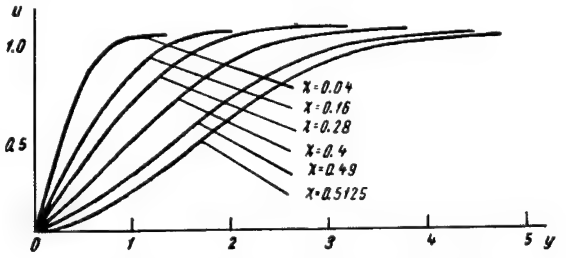


FIGURE 1. Velocity profiles $u$ for $a = 0.008$

The convergence of iterations was investigated for $x = 0.416$ and in the region near the separation point, i.e., $x = 0.476$. It was found that the convergence of iterations sharply deteriorated as we moved away from $y = 0$. A distinct deterioration of convergence was also observed near the separation point. For example, if we consider the relative convergence of iterations, $\delta u_i = \frac{|u_{i+1} - u_i|}{u_{i+1}}$ ($i$ is the iteration number), at points $y = 0.08$ for $x = 0.416$ and $x = 0.476$, then to obtain $\delta u_i < \varepsilon = 0.0003$ six iterations are needed at $x = 0.416$ as compared with twelve at $x = 0.476$.

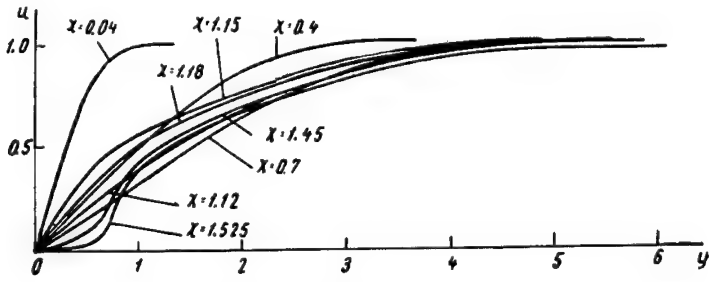


FIGURE 2. Velocity profiles $u$ for $a = 0.003$

On the strength of these results, in further calculations with various $a$ we halved the interval $\Delta x$ if the number of points in a layer more than doubled, or if the number of iterations had to be increased to more than 20 to satisfy the condition $\delta u_i < \varepsilon$ This condition (with $\varepsilon = 0.0003$) was checked at points $y = \Delta y_1$. The $y$-intervals were made variable: the first 11 points on the axis $y$ were taken with $\Delta y_1 = 0.04$, the other points with $\Delta y_2 = 0.08$. Initial $x$-interval was $\Delta x = 0.01$. As we approached the separation point, we gradually reduced $\Delta x$ until it decreased to less than 0.001. The separation was thus pinpointed to within 0.001.

Alternative claculations were made for $a = 0.01$, 0.008, 0.0065, 0.006, 0.005, 0.003, 0.002, 0.001. The results show that the amplitude $a_*$ for which separation first occurs at the first ridge lies in the interval $0.006 < a_* < 0.0065$, and at the second ridge, in the interval $0.002 < a_* < 0.003$. The separation point for various amplitudes $a$ varies as follows:

| $a$ | 0.01 | 0.008 | 0.0065 | 0.006 | 0.003 |
|---|---|---|---|---|---|
| $x_{sep}$ | 0.4775 | 0.5125 | 0.6925 | 1.45 | 1.54 |
| | first ridge | | | second ridge | |

For amplitudes $a$ at which separation occurs at the first ridge, the velocity profiles $u$ flatten out toward the separation point as $x$ increases. Figure 1 shows the velocity profiles $u$ for $a = 0.008$ (separation at first ridge), and Figure 2, for $a = 0.003$ (separation at second ridge). For the same alternatives Figure 3 gives the thickness of the boundary layer $\delta$ against $x$, as determined from matching conditions (see /4/). We see from the graphs that in the first case ($a = 0.008$) the boundary-layer thickness sharply increases toward the separation point; in the second case, there is only a slight increase in thickness.

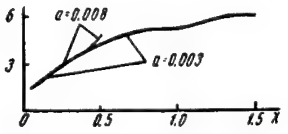


FIGURE 3. Variation of boundary-layer thickness for $a = 0.008$ and $a = 0.003$

We should also observe that for the amplitudes $a$ at which no separation occurred at the first ridge, the velocity profiles $u$ were very close to the profiles of the classical Blasius solution. For $a = 0.001$, the two profiles coincide up to $x = 0.76$.

In calculations we noted the number of iterations in each layer. The average number of iterations per layer was found to be 2—4. A somewhat higher number of iterations (5—7) was observed at the beginning of each new alternative. This is due to the fact that the initial profile did not satisfy our system of difference equations and the first stage of the computational procedure was in fact devoted to establishing a solution of adequate accuracy. As we have already observed, the number of iterations sharply increased near the separation point. It is remarkable that although for $a = 0.005$ and $a = 0.006$ no separation occurred at the first ridge, the number of iterations increased (to 6—9) for $0.58 < x < 0.7$. In this interval boundary-layer separation occurred at $a = 0.0065$.

BIBLIOGRAPHY

1. LOITSYANSKII, L.G. Mekhanika zhidkosti i gaza (Liquid and Gas Mechanics). — Gostekhteoretizdat, Moskva. 1950.

2. SOPRUNENKO, I.P. Pogranichnyi sloi na volnistoi stenke (Boundary Layer on Wavy Wall). — Izvestiya AN SSSR, seriya mekhanika i mashinostroeniya, No.2. 1962.

3. BAM-ZELIKOVICH, G.M. Raschet otryva pogranichnogo sloya (Calculation of Boundary-Layer Separation). — Izvestiya AN SSSR, otdelenie tekhnicheskikh nauk, No.12. 1954.

4. PASKONOV, V.M. A Standard Program for the Solution of Boundary-Layer Problems. — This volume.

*V. M. Paskonov and Yu. V. Polezhaev*

## *UNSTEADY MELTING OF VISCOUS MATERIAL NEAR STAGNATION POINT*

General statement of the problem of melting in a high-speed gas stream leads to simultaneous solution of a system of equations expressing the conservation of mass, momentum, and energy (for the gaseous, liquid, and solid phases, respectively).

Exact solutions available for some particular cases /1/ show that the motion of the molten film in itself does not affect the gaseous boundary layer. The equations for the gaseous phase and for the two other phases can therefore be solved separately. This considerably simplifies the problem, and we can assume that the heat flux $q_w$ and the friction $\tau_w$ satisfy the well-known formulas for a gaseous boundary layer at a stationary wall.

The present paper describes an attempt of a theoretical computation of the process of unsteady breakdown of a viscous glassy material.

The thickness of the liquid film, even in such viscous materials as molten quartz glass, is much less than the size of the body, and the equations describing the moving film therefore have the ordinary form of equations for a laminar boundary layer.

The density of the melt is practically independent of temperature, and the flow can therefore be regarded as incompressible. Specific heat and heat conductivity are also assumed constant, since their temperature dependence is substantially weaker than that of the viscosity of molten glass.

The system of equations of unsteady motion of the molten film thus has the form (in the coordinate system depicted in Figure 1):

$$\frac{\partial}{\partial x}(ru) + \frac{\partial}{\partial y}(rv) = 0, \tag{1}$$

$$\frac{\partial u}{\partial \tau} + u\frac{\partial u}{\partial x} + v\frac{\partial u}{\partial y} = -\frac{1}{\rho}\cdot\frac{\partial p}{\partial x} + \frac{1}{\rho}\cdot\frac{\partial}{\partial y}\left(\mu\frac{\partial u}{\partial y}\right), \tag{2}$$

$$\frac{\partial T}{\partial \tau} + u\frac{\partial T}{\partial x} + v\frac{\partial T}{\partial y} = \lambda\frac{1}{\rho c_p}\cdot\frac{\partial^2 T}{\partial y^2}. \tag{3}$$

Here $x$, $y$ are Cartesian coordinates; $\tau$ time; $u$, $v$ the velocity components along $x$, $y$ axes; $r$ the distance to the axis of symmetry of the body; $T$ the temperature; $p$ the pressure; $\rho$ the density; $\mu$ the viscosity; $\lambda$ the heat conductivity; $c_p$ is the specific heat at constant pressure.

We now make certain simplifying assumption.

1. If we confine ourselves to the motion of the molten film near the critical point of a bluff body, we may take $r = x$, $\frac{\partial T}{\partial x} = 0$, and consider the velocity component $u$ to be a linear function of $x$.

2. Provisional estimate show that inertia and time terms in equation (2) are of higher order of smallness than the terms in the right member. Equation (2) is therefore considerably simplified. Seeing that in the neighborhood of the critical point $\frac{dp}{dx} = ax$, where $a = \text{const}$, we can eliminate the variable $x$ and the velocity component $u$ from equations (1), (2), (3).

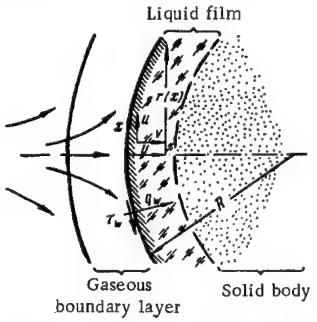


FIGURE 1. Schematic physical diagram of flow and the coordinate system

The problem is thus reduced to a system in two independent variables $(y, \tau)$ for two unknown functions $v$ and $T$:

$$\frac{\partial^2 v}{\partial y^2} + \frac{2}{\mu}\left(\frac{d\tau_w}{dx} + \frac{d^2p}{dx}\, y\right) = 0, \tag{4}$$

$$\frac{\partial T}{\partial \tau} - \frac{\lambda}{\rho c_p}\,\frac{\partial^2 T}{\partial y^2} + v\,\frac{\partial T}{\partial y} = 0, \tag{5}$$

where $\tau_w$ is the skin friction at the film surface, which is assumed to be known from the solution of the gaseous boundary layer.

Owing to the peculiar features of glassy materials, which do not have a fixed melting point, we should solve this system simultaneously in the liquid and in the solid phase, setting the boundary conditions in the form

$$\begin{gathered} \text{for } \tau = 0 \quad T = T_{\text{csa}}, v(y) = v_{\text{csa}}; \\ \text{for } y = 0 \quad \lambda \frac{dT}{dy} + q_w(T_w) = 0, \quad v(\tau) = 0; \\ \text{for } y = \infty \quad T(\tau) = T_{\text{csa}}, \quad \frac{\partial v}{\partial y} = 0. \end{gathered} \tag{6}$$

The heat flux to the film, $q_w$, should be known from the solution of the gaseous boundary layer. If we additionally assume that neither evaporation nor chemical reactions with the components of the incident gas stream occur at the surface of the film, the heat transfer to this surface is very simple to calculate, e. g., from the well-known formulas of Fay and Riddle /2/. Equations (4), (5) with boundary and initial conditions (6) were solved by the standard program for the solution of boundary-value problems /3/ developed at the Computational Center of the Moscow State University. The equations were approximated by a two-layer six-point implicit scheme utilizing a standard rectangular grid on the $(y, \tau)$ : $\tau = \tau_0 + n\Delta\tau$; $y = m\Delta y$. The system of difference equations was solved by the forcing method.

The choice of the corresponding mesh size $\Delta y$ on the initial layer was based on the analogy of this problem with the problem of heating. Indeed, it is clear that the moving film of molten glass will appear on the surface of the body only 1 - 2 seconds after the onset of heating, since the viscosity of quartz glass even at 2000°K is still very high (of the order of $10^{13}$ poise). Known analytical solutions of the problem of unsteady heating of solids /4/ enable us to determine the rate of variation of surface temperature and the depth of heating in the first 1 - 2 seconds before the formation of the liquid film. Physical considerations show that these rates at least should not increase after the molten film has formed. On the other hand, certain limitations on the time interval are imposed by the nonlinear variation of the heat flux $q_w$ with the surface temperature $T_w$. When approximating the boundary conditions for the $n$-th time layer we were forced to employ the values of $q_w\ (T_w)$ calculated on the $(n-1)$-th layer, and therefore the difference $q_w(T_w^{(n)}) - q_w(T_w^{(n-1)})$ had to be sufficiently small.

For these reasons we took $\Delta\tau$ equal to 0.02 sec and $\Delta y = 1.10^{-4}$m.

The process of unsteady heating increases the region of integration, in other words, the number of points on the $n$-th layer should be greater than or equal to the number of points on the $(n-1)$-th layer.

A provision is made in the program for the definition of the domain of integration from the condition of smooth matching of temperature with its value at infinity (since the temperature boundary layer here is much larger than the dynamic layer). The number of points on the layer is automatically determined by the inequality

$$\left| |T_M^n| - |T_{M-1}^n| \right| < \varepsilon, \qquad (7)$$

where $\varepsilon$ was set equal to 1. In some alternatives we even assumed $\varepsilon=10$, since this did not affect the flow of the film.

The results of test runs showed that the time required for a steady regime of melting to set in may be as high as 15 — 20 seconds. The unsteady-state curve leading to the steady state is very gentle, and variation of all parameters past the midpoint of the process is slight. With the object of reducing machine time, we made a provision for doubling $\Delta\tau$, $\Delta y$ and $\varepsilon$ when the number of points on a layer reached 128.

It was found, however, that with this program doubling the mesh size might lead to certain weakly damped fluctuations in temperature and velocity values. On the other hand, we could set up an alternative procedure for reducing the volume of computations. The behavior of the velocity and temperature profiles is such that the highest gradients are observed at the film surface, near $y=0$. It is therefore advisable to use a variable $y$-interval. This we did, and together with overall reduction in the number of points per layer substantially improved the approximation in the range of high gradients, since $\Delta y$ was reduced by an order of magnitude.

The $y$-mesh was defined as follows, starting with $y=0$: 6 intervals of $1 \cdot 10^{-5}$m each, 4 intervals of $2 \cdot 10^{-5}$m, 4 intervals of $4 \cdot 10^{-5}$m, 4 intervals of $8 \cdot 10^{-5}$ m, and all other intervals, up to the boundary defined by the condition of smooth matching, equal to $1.6 \cdot 10^{-4}$m.

This mesh size distribution was chosen on the basis of an analysis of previously calculated alternatives with the object of ensuring as fine a resolution as possible of the flow of the liquid film. One of the previous alternatives was re-run with the new $y$-mesh and constant $\Delta\tau = 0.02$ sec.

Comparison of results showed on the whole a good agreement of the ablation rate in both cases, but the steady surface temperature and the velocity profiles in the initial period somewhat differed.

Since allowance for nonlinearity of the system in the standard program makes it necessary to carry out iterations in every time section, we had to determine the number of iterations ensuring desired accuracy.

An analysis of the results showed that the convergence depends on various parameters of the problem: rate of heating, properties of the material, given time instant, etc. However, as a rule, satisfactory results could be obtained at the third step already, and the conclusive run of the problem therefore employed three iterations.

We see from the summary table of the alternative calculations that in the first five alternatives only the parameters of the incident flow were changed. The heat flux and the friction at the film surface, and also the second derivative of pressure and the enthalpy gradient in the boundary layer were determined from the following relations /5/:

$$\frac{q_w}{I_\infty - I_w} = \left(\frac{\alpha}{c_p}\right)_g = 0.763\sqrt{\beta\rho_g\mu_g}\,Pr_g^{0.6};$$

$$\frac{\partial\tau}{\partial x} = -1.7\,\frac{q_w}{I_\infty - I_w}\,\beta Pr_g^{0.6};$$

$$\frac{d^2p}{dx^2} = -\rho_g(\beta)^2;$$

$$I_\infty - I_w = \sqrt{a(T_w - T_0) + b}\,; \quad T_0 = 300^\circ\mathrm{K},$$

where $\rho_g$ is the density and $\mu_g$ the viscosity of the gas at stagnation temperature $T_\infty$, $Pr_g$ is the Prandtl number, $\beta$ the velocity gradient near the critical point, and the constants $a$ and $b$ are functions of the stagnation temperature and the properties of the incident gas. In particular, we assumed

$$a = -4013,\ b = 11.156 \cdot 10^6.$$

Individual alternatives (I-V) differed only in the velocity gradient at the critical point $\beta = \left(\frac{du}{dx}\right)_\infty$, which varied in the range $4 \cdot 10^4 \leqslant \beta \leqslant 1.2 \cdot 10^5$; This corresponded in our calculations to a variation of the heat flux from 400 kcal/m$^2$ sec to 700 kcal/m$^2$ sec at $T_w = 2800^\circ$K.

In alternative VI we altered the constants in the formula for the temperature dependence of the viscosity of molten glass. In alternative VII we changed the heat conductivity $\lambda$, keeping the thermal diffusivity $\frac{\lambda}{\rho c_p}$ constant.

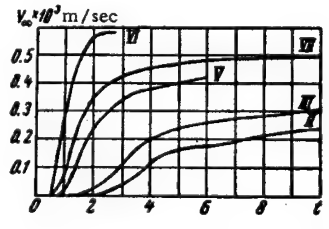


FIGURE 2. Rate of ablative mass loss vs. time in various alternatives

The results are plotted in Figures 2—9. The variation of the ablation rate $v_\infty$ in time is given in Figure 2. Clearly, an increase of the heat transfer coefficient $(\alpha/c_p)_g$ in alternatives I-V produces a sharp increase in the rate of approach to the steady state. In the limit, with very large heat fluxes, the steadying time should be

arbitrarily small. Decrease of viscosity (alternative VI) and decrease of heat conductivity of the material (alternative VII) produce a similarly directed effect. It is noteworthy that the thermal diffusivity $a = \frac{\lambda}{\rho c_p}$ and the parameters of the incident flow in alternative VII were as in alternative V. Heat conductivity thus affects the steadying trend not only directly, as a boundary condition, but also indirectly via thermal diffusivity.

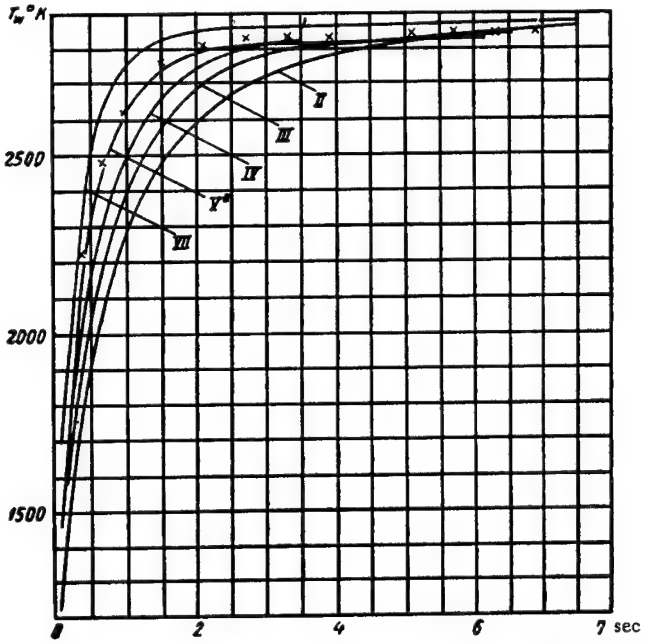


FIGURE 3. Surface temperature of liquid film vs. time in various alternatives

Figure 3 shows the variation of the surface temperature of the molten film as a function of time in various alternatives. The general trend of temperature toward the steady state is similar to the steadying curve of the ablation rate (alternatives I - V).

However, the effect of the properties of the material on the steadying process and on the stationary value of temperature is much more pronounced. For example, a reduction of viscosity by a factor of about 35 (alternative VI) sharply lowered the stationary temperature of the film surface (by more than 200°) and substantially accelerated the rate at which the system reached this temperature. We thus see that inaccuracies in the determination of viscosity, a parameter which is notoriously difficult to measure accurately, can produce considerable deviations of the calculated results from the experimental values.

Much weaker, though still marked, is the effect of the heat conductivity on surface temperature.

Figures 4 and 5 give dimensionless velocity and temperature profiles at three successive times, calculated for the incident flow parameters

and the material properties of alternative V. We have previously remarked that alternative V was run with two grids: one with a constant mesh size and one with a variable $y$-interval.

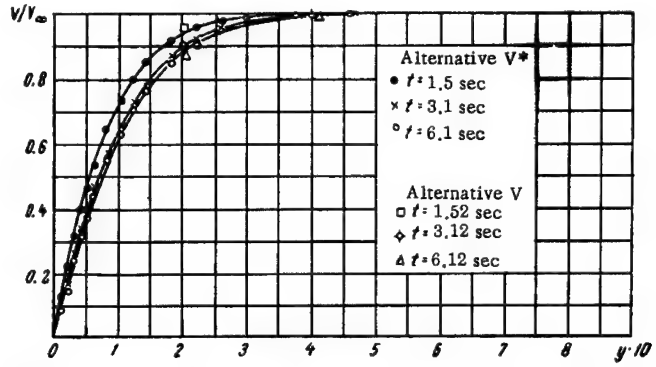


FIGURE 4. Comparison of dimensionless profiles of ablation rate for three time instants and different $\Delta y$ (alternatives V and V*)

Figures 4 and 5 illustrate the changes in temperature and velocity distributions produced by change of mesh size. It should be observed that the constant and fairly coarse mesh size $\Delta y$ in alternative V made a poor allowance for the liquid layer. It suffices to say that even when the molten film flowed freely, the entire liquid layer was represented by 3 - 4 points. This clearly did not enable the velocity gradient to be allowed for accurately and consequently gave a low value of the ablation rate. Nevertheless, the general trend of the ablation rate and the surface temperature in alternative V with constant mesh and alternative V* with variable mesh was the same (see Figures 2 and 3).

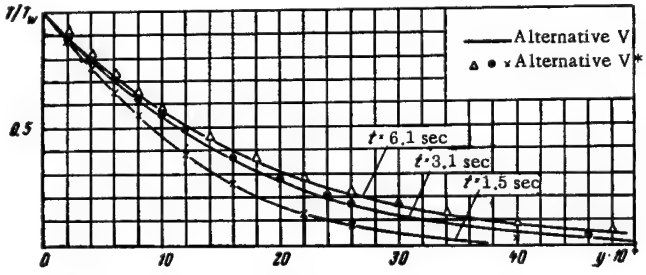


FIGURE 5. Comparison of dimensionless temperature profiles for the interior of the body for three time instants and different $\Delta y$ (alternatives V and V*)

Of considerable interest are the results plotted in Figure 6. It shows the effect of the material properties and the incident flow parameters on the unsteady temperature profile.

Comparison of curves I and V* shows that the heat transfer coefficient $(\alpha/c_p)_g$, which characterizes the rate of heating, has a considerable influence on the heating depth and the film flow. With small heat transfer

coefficients, the material is heated to a considerable depth, the film formed is very thin (since the external forces, namely friction and surface pressure gradient, are small), and the major part of the heat is transmitted to the interior layers. A concurrent reduction of heat conductivity (alternative VII) substantially reduces the heating depth.

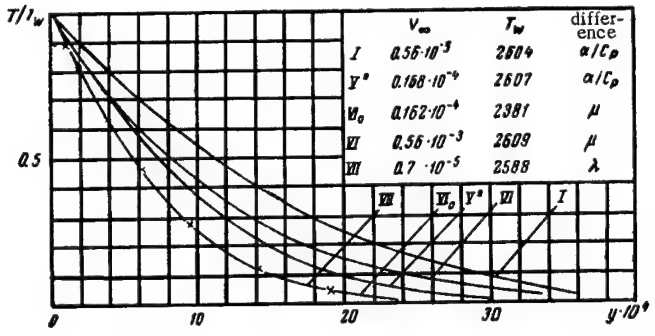


FIGURE 6. The effect of material properties and incident flow parameters on the unsteady temperature profile

Of special interest is a comparison of curves V* and VI. It is known /6/ that in the case of stationary film melting, the temperature profile is adequately approximated by the exponential curve

$$\frac{T-T_0}{T_w-T_0}=e^{-\frac{v_\infty y}{a}},$$

where $a=\frac{\lambda}{\rho c_p}$ is the thermal diffusivity. It might appear that an exponential dependence would also apply in the unsteady case, letting the ablation rate $v_\infty$ vary with time. Curves $VI_0$ and V* in Figure 6 show this to be wrong. Moreover, in spite of the constancy of $a=\frac{\lambda}{\rho c_p}$ and nearly equal values of $v_\infty$ in the two alternatives, the surface temperature gradients and the heating depths are entirely different. This simple dependence thus does not hold in the unsteady case, and this clearly imposes definite limitations on the validity of integral methods for these problems.

The coincidence of curves VII (crosses) and $VI_0$ in Figure 6 is purely accidental.

The numerical results obtained show that the time required to reach equilibrium between the processes of heating, heat conduction, and transfer of heat by the liquid phase may in some cases be 10 seconds and more. This can have a decisive influence in calculating the mass loss by viscous glassy materials in gas streams, whose parameters vary with time (in particular, in the case of an atmospheric entry trajectory). The accuracy provided for these problems by the quasistationary equations of heat conduction and liquid-film motion will apparently be very low.

It is noteworthy that the time required to reach steady surface temperature is much lower than that corresponding to the ablation rate.

Table of alternative calculations

| Alternative | $\Delta x$ | $\Delta y$ | $\varepsilon$ | Heat flux | | | Material properties | | Viscosity $\mu=\exp\left(\frac{\bar{\alpha}}{T+300}-\bar{\beta}\right)$ | | $2\frac{d^2p}{dx^2}$ | $2\frac{d\tau_w}{dx}$ |
|---|---|---|---|---|---|---|---|---|---|---|---|---|
| | | | | $\frac{a}{c_p}$ | $-a$ | $b$ | $1/\lambda$ | $\frac{\lambda}{\rho c_p}$ | $\bar{\alpha}$ | $\bar{\beta}$ | | |
| I | 0.33 | $9\cdot10^{-5}$ | 1 | 0.39 | 4013 | $11.156\cdot10^6$ | $0.2\cdot10^4$ | $0.842\cdot10^{-6}$ | 68800 | 24.59 | $0.178\cdot10^8$ | $0.43\cdot10^4$ |
| II | 0.02 | $1\cdot10^{-4}$ | 1 | 0.39 | 4013 | $11.156\cdot10^6$ | $0.2\cdot10^4$ | $0.842\cdot10^{-6}$ | 68800 | 24.59 | $0.29\cdot10^8$ | $0.63\cdot10^4$ |
| III | 0.02 | $1.10^{-4}$ | 1 | 0.5 | 4013 | $11.156\cdot10^6$ | $0.2\cdot10^4$ | $0.842\cdot10^{-6}$ | 68800 | 24.59 | $0.55\cdot10^8$ | $0.97\cdot10^4$ |
| IV | 0.02 | $1.10^{-4}$ | 1 | 0.57 | 4013 | $11.156\cdot10^6$ | $0.2\cdot10^4$ | $0.842\cdot10^{-6}$ | 68800 | 24.59 | $0.11\cdot10^9$ | $0.15\cdot10^5$ |
| V | 0.02 | $2\cdot10^{-4}$ | 1 | 0.65 | 4013 | $11.156\cdot10^6$ | $0.2\cdot10^4$ | $0.842\cdot10^{-6}$ | 68800 | 24.59 | $0.18\cdot10^9$ | $0.22\cdot10^5$ |
| V* | 0.02 | $1\cdot10^{-5}$ var. | 10 | 0.65 | 4013 | $11.156\cdot10^6$ | $0.2\cdot10^4$ | $0.842\cdot10^{-6}$ | 68800 | 24.59 | $0.18\cdot10^9$ | $0.22\cdot10^5$ |
| VI | 0.02 | » | 10 | 0.65 | 4013 | $11.156\cdot10^6$ | $0.2\cdot10^4$ | $0.842\cdot10^{-6}$ | 68800 | 28.0 | $0.18\cdot10^9$ | $0.22\cdot10^5$ |
| VII | 0.02 | » | 10 | 0.65 | 4013 | $11.156\cdot10^6$ | $0.25\cdot10^4$ | $0.842\cdot10^{-6}$ | 68800 | 28.0 | $0.18\cdot10^9$ | $0.22\cdot10^5$ |

This shows that the flow of the liquid film substantially modifies the rate of heat redistribution in the body.

In conclusion we should observe that in so far as the data on the physicochemical properties of materials are widely scattered in the literature, no reliable computations can be made of the processes of heating and ablation followed by a comparison of the results with adequate experimental data.

BIBLIOGRAPHY


1. SCALA and SUTTON. The Two-Phase Hypersonic Laminar Boundary Layer — A Study of Surface Melting. — Heat Transfer and Fluid Mechanics Institute. 1958.
2. FAY and RIDDLE. Theoretical Analysis of Heat Transfer at the Frontal Point Ablated by Dissociated Air. [Russian translation. 1959.]
3. PASKONOV, V.M. A Standard Program for the Solution of Boundary-Layer Problems. — This volume.
4. LYKOV, A.V. Teoriya teploprovodnosti (Theory of Heat Conduction). — GITTL, Moskva. 1952.
5. SIBULKIN, M. .Teploperedacha vblizi perednei kriticheskoi techki tela vrashcheniya (Heat Transfer near the Frontal Critical Point of a Body of Revolution). — In: "Mekhanika," No. 3. 1943.
6. BETHE, H.A. and ADAMS, M.C. A Theory for the Ablation of Glassy Material. — Journal of the Aero Space Sciences, Vol. 26, No. 6. 1959.

*T. S. Varzhanskaya, E. I. Obroskova, and E. N. Starova*

## *BOUNDARY LAYER NEAR THE CRITICAL POINT*

1. The paper presents an analysis of compressible laminar boundary layer near a critical point on a porous flat wall in a stream of air. A light gas — hydrogen — permeates through the wall at a constant rate. The boundary-layer equations with an allowance for diffusion have the following form in dimensionless coordinates:

$$\begin{gathered}
\rho u \frac{\partial u}{\partial x} + \rho v \frac{\partial u}{\partial y} = \frac{\partial}{\partial y}\left(\mu \frac{\partial u}{\partial y}\right) + x, \\
\frac{\partial}{\partial x}(\rho u) + \frac{\partial}{\partial y}(\rho v) = 0, \\
\rho u \frac{\partial c}{\partial x} + \rho v \frac{\partial c}{\partial y} = \frac{\partial}{\partial y}\left(\rho D_{12} \frac{\partial c}{\partial y}\right) \frac{1}{Pr_{g\infty}}, \\
\bar{\rho} \bar{c}_p \left(u \frac{\partial \theta}{\partial x} + v \frac{\partial \theta}{\partial y}\right) = \frac{\partial}{\partial y}\left(\lambda \frac{\partial \theta}{\partial y}\right) \frac{1}{Pr_\infty} + \\
+ \rho D_{12} \tilde{c}_p \frac{\partial c}{\partial y} \frac{\partial \theta}{\partial y} \cdot \frac{1}{Pr_{g_\infty}}.
\end{gathered} \tag{1}$$

Since the external flow velocity near the critical point is low ($M_\infty \approx 0$), we neglect energy dissipation.

The boundary conditions are

$$\begin{gathered}
\text{for } y = 0, \quad u = 0, \quad c = c_w, \quad \theta = 1, \\
v = -\frac{D_{12}}{1 - c_w} \cdot \frac{\partial c}{\partial y} \cdot \frac{1}{Pr_{g_\infty}}; \\
\text{for } y = \infty, \quad u = x, \quad c = 0, \quad \theta = 0.
\end{gathered} \tag{2}$$

The condition for $v$ at the wall is derived in /1/. The following notations are used here: $x$, $y$ the Cartesian coordinates reckoned from the critical point, with the $x$-axis directed parallel to the wall and the $y$-axis perpendicular to it; $u, v$ the horizontal and the vertical velocity components; $\theta = \frac{T - T_\infty}{T_w - T_\infty}$, where $T$ is the absolute temperature; $c$ the concentration of inblown hydrogen (ratio of the hydrogen density to the density of the air-hydrogen mixture); $\rho$ density; $\mu$ viscosity; $D_{12}$ diffusivity; $\lambda$ heat conductivity; $\nu = \frac{\mu}{\rho}$; $c_{p1}$, $c_{p2}$ the specific heats at constant pressure for the

first and second components of the gas mixture, respectively, $\bar{c}_p = cc_{p1} + (1-c)c_{p2}$; $Pr_\infty$ the Prandtl number; $Pr_{g\infty}$ the diffusion Prandtl number.

The subscript «$w$» indicates values at the wall, i. e., at $y=0$, and the subscript «$\infty$» refers to the point at infinity. The unknown functions in this system are $\theta$, $c$, $u$, $v$. The physical parameters of the boundary layer $\mu$, $\rho$, $D_{12}$ etc., are assumed to vary with concentration and temperature:

$$\lambda = \frac{18.0c^3 + 3.71c^2 + 0.224c + 0.0034}{1.99c^3 + 0.8c^2 + 0.0946c + 0.0034} \cdot \frac{1.2}{1.2 - 0.5\theta}(1 - 0.5\theta)^{1.5},$$

$$\rho = \frac{1}{(1-0.5\theta)(1+13.5c)},$$

$$\mu = \frac{1.2}{1.2-0.5\theta}(1-0.5\theta)^{1.5} \times$$

$$\times \left( \frac{0.479}{1 + 0.13\frac{1-c}{c}} + \frac{1}{1 + 3.95\frac{c}{1-c}} \right), \qquad (3)$$

$$\bar{c}_p = (1 - 0.5\theta)^{0.19}(13.15c + 1),$$

$$D_{12} = (1 - 0.5\theta)^2,$$

$$\tilde{c}_p = \frac{c_{p_1\infty}}{c_{p_2\infty}} c_{p_1} - c_{p_2} = 13.15(1 - 0.5\theta)^{0.19},$$

$$Pr_{g\infty} = 0.151, \quad Pr_\infty = 0.73.$$

These relations are taken over from /2/ for the case $\frac{T_w}{T_\infty} = 0.5$.

2. The system of partial differential equations near the critical point in the case $\rho_w u_w = \text{const}$ (constant flow rate at the wall) can be reduced by Dorodnitsyn's transformation /3/ $x = x$, $Y = \int_0^y \rho dy$, $V = \rho v + u\frac{dY}{dx}$ and the similarity transformation /4/ $x = x$, $\eta = Y$, $\psi = xf$, where $f' = \frac{u}{x}$, and $\psi$ is a dimensionless stream function such that $\frac{\partial\psi}{\partial Y} = u$, $\frac{\partial\psi}{\partial x} = -V$, to a system of nonlinear ordinary differential equations in $c(\eta)$, $\theta(\eta)$ and $f(\eta)$:

$$(\mu\rho f'')' + ff'' - f'^2 = -\frac{1}{\rho},$$

$$(\lambda\rho\theta')'\frac{1}{Pr_\infty} + \frac{\rho^2 D_{12}}{Pr_{g\infty}}\tilde{c}_p c'\theta' + \bar{c}_p f\theta' = 0,$$

$$\frac{1}{Pr_{g\infty}}(\rho^2 D_{12}c')' + fc' = 0 \qquad (4)$$

with the boundary conditions

$$\eta = 0: \; f' = 0, \; \theta = 1, \; c = c_w, \; f = \frac{(\rho^2 D_{12})_w}{1 - c_w} c_w \frac{1}{Pr_{g\infty}};$$

$$\eta = \infty: \quad f' = 1, \quad \theta = 0, \quad c = 0. \qquad (5)$$

We solved system (4) by the following iterative procedure:

1°. Choose a zero approximation for functions $f$, $\theta$, $c$: $f^0(\eta)$, $\theta^0(\eta)$, $c^0(\eta)$.

2°. Insert the zero approximation $f^0(\eta)$, $\theta^0(\eta)$, $c^0(\eta)$ in the coefficients of the third equation.

Solving the boundary-value problem for the new linear equation, we find the first approximation $c^1(\eta)$ for the function $c(\eta)$.

3°. Substituting $f^0$ and $\theta^0$ for the functions $f$ and $\theta$ in the coefficients of the second equation, and $c^1$ for $c$, we find $\theta^1(\eta)$.

4°. Substituting $f^0$, $\theta^1$, $c^1$ for the functions $f$, $\theta$, $c$ in the coefficients of the first equation, we solve it for $f^1(\eta)$. We now iterate the entire procedure with the first approximation to find the second approximation $f^2(\eta)$, $\theta^2(\eta)$, $c^2(\eta)$, etc. The process is continued until the difference between two successive approximations (for every function for all $\eta$) becomes less than a preassigned $\varepsilon$. The linear boundary-value problems arising in every step are solved by the forcing method. Application of the forcing method to the solution of equations of second order is described, e. g., in /6/. We shall therefore dwell on the solution of the first equation only.

We rewrite this equation in the form

$$Pf''' + Qf'' - Kf' + L = 0,$$

where

$$P = \mu\rho, \quad Q = (\mu\rho)' + f, \quad K = f', \quad L = \frac{1}{\rho}$$

are unknown functions of $\eta$.

For $\eta = 0$ we have to satisfy the boundary conditions $f = f_w$, $f' = 0$. The condition $f' = 1$ at infinity is transferred to the point $\eta = l$ and we solve the boundary-value problem in the interval $0 < \eta < l$ (in our case, with $c_w = 0 - 0.9$ and $\varepsilon = 10^{-3}$, we could take $l = 7.5$). The interval $l$ is divided into $n$ equal parts. At the grid points $\eta_0 = 0$, $\eta_1 = h$, ..., $\eta_k = kh$, ..., $\eta_n = l$, the equation is approximated by the following finite-difference relations ($f_k = f(kh)$. $h = \frac{l}{n}$):

$$P_k \frac{f_{k+2} - 2f_{k+1} + 2f_{k-1} - f_{k-2}}{2h^3} + Q_k \frac{f_{k+1} - 2f_k + f_{k-1}}{h^2} -$$

$$- K_k \frac{f_{k+1} - f_{k-1}}{2h} + L_k = 0 \text{ for } k = 2\ 3, \ldots n-2. \tag{6}$$

$$P_{n-1} \frac{1}{h^3} \left[ f_n - 3f_{n-1} + 3f_{n-2} - f_{n-3} + \frac{1}{2}(f_n - 4f_{n-1} + 6f_{n-2} - \right.$$

$$\left. - 4f_{n-3} + f_{n-4}) \right] + Q_{n-1} \frac{1}{h^2} \left[ f_n - 2f_{n-1} + f_{n-2} - \right.$$

$$\left. - \frac{1}{12}(f_n - 4f_{n-1} + 6f_{n-2} - 4f_{n-3} + f_{n-4}) \right] -$$

$$- K_{n-1} \frac{1}{2h}(f_n - f_{n-2}) + L_{n-1} = 0 \tag{7}$$

at the point $\eta_{n-1} = (n-1)h$.

The boundary conditions are written in finite differences in the form

$$\eta = 0: \quad \frac{-f_2 + 4f_1 - 3f_0}{2h} = 0,$$

$$f_0 = \frac{(\rho^2 D_{12})_w}{1 - c_w} \cdot \frac{(-c_2 + 4c_1 - 3c_0)}{2h} \cdot \frac{1}{Pr_{g\infty}};$$

$$\eta = l: \quad \frac{f_{n-2} - 4f_{n-1} + 3f_n}{2h} = 1.$$

From (6) we find that the coefficients $A_k$, $B_k$, $C_k$ in the forcing equation

$$f_k = A_k f_{k+1} + B_k f_{k+2} + C_k \tag{8}$$

satisfy the following recursion formulas

$$A_k = \frac{\gamma_k + \delta_k B_{k-1} + \lambda_k A_{k-2} B_{k-2}}{\alpha_k - \delta_k A_{k-1} - \lambda_k B_{k-2} - \lambda_k A_{k-2} A_{k-1}},$$

$$B_k = \frac{\beta_k}{\alpha_k - \delta_k A_{k-1} - \lambda_k B_{k-2} - \lambda_k A_{k-2} A_{k-1}},$$

$$C_k = \frac{\delta_k C_{k-1} + \lambda_k C_{k-2} + \lambda_k A_{k-2} C_{k-1} + \nu_k}{\alpha_k - \delta_k A_{k-1} - \lambda_k B_{k-2} - \lambda_k A_{k-2} A_{k-1}},$$

where

$$\alpha_k = 2Q_k h, \quad \beta_k = \frac{P_k}{2}, \quad \gamma_k = Q_k h - \left(P_k + \frac{K_k}{2} h^2\right),$$

$$\delta_k = Q_k h + \left(P_k + \frac{K_k}{2} h^2\right), \quad \lambda_k = -\frac{P_k}{2}, \quad \nu_k = L_k h^2,$$

$$P_k = (\mu\rho)_k, \quad Q_k = \frac{(\mu\rho)_{k+1} - (\mu\rho)_{k-1}}{2h} + f_k, \quad K_k = \frac{f_{k+1} - f_{k-1}}{2h}.$$

From these formulas we can compute all the forcing coefficients starting with $A_2$, $B_2$, $C_2$, and ending with $A_{n-2}$, $B_{n-2}$, $C_{n-2}$. The coefficients $A_0$, $B_0$, $C_0$, $A_1$, $B_1$, $C_1$ are determined using the left-hand boundary conditions:

$$A_0 = 0, \quad B_0 = 0, \quad C_0 = f_w,$$

$$A_1 = \frac{1}{4}, \quad B_1 = 0, \quad C_1 = \frac{3}{4} f_w.$$

Applying (7) and the right-hand boundary conditions, and also the forcing relations at points $n-2$, $n-3$, $n-4$, we find $f_n$ and $f_{n-1}$. Then by reverse forcing, from (8) we find $f_{n-2}$, $f_{n-3}, \ldots, f_1$. To improve the convergence of the scheme, having calculated $f^i$, $\theta^i$, $c^i$, we substitute the functions $\frac{f^{i-1} + f^i}{2}$, $\frac{\theta^{i-1} + \theta^i}{2}$, $\frac{c^{i-1} + c^i}{2}$ $(i = 1, 2, \ldots)$ in the coefficients of the equation to obtain the next approximation. We tried several alternatives for various hydrogen concentrations at the wall: $c_w = 0$; 0.2; 0.4; 0.6; 0.8; 0.9, for $\varepsilon = 10^{-3}$ and $l = 7.5$.

For $c_w = 0.2$, we assumed as zero approximation linear functions for $c$ and $\theta\left(c^0 = \frac{c_w}{l}(l-\eta), \theta^0 = \frac{1}{l}(l-\eta)\right)$, and the Blasius function for $f^0(\eta)$ (except for the value on the wall, where $f_w = \frac{(\rho^2 D_{12})_w}{1 - c_w} c_w' \frac{1}{Pr_{g\infty}}$).

For $c_w = 0.4$, as the zero approximation for all $\eta > 0$ served the solution obtained with $c_w = 0.2$, and for $\eta = 0$, $c = c_w = 0.4$.

For $c_w = 0.6$, as the zero approximation for all $\eta > 0$ served the solution obtained with $c_w = 0.4$, and $c = 0.6$ with $\eta = 0$, etc.

For $c_w = 0$, the zero approximation was $c^0 = 0$ for all $\eta$, $\theta^0 = \frac{1}{l}(l-\eta)$, and $f^0$ was taken as $f = f(\eta)$ obtained for $c_w = 0.9$.

For $c_w = 0.2$ we tried $h = 0.15$, 0.075, and 0.0375.

Comparison of the results at corresponding points $\eta$ shows that $h = 0.15$ is too coarse (this shortcoming is particularly pronounced near the wall). Mesh size $h = 0.075$ gives much more satisfactory results, while for identical $\eta$ the results obtained with $h = 0.075$ and $h = 0.0375$ differ only slightly.

Subsequent computations for high concentrations $c_w$ were made with $h = 0.0375$.

The variation of $c$, $\theta$, $f$, $f'$ with $\eta$ for various $c_w$ on the wall is shown in Figures 1 - 4. We see that the functions $c$, $\theta$, $f'$ reach an asymptote at $\eta < 7.5$. Figure 4 gives the velocity profiles $\frac{u}{x} = f'$. We see from these plots that for $c_w = 0$, $f'$ is always less than 1, i. e., the velocity in the layer is less than the velocity at exterior points. For all $c_w > 0$, $f'$ reaches a maximum in the layer, i. e., in the layer the velocity is higher than the velocity at exterior points. As the hydrogen concentration at the wall increases, $f'$ rises considerably and $f''$ at the wall also increases.

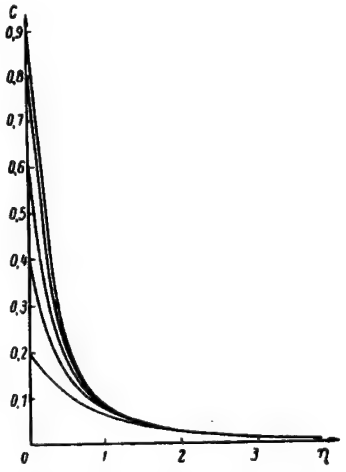


FIGURE 1. Concentration $c$ of the inblown gas (hydrogen) vs. $\eta$ for various $c$ values at the wall

3. Problem (1), (2) was also solved by an alternative method — the method of the two-layer implicit difference scheme described in /5/.

The initial data were defined for $x_0 = 0.01$. Twenty-six points were chosen in the initial layer with $\Delta y = 0.2$ for $0 \leqslant y \leqslant 2.8$, $\Delta y = 0.4$ for $2.8 < y \leqslant 7.2$. The $x$-interval was made equal to 0.0025. The first 6 layers were run with 8 iterations per layer and $s = 1$, the other layers with 6 iterations and $s = 0.7$ ($s$ is the averaging parameter, see /5/).

As the boundary layer expanded, the points on layers increased in number. The condition of smooth matching (see /5/) was checked for the concentration $c$ and for the velocity component $u$. In our case, the asymptotic behavior of $\frac{u}{x}$ is the slowest. Several alternatives with $c_w = 0.2$ were run on the STRELA computer to determine the effect of the initial profiles on the final solution.

1) In the first alternative, the initial data were borrowed from the previous solution of the problem in the self-similar variable $\eta$.

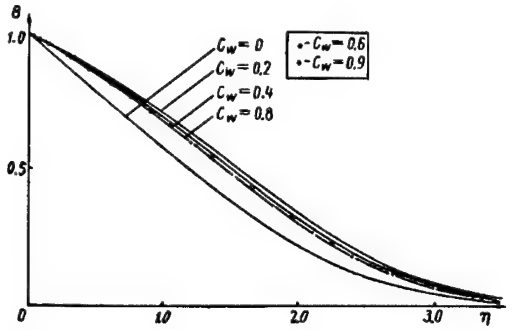


FIGURE 2. The temperature functions $\theta = \frac{T - T_\infty}{T_w - T_\infty}$ vs. $\eta$ for various $c$ values at the wall

Calculations were made on the $0.01 \leqslant x \leqslant 0.0475$ interval. Since the solution was self-similar, the values of $\theta$, $c$ and $u$ obtained by difference method for different $x$ should coincide when passing to the similarity variable $\eta(x,y)$. The results showed that the solution steadied already at $x = 0.0375$. After reducing the results to the self-similar variable on the interval $0.0375 \leqslant x \leqslant 0.0475$, the scatter of the functions for identical $\eta$ was 0.1 % for $u$, 0.7% for $c$, and 2 % for $\theta$.

2) In the second alternative, the functions $\theta$, $c$ and $v$ in the initial layer were the same as in alternative 1, while $u = y$ for $0 \leqslant y \leqslant 1$ and $u = 1$ for $1 < y \leqslant 7.2$. Computations were made for $0.01 \leqslant x \leqslant 0.095$. The solution steadied (i. e., the effect of the initial data disappeared entirely) for $0.01 \leqslant x \leqslant 0.0475$. For $x \geqslant 0.0475$, after reducing the results to the self-similar variable, the departure from the solution of alternative 1 did not exceed 0.1 % in $u$, 1 % in $c$, and 4 % in $\theta$ (for $0.1 \leqslant \theta \leqslant 1$, the scatter in the values of $\theta$ did not exceed 1.3 %).

3) In the third alternative, the initial data were the functions $c$, $u$, $v$ from the self-similar solution, and $\theta = 1 - \frac{y}{4.4}$ for $0 \leqslant y \leqslant 4.4$, $\theta = 0$ for $4.4 < y \leqslant 7.2$. Computations were made for $0.01 \leqslant x \leqslant 0.135$. The effect of the initial data disappeared more slowly than in alternative 2; the solution steadied only at $x \geqslant 0.085$. After reducing the results to the self-similar variable for $x \geqslant 0.085$, the departure from alternative 1 did not exceed 0.3 % in $u$, 0.73 % in $c$, and 1.2 % in $\theta$. The departure from the solution of alternative 2 did not exceed 0.3 % in $u$, 0.9 % in $c$, and 4 % in $\theta$ (for $0.1 \leqslant \theta \leqslant 1$ the scatter in $\theta$ did not exceed 1.2 %).

4) In the first alternative the initial data were chosen as follows: $\theta$ was as in alternative 3, $u$ as in alternative 2, $c = 0.2 - \frac{y}{14}$ for $0 \leqslant y \leqslant 2.8$, and $c = 0$ for $2.8 < y \leqslant 7.2$; $v$ was taken as linear, satisfying the boundary value at the wall and assuming at $y = 7.2$ the same value as in alternative 1.

Computation was made for $0.01 \leqslant x \leqslant 0.075$. The effect of the initial data disappeared much more rapidly than in alternative 3. The solution steadied for $x \geqslant 0.0525$. Reducing the results to the self-similar variable for $x \geqslant 0.0525$, the departure from alternative 1 did not exceed 0.28% in $u$, 0.85% in $c$, and 1% in $\theta$. The departure from the solution of alternative 2 did not exceed 0.3% in $u$, 0.97% in $c$, 3.8% in $\theta$. The departure from the solution of alternative 3 did not exceed 0.13% in $u$, 0.05% in $c$, 0.97% in $\theta$.

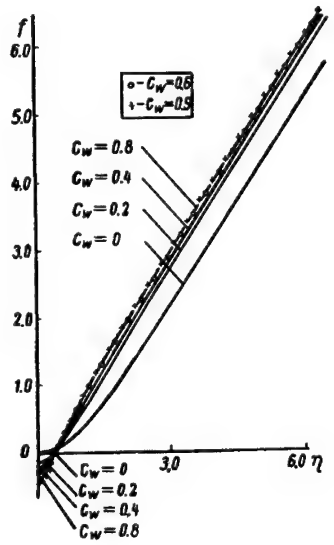


FIGURE 3. Function $f$ vs. $\eta$ for various $c$ values at the wall

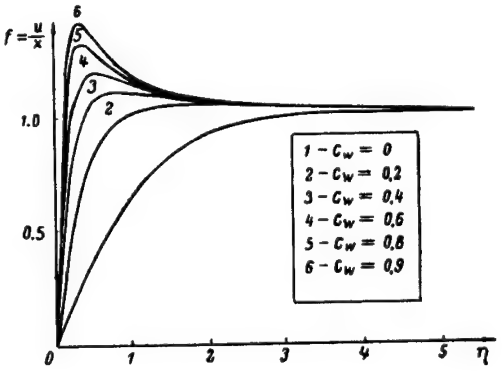


FIGURE 4. The velocity $\frac{u}{x} = f'$ vs. $\eta$ for various $c$ values at the wall

5) To check the choice of the $y$-interval, we re-ran alternative 1 with half the mesh spacing $\Delta y$, starting with $x = 0.0475$. After reducing the results to the self-similar variable $\eta$ for $0.0475 \leqslant x \leqslant 0.1025$, the scatter of the values of the functions for identical $\eta$ did not exceed 0.8% in $u$, 0.9% in $c$, and 7% in $\theta$ (for $0.1 \leqslant \theta \leqslant 1$, the scatter of $\theta$ did not exceed 0.98%). The departure from the solution of alternative 1 did not exceed 1.9% in $u$, 0.97% in $c$, and 6% in $\theta$ (for $0.1 \leqslant \theta \leqslant 1$, at most 1.2%). The departure from the solution of alternative 3 did not exceed 1.05% in $u$, 1.1% in $c$, 7% in $\theta$ (for $0.1 \leqslant \theta \leqslant 1$, at most 2.3%). The departure from the solution of alternative 4 did not exceed 0.8% in $u$, 0.8% in $c$, 8% in $\theta$ (for $0.1 \leqslant \theta \leqslant 1$, at most 1.45%).

We compared the results obtained when solving the problem in the self-similar variable $\eta$ with mesh size of $\Delta\eta = 0.075$ and $\Delta\eta = 0.0375$ with the results obtained by reducing the functions $\theta$, $c$, $u$ from the solution of alternative 1 in the variables $x$, $y$ to $\eta$. The scatter of functions for identical values of $\eta$ did not exceed 0.7% in $\theta$, 0.9% in $c$, and 1.7% in $u$.

BIBLIOGRAPHY


1. AVDUEVSKII, V.S. and E.I. OBROSKOVA. Issledovanie laminarnogo pogranichnogo sloya na poristoi plastine s uchetom teplo — i massoobmena (Investigation of Laminar Boundary Layer on a Porous Plate with Heat and Mass Transfer). — Izv. AN SSSR, seriya mekhanika i mashinostroeniya, No. 4. 1960.
2. HIRSHFIELDER, D., C.CURTISS, and R. BIRD. Molecular Theory of Gases and Liquids. [Russian translation. 1961.]
3. DORODNITSYN, A.A. Progranichnyi sloi v szhimaemom gaze (Boundary Layer in Compressible Gas). — PMM, No. 6, 1942.
4. SCHLICHTING, H. Grenzschichttheorie. [Russian translation. 1956.]
5. BRAILOVSKAYA, I. Yu. and L.A. CHUDOV. Reshenie uravnenii pogranichnogo sloya raznostnym metod (Solution of Boundary-Layer Equations by the Difference Method). — In: Vychislitel'nye metody i programmirovanie. Sbornik rabot Vychislitel'nogo tsentra MGU. Izdatel'stvo MGU. 1962.
6. BEREZIN, I.S. and N.P. ZHIDKOV. Metody vychislenii (Numerical Methods). — Fizmatgiz, Moskva. 1959.

*B. M. Budak, T. F. Bulatskaya, and F. P. Vasil'ev*

# *NUMERICAL SOLUTION OF A BOUNDARY-VALUE PROBLEM FOR THE SYSTEM OF NONLINEAR INTEGRO-DIFFERENTIAL EQUATIONS OF A HYPERSONIC BOUNDARY LAYER*

## § 1. STATEMENT OF PROBLEM

The equations of a hypersonic boundary layer on a slender body of revolution in a flow of viscous heat-conducting gas have the following form in the coordinates $xL$, $yL$, where $x$ is reckoned from the leading edge along the generatrix, and $y$ from the surface of the body along the normal /1/:

$$\left.\begin{aligned}
&\rho r\left(u\frac{\partial u}{\partial x}+v\frac{\partial u}{\partial y}\right)=-r\frac{\partial p}{\partial x}+\frac{1}{R}\cdot\frac{\partial}{\partial y}\left(r\mu\frac{\partial u}{\partial y}\right),\\
&\rho r\left(u\frac{\partial i}{\partial x}+v\frac{\partial i}{\partial y}\right)=ru\frac{\partial p}{\partial x}+\frac{1}{R}\cdot\frac{\partial}{\partial y}\left(r\frac{\mu}{\sigma}\cdot\frac{\partial i}{\partial y}\right)+\\
&\qquad+\frac{1}{R}r\mu\left(\frac{\partial u}{\partial y}\right)^2,\\
&\frac{\partial(\rho ru)}{\partial x}+\frac{\partial(\rho rv)}{\partial y}=0,
\end{aligned}\right\}\qquad(1)$$

where $uu_\infty$, $vu_\infty$ are the velocity components along the $x$ and $y$ axes, respectively, $iu_\infty^2$ the enthalpy, $\rho\rho_\infty u_\infty^2$ the pressure, $\rho\rho_\infty$ density of matter, $\mu\mu_\infty$ viscosity, $L$ the length of the body, $rL$ the distance to the axis of the body, $R=\frac{u_\infty\rho_\infty L}{\mu_\infty}$ the Reynolds number, $\sigma$ the Prandtl number.

The subscript «$\infty$» designates the parameters of the incident flow. For a slender body, $r=r_w(x)+y$, where $r=r_w(x)$ is the equation of the generatrix.

In the Dorodnitsyn variables the system (1) takes the form /1/

$$\left.\begin{aligned}
&u\frac{\partial u}{\partial\xi}+v_1\frac{\partial u}{\partial\eta}=-\frac{1}{\rho}\frac{\partial p}{\partial\xi}+2\frac{M^2}{R}\cdot\frac{\partial}{\partial\eta}\left(Yf\frac{\partial u}{\partial\eta}\right),\\
&u\frac{\partial i}{\partial\xi}+v_1\frac{\partial i}{\partial\eta}=\frac{u}{\rho}\cdot\frac{\partial p}{\partial\xi}+2\frac{M^2}{R}\cdot\frac{\partial}{\partial\eta}\left(Yf\frac{\partial i}{\partial\eta}\right)+\\
&\qquad+2\frac{M^2}{R},\\
&\frac{\partial u}{\partial\xi}+\frac{\partial v_1}{\partial\eta}=0,
\end{aligned}\right\}\qquad(2)$$

where

$$v_1 = 2\frac{u}{\rho r_w^2}\cdot\frac{\partial \eta}{\partial x}\bigg|_r + \frac{2r(v+ur_w')}{\rho r_w^2},$$
$$Y = \frac{r^3}{r_w^2}, \quad f = \frac{\mu\rho}{pM^3}, \tag{3}$$

and $M$ is the Mach number.

Equations (2) must be solved for the boundary conditions

$$u = v_1 = 0,\ i = i_w = \text{const, or } \frac{\partial i}{\partial \eta} = 0 \text{ for } \eta = 0,$$
$$u = 1,\ \ i = 0 \text{ for } \eta \to +\infty. \tag{4}$$

The solution of the boundary-value problem (2), (4) is sought in the form

$$u = \psi(\zeta), \quad i = i(\zeta), \text{where} \zeta = \frac{\sqrt{R}\,\eta}{2M\sqrt{\xi}}. \tag{5}$$

Inserting (5) in (2) and (4), we obtain a boundary-value problem for a system of nonlinear integro-differential Volterra equations:

$$\left.\begin{aligned}&(Yf)\psi'' + [(Yf)' + \varphi]\psi' - 2mF(i) = 0,\\ &\left(Y\frac{f}{\sigma}\right)i'' + \left[\left(Y\frac{f}{\sigma}\right)' + \varphi\right]i' + 2m\psi F(i) + (Yf)(\psi')^2 = 0,\end{aligned}\right\} \tag{6}$$

$$\left.\begin{aligned}&\psi(0) = 0,\ \ i(0) = i_w \text{ or } i'(0) = 0,\\ &\psi(\zeta) \to 1,\ \ i(\zeta) \to 0 \text{ for } \zeta \to +\infty,\end{aligned}\right\} \tag{7}$$

where

$$F(i) \approx \frac{\varkappa - 1}{\varkappa} i,\ \ Y = \frac{r^3}{r_w^2} = 1 + kI(\zeta),\ \ I(\zeta) = \int_0^\zeta F(i)\,d\zeta, \tag{8}$$
$$\varphi(\zeta) = \int_0^\zeta \psi(t)\,dt,$$

$$k = \frac{4M}{\sqrt{R}}\cdot\frac{\sqrt{\xi}}{r_w^2 p}, \quad m = \frac{\xi}{p}\cdot\frac{dp}{d\xi}, \tag{9}$$

$\varkappa$ is the ratio of specific heats,

$$f = f(i),\ \ \sigma = \sigma(i), \tag{10}$$

both given functions of $i$.

A self-similar solution of (5) exists if $k$ const and $m$ = const, where $k$ is a nonnegative root of the cubic

$$I(\infty)k^3 + k^2 - G^2 = 0, \tag{11}$$

where

$$G = \frac{8\beta_0}{3\sqrt{c}}, \quad \beta_0 = \frac{M}{a^2\sqrt{R}}\ ^*, \tag{12}$$

$a$ is the parameter entering the equation of the generatrix of the family of bodies admitting of a self-solution /1/:

$$r_w(x) = ax^{3/4}. \tag{13}$$

The boundary value problem (6), (7) for the integro-differential equations should be solved simultaneously with the cubic (11), where the coefficient $I(\infty)$ is a functional of the unknown function $i(\zeta)$. The convergence of the integral $I(\infty)$ is proved in /1/.

## § 2. GENERAL DESCRIPTION OF THE NUMERICAL METHOD OF SOLUTION OF (6), (7), (11)

We solve the problem (6), (7), (11) by the difference-iterative method. Since according to /1/

$$\frac{\partial u}{\partial \zeta} = \psi'(\zeta) = \varphi''(\zeta) \text{ and } i(\zeta) \text{ for } \zeta \to +\infty$$

decrease not slower than $e^{-H\zeta^2}$, where $H$ is a positive constant, it is advisable to employ a varying mesh, with mesh size increasing with increase of $\zeta$. Taking a sufficiently large interval $0 \leqslant \zeta \leqslant l$, we divide it by points $0 = \zeta_0 < \zeta_1 < \ldots < \zeta_n = l$ into $n$ unequal segments $[\zeta_{\nu-1}, \zeta_\nu]$, $\nu = 1,2,\ldots,n$ and replace at each point $\zeta_\nu$ the value of the unknown function and its derivatives, which are provisionally designated $y(\zeta_\nu)$, $y'(\zeta_\nu)$, $y''(\zeta_\nu)$, by the values of the discrete approximating function $y_\nu$ and the corresponding difference ratios $y'_\nu$ and $y''_\nu$ calculated from the values of $y_\nu$. The explicit form of these difference ratios will be given in what follows. The integrals of the unknown functions will be calculated using the trapezoid formula (Simpson's formula is not more advantageous). The cubic (11) will be numerically solved by Newton's method.

The boundary-value problem (6), (7), (11) in the infinite interval $0 \leqslant \zeta < +\infty$ is thus replaced by a difference boundary-value problem on the finite interval $0 \leqslant \zeta \leqslant l$:

$$(Yf)_\nu \psi''_\nu + [(Yf)'_\nu + \varphi_\nu]\,\psi'_\nu - 2mF(i_\nu) = 0, \tag{13a}$$

$$\left(Y\frac{f}{\sigma}\right)_\nu i''_\nu + \left[\left(Y\frac{f}{\sigma}\right)'_\nu + \varphi_\nu\right] i'_\nu + 2mF(i_\nu)\psi_\nu + (Yf)_\nu(\psi'_\nu)^2 = 0, \quad \nu = 1, 2, \ldots, n-1, \tag{13b}$$

$$\psi_0 = 0, \quad i_0 = i_w, \text{ or } i'_0 = 0, \tag{13c}$$

$$\psi_n = 1, \quad i_n = 0, \tag{13d}$$

$$I_n(l)\,k^3 + k^2 - G^2 = 0, \tag{13e}$$

* In notations of /1/ $\beta_0 = \frac{\varkappa}{M^2a^2}$.

where $(Yf)_\nu$, $\left(Y\frac{f}{\sigma}\right)_\nu$, $\varphi_\nu$, $I_n(l)$ denote the corresponding quadrature formulas substituted for the integrals

$$(Yf)|_{\zeta=\zeta_\nu}, \qquad \left(Y\frac{f}{\sigma}\right)\Big|_{\zeta=\zeta_\nu}, \qquad \varphi|_{\zeta=\zeta_\nu} \qquad I(\zeta)|_{\zeta=l}.$$

The interval $0 \leqslant \zeta \leqslant l$ and the mesh spacing along the axis are chosen so that as the length $l$ of the interval increases and the mesh becomes finer the values of the unknown functions stabilize at the corresponding mesh points over the entire interval; we should therefore mainly require that the behavior of $\psi_\nu$ and $i_\nu$ as $\nu$ approaches $n$ be analogous to the behavior of $\psi(\zeta)$ and $i(\zeta)$ as $\zeta \to +\infty$ (see the beginning of this section, and /5/).

Setting /1/

$$F(i) = \frac{\varkappa - 1}{\varkappa} i, \tag{14}$$

we solve the difference boundary-value problem (13a)-(13e) by the following iterative scheme:

$$[\overset{(s)}{Yf}]_\nu \overset{(s+1)}{\psi''_\nu} + [(\overset{(s)}{Yf})_\nu + \overset{(s)}{\varphi_\nu}] \overset{(s+1)}{\psi'_\nu} - 2m \frac{\varkappa - 1}{\varkappa} \overset{(s)}{i_\nu} = 0, \tag{15a}$$

$$\left[Y\frac{\overset{(s)}{f}}{\sigma}\right]_\nu \overset{(s+1)}{i''_\nu} + \left[\left(Y\frac{\overset{(s)}{f}}{\sigma}\right)'_\nu + \overset{(s+1)}{\varphi_\nu}\right] \overset{(s+1)}{i'_\nu} + 2m \frac{\varkappa - 1}{\varkappa} \overset{(s+1)}{\psi_\nu} \overset{(s+1)}{i_\nu} + $$

$$+ (\overset{(s)}{Yf})_\nu [\overset{(s+1)}{\psi'_\nu}]^2 = 0, \tag{15b}$$

$$\left.\begin{aligned} &\overset{(s)}{\psi_0} = 0, \quad \overset{(s)}{\psi_n} = 1, && \text{(15c)} \\ &\overset{(s)}{i_0} = i_w \ (\text{or } \overset{(s)}{i'_0} = 0), \quad \overset{(s)}{i_n} = 0 && \text{(15d)} \end{aligned}\right\} \text{ for all } s = 0, 1, 2, \ldots$$

$$\overset{(s)}{I_n}(l)\, \overset{(s)}{k^3} + \overset{(s)}{k^2} - G^2 = 0. \tag{15e}$$

If the initial approximation $\overset{(0)}{\psi_\nu}$, $\overset{(0)}{i_\nu}$ is known (concerning its choice, see § 3), the quadrature formulas can be applied to find $\overset{(0)}{\varphi_\nu}$, $\overset{(0)}{I_n}(l)$, and then from (15e), by Newton's method, to find $\overset{(0)}{k}$. Now for $s=0$, all the coefficients and the free term in the difference equation (15a), which is linear in $\overset{(1)}{\psi_\nu}$, are expressed in terms of the known quantities $\overset{(0)}{\varphi_\nu}$, $\overset{(0)}{i_\nu}$, $\overset{(0)}{k}$ and the equation is solved for $\overset{(1)}{\psi_\nu}$ with boundary conditions (15c) for $s=1$, i. e., with the boundary conditions $\overset{(1)}{\psi_0}=0$, $\overset{(1)}{\psi_n}=1$. Given $\overset{(1)}{\psi_\nu}$, we find $\overset{(1)}{\psi'_\nu}$ by numerical differentiation and $\overset{(1)}{\varphi_\nu}$ by numerical integration with the quadrature formula. The coefficients and the free term of the difference equation (15c), which is linear in $\overset{(1)}{i_\nu}$, are expressed for $s=0$ in terms of the known quantities $\overset{(1)}{\psi_\nu}$, $\overset{(1)}{\psi'_\nu}$, $\overset{(1)}{\varphi_\nu}$, $\overset{(0)}{i_\nu}$, $\overset{(0)}{k}$ and the resulting equation is solved with boundary conditions (15d) for $s=1$.

Given $\overset{(1)}{\psi_\nu}$, $\overset{(1)}{i_\nu}$, we can analogously find the next approximation $\overset{(2)}{\psi_\nu}$, $\overset{(2)}{i_\nu}$, $\overset{(1)}{k}$, and then the third approximation $\overset{(3)}{\psi_\nu}$, $\overset{(3)}{i_\nu}$, $\overset{(2)}{k}$, etc.

The iteration is terminated at $s=s_0$, when the inequalities

$$|\overset{(s+1)}{\varphi_\nu} - \overset{(s)}{\varphi_\nu}| < \varepsilon, \quad |\overset{(s+1)}{i_\nu} - \overset{(s)}{i_\nu}| < \varepsilon \tag{16}$$

are first satisfied for all $\nu=0, 1, 2, \ldots, n$; here $\varepsilon$ is a given positive number, which has been taken equal to $10^{-5}$.

## § 3. DESCRIPTION OF DIFFERENCE APPROXIMATIONS AND OF THE MAIN STAGES OF THE COMPUTATIONAL PROCESS

*1°. Difference approximation of derivatives and integrals in (6), (7), (11).* The difference approximation (13a) - (13e) for (6), (7), (11) is constructed as follows. The interval $0 \leqslant \zeta \leqslant l$ is divided into $r$ subintervals by points $0=l_0 < l_1 < \ldots < l_{r-1} < l_r = l$, and each of the subintervals $[l_{i-1}, l_i]$, $1 \leqslant i \leqslant r$, is in turn divided into several smaller segments of constant (for a given $i$) length $h_i$ so that

$$h_i = 2h_{i-1}, \quad i = 1, 2, \ldots, r. \tag{17}$$

The numbers

$$n_1 = \frac{l_1}{h_1}, \quad n_2 = n_1 + \frac{l_2 - l_1}{h_2}, \quad \ldots$$

$$\ldots, n_r = n_1 + \ldots + n_{r-1} + \frac{l_r - l_{r-1}}{h_r} = n \tag{18}$$

are integers.

Evidently,

$$l_i = \sum_{j=1}^{i} (n_j - n_{j-1}) h_j, \quad n_0 = 0, \ i = 1, 2, \ldots, r. \tag{19}$$

We have thus divided the segment $0 \leqslant \zeta \leqslant l$ into a nonuniform mesh with $n_r = n$ points: $\zeta_0=0, \zeta_1, \ldots \zeta_{n_r} = l$ where $\zeta_{n_i} = l_i$, $i=1, 2, \ldots, r$, such that the mesh spacing is doubled when passing from the interval $l_{i-1} \leqslant \zeta \leqslant l_i$ to the interval $l_i \leqslant \zeta \leqslant l_{i+1}$, i. e., $h_{i+1} = 2h_i$.

We provisionally denote any of the functions in equations (6) by $y(\zeta)$ and replace $y(\zeta_\nu)$ by $y_\nu$ for $0 \leqslant \nu \leqslant n$; the derivatives $y'(\zeta_\nu)$ and $y''(\zeta_\nu)$ are replaced by

$$y'(\zeta_\nu) \approx y'_\nu = \begin{cases} \dfrac{y_{\nu+1} - y_{\nu-1}}{2h_i} \\ \text{for } n_{i-1} < \nu < n_i, \ i = 0, 1, \ldots, r, \\ \dfrac{y_{\nu+1} - y_{\nu-2}}{2h_{i+1}} \\ \text{for } \nu = n_i, \ i = 1, 2, \ldots, r-1, \end{cases} \tag{20}$$

$$y''(\zeta_\nu) \approx \dot{y}_\nu = \begin{cases} \dfrac{y_{\nu+1} - 2y_\nu + y_{\nu-1}}{h_i^2} \\ \text{for } n_{i-1} < \nu < n_i,\ i = 0, 1, \ldots, r, \\ \dfrac{y_{\nu+1} - 2y_\nu + y_{\nu-2}}{h_{i+1}^2} \\ \text{for } \nu = n_i,\ i = 1, 2, \ldots, r-1. \end{cases} \tag{21}$$

Boundary conditions of the form

$$\left.\begin{aligned} y(0) = Y_1, \quad y(l) = Y_2 \\ y'(0) = Y_1',\ y(l) = Y_2 \end{aligned}\right\} \tag{22}$$

or

are respectively replaced by

$$y_0 = Y_1, \quad y_n = Y_2, \tag{23}$$

or

$$y'(0) \approx \frac{-y_2 + 4y_1 - 3y_0}{2h_1} = Y_1', \quad y_n = Y_2. \tag{24}$$

The integral over $y(\zeta)$ is replaced according to the trapezoid formula by

$$\begin{aligned} \int_0^{\zeta_\nu} y(\zeta)\, d\zeta \approx h_1 \left( \frac{y_1 + y_2}{2} + \ldots + \frac{y_{n_1-1} + y_{n_1}}{2} \right) + \\ + h_2 \left( \frac{y_{n_1} + y_{n_1+1}}{2} + \ldots + \frac{y_{n_2-1} + y_{n_2}}{2} \right) + \ldots \\ \ldots + h_i \left( \frac{y_{n_{i-1}} + y_{n_{i-1}+1}}{2} + \ldots + \frac{y_{\nu-1} + y_\nu}{2} \right) \\ \text{for } n_{i-1} \leqslant \nu \leqslant n_i. \end{aligned} \tag{25}$$

The derivative at the right end point of the interval $0 \leqslant \zeta \leqslant l$ is replaced by

$$y'(\zeta_n) = y'(l) \approx \dot{y}_n = \frac{y_{n-2} - 4y_{n-1} + 3y_n}{2h_r} \tag{26}$$

(the derivative at the left end point is determined from the first formula in (24)).

If the known given functions and the functions constituting the solution of boundary-value problem (6), (7), (11) are sufficiently smooth, then with this method of approximation of the derivatives and the integrals, taking $l$ sufficiently large, the difference scheme (13a) - (13e) gives an approximation accurate to $O(h^2)$, where $h$ is the maximum spacing of the mesh chosen.

*2°. Solution for a linear difference equation by the forcing method on variable mesh.* In the course of iteration (15a) -(15e), each step involves the solution of a boundary-value problem for the linear difference equation of second order

$$\begin{aligned} c_1(\zeta_\nu)\, \dot{y}_\nu + c_2(\zeta_\nu)\, \dot{y}_\nu + c_3(\zeta_\nu)\, y_\nu + c_4(\zeta_\nu) = 0, \\ \nu = 1, 2, \ldots, n-1, \end{aligned} \tag{27}$$

with boundary conditions

$$y_0 = Y_1, \quad y_n = Y_2, \tag{$28_1$}$$

or

$$y_0' = \frac{-y_2 + 4y_1 - 3y_0}{2h_1} = Y_1', \quad y_n = Y_2 \tag{$28_2$}$$

to obtain the $(s+1)$-th approximation from the $s$-th approximation we proceed as follows: $y_\nu'$ and $y_\nu''$ in (27) have the form (20) and (21). We seek the solution of problem (27), ($28_1$) or (27), ($28_2$) in the form

$$y_\nu = a_1^{(\nu)} y_{\nu+1} + a_2^{(\nu)}, \quad \nu = 1, 2, \ldots, n-1, \tag{29}$$

$$y_0 = a_1^{(0)} y_1 + a_2^{(0)} + a_3^{(0)} y_2,$$
$$y_n = Y_2,$$

where

$$a_1^{(1)} = \frac{-L_1 a_3^{(0)} + \left(c_{11} + \frac{1}{2} h_1 c_{21}\right)}{L_1 a_1^{(0)} + (2c_{11} - h_1^2 c_{31})}, \tag{30}$$

$$a_2^{(1)} = \frac{-L_1 a_2^{(0)} + h_1^2 c_{41}}{L_1 a_1^{(0)} + (2c_{11} - h_1^2 c_{31})},$$

$$a_1^{(\nu)} = \begin{cases} \dfrac{c_{1\nu} + \frac{1}{2} h_i c_{2\nu}}{L_\nu a_1^{(\nu-1)} + (2c_{1\nu} - h_i^2 c_{3\nu})} \\ \text{for } n_{i-1} < \nu < n_i, \ i = 1, 2, \ldots, r, \\ \dfrac{c_{1\nu} + \frac{1}{2} h_{i+1} c_{2\nu}}{L_\nu A_1^{(\nu-1)} + (2c_{1\nu} - h_{i+1}^2 c_{3\nu})}, \ A_1^{(\nu-1)} = a_1^{(\nu-2)} a_2^{(\nu-1)} \\ \text{for } \nu = n_i, \ i = 1, \ldots, r-1, \end{cases} \tag{31}$$

$$a_2^{(\nu)} = \begin{cases} \dfrac{-L_\nu a_2^{(\nu-1)} + c_{4\nu} h_i^2}{L_\nu a_1^{(\nu-1)} + (2c_{1\nu} - h_i^2 c_{3\nu})} \\ \text{for } n_{i-1} < \nu < n_i, \ i = 1, 2, \ldots, r, \\ \dfrac{-L_\nu A_2^{(\nu-1)} + h_{i+1}^2 c_{4\nu}}{L_\nu A_1^{(\nu-1)} + (2c_{1\nu} - h_{i+1}^2 c_{3\nu})}, \\ A_2^{(\nu-1)} = a_1^{(\nu-1)} a_2^{(\nu-1)} + a_2^{(\nu-2)}, \\ \text{for } \nu = n_i, \ i = 1, 2, \ldots, r-1, \end{cases} \tag{32}$$

$$L_\nu = \begin{cases} -c_{1\nu} + \frac{1}{2} h_i c_{2\nu} \text{ for } n_{i-1} < \nu < n_i, \ i = 1, 2, \ldots, r, \\ -c_{1\nu} + \frac{1}{2} h_{i+1} c_{2\nu} \text{ for } \nu = n_i, \ i = 1, 2, \ldots, r-1, \end{cases} \tag{33}$$

$$c_{j\nu} = c_j(\zeta_\nu), \quad j = 1, 2, 3, 4. \tag{34}$$

With boundary conditions $(28_1)$

$$a_1^{(0)} = a_3^{(0)} = 0, \quad a_2^{(0)} = Y_1,$$

and with boundary conditions $(28_2)$

$$a_1^{(0)} = \frac{4}{3}, \; a_2^{(0)} = -\frac{2}{3} h_1 Y_1', \; a_3^{(0)} = -\frac{1}{3}.$$

From (30)—(34) we find the forcing coefficients, going in the direction of increasing $\nu(\nu=1, 2, 3, \ldots, n)$, and then back in the reverse direction $(\nu=n-1, n-2, \ldots, 1, 0)$ we find from (29) the value of $y_\nu$.

The forcing formulas (29)—(34) are derived as in /3/ or /4/ for a fixed-size mesh*.

*3°. Newton's method for the solution of the cubic in the case of equation (15e)* is reduced for every given $s$ to the iteration /3/

$$\overset{(s)}{k}_{q+1} = \frac{\overset{(s)}{k}_q^2 (2\overset{(s)}{I}_n(l)\overset{(s)}{k}_q + 1) + G^3}{\overset{(s)}{k}_q (3\overset{(s)}{I}_n(l)\overset{(s)}{k}_q + 2)}, \quad q = 0, 1, 2, \ldots \tag{35}$$

As the initial approximation we assume $\overset{(s)}{k}_0 = |G|$. The iteration is terminated at $q=q_0$ for which the inequality

$$|\overset{(s)}{k}_{q+1} - \overset{(s)}{k}_q| < \varepsilon_0 = 10^{-8} \tag{36}$$

is first satisfied. By virtue of $\overset{(s)}{I}_n(l) > 0$, the cubic (15e) has a single positive root in the interval $|0, |G||$.

*4°. Choice of given functions, constants, and initial approximations.* We have made our calculations for $f=1$, $\sigma=0.72$ and for various values of the constants $\varkappa$, $m$ and $\beta_0$. Numerical trials showed that the results are highly stable with regard to the choice of the initial approximations $\overset{(0)}{i}_\nu$, $\overset{(0)}{\psi}_\nu$, but the number of iterations $s_0$ required to achieve the predetermined accuracy $\varepsilon$ depends on the initial data $\overset{(0)}{i}_\nu$, $\overset{(0)}{\psi}_\nu$. For example, when $\overset{(0)}{\psi}_\nu$ was taken from the table in /2/, p. 529 (the column corresponding to $\beta=2.0$), applying linear interpolation for the corresponding intermediate grid points, and $\overset{(0)}{i}_\nu$ was calculated from

$$\overset{(0)}{i}_\nu = \frac{1}{2}(1 - \overset{(0)}{\psi}_\nu^2) + B(1 - \overset{(0)}{\psi}_\nu), \tag{37}$$

where

$$B = \begin{cases} 0 \text{ for } i'(0) = 0, \\ i_w - \frac{1}{2}, \text{ for } i(0) = i_w, \end{cases}$$

the number of iterations for $\varepsilon=10^{-5}$ varied from 7 to 10 depending on the parameters $\varkappa$, $m$, $\beta_0$.

If we set $\overset{(0)}{i}_\nu \equiv \overset{(0)}{\psi}_\nu \equiv 0$, then for $\varepsilon=10^{-5}$ and the same parameters 18—20 iterations will be required.

* The forcing scheme for difference equations of second order in the case of variable-size mesh has been previously used at the Computational Center of Moscow State University, see, e. g., /6/.

Since using the tabulated values from /2/ as the initial approximation $\overset{(0)}{\psi}_v$ involves storing a great many numbers in the computer memory, we assumed the following initial approximation

$$\overset{(0)}{\psi}_v = \begin{cases} 0{,}4\,\zeta_v \text{ for } 0 \leqslant \zeta_v \leqslant \zeta' = 2.5, \\ 1 \text{ for } \zeta_v > 2.5, \end{cases} \tag{38}$$

and calculated $\overset{(0)}{i}_v$ from (37). We thus avoided the necessity of interpolation to determine the values $\overset{(0)}{\psi}_v$ at the intermediate points (a necessary procedure when the tables from /2/ are used). This choice of initial approximations requires the same number of iterations as are necessitated by the tabulated data from /2/. The function (38) is a rough piecewise-linear approximation to the function $\psi_v$ given in /2/.

## § 4. VERIFICATION OF THE NUMERICAL METHOD AND ITS CONVERGENCE

To verify this numerical method, we made a control calculation for the Blasius case and compared the results with the table in /2/, p. 529. We minded mainly the column for $\beta = 2.0$. If we take $i = \frac{1}{2}(1 - \varphi'^2)$, the boundary-value problem for the system of integro-differential equations $\left(\varphi' = \psi,\ \varphi(\zeta) = \int_0^\zeta \psi(t)\,dt\right)$ reduces to the differential equation $\varphi''' + \varphi\varphi'' = \gamma(\varphi'^2 - 1)$, where $\gamma = -m\frac{\varkappa - 1}{\varkappa}$, with the boundary conditions $\varphi(0) = \varphi'(0) = 0$, $\varphi'(\infty) = 1$, or an equivalent integro-differential equation $\psi'' + \varphi\psi' = \gamma(\psi^2 - 1)$, where $\gamma = -m\frac{\varkappa - 1}{\varkappa}$ with boundary conditions $\psi(0) = 0$, $\psi(\infty) = 1$.

In notations of § 1 the following values of the parameters correspond to this problem: $m = -7$, $\beta_0 = 0$, $f = 1$, $\sigma = 1$, $\varkappa = 1.4$. Replacing the interval $0 \leqslant \zeta < +\infty$ by the interval $0 \leqslant \zeta \leqslant 5$ and making in this interval calculations with constant mesh size $h = 0.05$ and constant mesh size $h = 0.0125$, we obtain approximate values of the function $\varphi'(\zeta) = \psi(\zeta)$ which show a maximum deviation of 1.4% and 0.12%, respectively, from the corresponding values in /2/. Making in this interval $0 \leqslant \zeta \leqslant 5$ a calculation with variable mesh size $h_1 = 0.005$, $n_1 = 100$, $h_2 = 0.01$, $n_2 = 250$, $h_3 = 0.02$, $n_3 = 400$, we obtained approximate values of $\varphi'(\zeta) = \psi(\zeta)$ which deviated at most by 0.06% from the corresponding values in /2/. The approximate values of $\varphi'(\zeta) = \psi(\zeta)$ corresponding to grid points in the interval $3 \leqslant \zeta \leqslant 5$ in all these cases differed by at most $10^{-4}$ from 1. Note that for $\zeta \to +\infty$, $\psi(\zeta)$ behaves as $1 + \text{const} \cdot e^{-H\zeta}$, where $H = \text{const} > 0$, and that in choosing the interval $0 \leqslant \zeta \leqslant 5$ for calculations we set $\psi(5) = 1$. Replacing the interval $0 \leqslant \zeta \leqslant 5$ by the interval $0 \leqslant \zeta \leqslant 3$ and making a calculation with constant mesh size $h = 0.0125$ and boundary value $\psi(3) = 1$, we obtained approximate values of $\varphi'(\zeta) = \psi(\zeta)$ differing by at most 0.1% from the corresponding values obtained with the same mesh size $h = 0.0125$ in the interval $0 \leqslant \zeta \leqslant 5$. This agreement in numerical results seemed to us to prove satisfactorily the accuracy of our method.

The choice of the length $l$ of the interval $0 \leqslant \zeta \leqslant l$ and of the mesh size $h$ is made analogously in cases of other combinations of the known constants $m$, $\varkappa$, $\beta_0$, $\sigma$, $i_w$, $i_w$. The mesh size was assumed sufficiently fine and the length of the $0 \leqslant \zeta \leqslant l$ interval sufficiently large if the values $i(\zeta)$, $\psi(\zeta)$ in the interval $^3/_4 l \leqslant \zeta \leqslant l$ differed at most by $10^{-4}$ from the boundary values $i(l)=0$, $\psi(l)=1$, and if reduction of the interval to $0 \leqslant \zeta \leqslant {}^3/_4 l$ and doubling of the mesh size altered the values of $\psi(\zeta)$ and $i(\zeta)$ at the corresponding points by at most 0.1%.

We observe that increase of $\beta_0$ entails an increase of the interval length $l$. For example, we had to take the interval $0 \leqslant \zeta \leqslant 30$ for the following parameter values: $m=0.25$, $\varkappa=1.4$, $\beta_0=100$, $\sigma=0.72$, $i_w=0.25$. With this large interval, fixed-mesh calculation occupying minimum working memory gives too low accuracy. We therefore had to resort to variable mesh size.

In all the alternatives calculated, as the mesh was made finer, the approximate values $\psi(\zeta)=\varphi'(\zeta)$ for any given $\zeta$ monotonically increased, and $i(\zeta)$ monotonically decreased, both approaching definite limits*.

## § 5. ANALYSIS OF RESULTS FOR SEVERAL ALTERNATIVES

The above method was used in calculations for the following values of parameters and boundary values:

$f=1$, $\sigma=0.72$;

$\varkappa=1.4$;

$m=-1$; $i_w=0$; 0.1; 0.25; $i'_w=0$; $\beta_0=0$;

$m=-\frac{1}{4}$; $i_w=0$; 0.25; $i'_w=0$; $\beta_0=0$; 0.5; 2; 10; 100;

$m=-\frac{1}{4}$; $i_w=0.1$; $\beta_0=0$; 10;

$\varkappa=1,2$;

$m=-1$; $i_w=0$; $i'_w=0$; $\beta_0=0$;

$m=-\frac{1}{4}$; $i_w=0$; $i'_w=0$; $\beta_0=0$; 0.5; 2; 10; 100.

The numerical results are plotted in Figures 1—4.

The results reveal the substantial effect of the parameter $\beta_0$ on the value $\zeta=l$ characterizing the limit of the boundary layer. For example, with $\beta_0=100$ and $i'_w=0$, $l \approx 25$, i.e., five times as great as in the Blasius case. This is probably so because as $\beta_0$ increases, $k$ and $y$ also increase, and the effect of increasing $y$ on the solution formally resembles the effect of increasing viscosity in the boundary-layer equation.

The parameter $\zeta=l$ decreases with decreasing $i_w$, which is apparently due to the resulting overall drop in enthalpy.

It is noteworthy that the boundary value of $\zeta$ for the velocity $u=\psi(\zeta)$ (characterizing the limit of the boundary layer so far as velocity is concerned) is much lower than for the enthalpy.

* This regularity may be established theoretically. The theoretical proof of the convergence of this method will be discussed in another paper.

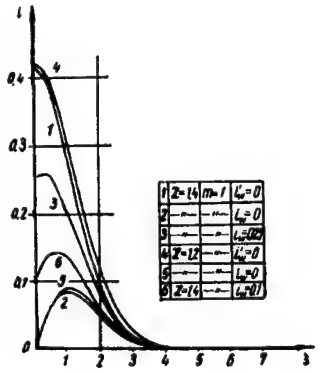

FIGURE 1. Enthalpy $i$ vs. $\zeta = \dfrac{\sqrt{R}\cdot\eta}{2M\sqrt{\xi}}$ ($\eta$, $\xi$ are the Dorodnitsyn variables) in boundary layer with $\beta=0$

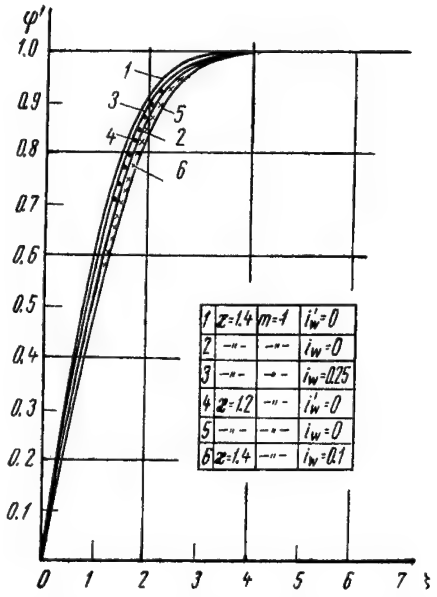

FIGURE 2. Velocity profiles $u=\varphi'(\zeta)$ in boundary layer with $\beta=0$

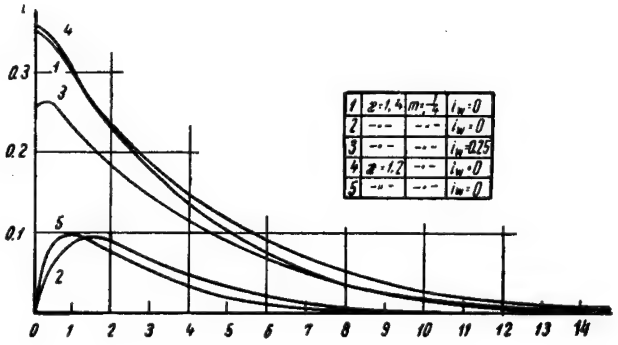

FIGURE 3. Enthalpy $i$ vs. $\zeta$ for $\beta=100$

The boundary value of enthalpy for $\zeta=0$ and the parameter $\varkappa$ have virtually no effect on the velocity profile $u=\psi(\zeta)$ for $\beta_0=0$; 0.5, but have a marked effect at higher $\beta_0$.

The calculations made enable us to estimate the effect of the interaction of the boundary layer with the exterior stream on the pattern of flow past slender bodies at high supersonic velocities, over a wide range of flow conditions and values of the parameter $\beta_0$, characterizing the slenderness ratio of the body.

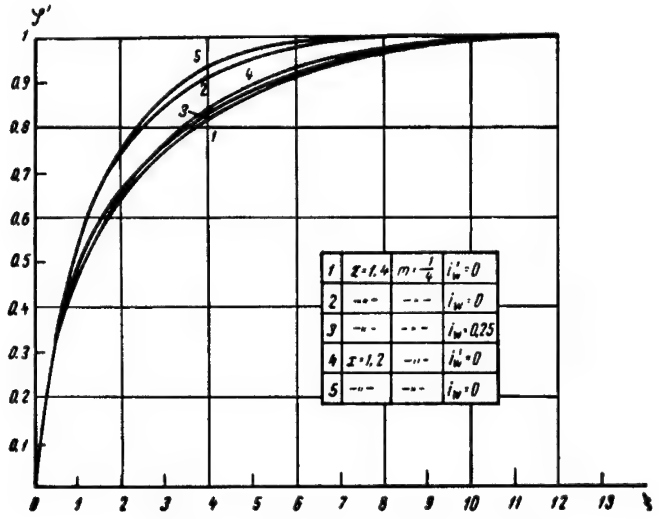


FIGURE 4. Velocity profiles $u=\varphi'(\zeta)$ for $\beta=100$

In conclusion, we extend our thanks to V. V. Lunev for the discussion of the physical formulation of the problem, the choice of numerical values of the parameters, and discussion of the results. We are also thankful to G. S. Roslyakov for constant attention to our work and to Kh. A. Rakhmatulin and participants of his seminar for discussion of results.

BIBLIOGRAPHY

1. LUNEV, V.V. Avtomodel'nyi sluchai giperzvukovogo obtekaniya osesimmetrichnogo tela vyazkim teploprovodnym gazom (Self Similar Hypersonic Flow of Viscous Heat-Conducting Gas Past an Axisymmetric Body). — PMM, Vol. 24, No. 3. 1960.
2. LOITSYANSKII, L.G. Mekhanika zhidkosti i gaza (Mechanics of Liquids and Gases).— GITTL, Moskva. 1957.
3. BEREZIN, I.S. and N.P. ZHIDKOV. Metody vychislenii (Numerical Methods), Vol. II. — Fizmatgiz, Moskva. 1960.
4. RICHTMEYER, R.D. Difference Methods for the Solution of Boundary-Value Problems. [Russian translation. 1960.]
5. COLLATZ, L. Numerische Methoden Zur Auflösung von Differentialgleichungen. — Springer (Berlin).
6. PASKONOV, V.M. A Standard Program for the Solution of Boundary-Layer Problems. — This volume.

## *III. VISCOUS FLOW*

*A. L. Krylov*

# *FINITE-DIMENSIONAL MODELS FOR EQUATIONS OF MATHEMATICAL PHYSICS*

A large class of partial differential equations of mathematical physics has the following property: the equations express laws of conservation of certain physical quantities (e.g., momentum, energy, mass) and, moreover, some "additional" conservation principle follows from the basic equations. For equations of gas dynamics, this is the conservation of entropy; for equations of crystal optics (in particular, for Maxwell equations), this is the conservation of energy, etc. Following S. K. Godunov /1/, we shall consider equations of the form

$$\frac{\partial L^0_{q_i}}{\partial t} + \sum_{j=1}^{n} \frac{\partial L^j_{q_i}}{\partial x_j} = 0, \quad i = 1, 2, \ldots, m, \tag{1}$$

where

$$L^k = L^k(q_1, q_2, \ldots, q_m), \qquad k = 0, 1, \ldots, n.$$

This is the general form for the equations of variational calculus, gas dynamics (ordinary and relativistic), crystal optics, mixture of gases, etc. The smooth solutions of system (1) satisfy the following conservation law

$$\frac{\partial}{\partial t}\left(\sum_{i=1}^{m} q_i L^0_{q_i} - L^0\right) + \sum_{j=1}^{n} \frac{\partial}{\partial x_j}\left(\sum_{i=1}^{m} q_i L^j_{q_i} - L^j\right) = 0, \tag{2}$$

which can be interpreted as the conservation of energy or entropy. The equations can be extended in a natural manner to irreversible processes, in which case (2) is regarded as the equation of dissipation of energy.

The present paper is devoted to the construction of finite-dimensional models for systems having an "exact" law of energy conservation of the form (2). This problem was first posed for the Navier-Stokes equations for viscous incompressible flow (which, incidentally, do not belong to class (1)) by A. N. Kolmogorov at the seminar on problems of turbulence held in 1958-1959. A study of the ergodic properties of these models will possibly imply some properties of the continuous case also. The author is not familiar with any work in this direction.

We first consider the case $i=j=1$, so that the equation takes the form

$$\frac{\partial}{\partial t} A_q(q) + \frac{\partial}{\partial x} B_q(q) = \frac{\partial}{\partial x}\left(C(q)\frac{\partial q}{\partial x}\right) \tag{3}$$

(the dissipative term has been added in the right-hand side), where it is assumed that $A_q(q)\,q - A(q) > 0$ and $C(q) > 0$. For simplicity we shall consider a Cauchy problem with periodic boundary condition for $x$:

$$\frac{\partial^k q}{\partial x^k}(t, 0) = \frac{\partial^k q}{\partial x^k}(t, l), \qquad k = 0;\ 1. \tag{4}$$

Other boundary conditions can be analogously treated, including the case of a region unbounded in $x$ with the relevant functions vanishing at infinity.

We multiply equation (3) by $q$ and transform the individual terms as follows:

$$q\frac{\partial}{\partial t}A_q(q) = \frac{\partial}{\partial t}(A_q(q)\,q - A(q)), \tag{$\alpha$}$$

$$q\frac{\partial}{\partial x}B_q(q) = \frac{\partial}{\partial x}(B_q(q)\,q - B(q)), \tag{$\beta$}$$

$$q\frac{\partial}{\partial x}\left(C(q)\frac{\partial q}{\partial x}\right) = \frac{\partial}{\partial x}\left(C(q)\frac{\partial q}{\partial x}q\right) - C(q)\left(\frac{\partial q}{\partial x}\right)^2. \tag{$\gamma$}$$

Hence, in view of (4), we obtain the identity

$$\int_0^l [A_q(q)\,q - A(q)]\,dx\Big|_{t=0}^{t=T} = \int_0^T\int_0^l C(q)\left(\frac{\partial q}{\partial x}\right)^2 dx\,dt \tag{5}$$

(the law of dissipation of "energy" $A_q q - A$). We shall attempt to construct a finite-dimensional model of the problem (3), (4) which would allow analogous transformations to be made in the difference equation approximating (3). In the interval $(0, l)$ we define points with abscissas $x_k$ equal to $kh$; $k = 0, 1, \ldots, N$, $h = \frac{l}{N}$; the points $x_0$ and $x_N$ are considered as coinciding. Points with the abscissas $(k + 1/2)h$ will be called half-integral points; they will play an auxiliary role in our construction. The required functions $q^k(t)$, $k = 0, 1, \ldots, N$, approximating the solution of equation (3) at $x_k$ are assumed to be defined for the integral values of the index, while their explicit and implicit "derivatives" with respect to $x$ are considered at half-integral values of the index, i.e., we shall write $\delta q^{k+\frac{1}{2}} = \frac{1}{h}(q^{k+1} - q^k)$. We also determine the "drift" of a function $q^k$ at half-integral points:

$$\mu q^{k+1/2} = \frac{1}{2}(q^{k+1} + q^k).$$

For functions $a^k$ and $b^{k+\frac{1}{2}}$ which are periodic on the grid, we obviously have the following rule of "summation by parts":

$$\sum a^k \delta b^k = -\sum b^{k+\frac{1}{2}}\delta a^{k+\frac{1}{2}}; \quad \sum b^{k+\frac{1}{2}}\delta a^{k+\frac{1}{2}} = -\sum a^k \delta b^k,$$

of which we will make much use.

Consider the approximation to equation (3). The term $\frac{\partial}{\partial t}A_q(q)$ is clearly approximated by the trivial expression $\frac{d}{dt}A_q(q^k)$.

To approximate the dissipative term $\frac{\partial}{\partial x}\left(C(q)\frac{\partial q}{\partial x}\right)$, we reason as follows: the approximation must apply at integral points, i.e., the function $C(q)\frac{\partial q}{\partial x}$

should be approximated at half-integral points; it is natural to assume the approximation $C(\mu q^{k+\frac{1}{2}})\delta q^{k+\frac{1}{2}}$ (in case of a single variable, we could even take $\mu C(q)^{k+\frac{1}{2}}\delta q^{k+\frac{1}{2}}$; with many variables, however, this is not so — see below). We now write down the analog of (γ):

$$\sum_k \delta\,(C(\mu q)\,\delta q)^k q^k = -\sum_k C(\mu q^{k+\frac{1}{2}})(\delta q^{k+\frac{1}{2}})^2$$

(here the periodicity of $q^k$ is taken into consideration, i.e., $q^0 = q^{N-1}$, $q^1 = q^N$). As $C(q)$ is assumed positive, the last sum is negative and can be regarded as the dissipated "energy" per unit time. We finally consider the most complicated terms, $\frac{\partial}{\partial x} B_q(q)$. The expression for $B_q(q)$ should be written for half-integral points, and we moreover must obtain an analog of the formula $B_q(q)\frac{\partial q}{\partial x} = \frac{\partial}{\partial x} B(q)$. These requirements lead us to the expression

$$\frac{B(q^{k+1}) - B(q^k)}{q^{k+1} - q^k} = B_q^{k+\frac{1}{2}}(q).$$

We then have

$$\sum_k \delta\,(B_q(q))^k q^k = -\sum_k B_q^{k+\frac{1}{2}}(q)\,\delta q^{k+\frac{1}{2}} =$$
$$= -\sum_k (B(q^{k+1}) - B(q^k)) = 0.$$

The transformation of the first term does not differ from (α).

We thus see that the system

$$\frac{d}{dt} A_q(q^k) + \delta\,(B_q(q))^k = \delta\,(C(\mu q)\,\delta q)^k, \qquad k = 0, 1, \ldots, N, \tag{6}$$

with the periodicity conditions

$$q^0 = q^{N-1}, \quad q^1 = q^N \tag{7}$$

has the "law of energy dissipation"

$$\sum_k (A_q(q^k)\,q^k - A(q^k))\Big|_{t=0}^{t=T} = -\int_0^T \sum_k C(\mu q)^{k+\frac{1}{2}}(\delta q^{k+\frac{1}{2}})^2\,dt. \tag{8}$$

The sum in the integrand in the right-hand side is made up of nonnegative terms, which are all dissipation densities at corresponding grid points per unit time.

For general systems of the form

$$\frac{\partial L^0 q_i}{\partial t} + \sum_{j=1}^n \frac{\partial L^j q_i}{\partial x_j} = \sum_{j,l,s} \frac{\partial}{\partial x_j} b_{il}^{js} \frac{\partial q_l}{\partial x_s}, \qquad i = 1, 2, \ldots, m, \tag{1'}$$

with a symmetric and positive-definite matrix $|b_{il}^{js}|$ (Onsager conditions for irreversible processes), the construction is carried out analogously. The

author has not succeeded in his attempt to construct a difference scheme with a rectangular mesh for the case of more than one space variable; tetrahedral nets were used, which had been first introduced for similar (and more general) purposes by V. I. Lebedev /2/, whose work we shall closely follow. For simplicity, consider the case of two space variables $p_1$, $p_2$ with the metric

$$ds^2 = (g^1)^2 dp_1^2 + (g^2)^2 dp_2^2, \quad d\sigma = g^1 g^2 dp_1 dp_2 \tag{9}$$

(curvilinear orthogonal coordinates).

The linear differential operators of mathematical physics in these coordinates have the form

$$\begin{aligned}
\operatorname{grad}\Psi &= \left\{\frac{1}{g^1}\frac{\partial\Psi}{\partial p_1},\ \frac{1}{g^2}\frac{\partial\Psi}{\partial p_2}\right\},\\
\operatorname{div}\vec{A} &= \frac{1}{g^1 g^2}\left[\frac{\partial}{\partial p_1}(g^2 A^1) + \frac{\partial}{\partial p_2}(g^1 A^2)\right],\\
\operatorname{rot}\vec{A} &= \frac{1}{g^1 g^2}\left[\frac{\partial}{\partial p_1}(g^2 A^2) - \frac{\partial}{\partial p_2}(g^1 A^1)\right],\\
\operatorname{rot}\Psi &= \left\{\frac{1}{g^2}\frac{\partial\Psi}{\partial p_2},\ -\frac{1}{g^1}\frac{\partial\Psi}{\partial p_1}\right\},
\end{aligned} \tag{10}$$

($\vec{A}$ being a vector, $\Psi$ a scalar function of $p_1$, $p_2$). Formulas (10) are as suitable for the verification of relations such as $\operatorname{rot}\operatorname{grad}\Psi = 0$ and $\operatorname{div}\operatorname{rot}\vec{A} = 0$, and of various forms of the Gauss formula of the type $\int \operatorname{rot}\Psi\,\vec{A}\,d\sigma = -\int \Psi \operatorname{rot}\vec{A}\,d\sigma$, as the corresponding formulas in Cartesian coordinates. The difference approximation to the operators (10) amounts to the following. A uniform grid of points is introduced on the $p_1$, $p_2$-plane, as shown in the diagram. These points are labeled by indexes $(m, n)$ and $(m + 1/2, n + 1/2)$, and called integral points. Between every two such "integral" points we introduce an auxiliary "half-integral" point $(m, n + 1/2)$ or $(m + 1/2, n)$:

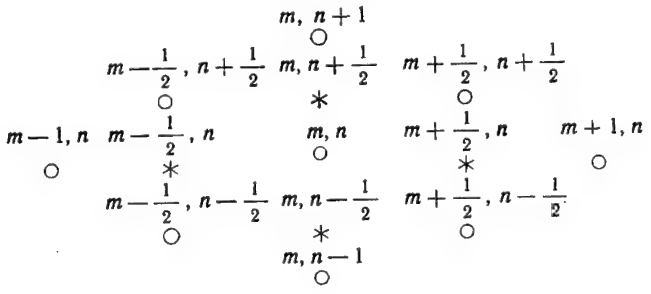


The function and the "differential" operators of even orders are defined at integral points, while "differential" operators of odd orders are defined at half-integral points. The operators are expanded by using analogs of formulas (10), with $\delta^i$ $(i = 1, 2)$ substituted for $\frac{\partial}{\partial p_i}$

For example,

$$\operatorname{rot}_h \vec{A}_{0,0} = \frac{1}{g^1_{0,0} g^2_{0,0}} [\delta^1 (g^2 A^2)_{0,0} - \delta^2 (g^1 A^1)_{0,0}] =$$

$$= \frac{1}{g^1_{0,0} g^2_{0,0}} [(g^2_{\frac{1}{2},0} A^2_{\frac{1}{2},0} - g^2_{-\frac{1}{2},0} A^2_{-\frac{1}{2},0}) -$$
$$- (g^1_{0,\frac{1}{2}} A^1_{0,\frac{1}{2}} - g^1_{0,-\frac{1}{2}} A^1_{0,-\frac{1}{2}})]$$

(to obtain the value of $\operatorname{rot}_h \vec{A}$ at point (0,0) we clearly should consider the vector $\vec{A}=(A^1, A^2)$ defined at the half-integral points $\left(\pm\frac{1}{2}, 0\right), \left(0, \pm\frac{1}{2}\right)$).

We observe that the "surface element", i.e., the weight with which the functions are to be summed, is $\sigma = g^1 g^2$ (for unit $p_1, p_2$ intervals).

We now return to equations (1′). Their finite-difference analog at (0,0) (taking $n=2$) is found to be

$$L^1_{q_l} = \frac{L^1(q_1^{\frac{1}{2},0}, \ldots, q_m^{\frac{1}{2},0}) - L^1(q_1^{-\frac{1}{2},0}, \ldots, q_m^{-\frac{1}{2},0})}{q_l^{\frac{1}{2},0} - q_l^{-\frac{1}{2},0}},$$

$$L^2_{q_l} = \frac{L^2(q_1^{0,\frac{1}{2}}, \ldots, q_m^{0,\frac{1}{2}}) - L^2(q_1^{0,-\frac{1}{2}}, \ldots, q_m^{0,-\frac{1}{2}})}{q_l^{0,\frac{1}{2}} - q_l^{0,-\frac{1}{2}}}, \qquad (11)$$

$$\mu q_i^{0,\frac{1}{2}} = \frac{1}{4}(q_i^{0,0} + q_i^{0,1} + q_i^{\frac{1}{2},\frac{1}{2}} + q_i^{\frac{1}{2},-\frac{1}{2}})$$

(the manner of averaging may also be different). The other manipulations are carried out as in the one-dimensional case. The law of energy dissipation has the form

$$\sum_{\alpha,\beta} \left( \sum_{i=1}^{m} L^0_{q_i} q_i - L^0 \right)^{\alpha,\beta} \Big|_{t=0}^{t=T} =$$

$$= -\int_0^T dt \sum_{\alpha',\beta'} \left( \sum_{j,s,k} b^{js}_{ik} (\mu q_1, \ldots, \mu q_m) \delta^s q_i \delta^j q_k \right)^{\alpha',\beta'},$$

where $\alpha$, $\beta$ run through all integral and $\alpha'$, $\beta'$ through all half-integral points. The assumptions of symmetry and positiveness of the matrix $\| b^{js}_{ik} \|$ (Onsager relations) imply that every term of the sum over $\alpha'$, $\beta'$ is positive and can be interpreted as density of energy dissipation rate.

Finally, let us consider the problem of the difference model for viscous incompressible flow. The Navier-Stokes equation in the plane case has the form

$$\frac{\partial u_i}{\partial t} + \sum_{j=1}^{2} u_j \frac{\partial u_i}{\partial x_j} = \nu \Delta u_i, \quad i = 1, 2,$$

$$\operatorname{div} \vec{u} = 0.$$

Let us again consider periodic boundary conditions (conditions of adherence are treated analogously). Integrating the incompressibility equation by introducing a stream function $\psi(x_1, x_2)$ such that $\frac{\partial \psi}{\partial x_1} = -u_2$, $\frac{\partial \psi}{\partial x_2} = u_1$, we obtain an equation for $\psi$:

$$\frac{\partial}{\partial t}\Delta\psi + \frac{\partial(\psi, \Delta\psi)}{\partial(x_1, x_2)} = \nu\Delta^2\psi. \tag{12}$$

This equation gives the enrgy dissipation law

$$\iint |\operatorname{rot}\psi|^2 dx_1 dx_2 \Big|_{t=0}^{t=T} = -\nu\int_0^T dt \iint |\Delta\psi|^2 dx_1 dx_2, \tag{13}$$

which is obtained by multiplying (12) by $\psi$ and integrating by parts. The nonlinear term $\frac{\partial(\psi, \Delta\psi)}{\partial(x_1, x_2)}$ does not enter (13), which is apparently very significant for the interpretation of the phenomenon. However, it is by no means immediately clear how to write a difference scheme with an expansion of the nonlinear term which would have this property (this is chiefly due to complications in constructing difference quotients for products). We therefore rewrite equation (12) in the form

$$\frac{\partial}{\partial t}\Delta\psi = \operatorname{rot}[\operatorname{rot}\psi \times \Delta\psi] + \nu\Delta^2\psi. \tag{14}$$

The nonlinear term does not enter (13) because of the evident relation

$$\iint (\operatorname{rot}[\operatorname{rot}\psi \times \vec{A}], \psi)\, dx_1\, dx_2 = -\iint (\operatorname{rot}\psi \times \vec{A}, \operatorname{rot}\psi)\, dx_1\, dx_2;$$

the mixed product in the integrand identically vanishes because $\operatorname{rot}\psi$ enters twice. It follows from our method of approximation of differential operators that this property is also retained in difference formulas (in any curvilinear orthogonal coordinates). "Integration" in differences of the linear terms is trivial. We have thus shown that the system

$$\frac{\partial}{\partial t}\Delta_h\psi^{m,n} = \operatorname{rot}_h[\operatorname{rot}_h\psi \times \Delta_h\psi]^{m,n} + \nu\Delta_h^2\psi^{m,n}$$

with periodic (or adherence) boundary conditions has the energy dissipation law

$$\sum_{\alpha',\beta'} (\operatorname{rot}_h \psi^{\alpha',\beta'})^2 \Big|_{t=0}^{t=T} = -\nu\int_0^T dt \sum_{\alpha,\beta} (\Delta_h\psi^{\alpha,\beta})^2,$$

where $\alpha$, $\beta$ run through integral, and $\alpha'$, $\beta'$ through half-integral points. Note that

$$\Delta_h = \operatorname{div}_h \operatorname{grad}_h = -\operatorname{rot}_h \operatorname{rot}_h, \quad \Delta_h^2 = \Delta_h\Delta_h.$$

In conclusion we observe that finite-dimensional models can apparently be used to obtain difference schemes having the same properties. For a very large class of ordinary differential equations these schemes (to arbitrary accuracy) were constructed and investigated by A. N. Tikhonov and A. A. Samarskii (see, e.g., /3/).

BIBLIOGRAPHY

1. GODUNOV, S.K. Interesnyi klass kvazilineinykh sistem (An Interesting Class of Quasilinear Systems). — DAN SSSR, Vol. 139, No. 3. 1961.
2. LEBEDEV, V.I. O metode setok dlya odnoi sistemy uravnenii v chastnykh proizvodnykh (On a Difference Method for a Certain System of Partial Differential Equations). — Izvestiya AN SSSR, seriya matematicheskaya, 22: 717-734. 1958.
3. TIKHONOV, A.N. and A.A. SAMARSKII. Ob odnorodnykh raznostnykh skhemakh (On Uniform Difference Schemes). — Zhurnal Vychislitel'noi Matematicheskoi Fiziki, Vol. 1, No. 1. 1961.

*A. L. Krylov and E. K. Proizvolova*

# *NUMERICAL STUDY OF FLOW BETWEEN ROTATING CYLINDERS*

We consider here the following problem (for more details, see /1/, §§ 18, 26, 28): a viscous incompressible fluid is enclosed between coaxial cylinders of radii $r_1$, $r_2$ $(r_1 < r_2)$ and unlimited height. When the cylinders rotate at angular velocities $\Omega_1$ and $\Omega_2$ then at certain relationships between the Reynolds numbers $\mathrm{Re}_1 = \frac{\Omega_1 r_1^2}{\nu}$ and $\mathrm{Re}_2 = \frac{\Omega_2 r_2^2}{\nu}$ (where $\nu$ is the viscosity) the simple stationary flow independent of angle and height becomes unstable and gives way to a different regime of stationary flow which, although still independent of the angle, periodically varies with height. These facts were obtained by Taylor experimentally, and also numerically (using small perturbations). Our aim is to carry out a numerical analysis of the phenomenon for the general nonlinear formulation, in accordance with experiment. However, we assume the flow to be periodic in height and axisymmetric.

The equations of motion in cylindrical coordinates have the form (see /2/, Ch. 1)

$$\frac{\partial u}{\partial t} + u\frac{\partial u}{\partial r} + w\frac{\partial u}{\partial z} - \frac{v^2}{r} = -\frac{\partial p}{\partial r} + \nu\left(\Delta u - \frac{u}{r^2}\right),$$

$$\frac{\partial v}{\partial t} + u\frac{\partial v}{\partial r} + w\frac{\partial v}{\partial z} + \frac{uv}{r} = \nu\left(\Delta v - \frac{v}{r^2}\right),$$

$$\frac{\partial w}{\partial t} + u\frac{\partial w}{\partial r} + w\frac{\partial w}{\partial z} = -\frac{\partial p}{\partial z} + \nu\Delta w$$

and the incompressibility condition

$$\frac{1}{r}\cdot\frac{\partial}{\partial r}(ru) + \frac{\partial w}{\partial z} = 0.$$

Here $\{u, v, w\}$ are the velocity components along the coordinates $r$, $\varphi$, $z$, $\Delta = \frac{\partial^2}{\partial r^2} + \frac{1}{r}\cdot\frac{\partial}{\partial r} + \frac{\partial^2}{\partial z^2}$. Introducing a stream function, such that

$$u = -\frac{1}{r}\cdot\frac{\partial}{\partial z}(r\psi); \quad w = \frac{1}{r}\cdot\frac{\partial}{\partial r}(r\psi),$$

we integrate the equation of incompressibility and, eliminating the pressure $p$, obtain a system for $\psi$ and $v$:

$$\frac{\partial L\psi}{\partial t} = \nu L^2\psi + \frac{\partial\psi}{\partial z}\left(\frac{\partial L\psi}{\partial r} - \frac{L\psi}{r}\right) - \frac{\partial L\psi}{\partial z}\left(\frac{\partial\psi}{\partial z} + \frac{\psi}{r}\right) - \frac{2v}{r}\frac{\partial v}{\partial z}, \qquad (1)$$

$$\frac{\partial v}{\partial t} = \nu Lv + \frac{\partial \psi}{\partial z}\left(\frac{\partial v}{\partial r} + \frac{v}{r}\right) - \frac{\partial v}{\partial z}\left(\frac{\partial \psi}{\partial r} + \frac{\psi}{r}\right), \tag{1}$$

where

$$L = \frac{\partial^2}{\partial r^2} + \frac{1}{r}\frac{\partial}{\partial r} + \frac{\partial^2}{\partial z^2} - \frac{1}{r^2}.$$

We seek a solution in the domain $r_1 \leqslant r \leqslant r_2, -H \leqslant z \leqslant H$. We set down periodic boundary conditions in $z$:

$$\left.\frac{\partial^l v}{\partial z^l}\right|_{z=-H} = \left.\frac{\partial^l v}{\partial z^l}\right|_{z=H}; \quad \left.\frac{\partial^m \psi}{\partial z^m}\right|_{z=-H} = \left.\frac{\partial^m \psi}{\partial z^m}\right|_{z=H} \tag{2'}$$
$$l = 0,1; \quad m = 0, 1, 2, 3;$$

and adherence conditions at the solid boundaries

$$v|_{r=r_i} = \Omega_i r_i, \quad \psi = \left.\frac{\partial \psi}{\partial r}\right|_{r=r_i} = 0, \qquad i = 1, 2. \tag{2''}$$

The simplest stationary solution mentioned above has the form

$$\psi \equiv 0, \quad v = Ar + \frac{B}{r},$$

where $A$ and $B$ are constants which are expressed in terms of $\Omega_i$ and $r_i$, $i = 1,2$, and are independent of $\nu$. For $\Omega_2 = 0$ this flow is stable for all sufficiently large $\nu$ (with constant $r_i$ and $\Omega_1$), and becomes unstable for $\nu = \nu_{cr}$. This phenomenon is the object of our study.

Equation (1) and the boundary conditions (2) are replaced by corresponding difference equations and boundary conditions. On the cylinder $r_1 \leqslant r \leqslant r_2$, $-H \leqslant z \leqslant H$ we set up a net with constant $r$ and $z$ intervals:

$$r_m = r_1 + mh; \quad m = 0,1,\ldots, M; \quad h = \frac{r_2 - r_1}{M};$$
$$z_n = nk; \quad n = -2, -1, 0, 1, \ldots, N, N+1; \quad k = \frac{H}{N}; \tag{3}$$
$$t_p = t_0 + p\tau; \quad p = 0, 1, \ldots, P.$$

The values of $\psi$ and $v$ at the point $(r_m, z_n)$ at a time $p\tau$ will be denoted by $\psi^p_{mn}$, $v^p_{mn}$. The difference approximation for (1) is taken in the form

$$\frac{L_h\psi^{p+1}_{mn} - L_h\psi^p_{mn}}{\tau} = \nu L_h^2\psi^{p+1}_{mn} + M_h(\psi^p_{mn}, v^p_{mn}),$$
$$\frac{v^{p+1}_{mn} - v^p_{mn}}{\tau} = \nu L_h v^{p+1}_{mn} + N_h(\psi^p_{mn}, v^p_{mn}), \tag{4}$$

where $L_h$, $M_h$, $N_h$ are difference operators approximating the corresponding differential operators ($L_h$ is a linear and $M_h$, $N_h$ are nonlinear operators; in more detail, see /3/).

This amounts to a two-layer scheme, and the system to be solved at the upper layer has the form

$$\tau\nu L_h^2\psi^{p+1}_{mn} - L_h\psi^{p+1}_{mn} = f(\psi^p_{mn}, v^p_{mn}),$$
$$\tau\nu L_h v^{p+1}_{mn} - v^{p+1}_{mn} = g(\psi^p_{mn}, v^p_{mn}), \tag{5}$$

i.e., can be divided into subsystems in $\psi^{p+1}_{mn}$ and $v^{p+1}_{mn}$. The stability of our scheme depends on the viscosity $\nu$ and deteriorates as $\nu \to 0$; we therefore

cannot hope to compute with this scheme the range of high Reynolds numbers. Fortunately, the phenomenon in question is observed in the range of moderate Reynolds numbers, around 100 — 200.

The system for the determination of $\psi$ at the $(p+1)$-th layer, after introducing the notations $\{\psi^p_{m0}, \psi^p_{m1}, \ldots, \psi^p_{mN-1}\} = \overline{\psi}^p_m$ can be written in the matrix form

$$A_m\overline{\psi}^{p+1}_{m+2} + B_m\overline{\psi}^{p+1}_{m+1} + C_m\overline{\psi}^{p+1}_m + D_m\overline{\psi}^{p+1}_{m-1} + E_m\overline{\psi}^{p+1}_{m-2} = \overline{f}^{p+1}_m, \quad m = 2, 3, \ldots, M-2; \tag{6}$$

with boundary conditions

$$\begin{cases} \overline{\psi}^{p+1}_0 = 0, \\ \overline{\psi}^{p+1}_1 = \frac{1}{4}\overline{\psi}^{p+1}_2, \end{cases} \qquad \begin{cases} \overline{\psi}^{p+1}_{M-1} = \frac{1}{4}\overline{\psi}^{p+1}_{M-2}, \\ \overline{\psi}^{p+1}_M = 0. \end{cases} \tag{7}$$

The vectors $\overline{\psi}$ satisfy the periodicity condition

$$\psi^{p+1}_{m,-2} = \psi^{p+1}_{m,N-2}, \quad \overline{\psi}^{p+1}_{m,-1} = \overline{\psi}^{p+1}_{m,N-1}, \qquad \psi^{p+1}_{m,0} = \psi^{p+1}_{m,N}, \quad \psi^{p+1}_{m,1} = \psi^{p+1}_{m,N+1}. \tag{8}$$

The matrices $A_m$, $B_m$, $C_m$, $D_m$, $E_m$ in (6) are all symmetric and cyclic. A matrix is said to be cyclic if every one of its rows can be obtained from the preceding row by a cyclic shift to the right, i.e.,

$$a_{i+1,j} = a_{i,j-1} \quad (j \neq 0) \text{ and } a_{i+1,0} = a_{i,N-1},$$

$(i, j = 0,1,\ldots,N-1)$. A cyclic matrix is thus completely defined by its first row. The cyclic matrices constitute a ring; the inverse of a cyclic matrix is also a cyclic matrix. It is convenient to interpret cyclic matrices as "vectors" $\overline{X} = \{x_i\}$ with the operations

$$\overline{X} + \overline{Y} = \{x_i + y_i\}; \quad c\overline{X} = \{cx_i\};$$

$$\overline{X}\cdot\overline{Y} = \left\{\sum_{k=0}^{i} x_k y_{i-k} + \sum_{k=i+1}^{N-1} x_k y_{N+i-k}\right\};$$

$$\overline{X}^{-1} = \left\{ \frac{1}{N} \sum_{l=0}^{N-1} \frac{\cos\frac{2\pi}{N} li}{\sum_{k=0}^{N-1} x_k \cos\frac{2\pi}{N} kl} \right\}$$

($\overline{X}^{-1}$ is the first row of the cyclic matrix which is the inverse of the cyclic matrix whose first row is $\overline{X}$). Observe that operations with cyclic matrices are essentially simpler. These matrices always appear when one of the coordinates is implicit in an equation (in our case, also in boundary conditions; for more details, see /3/).

System (6)-(7) will be solved by the method of matrix forcing, which in this case amounts to the following. Consider two relations for three consecutive vectors

$\bar{\psi}_i^{p+1}$, $\bar{\psi}_{i+1}^{p+1}$, $\bar{\psi}_{i+2}^{p+1}$, which for $i = m-2$, $m-1$, take the form:

$$\bar{\psi}_{m-2}^{p+1} = X_{m-2}\bar{\psi}_{m-1}^{p+1} + Y_{m-2}\bar{\psi}_m^{p+1} + \bar{Z}_{m-2}^{p+1},$$
$$\bar{\psi}_{m-1}^{p+1} = X_{m-1}\bar{\psi}_m^{p+1} + Y_{m-1}\bar{\psi}_{m+1}^{p+1} + \bar{Z}_{m-1}^{p+1}.$$

Inserting these relations in (6) we obtain the analogous relation for $i = m$:

$$\bar{\psi}_m^{p+1} = X_m\bar{\psi}_{m+1}^{p+1} + Y_m\bar{\psi}_{m+2}^{p+1} + \bar{Z}_m^{p+1}. \qquad (9)$$

Relation (9) can easily be written for $m = 0, 1$ using the boundary conditions at the inner cylinder:

$$X_0 = Y_0 = Y_1 = 0, \quad X_1 = \frac{1}{4}E, \quad \bar{Z}_0^{p+1} = \bar{Z}_1^{p+1} = 0,$$

where $E$ is the unit matrix.

Direct forcing involves successive determinations of matrices $X_m$, $Y_m$ and vectors $\bar{Z}_m^{p+1}$ from recurrence formulas; $X_m$, $Y_m$ should be determined only once (for all $p$), where $\bar{Z}_m^p$ depends on the layer number. Having obtained the last forcing relation

$$\bar{\psi}_{M-2}^{p+1} = X_{M-2}\bar{\psi}_{M-1}^{p+1} + Y_{M-2}\bar{\psi}_M^{p+1} + \bar{Z}_{M-2}^{p+1},$$

we apply the second boundary conditions $\bar{\psi}_M^{p+1} = 0$; $\bar{\psi}_{M-1}^{p+1} = \frac{1}{4}\bar{\psi}_{M-3}^{p+1}$,

to determine $\bar{\psi}_{M-1}^{p+1}$ and then, from (9), we successively determine $\bar{\psi}_m^{p+1}$ for $m = M-2, M-3, \ldots, 2$. This is the reverse forcing. The system for $\bar{V}_{mn}^{p+1}$ is solved analogously; the corresponding boundary conditions at the cylinders have the form

$$\bar{v}_0^{p+1} = \Omega_1 r_1 \bar{e}, \qquad \bar{v}_M^{p+1} = \Omega_2 r_2 \bar{e},$$

where $\bar{e} = (1, 1, \ldots, 1)$.

We now proceed with an analysis of the numerical results. Computations were made for a grid with $M = 20$, $N = 10$ for $\Omega_1 = 1$, $\Omega_2 = 0$, $r_1 = 1$, $r_2 = 2$ (the Reynolds number was thus specified by the dimensionless viscosity $\nu$).

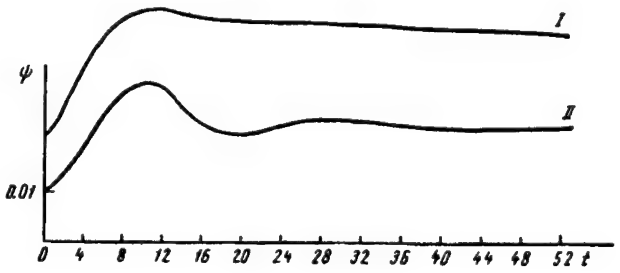


FIGURE 1. Variation of $\Psi$ in time:

I — $\tau = \frac{1}{4}$, $H = l$; II — $\tau = \frac{1}{32}$, $H = 2l$.

As initial values $\psi^0_{mn}$, $v^0_{mn}$ we assumed a distribution of $\psi$, $v$ close to the simplest stationary solution.

We were mostly concerned with the following problem: given a constant Reynolds number $\nu = \frac{1}{200}$, find the possible periodic regimes; in particular, establish the existence of "stronger" frequencies in the part of the spectrum which is unstable under infinitesimal perturbations.

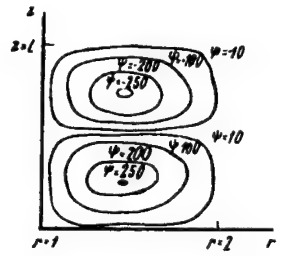


FIGURE 2. $\Psi$-field for $H=l$ (flow I) at time $t=40$; $\tau=\frac{1}{4}$

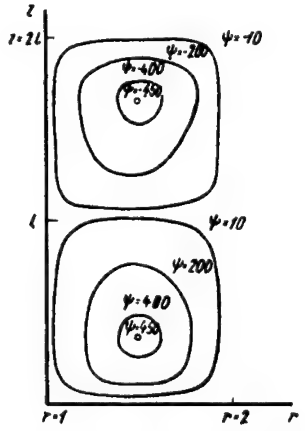


FIGURE 3. $\Psi$-field for $H=2l$ (flow II) at time $t=30$; $\tau=\frac{1}{32}$

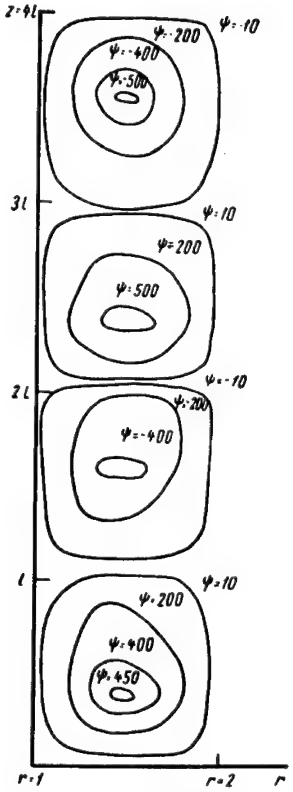


FIGURE 4. $\Psi$-field for $H=4l$ (flow III) at time $t=70$; $\tau=\frac{1}{32}$

Computations were made for

$$\nu=\frac{1}{200};\quad H=l,\ 2l,\ 4l,\quad \left(l=\frac{\pi}{3,2}\right).$$

In the first and the second cases analogous flow patterns were obtained, with a pair of counter-rotating vortices per period. The evolution to stationary regime is shown in Figure 1. Observe that the initial growth of $\psi_{mn}$, $v_{mn}$ in flow I is gentler than in flow II and that its amplitude (in $\psi$) is

smaller. Flow I is less intense than flow II. In the second case the principal harmonic of flow I is "offset" by the gentler flow II.

The situation in case III ($H = 4l$) is entirely different. Here the gentle harmonic of period $4l$, which in the infinitesimal approximation has a time growth one order smaller, is offset by the principal harmonic $2l$ so that the stationary flow in case III is simply twice repeated flow II (Figures 2, 3, 4).

This confirms the hypothesis of M. A. Lavrent'ev that, of the possible spectrum of unstable frequencies, only the frequency which has the fastest rate of time growth in the linear approximation is actually observed /4/ (Lavrent'ev originally analyzed the behavior of a rod beyond the stability limit). In our problem, the strongest period is $2l$ (frequency $\alpha = \frac{2\pi}{H} = 3.2$). This conclusion also follows from the linear theory.

We wish to thank I. M. Gel'fand whose influence and active participation contributed greatly to the initiation of projects on numerical investigation of stability of viscous flow. The present work, in particular, is a continuation of /3/ carried out under the guidance of I. M. Gel'fand. We are also grateful to S. B. Mostinskaya and Yu. Gormatyuk who participated in the compilation of the program.

BIBLIOGRAPHY

1. LANDAU, L.D. and E.M. LIFSHITS. Mekhanika sploshnykh sred (Mechanics of Continuous Media). — GITTL, Moskva. 1954.
2. LIN, C.C. Theory of Hydrodynamic Stability. — Cambridge Univ. Press. [Russian translation. 1958.]
3. ZHIDKOV, N.P., A.A. KORNEICHUK, A.L. KRYLOV, and S.B. MOSTINSKAYA. Ploskoparallel'noe dvizhenie vyazkoi zhidkosti mezhdu vrashchayushchimisya tsilindrami (Plane-Parallel Motion of Viscous Fluid between Rotating Cylinders). — In: "Vychislitel'nye metody i programmirovanie," Izdatel'stvo MGU. 1962.
4. LAVRENT'EV, M.A. Kumulyativnyi zaryad i printsipy ego raboty (Cumulative Charge and Its Working Principles). — UMN, 12(4): 76. 1957.

*A. L. Krylov and A. F. Misnik*

# *STABILITY OF VISCOUS FLOW BETWEEN TWO ROTATING CYLINDERS*

We present here the results of numerical integration of the Orr-Sommerfeld equation for viscous fluid enclosed between rotating cylinders (Taylor flow). A neutral curve was plotted in the $(R,\lambda)$ plane, where $R$ is the Reynolds number of undisturbed flow, and $\lambda$ is the frequency at which loss of stability occurs (the disturbance has the form $f(r)e^{\sigma t+i\lambda z}$).

The equation of stability of Taylor flow was found to reveal spectral properties which strongly differ from those of the equation of stability of Poiseuille flow.

1. Consider incompressible viscous flow between rotating concentric cylinders of unlimited length. If $u, v, w$ are the velocity components along $r, \theta, z$, the problem has the "trivial" stationary solution

$$\bar{u}=\bar{w}=0, \quad \bar{v}=Ar+\frac{B}{r}, \tag{1}$$

where

$$A=\frac{\left(\frac{R_2}{R_1}\right)^2\frac{\Omega_2}{\Omega_1}-1}{\left(\frac{R_2}{R_1}\right)^2-1}, \quad B=-\frac{\frac{R_2}{R_1}\left(\frac{\Omega_2}{\Omega_1}-1\right)}{\left(\frac{R_2}{R_1}\right)^2-1},$$

$R_j$ being the radii of the cylinders, $\Omega_j$ their angular velocities $(j=1,2)$.

An investigation of the stability of this solution amounts (see /1/, Ch. 1) to investigation of the spectral properties of the system

$$\begin{gathered}(L-\lambda^2-\sigma R)(L-\lambda^2)\psi=2\lambda R\left(A+\frac{B}{r^2}\right)v,\\ (L-\lambda^2-\sigma R)v=2\lambda RA\psi,\\ \psi=\frac{d\psi}{dr}=v=0 \quad \text{for } r=R_j \qquad (j=1,2),\\ L\equiv\frac{d^2}{dr^2}+\frac{1}{r}\frac{d}{dr}-\frac{1}{r^2}.\end{gathered} \tag{2}$$

Here $\lambda$ and $\sigma$ are parameters which can physically be interpreted as $z$- and $t$-frequencies of the solution for small perturbations of the "trivial" solution $(\lambda>0,\ \sigma=\sigma_1+i\sigma_2)$. For given $\lambda$ and $\sigma$ we must find a Reynolds number $R$ for which the homogeneous problem (2) has a nontrivial solution. The case $\sigma=0$ is called neutral and corresponds to stationary secondary flow; the curve in the $(R,\lambda)$-plane corresponding to the neutral case is called the

neutral curve. The least (in $\lambda$) Reynolds number on this curve is called the critical Reynolds number; it is the stability limit of the "trivial" solution.

The critical Reynolds number for this problem was first determined by Taylor /2/. The basic ideas of Taylor, who approximated the solution by a linear combination of functions and determined the coefficients by equation of the infinite determinant of the system to zero, were further developed in /3, 4/.

With high-speed computers, it is more expedient to solve problem (2) by the method of finite differences, which provides a more direct way to the solution. This is particularly evident for related, but more complicated problems, e.g., the study of stability of Poiseuille flow where instability sets in at very high Reynolds numbers, giving a small coefficient for the leading derivatives (see /1/). None of the above papers, however, gives the neutral curve for Taylor flow. Our procedure is close to that of Thomas /5/.

2. To obtain a difference approximation to system (2), we use a procedure first devised by Gauss, and later developed by Numerov, Jackson, and Thomas (see /5/).

Setting $\psi = r^{-\frac{1}{2}}\varphi$ and $v = r^{-\frac{1}{2}}u$, we remove the derivatives $\frac{d^3\psi}{dr^3}$ and $\frac{dv}{dr}$ from equations (2).

After this substitution, system (2) takes the form

$$\varphi^{(IV)} + B\varphi'' + C\varphi' + D\varphi + Eu = 0, \qquad (2')$$
$$u'' + Gu + F\varphi = 0,$$

where

$$B = -\left(\frac{3}{2r^2} + 2\lambda^2\right),$$
$$C = \frac{3}{r^3},$$
$$D = \lambda^4 + \frac{3}{2}\frac{\lambda^2}{r^2} - \frac{63}{16r^4},$$
$$E = -2\lambda R\left(A + \frac{B}{r^2}\right),$$
$$G = -\left(\frac{3}{4r^2} + \lambda^2\right),$$
$$F = -2\lambda RA.$$

If we replace the derivatives using the ordinary difference formulas

$$\varphi^{(IV)} \sim \frac{1}{h^4}(\varphi_{i+2} - 4\varphi_{i+1} + 6\varphi_i - 4\varphi_{i-1} + \varphi_{i-2}),$$

we obtain a truncation error of the order of $h^2$ per step. A similar error occurs in the approximation

$$u'' \sim \frac{1}{h^2}(u_{i+1} - 2u_i + u_{i-1}).$$

To reduce the truncation error, we make a different substitution:

$$\varphi = (1 + k_1\delta^2 + k_2\delta^4 + \ldots)g,$$
$$u = (1 + l_1\delta^2 + l_2\delta^4 + \ldots)f,$$

where $\delta^2$ is the second central difference operator

$$\delta^2 x = x_{i+1} - 2x_i + x_{i-1} = x(r+h) - 2x(r) + x(r-h),$$

and the coefficients $k_\nu$, $l_\nu$ are determined from the conditions of best approximation. It is easily seen that setting $k_1 = \frac{1}{6}$, $l_1 = \frac{1}{12}$ and $k_\nu = l_\nu = 0$ ($\nu = 2, 3, \ldots$), we obtain an accuracy of the order of $h^4$. We finally obtain the following formulas and estimates:

$$\varphi_i = \frac{1}{6} g_{i+1} + \frac{2}{3} g_i + \frac{1}{6} g_{i-1},$$

$$u_i = \frac{1}{12} f_{i+1} + \frac{5}{6} f_i + \frac{1}{12} f_{i-1},$$

$$\frac{d^4}{dr^4} \varphi_i = \frac{1}{h^4} \delta^4 g_i + \left[ -\frac{3103}{50400} h^4 g^{(8)} \right],$$

$$\frac{d^2}{dr^2} \varphi_i = \frac{1}{h^2} \left( \delta^2 + \frac{1}{12} \delta^4 \right) g_i + \left[ -\frac{h^4}{360} g^{(6)} \right],$$

$$\frac{d}{dr} \varphi_i = \frac{1}{h} (g_{i+1} - g_{i-1}) + \left[ -\frac{7}{135} h^4 g^{(5)} \right],$$

$$\frac{d^2}{dr^2} u_i = \frac{1}{h^2} \delta^2 g_i + \left[ \frac{1}{240} h^4 f^{(6)} \right].$$

Omitting terms of the order of $h^4$, we rewrite system (2') in the form

$$\begin{gathered} A_i g_{i+2} + B_i g_{i+1} + C_i g_i + D_i g_{i-1} + A_i g_{i-2} + \\ + E_i f_{i+1} + 10 E_i f_i + E_i f_{i-1} = 0, \\ F_i g_{i+1} + 4F_i g_i + F_i g_{i-1} + G_i f_{i+1} + H_i f_i + G_i f_{i-1} = 0, \\ i = 0, 1, \ldots, n-1, \end{gathered} \tag{3}$$

where

$$A_i = 1 - \frac{h^2}{12} \left( \frac{3}{2r_i^2} + 2\lambda^2 \right),$$

$$B_i = -4 - \frac{2}{3} h^2 \left( \frac{3}{2r_i^2} + 2\lambda^2 \right) + \frac{3}{2} \frac{h^3}{r_i^3} + \\ + \frac{h^4}{6} \left( \lambda^4 + \frac{3}{2} \frac{\lambda^2}{r_i^2} - \frac{63}{16 r_i^4} \right),$$

$$C_i = 6 + \frac{3}{2} h^2 \left( \frac{3}{2r^2} + 2\lambda^2 \right) + \frac{2}{3} h^4 \left( \lambda^4 + \frac{3}{2} \frac{\lambda^2}{r_i^2} - \frac{63}{16 r_i^4} \right),$$

$$D_i = -4 - \frac{2}{3} h^2 \left( \frac{3}{2r_i^2} + 2\lambda^2 \right) - \frac{3}{2} \cdot \frac{h^3}{r_i^3} + \\ + \frac{h^4}{6} \left( \lambda^4 + \frac{3}{2} \frac{\lambda^2}{r_i^2} - \frac{63}{16 r_i^4} \right),$$

$$E_i = -\frac{h^4}{6} \left( 1 + \frac{B}{r_i^2} \right) R\lambda,$$

$$F_i = -\frac{h^3}{3} R\lambda,$$

$$G_i = 1 - \frac{h^2}{12} \left( \frac{3}{4r_i^2} + \lambda^2 \right),$$

$$H_i = -2 - \frac{5}{6} h^2 \left( \frac{3}{4r_i^2} + \lambda^2 \right).$$

The boundary conditions are also approximated to within $h^4$, as in /5/ (note that the variables $g_i$, $f_i$ require the addition of one point at each end of the interval). System (3) with the boundary conditions is solved by the forcing method, i.e., by successive elimination of the pairs $(g_i, f_i)$ from left to right. We thus obtain the recurrence formulas

$$\begin{aligned} g_i &= X_i g_{i+1} + Y_i g_{i+2} + Z_i f_{i+1}, \\ f_i &= \alpha_i g_{i+1} + \beta_i g_{i+2} + \gamma_i f_{i+1}, \end{aligned} \tag{4}$$

where the coefficients $X_i$, $Y_i$, $Z_i$, $\alpha_i$, $\beta_i$, $\gamma_i$ are expressed by certain recurrence formulas in terms of the coefficients of system (3) at the $i$-the point and the forcing coefficients at two preceding points. At points $r_{-1}$ and $r_0$ the forcing coefficients are simply expressed in terms of the coefficients of the equation.

For given $\lambda$ and $R$ we can compute the forcing coefficients and find a relation between $f$ and $g$ at the right endpoint. It has the form

$$\left(Y_{n-2} - \frac{1}{2} X_{n-2} - 1\right) g_n = 0. \tag{5}$$

If the factor preceding $g_n$ does not vanish, then $g_n = 0$ and, as is readily seen, $f_{n+1} = f_n = 0$. It then follows from (4) that $f_i = g_i = 0$ $(i = -1, 0, \ldots, n+1)$, i.e., the problem has a trivial solution only. The equation of the neutral curve can thus be written

$$M(\lambda, R) \equiv Y_{n-2} - \frac{1}{2} X_{n-2} - 1 = 0. \tag{6}$$

If $M = 0$, we can take $g_n \neq 0$ and find a neutral solution, which is the corresponding eigenfunction.

Computations were made for $n = 11, 16, 26$ points. An analysis of the numerical data shows that the results with $n = 16$ and $n = 26$ do not differ for all practical purposes, i.e., the solution is independent of $h$ and therefore solves the differential, as well as the difference equation. 20—25 sec of the STRELA computer time were required to find the root $R$ of the equation $M(\lambda, R) = 0$ to within $10^{-3}$ for a given $\lambda$ with $n = 16$.

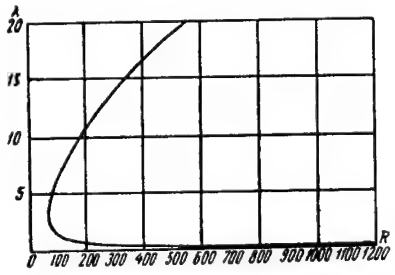


3. We see from the graph that the Taylor flow has a neutral curve with two branches, one of which approaches the axis $\lambda = 0$, and the other recedes to infinity in both $R$ and $\lambda$. Therefore, unlike Poiseuille flow, all the frequencies of Taylor flow eventually become unstable. The critical Reynolds number $R$ which is the smallest (in $\lambda$) root of the equation of the neutral curve (6) is equal to 68.191 for $\lambda = 3.2$. The general nonstationary case $\sigma = \sigma_1 + i\sigma_2$ was calculated analogously to the neutral curve for $\sigma = 0$. The program was run on the STRELA computer at the Computational Center of the Moscow State University. The critical Reynolds number was calculated in the M. Sc. thesis of G. Tolstova in 1959/60.

Table of results

| $\lambda$ | $R$ | $\lambda$ | $R$ | $\lambda$ | $R$ |
|---|---|---|---|---|---|
| 0.1 | 1189.725 | 4.7 | 76.963 | 9.3 | 162.060 |
| 0.2 | 596.167 | 4.8 | 78.013 | 9.4 | 164.569 |
| 0.3 | 398.941 | 4.9 | 79.109 | 9.5 | 167.101 |
| 0.4 | 300.726 | 5.0 | 80.251 | 9.6 | 169.652 |
| 0.5 | 242.135 | 5.1 | 81.437 | 9.7 | 172.230 |
| 0.6 | 203.368 | 5.2 | 82.668 | 9.8 | 174.829 |
| 0.7 | 175.941 | 5.3 | 83.941 | 9.9 | 177.451 |
| 0.8 | 155.594 | 5.4 | 85.256 | 10.0 | 180.095 |
| 0.9 | 138.978 | 5.5 | 86.610 | 10.1 | 182.761 |
| 1.0 | 127.651 | 5.6 | 88.004 | 10.2 | 185.449 |
| 1.1 | 117.731 | 5.7 | 89.438 | 10.3 | 188.159 |
| 1.2 | 109.627 | 5.8 | 90.909 | 10.4 | 190.891 |
| 1.3 | 102.921 | 5.9 | 92.417 | 10.5 | 193.645 |
| 1.4 | 97.295 | 6.0 | 93.964 | 10.6 | 196.413 |
| 1.5 | 92.566 | 6.1 | 95.543 | 10.7 | 199.117 |
| 1.6 | 88.541 | 6.2 | 97.161 | 10.8 | 202.009 |
| 1.7 | 85.119 | 6.3 | 98.812 | 10.9 | 204.847 |
| 1.8 | 82.182 | 6.4 | 100.498 | 11.0 | 207.732 |
| 1.9 | 79.667 | 6.5 | 102.217 | 11.1 | 210.613 |
| 2.0 | 77.518 | 6.6 | 103.969 | 11.2 | 213.515 |
| 2.1 | 75.674 | 6.7 | 105.752 | 11.3 | 216.437 |
| 2.2 | 74.102 | 6.8 | 107.563 | 11.4 | 219.380 |
| 2.3 | 72.769 | 6.9 | 109.409 | 11.5 | 222.345 |
| 2.4 | 71.648 | 7.0 | 111.287 | 11.6 | 225.330 |
| 2.5 | 70.717 | 7.1 | 113.195 | 11.7 | 228.335 |
| 2.6 | 69.954 | 7.2 | 115.131 | 11.8 | 231.360 |
| 2.7 | 69.347 | 7.3 | 117.097 | 11.9 | 234.407 |
| 2.8 | 68.879 | 7.4 | 119.092 | 12.0 | 237.473 |
| 2.9 | 68.541 | 7.5 | 121.115 | 12.1 | 240.560 |
| 3.0 | 68.318 | 7.6 | 123.166 | 12.2 | 243.667 |
| 3.1 | 68.204 | 7.7 | 125.249 | 12.3 | 246.795 |
| 3.2 | 68.191 | 7.8 | 127.356 | 12.4 | 249.942 |
| 3.3 | 68.272 | 7.9 | 129.491 | 12.5 | 253.110 |
| 3.4 | 68.443 | 8.0 | 131.653 | 12.6 | 256.298 |
| 3.5 | 68.697 | 8.1 | 133.842 | 12.7 | 259.505 |
| 3.6 | 69.030 | 8.2 | 136.057 | 12.8 | 262.733 |
| 3.7 | 69.438 | 8.3 | 138.296 | 12.9 | 265.980 |
| 3.8 | 69.916 | 8.4 | 140.560 | 13.0 | 269.248 |
| 3.9 | 70.463 | 8.5 | 142.851 | 13.1 | 272.535 |
| 4.0 | 71.075 | 8.6 | 145.168 | 13.2 | 275.843 |
| 4.1 | 71.749 | 8.7 | 147.508 | 13.3 | 279.170 |
| 4.2 | 72.483 | 8.8 | 149.874 | 13.4 | 282.517 |
| 4.3 | 73.274 | 8.9 | 152.267 | 13.5 | 285.870 |
| 4.4 | 74.114 | 9.0 | 154.675 | 15.0 | 340.080 |
| 4.5 | 75.013 | 9.1 | 157.113 | 17.0 | 415.920 |
| 4.6 | 75.963 | 9.2 | 159.575 | 20.0 | 546.510 |

BIBLIOGRAPHY


1. LIN, C.C. Theory of Hydrodynamic Stability. — Cambridge Univ. Press. [Russian translation. 1958.]
2. TAYLOR, G.J. Stability of a Viscous Liquid Contained between Two Rotating Cylinders. — Phil. Trans., A, 223, 289-343. 1923.
3. CHANDRASEKHAR, S. The Stability of Viscous Flow between Rotating Cylinders. — Proc. Royal Soc., ser. A, G, B. 246:(1246): 301-311. 1958.
4. DI PRIMA, R.C. Application of the Galerkin Method to the Calculation of the Stability of Curved Flows. —Quart. Appl. Math., 13; 55–62. 1955.
5. THOMAS, L.H. The Stability of Plane Poiseuille Flow. — Phys. Rev., 93(4): 780-783. 1953.

*L. A. Chudov and T. V. Kuskova*

# *APPLICATION OF DIFFERENCE SCHEMES TO COMPUTATION OF NONSTATIONARY FLOW OF VISCOUS INCOMPRESSIBLE FLUID*

## § 1. INTRODUCTION

Two-dimensional nonstationary flow of a viscous incompressible fluid is described by the equation

$$\frac{\partial}{\partial t}\Delta\psi = \nu\Delta\Delta\psi - \frac{\partial\psi}{\partial y}\frac{\partial\Delta\psi}{\partial x} + \frac{\partial\psi}{\partial x}\frac{\partial\Delta\psi}{\partial y}, \qquad (1)$$

where $\psi$ is the stream function, $\frac{\partial\psi}{\partial y} = u$ is the velocity component along the $x$-axis, $-\frac{\partial\psi}{\partial x} = v$ is the velocity component along the $y$-axis, $\nu$ the kinematic viscosity.

Numerical solution of equation (1) involves considerable difficulties. These difficulties are due to the following reasons: first, equation (1) is not explicit in the time derivative, second, it is nonlinear, third, at small $\nu$ the solution of equation (1) near the boundary of the region in which the solution is sought generally behaves as a boundary layer, i.e., intensely varies along the normal to the boundary.

Attempts to apply semi-analytical methods, as the methods of Kantorovich (the ray method) and Galerkin, to computation of nonstationary viscous flow show that as the problem becomes more complicated, the programming difficulties mount rapidly owing to lack of standard procedures. Moreover, estimating the computational error is a very difficult task with these methods. Difference methods seem more promising as regard the possibilities of programming and estimating the computational accuracy.

It is quite obvious that the solution of equation (1) by difference methods is a complicated problem. Since in this equation $\Delta\psi$ has to be differentiated with respect to $t$, at every time section we must solve (by some iterative method) a difference Poisson equation for $\psi$. As the equation is nonlinear, to ensure second order accuracy with respect to the time interval, additional iterations must be made at every time section, or alternatively more complicated schemes should be employed (the three-layer scheme, the "tripod" scheme, etc.). The fourth-order derivatives in the equation substantially complicate the computational algorithm, and the abrupt variation of the solution near the boundaries requires either a nonuniform mesh or a very fine one.

Until now only very few papers have been published on the application of difference methods to the solution of nonstationary, or even stationary problems of viscous incompressible flow described by the complete Navier-Stokes equation (see /1/—/6/). These works, however, mostly give no estimates of the accuracy of the results. This is due to the exceeding cumbersomeness of the computations which generally strained to the limit the capacities of the techniques used, and also to obvious difficulties of deriving theoretical estimates of errors in difference schemes used to approximate equation (1). It was therefore necessary to devise model problems for evaluating the effectiveness of difference methods, in particular, to investigate such problems as choice of schemes, determination of grid parameters, and of iterative processes.

In the present article the analysis is made for the model equation

$$\frac{\partial \Delta\psi}{\partial t} = \nu \Delta\Delta\psi + A\frac{\partial \Delta\psi}{\partial x} + B\frac{\partial \Delta\psi}{\partial y} \qquad (2)$$

with constant coefficients $A$, $B$, $\nu$. The Cauchy problem for equation (2) is considered (on the entire $x$, $y$ plane for $t > 0$).

With suitable requirements satisfied by the initial conditions, the solution of this problem can be represented as a Fourier integral

$$\psi(x, y, t) = \iint e^{\lambda t} e^{i\omega_1 x} e^{i\omega_2 y} \tilde{\psi}_0(\omega_1, \omega_2)\, d\omega_1\, d\omega_2, \qquad (3)$$

where

$$\lambda = \lambda(\omega_1, \omega_2) = -\nu(\omega_1^2 + \omega_2^2) + iA\omega_1 + iB\omega_2. \qquad (4)$$

The approximate solution obtained with any of the difference schemes can be represented in the form (3) by substituting $\overline{\lambda}$ for $\lambda$, where $\overline{\lambda}$ depends on the choice of the scheme, the mesh size, and also the iterative processes and their respective parameters. The accuracy of the results is estimated here by comparison of the factors $e^{\lambda t}$ and $e^{\overline{\lambda} t}$ which specify the variation in time of the exact and the approximate solution. Given the accuracy with which the approximate solution should be computed, we can determine the mesh size and the parameters of the iterative processes for the scheme in question.

In the present article we only deal with the choice of mesh size for certain difference schemes. In future we intend to investigate by this method various iterative processes which can be applied to the solution of difference equations at layers corresponding to these particular schemes*.

As an example of the application of the results, we considered the stability of Poiseuille flow.

* The results of an investigation of one simple iterative process are presented in the author's paper "Issledovanie skhodimosti prosteishikh iteratsionnykh protsessov i ustoichivosti raznostnykh skhem s uchetom iteratsionnykh oshibok dlya uravneniya Nav'e-Stoksa" (A Study of Convergence of Simple Iterative Processes and of Stability of Difference Schemes with an Allowance for Iteration Errors for the Navier-Stokes Equation). — Report of the Computational Center of Moscow State University. 1962.

## § 2. THE PRINCIPAL HARMONIC, THE MAIN RECTANGLE. CHARACTERISTIC TIME. ACCURACY STANDARD*

Let us first define some necessary concepts. Suppose that the solution $\psi(x, y, t)$ does not change (to within pre-assigned accuracy) if the integral (3) is "truncated", i.e., if the infinite integration domain is replaced by the rectangle

$$0 \leqslant |\omega_1| \leqslant \omega_1^0, \qquad 0 \leqslant |\omega_2| \leqslant \omega_2^0.$$

The sides $\omega_1^0$, $\omega_2^0$ are determined by the smoothness of the solution required; they sometimes can be inferred from some previously found approximate solutions, and sometimes from experimental data. A solution of the form $e^{\lambda t}\, e^{i\omega_1^0 x}\, e^{i\omega_2^0 y}$ will be called the principal harmonic, and the rectangle $\left\{0 \leqslant x \leqslant \frac{\pi}{\omega_1^0},\ 0 \leqslant y \leqslant \frac{\pi}{\omega_2^0}\right\}$ the main rectangle. The mesh size required for sufficiently accurate computation of the principal harmonic will be characterized by the number of grid points $N(\omega_1^0, \omega_2^0)$ in the main rectangle. We shall show (§ 4) that $N$, in a certain sense, is a constant number independent of $\omega_1^0$, $\omega_2^0$. Let the region $\Omega$ where the solution is being determined by $L_1$ long on the side parallel to the $x$-axis and $L_2$ along the axis $y$. In view of the preceding remark concerning $N$, we see that the total number of grid points required to compute the principal harmonic with pre-assigned accuracy is proportional to the number of rectangles, equal in area to the main rectangle, necessary to cover the domain $\Omega$. The total number of mesh points is thus equal in order of magnitude to $\frac{L_1 L_2}{\pi^2}\, \omega_1^0 \omega_2^0\, N$. For the schemes considered below, the truncation error decreases with decreasing $\omega_1$ and $\omega_2$, so that for purposes of estimating the accuracy of the solution it is sufficient to concentrate on the principal harmonic. To simplify the notations, we shall write in what follows $\omega_1$, $\omega_2$ for $\omega_1^0$, $\omega_2^0$. The relative error of the approximate solution for the principal harmonic at time $t$ is

$$\left|\frac{e^{\lambda t} - e^{\lambda t}}{e^{\lambda t}}\right| = |e^{(\bar{\lambda}-\lambda)t} - 1|.$$

For small $t$ this error is approximately proportional to $|\bar{\lambda} - \lambda|\, t$. The difference $|\bar{\lambda} - \lambda|\, t$ thus characterizes the relative error. To make this characteristic independent of $t$, we introduce the concept of characteristic time. We define it as

$$T_{\text{char}} = \frac{1}{|\lambda|} = \frac{1}{\sqrt{\nu(\omega_1^2 + \omega_2^2) + (A\omega_1 + B\omega_2)^2}}. \tag{5}$$

This definition of characteristic time can be justified as follows. According to (4), the time variation of the principal harmonic amounts, first, to a change of amplitude (due to the term $\nu(\omega_1^2 + \omega_2^2)$) and, second, to a change of phase (due to $iA\omega_1 + iB\omega_2$). If $A = B = 0$, then during the time $T_{\text{char}}$ the logarithm of the amplitude will change by 1, and the phase will remain

* The concepts introduced in this section and the general procedure employed were developed by L. A. Chudov in application to the equation $u_t = \nu\Delta u + Au_x + Bu_y$ in his special course "Difference Methods for Solution of Parabolic Equations" given at the Moscow University in 1960/61.

constant. If $\nu = 0$ (and $A\omega_1 + B\omega_2 \neq 0$), the phase will change by 1, and the amplitude will retain its previous value. In the general case, during the time $T_{char}$, either the logarithm of the amplitude or the phase will change considerably (but by no more than 1).

The relative error of the approximate solution during time $T_{char}$ is

$$\delta = |e^{(\overline{\lambda}-\lambda)|\lambda|} - 1| \approx \left|\frac{\overline{\lambda}-\lambda}{\lambda}\right|. \tag{6}$$

The overall error is made up of the errors due to approximation of the derivatives with respect to $x$ and $y$, of the derivative with respect to $t$, and to iterative processes. When choosing the mesh parameters and the iterative processes, we shall require that each of these errors will be of the same order of smallness as a small number $k$, which will be called the accuracy standard (technically this is more convenient than to impose the requirement of smallness directly on $\delta$). Approximate equality of these errors clearly characterizes optimum choice of parameters. In this case $\delta = 3k$.

## § 3. DIFFERENCE SCHEMES. STABILITY

We first consider two two-layer difference schemes which can be written in the general form

$$\frac{\Delta_{h,l}\psi^{n+1}_{m,k} - \Delta_{h,l}\psi^{n}_{m,k}}{\tau} = \alpha_1 L_{h,l}\psi^{n+1}_{m,k} + \alpha_2 L_{h,l}\psi^{n}_{m,k}. \tag{7}$$

Here $\Delta_{h,l}$ is the approximation to the operator $\Delta = \frac{\partial^2}{\partial x^2} + \frac{\partial^2}{\partial y^2}$ on a grid with $\Delta x = h$, $\Delta y = l$; $L_{h,l}$ is the approximation to the operator on the right-hand side of equation (2); $\Delta t = \tau$ the time interval; $\alpha_1$, $\alpha_2$ weights, satisfying the conditions $\alpha_1 + \alpha_2 = 1$, $\alpha_1 \geqslant 0$, $\alpha_2 \geqslant 0$; $\psi^n_{m,k} = \psi(mh, kl, n\tau)$.

We now proceed with the description of the difference operators $\Delta_{h,l}$ and $L_{h,l}$. We shall consider two alternatives differing in order of approximation.

Alternative A. Approximation error $O(h^2 + l^2)$.

$$\Delta^{(A)}_{h,l}\psi_{m,k} = \frac{\psi_{m+1,k} - 2\psi_{m,k} + \psi_{m-1,k}}{h^2} + \frac{\psi_{m,k+1} - 2\psi_{m,k} + \psi_{m,k-1}}{l^2}, \tag{8}$$

$$L^{(A)}_{h,l}\psi_{m,k} = \nu\Delta^{(A)}{}_{h,l}\Delta^{(A)}_{h,l}\psi_{m,k} + A\delta_x\Delta^{(A)}_{h,l}\psi_{m,k} + B\delta_y\Delta^{(A)}_{h,l}\psi_{m,k}, \tag{9}$$

where

$$\delta_x\Delta\psi_{m,k} = \frac{\Delta\psi_{m+1,k} - \Delta\psi_{m-1,k}}{2h}; \quad \delta_y\Delta\psi_{m,k} = \frac{\Delta\psi_{m,k+1} - \Delta\psi_{m,k-1}}{2l}.$$

Alternative B. Approximation error $O(h^4 + l^4)$.

$$\Delta^{(B)}_{h,l}\psi_{m,k} = \Delta^{(A)}_{h,l} - \frac{h^2\delta^4_{xxxx}\psi_{m,k} + l^2\delta^4_{yyyy}\psi_{m,k}}{12}, \tag{10}$$

$$L_{h,l}^{(B)}\psi_{m,k} = L_{h,l}^{(A)}\psi_{m,k} - \frac{\nu}{6}[\Delta(\delta_{xxxx}^4 + \delta_{yyyy}^4)\psi_{m,k}] -$$

$$-\frac{A}{12}[\delta_x(h^2\delta_{xxxx}^4 + l^2\delta_{yyyy}^4)\psi_{m,k} + 2h^2\delta_{xxx}^3(\delta_{xx}^2 + \delta_{yy}^2)\psi_{m,k}] - \qquad (11)$$

$$-\frac{B}{12}[\delta_y(h^2\delta_{xxxx}^4 + l^2\delta_{yyyy}^4)\psi_{m,k} + 2l^2\delta_{yyy}^3(\delta_{xx}^2 + \delta_{yy}^2)\psi_{m,k}].$$

Here $\delta_x\psi_{m,k}$; $\delta_{xx}\psi_{m,k}$;...; $\delta_{yyyy}\psi_{m,k}$ is the central difference approximation to the derivatives $\frac{\partial\psi}{\partial x}, \frac{\partial^2\psi}{\partial x^2}, \ldots, \frac{\partial^4\psi}{\partial y^4}$; $\Delta(\delta_{xxxx}^4+\delta_{yyyy}^4)\psi_{m,k}$ is the analogous approximation to the expression

$$\frac{\partial^2}{\partial x^2}\left(\frac{\partial^4\psi}{\partial x^4} + \frac{\partial^4\psi}{\partial y^4}\right) + \frac{\partial^2}{\partial y^2}\left(\frac{\partial^4\psi}{\partial x^4} + \frac{\partial^4\psi}{\partial y^4}\right). \qquad (12)$$

The difference expressions (10) and (11) were obtained from (8), (9) by computing the main terms of the error with subsequent substitution of difference quotients for the corresponding derivatives. The stability of difference equation (7) for every alternative will be investigated in the case of time-symmetric implicit scheme ($\alpha_1 = 1/2$, $\alpha_2 = 1/2$) and in the case of "explicit" scheme ($\alpha_1 = 0$, $\alpha_2 = 1$)*.

We investigate stability using the Fourier transform, i.e., we seek a solution of the form $\psi_{m,k}^n = s^n e^{i\omega_1 mh} e^{i\omega_2 kl}$. For these solutions, application of operators $\Delta_{h,l}$ and $L_{h,l}$ amounts to multiplication by $\Delta_{h,l}(\omega_1, \omega_2)$ and $L_{h,l}(\omega_1, \omega_2)$.

Computing $s$, we obtain

$$s = \frac{1 + \tau\alpha_2 \dfrac{L_{h,l}(\omega_1, \omega_2)}{\Delta_{h,l}(\omega_1, \omega_2)}}{1 - \tau\alpha_1 \dfrac{L_{h,l}(\omega_1, \omega_2)}{\Delta_{h,l}(\omega_1, \omega_2)}}. \qquad (13)$$

For alternative A we have

$$s^{(A)} = \frac{1 - \alpha_2\left[4\nu\tau\left(\dfrac{\sin^2\frac{\omega_1 h}{2}}{h^2} + \dfrac{\sin^2\frac{\omega_2 l}{2}}{l^2}\right) - i\tau\left(A\dfrac{\sin\omega_1 h}{h} + B\dfrac{\sin\omega_2 l}{l}\right)\right]}{1 + \alpha_1\left[4\nu\tau\left(\dfrac{\sin^2\frac{\omega_1 h}{2}}{h^2} + \dfrac{\sin^2\frac{\omega_2 l}{2}}{l^2}\right) - i\tau\left(A\dfrac{\sin\omega_1 h}{h} + B\dfrac{\sin\omega_2 l}{l}\right)\right]}. \qquad (14)$$

For alternative B we have

$$s^{(B)} = \frac{1 + \alpha_2\tau(P + Q)}{1 - \alpha_1\tau(P + Q)}, \qquad (15)$$

where

$$P = -\frac{4\nu}{1 + C_1}\left[\frac{1}{h^2}\sin^2\frac{\omega_1 h}{2}\left(1 + \frac{2}{3}\sin^2\frac{\omega_1 h}{2}\right) + \right.$$

$$\left. + \frac{1}{l^2}\sin^2\frac{\omega_2 l}{2}\left(1 + \frac{2}{3}\frac{\sin^2\omega_2 l}{2}\right)\right],$$

$$Q = i\frac{1}{1 + C_1}\left[\frac{A\sin\omega_1 h}{h}A_1 + \frac{B\sin\omega_2 l}{l}B_1\right];$$

$$A_1 = 1 + \frac{2}{3}\sin^2\frac{\omega_1 h}{2} + C_1;$$

$$B_1 = 1 + \frac{2}{3}\sin^2\frac{\omega_2 l}{2} + c_1;$$

* This scheme is actually implicit, since only $\Delta_{h,l}\psi^{n+1}$ is determined explicitly; to find $\psi^{n+1}$ a difference Poisson equation should be solved.

$$C_1 = \frac{1}{3}\,\frac{\frac{1}{h^2}\sin^4\frac{\omega_1 h}{2} + \frac{1}{l^2}\sin^4\frac{\omega_2 l}{2}}{\frac{1}{h^2}\sin^2\frac{\omega_1 h}{2} + \frac{1}{l^2}\sin^2\frac{\omega_2 l}{2}}.$$

It is easily seen that for $\alpha_1 = \alpha_2 = \frac{1}{2}$ the scheme (7) is stable for both alternatives. Indeed, in both cases $|s|^2 \leqslant 1$.

Let us now consider the "explicit" scheme ($\alpha_1 = 0$, $\alpha_2 = 1$). For alternative A we have

$$s = 1 - 4\nu\tau\left(\frac{\sin^2\frac{\omega_1 h}{2}}{h^2} + \frac{\sin^2\frac{\omega_2 l}{2}}{l^2}\right) + i\tau\left(\frac{A\sin\omega_1 h}{h} + \frac{B\sin\omega_2 l}{l}\right). \tag{16}$$

We now consider two particular cases.

Case I. $A = B = 0$. Then

$$s = 1 - 4\nu\tau\left(\frac{\sin^2\frac{\omega_1 h}{2}}{h^2} + \frac{\sin^2\frac{\omega_2 l}{2}}{l^2}\right).$$

From $|s| \leqslant 1$ we have

$$\tau\left(\frac{1}{h^2} + \frac{1}{l^2}\right) \leqslant \frac{1}{4\nu}. \tag{17}$$

Case II. $\nu = 0$. Then

$$s = 1 + i\tau\left(A\frac{\sin\omega_1 h}{h} + B\frac{\sin\omega_2 l}{l}\right), \tag{18}$$

$$|s|^2 = 1 + \tau^2\left(\frac{A\sin\omega_1 h}{h} + B\frac{\sin\omega_2 l}{l}\right)^2. \tag{19}$$

Let $\frac{\tau}{h} = \text{const}$, $\frac{\tau}{l} = \text{const}$, then from (19) we have, for the corresponding values of $\omega_1$, $\omega_2$ $|s|^2 > 1 + \mu$, $\mu > 0$, which indicates instability.

Let now $\frac{\tau}{h^2} = a = \text{const}$, $\frac{\tau}{l^2} = b = \text{const}$. We have

$$|s|^2 = 1 + \tau\left(\sqrt{a}\,A\sin\omega_1 h + \sqrt{b}\,B\sin\omega_2 l\right)^2.$$

Whence

$$|s|^n < \exp\left[\frac{1}{2}\left(\sqrt{a}|A| + \sqrt{b}|B|\right)^2 T\right], \tag{20}$$

if

$$0 \leqslant n\tau \leqslant T.$$

The scheme is thus stable on any finite interval $0 \leqslant t \leqslant T$. However, if the right-hand side of (20) is large, the error of the approximate solution will be high even with small $h$, $l$ and $\tau$.

## § 4. DETERMINATION OF SPACE INTERVALS FOR SCHEMES OF SECOND-ORDER ACCURACY IN $h$ AND $l$

As we have stated in § 2, we investigate errors of approximate solution due to $h$, $l$ and $\tau$ in the principal harmonic only. We write an approximate solution $s^n e^{i\omega_1 x} e^{i\omega_2 y}$ in the form $e^{\lambda t} e^{i\omega_1 x} e^{i\omega_2 y}$ i.e., we set

$$\bar{\lambda} = \bar{\lambda}(\omega_1, \omega_2, h, l, \tau) = \frac{1}{\tau}\ln s(\omega_1, \omega_2, h, l, \tau).$$

Taking first $\tau = 0$ we find $h$ and $l$ so that

$$\left|\frac{\bar{\lambda}-\lambda}{\lambda}\right| \approx k,$$

where $k$ is the accuracy standard. From the general formula (13) we have

$$\bar{\lambda}(\omega_1, \omega_2, h, l, 0) = \frac{L_{h,l}(\omega_1, \omega_2)}{\Delta_{h,l}(\omega_1, \omega_2)}. \tag{21}$$

The expression of $\lambda$ for the complete differential equation is given in §1, (4).

We now proceed with alternative A (scheme with second order error in $h$ and $l$). We again consider two particular cases.

Case I. $A = B = 0$. Then

$$\bar{\lambda} = -4\nu\left(\frac{\sin^2\frac{\omega_1 h}{2}}{h^2} + \frac{\sin^2\frac{\omega_2 l}{2}}{l^2}\right),$$

$$\lambda = -\nu(\omega_1^2 + \omega_2^2).$$

The permissible $h$ and $l$ should thus be found from the condition

$$\left|1 - \frac{4}{\omega_1^2 + \omega_2^2}\left(\frac{\sin^2\frac{\omega_1 h}{2}}{h^2} + \frac{\sin^2\frac{\omega_2 l}{2}}{l^2}\right)\right| \sim k. \tag{22}$$

The left-hand side of (22) can be rewritten

$$\left(1 - \frac{4}{\omega_1^2 h^2}\sin^2\frac{\omega_1 h}{2}\right)\frac{\omega_1^2}{\omega_1^2 + \omega_2^2} + \left(1 - \frac{4}{\omega_2^2 l^2}\sin^2\frac{\omega_2 l}{2}\right)\frac{\omega_2^2}{\omega_1^2 + \omega_2^2}, \tag{23}$$

whence it is obvious that the errors due to $h$ and $l$ are averaged with weights proportional to $\omega_1^2$ and $\omega_2^2$. We shall first require that each of the errors for the principal harmonic be of the order of $k$. Designating the permissible values of $\frac{\omega_1 h}{2}$ and $\frac{\omega_2 l}{2}$ by $\varphi$, we obtain the following equation for $\varphi$:

$$1 - \frac{\sin^2\varphi}{\varphi^2} = k. \tag{24}$$

Solving this equation for $\varphi$ and various $k$, we obtain the following table:

| $k$ | 0.001 | 0.01 | 0.05 |
|---|---|---|---|
| $\varphi$ | 0.055 | 0.17 | 0.392 |
| $N = N_1 \times N_2$ | $28 \times 28 = 784$ | $10 \times 10 = 100$ | $4 \times 4 = 16$ |

(25)

The third row gives the approximate number of points in the main rectangle which ensures the required accuracy. This number is determined as follows. The length of the side of the main rectangle parallel to the $x$-axis is $\frac{\pi}{\omega_1}$, the mesh size $h$ is determined from the equality $\frac{\omega_1 h}{2} = \varphi$, i.e., $h = \frac{2\varphi}{\omega_1}$. The number of mesh intervals in this side of the rectangle is therefore $N_1 \sim \frac{\pi}{\omega_1} \Big/ \frac{2\varphi}{\omega_1} = \frac{\pi}{2\varphi}$. For the other side, the one parallel to the $y$-axis, we have $N_2 \sim \frac{\pi}{\omega_2} \Big/ \frac{2\varphi}{\omega_2} = \frac{\pi}{2\varphi}$, which is equal to $N_1$. As we have previously observed (§2), $N$ remains constant, regardless of $\omega_1$ and $\omega_2$ (it

must be remembered that the ratio of the sides is $\frac{\omega_2}{\omega_1}$ which is exactly equal to the ratio of the mesh spacings $\frac{h}{l} = \frac{\omega_2}{\omega_1}$). In case of frequencies which considerably differ in order of magnitude, say, $\omega_1 \ll \omega_2$, a case encountered in some problems (e.g., the stability of Poiseuille flow), we see that $\left(1 - \frac{4}{\omega^2 h^2}\sin^2\frac{\omega_1 h}{2}\right)$ enters (23) with a very small weight and it would seem that we can determine $\varphi_1 = \frac{\omega_1 h}{2}$, $\varphi_2 = \frac{\omega_2 l}{2}$, using the formulas

$$1 - \frac{\sin^2\varphi_1}{\varphi_1^2} = k\,\frac{\omega_1^2 + \omega_2^2}{\omega_1^2},$$

$$1 - \frac{\sin^2\varphi_2}{\varphi_2^2} = k\,\frac{\omega_1^2 + \omega_2^2}{\omega_2^2}.$$

The second formula is close to the original (24), while the first, already with $\omega_1 = \frac{\omega_2}{10}$, gives

$$1 - \frac{\sin^2\varphi_1}{\varphi_1^2} \sim 100k.$$

Using this formula we could apparently increase $h$ several times. However, this applies only for the main frequencies. As $\omega_2$ decreases, the weights are redistributed and in this case the error could increase. In what follows we therefore determine $\varphi$ (and consequently also $h$ and $l$) from conditions (2), (4), whose accuracy is unaffected by the decrease of $\omega_1$ and $\omega_2$.

Case II. $\nu = 0$. We have

$$\bar{\lambda} = iA\sin\frac{\omega_1 h}{h} + iB\,\frac{\sin\omega_2 l}{l}, \quad \lambda = iA\omega_1 + iB\omega_2$$

Then

$$\left|\frac{\lambda - \bar{\lambda}}{\lambda}\right| = \left|\frac{A\omega_1}{A\omega_1 + B\omega_2}\left(1 - \frac{\sin\omega_1 h}{\omega_1 h}\right) + \right.$$
$$\left. + \frac{B\omega_2}{A\omega_1 + B\omega_2}\left(1 - \frac{\sin\omega_2 l}{\omega_2 l}\right)\right|.$$

We first assume that the weights $\frac{A\omega_1}{A\omega_1 + B\omega_2}$ and $\frac{B\omega_2}{A\omega_1 + B\omega_2}$ have the same sign. Then, as in the previous case, the condition of accuracy for $h$ and $l$ has the form

$$\omega_1 h \leqslant \eta, \quad \omega_2 l \leqslant \eta, \tag{26}$$

where $\eta$ is the root of the equation

$$1 - \frac{\sin\eta}{\eta} = k.$$

We obtain the following table:

| $k$ | 0.001 | 0.01 | 0.05 |
|---|---|---|---|
| $\eta$ | 0.0775 | 0.245 | 0.55 |
| $N = N_1 \times N_2$ | $40 \times 40 = 1600$ | $13 \times 13 = 169$ | $6 \times 6 = 36$ |

(27)

If $A\omega_1$ and $B\omega_2$ have different signs, it is more difficult to estimate the accuracy, since the "weights" $\frac{A\omega_1}{A\omega_1 + B\omega_2}$ and $\frac{B\omega_2}{A\omega_1 + B\omega_2}$ may then have large absolute values. This case requires further analysis with special

consideration of the actual values of A and B, and will not be discussed here any further.

Let us now consider the general case of equation (2).

We have $\overline{\lambda} = \overline{\lambda}_I + \overline{\lambda}_{II}$, $\lambda = \lambda_I + \lambda_{II}$, where

$$\overline{\lambda}_I = -4\nu\left(\frac{\sin^2\frac{\omega_1 h}{2}}{h^2} + \frac{\sin^2\frac{\omega_2 l}{2}}{l^2}\right),$$

$$\overline{\lambda}_{II} = i\overline{\mu}_{II} = i\left(A\frac{\sin\omega_1 h}{h} + B\frac{\sin\omega_2 l}{l}\right),$$

$$\lambda_I = -\nu(\omega_1^2 + \omega_2^2), \quad \lambda_{II} = i\mu_{II} = i(A\omega_1 + B\omega_2)$$

Then

$$\left|\frac{\lambda - \overline{\lambda}}{\lambda}\right|^2 = \frac{\lambda_I^2}{\lambda_I^2 + \mu_{II}^2}\left(\frac{\lambda_I - \overline{\lambda}_I}{\lambda_I}\right)^2 + \frac{\mu_{II}^2}{\lambda_I^2 + \mu_{II}^2}\left(\frac{\mu_{II} - \overline{\mu}_{II}}{\mu_{II}}\right)^2 \qquad (28)$$

Hence it follows that in the general case the relative error of $\overline{\lambda}$ does not exceed $k$, if $h$ and $l$ are chosen so that this error for each of the previously considered cases does not exceed $k$. Stronger requirements are imposed on $h$ and $l$ by the second case. To obtain more exact estimates of $h$ and $l$ in particular problems we should take into consideration the weights of the errors of the two different cases (i.e., allow for the relationship between $\lambda_I$ and $\mu_{II}$). We see from a comparison of the grids for cases I and II that the gain in the number of mesh points achieved in this way is relatively small, since

$$N_{II} \sim 1.7 N_I.$$

## § 5. DETERMINATION OF SPACE INTERVALS FOR SCHEMES OF FOURTH ORDER ACCURACY IN $h$ AND $l$

Consider alternative B of approximation to $\Delta$ and $L$ which ensures fourth order of accuracy relative to $h$ and $l$. As in the preceding section, we first consider particular case I, determining $\overline{\lambda}$ from (21).

Case I. $A = B = 0$. Here $\overline{\lambda} = P$, where $P$ is determined from (15), $\lambda = \nu(\omega_1^2 + \omega_2^2)$.

Proceeding from the results of the preceding section for schemes of second order accuracy, we obtain for $h$ and $l$

$$\varphi = \frac{\omega_1 h}{2} = \frac{\omega_2 l}{2}. \qquad (29)$$

Then

$$\left|\frac{\lambda - \overline{\lambda}}{\lambda}\right| = \left|1 - \frac{\sin^2\varphi}{\varphi^2}\,\frac{1 + \frac{2}{3}\sin^2\varphi}{1 + \frac{1}{3}\sin^2\varphi}\right|.$$

Thus $\varphi$ is found from the equation

$$1-\frac{\sin^2\varphi}{\varphi^2}\,\frac{1+\frac{2}{3}\sin^2\varphi}{1+\frac{1}{3}\sin^2\varphi}=k.$$

The results of computations for various $k$ are given in the following table:

| $k$ | 0.001 | 0.01 | 0.05 |
|---|---|---|---|
| $\varphi$ | 0.2437 | 0.431 | 0.664 |
| $N=N_1\times N_2$ | 7×7=49 | 4×4=16 | 2×2=4 |

(30)

Comparing these results with table (25), we see that the fourth-order scheme enables $h$ and $l$ to be considerably increased (by a factor of some 2.5 for $k=0.01$).

Case II. $\nu=0$. We have $\bar{\lambda}=Q$, where $Q$ is determined from (15), $\lambda=i(A\omega_1+B\omega_2)$. Setting

$$\eta=\omega_1 h=\omega_2 l, \tag{31}$$

we find $\eta$ from

$$\left|\frac{\lambda-\bar{\lambda}}{\lambda}\right|=\left|1-\frac{\sin\eta}{\eta}\,\frac{1+\sin^2\frac{\eta}{2}}{1+\frac{1}{3}\sin^2\frac{\eta}{2}}\right|=k.$$

The results are

| $k$ | 0.001 | 0.01 | 0.05 |
|---|---|---|---|
| $\eta$ | 0.3827 | 0.6846 | 1.223 |
| $N=N_1\times N_2$ | 9×9=81 | 5×5=25 | 3×3=9 |

(32)

For $k=0.01$, $h$ and $l$ can be increased, as in case I, by a factor of about 3 over the mesh size used with the scheme of second-order accuracy.

The general case of equation (2) is investigated as in the preceding section for second order schemes in $h$ and $l$ (see (28) and what follows).

Note 1. To determine the limit values of $h$ and $l$, we introduced the expressions (29) and (31) by analogy with second order schemes. It can be shown that the justification of equations (24) and (26) given in §4 can be extended to this scheme also.

Note 2. As in the preceding section, $A$ and $B$ are assumed to have like signs. Otherwise the results would essentially depend on $A$, $B$, $\omega_1$, $\omega_2$.

## §6. DETERMINATION OF THE TIME INTERVAL

In choosing the time interval $\tau$ we shall assume $h$ and $l$ to have been chosen in accordance with the procedure outlined in §4, 5. According to (13) and (21) we have

$$s=\frac{1-\tau\alpha_2\bar{\lambda}_0}{1+\tau\alpha_1\bar{\lambda}_0},\ (\alpha_1+\alpha_2=1,\ \alpha_1\geqslant 0,\ \alpha_2\geqslant 0),$$

where $\bar{\lambda}_0=\bar{\lambda}(\omega_1\omega_2;\ h,\ l,\ 0)$ (in the two previous sections this parameter was simply designated $\bar{\lambda}$).

Hence

$$\bar{\lambda}=\frac{1}{\tau}\ln s=\bar{\lambda}_0+\frac{1}{2}\tau(\alpha_1-\alpha_2)\,\bar{\lambda}_0^2+\frac{1}{3}\tau^2(\alpha_1^3+\alpha_2^3)\bar{\lambda}_0^3+\ldots$$

The contribution of $\tau$ to the relative error

$$\delta = \left| \frac{\lambda - \bar{\lambda}}{\lambda} \right|$$

is estimated by the expression

$$\delta_1 = \frac{1}{2}(\alpha_1 - \alpha_2)\tau\lambda + \frac{1}{3}(\alpha_1^3 + \alpha_2^3)\tau^2\lambda^2.$$

In choosing $\tau$, we require that $\delta \sim k$. The characteristic time $T_{\text{char}}$ is defined as $T_{\text{char}} = \frac{1}{|\lambda|}$, so that $\tau|\lambda| = \frac{\tau}{T_{\text{char}}} = \frac{1}{n}$, where $n$ is the number of time intervals in the characteristic time period; $n$ should therefore be determined from the condition

$$\frac{1}{2}|\alpha_1 - \alpha_2|\frac{1}{n} + \frac{1}{3}(\alpha_1^3 + \alpha_2^3)\frac{1}{n^2} \sim k. \tag{33}$$

Let us first consider the case of the implicit symmetric scheme $\left(\alpha_1 = \alpha_2 = \frac{1}{2}\right)$. Then from (33) it follows that $n \sim \frac{1}{\sqrt{12k}}$. For the relevant values of $k$ we have

| $k$ | 0.001 | 0.01 | 0.05 |
|---|---|---|---|
| $n$ | 10 | 3 | 1÷2 |

(34)

For "explicit" schemes ($\alpha_1 = 0$, $\alpha_2 = 1$), retaining only the leading term on the left-hand side of (33), we obtain

$$n \sim \frac{1}{2k}.$$

Hence

| $k$ | 0.001 | 0.01 | 0.05 |
|---|---|---|---|
| $n$ | 500 | 50 | 10 |

(35)

## § 7. ON THE CHOICE OF THE ACCURACY STANDARD FOR THE PROBLEM OF STABILITY OF POISEUILLE FLOW

In order to have an idea of the amount of computational work involved in the solution of problems of stability of viscous incompressible flow by the difference method, let us consider the problem of stability of Poiseuille flow. Of the several papers on approximate solution of the linearized problem, the work of Thomas /7/ is the only one to utilize difference methods.

We give here some of Thomas's results. Linearization of equation (1) enables the solution to be represented as

$$\psi = \varphi(y)\, e^{-i(\alpha x - ct)}. \tag{36}$$

The well-known Orr-Sommerfeld equation is solved for $\varphi$,

$$\frac{d^4\varphi}{dy^4} - 2\alpha^2\frac{d^2\varphi}{dy^2} + \alpha^4\varphi + i\alpha R\left\{(1 - c - y^2)\left(\frac{d^2\varphi}{dy^2} - \alpha^2\varphi\right) + 2\varphi = 0\right\}, \tag{37}$$

where $R = \frac{u_0 b}{\nu}$, $b$ the channel half-width, $u_0$ the midstream velocity, $\nu$ the kinematic viscosity. For given $\alpha$ and $R$, $c$ can be regarded as an eigenvalue.

If Im$c$ is negative, the solution infinitely increases in time, which indicates flow instability. The eigenvalues of equation (37) were found by Thomas by introducing a difference equation with fourth-order approximation error. The number of mesh intervals was quite large (50—100 in the main work), because the solution showed very sharp variations. We give the values of $c$ computed by Thomas for $\alpha = 1$ and various Reynolds numbers:

| $R$ | 1600 | 2500 | 6400 | 1000 | 35000 |
|---|---|---|---|---|---|
| $c$ | $0.3231+$ $+i0.0262$ | $0.3011+$ $+i0.0142$ | $0.2569+$ $+i0.0009$ | $0.2375-$ $-i0.0037$ | $0.1886+$ $+i0.0009$ |

(38)

We see from this table that the eigenvalues had to be determined with a relative error of from 0.005 to 0.08 to enable the sign of the imaginary part of $c$ to be determined with any degree of reliability. Extending this requirement to $\lambda$, we obtain

$$\delta = \left|\frac{\lambda - \overline{\lambda}}{\lambda}\right| \sim 0.005.$$

We thus obtain an accuracy standard $k = 0.001$. A second order difference scheme in $h$ and $l$ thus gives a grid of $40 \times 40 = 1600$ points for the main rectangle. For the fourth-order scheme, a grid of $9 \times 9 = 81$ suffices. Let us now consider the question of the number of main rectangles in the domain $\Omega$, in which the difference computations are made. In Thomas's variables, for $\alpha = 1$, this domain is the rectangle

$$\begin{aligned} -\pi \leqslant x \leqslant \pi, \\ 0 \leqslant y \leqslant 1. \end{aligned} \qquad (39)$$

For $x = \pm\pi$ we have periodicity conditions; for $y = 1$ the adherence conditions $\varphi = \varphi' = 0$; for $y = 0$ symmetry conditions: $\varphi' = \varphi''' = 0$. Since in the $x$-direction we have two half-waves, the main rectangle is contained two times in this direction, i.e., in the $x$-direction we should have 80 intervals for second-order scheme and 18 intervals for fourth-order scheme.

More complicated is the problem of the length of the main rectangle in the $y$-direction, i.e., the value of $\omega_2$. To determine $\omega_2$, let us consider the graph of the function $\varphi_1(y) = \mathrm{Im}\varphi(y)$, which is less smooth than $\varphi_2 = \mathrm{Re}\varphi(y)$, for Reynolds number $R = 10\,000$ and $\alpha = 1$ (see Figure).

Clearly $\omega_2$ is of the same order of magnitude as $\frac{Y}{d}\pi$, where $Y$ is the length of the entire $y$-range (1 in this case), and $d$ is the "width" of the peak (here $d \sim 0.1$). We can conclude from the graph that $\omega_2$ is not less than $10\pi$. In the $y$-direction, for $0 \leqslant y \leqslant 1$, we should thus repeat the main rectangle at least 10 times. In the range of space variables (39) we thus obtain a grid of $400 \times 80 = 32000$ points for the second-order scheme and $20 \times 100 = 2000$ points for the fourth-order scheme.

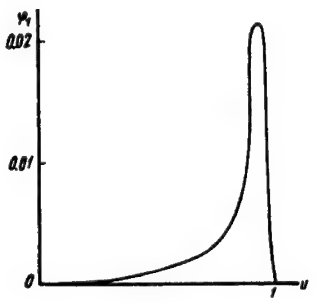


It is noteworthy that with regards to the $y$-length of the grid we arrived at close agreement with the number of intervals in Thomas's work (for the fourth-order scheme).

The estimates in this section are all quite provisional. In fact, they even do not apply for a linear equation with variable coefficients. Indeed, the Fourier transform method can be applied only locally, in regions which, although

large in comparison with the main rectangle, are small in comparison with the distance over which the coefficients of the equations vary noticeably. Still we apply the estimates obtained by the Fourier method to the entire domain $\Omega$. However, proceeding from the experience gained in work with difference schemes, we submit that the above estimates are necessary in the sense that in the case of variable coefficients $A$ and $B$ and particularly for the nonlinear equation it is impossible to achieve the accuracy required in the problem of stability of Poiseuille flow with sparser grids.

BIBLIOGRAPHY


1. THOM, A. The Flow Past Circular Cylinders at Low Speeds. — Proc. Roy. Soc. (A), 141: 651. 1933.
2. ALLEN, D. N., R.V. SOUTHWELL. Relaxation Methods Applied to Determine the Motion, in Two Dimensions, of a Viscous Fluid Past a Fixed Cylinder. —Quart. J. Mech. and Appl. Math., 8: 129. 1955.
3. JANSSEN, E. Flow Past a Flat Plate at Low Reynolds Numbers. —Journal of Fluid Mechanics. Vol. 3, No. 4. p. 329. 1958.
4. JENSON, V.G. Viscous Flow Round a Sphere at a Low Reynolds Number. — Proc. Roy. Soc. (A), Vol. 249, p. 343. 1959.
5. ZHIDKOV, N.P., A.A. KORNEICHUK, A.L. KRYLOV, and S.B. MOSTINSKAYA. Ploskoparallel'noe dvizhenie vyazkoi zhidkosti mezhdu vrashchayushchimisya tsilindrami (Plane-Parallel Motion of Viscous Fluid Between Rotating Cylinders). — In: "Vychislitel'nye metody i programmirovanie", Izdatel'stvo MGU. 1962.
6. KRYLOV, A.L. and E.K. PROIZVOLOVA. Numerical Study of Flow between Rotating Cylinders.— This volume.
7. THOMAS, L.H. The Stability of Plane Poiseuille Flow. — The Physical Review. Vol. 91, No. 4. 1953.

## IV. SEEPAGE PROBLEMS

*B. M. Budak and F. P. Vasil'ev*

# CONVERGENCE AND ERROR ESTIMATES IN THE RAY METHOD FOR THE SOLUTION OF SOME SEEPAGE PROBLEMS

In this paper we consider the problem of convergence and error estimation in the ray method for the solution of the nonstationary and the stationary seepage problems. These problems arise, e.g., when considering the influx of oil to an imperfect borehole in the radial-symmetric case.

In /1/ the ray method was applied without theoretical substantiation to the solution of the stationary problem, which amounts to a mixed boundary-value problem for an elliptic equation with variable coefficients in the "rectangle" $D\{0 < r_1 \leqslant r \leqslant r_2, 0 \leqslant z \leqslant H\}$, where $r$ and $z$ are cylindrical coordinates; it is assumed that on some parts of the boundary the values of the required function are given, while on other parts the values of its normal derivative.

In the present paper we apply the ray method to a nonstationary or stationary problem which is reduced to an analogous mixed boundary-value problem for a two-dimensional* parabolic equation. The ray method in this case suggests itself as a natural combination of the plane method applied in /2, 3, 4/ to the two-dimensional parabolic equation, and the ray method applied in /1, 5, 6/ to the two-dimensional elliptic equation.

The ray method in both the stationary and the nonstationary cases enables the problem to be solved not only in a bounded domain $D\{0 < r_1 \leqslant r \leqslant r_2, 0 \leqslant z \leqslant H\}$, but also in the unbounded domain $D\{0 < r_1 \leqslant r < +\infty, 0 \leqslant z \leqslant H\}$. However, we shall dwell in detail on the bounded case only, noting that in the unbounded case the solution of the system of ordinary differential equations of the ray method is by no means simple and convenient for computations.

The nonstationary boundary-value problem is stated as follows: in the paralelepiped $Q = D \times [0, T]$ we seek a function $u(r, z, t)$ satisfying the equation

$$Lu \equiv \frac{\partial^2 u}{\partial r^2} + \frac{1}{r}\frac{\partial u}{\partial r} + \frac{\partial^2 u}{\partial z^2} - \frac{\partial u}{\partial t} = f(r, z, t) \text{ inside } Q, \qquad (1.0)$$

the boundary conditions

$$u|_{r=r_1} = \varphi_1(z, t) \quad \text{for } H_0 < z < H, \quad 0 \leqslant t \leqslant T, \quad \text{where } 0 \leqslant H_0 \leqslant H; \qquad (1.1)$$

$$u|_{r=r_2} = \varphi_2(z, t) \quad \text{for } 0 < z < H, \quad 0 \leqslant t \leqslant T, \qquad (1.2)$$

* That is, with two independent space coordinates $r$, $z$ and the time $t$.

$$\left.\frac{\partial u}{\partial z}\right|_{z=0} = \psi_1(r, t), \quad \left.\frac{\partial u}{\partial z}\right|_{z=H} = \psi_2(r, t)$$

$$\text{for } r_1 < r < r_2, 0 \leqslant t \leqslant T, \tag{1.3}$$

$$\left.\frac{\partial u}{\partial r}\right|_{r=r_1} = \psi_0(z, t) \quad \text{for } 0 < z < H_0, \qquad 0 \leqslant t \leqslant T, \tag{1.4}$$

and the initial condition

$$u|_{t=0} = \varphi_0(r, z) \text{ in } D, \tag{1.5}$$

always assuming that the natural matching conditions are satisfied:

$$\varphi_1(z, 0) \equiv \varphi_0(r_1, z), \quad \varphi_2(z, 0) \equiv \varphi_0(r_2, z), \ 0 \leqslant z \leqslant H. \tag{1.6}$$

The following scheme of the ray method is proposed for solving this problem. We construct the planes $z=ih$, $i=0, 1, \ldots, M+1$, where $(M+1)h=H$ and $t = k\tau$, $k = 0, 1, \ldots, N$, where $N\tau = T$. The intersection lines of these planes will be called nodal lines. The segments of the nodal lines in the parallelepiped $Q$ form a "grid" consisting of points with the coordinates $(r, ih, k\tau) = (r, z_i, t_k, )$, where $r_1 \leqslant r \leqslant r_2$, $0 \leqslant i \leqslant M+1$, $0 \leqslant k \leqslant N$. Equation (1.0) is then approximated on the nodal lines by the following system of ordinary differential equations

$$L_{h\tau}[u_{ik}(r)] \equiv \frac{d^2u_{ik}(r)}{dr^2} + \frac{1}{r}\frac{du_{ik}(r)}{dr} + \delta_{z\bar{z}}u_{ik}(r) - \delta_{\bar{t}}u_{ik}(r) = f_{ik}(r) \tag{2.0}$$

for $r_1 < r < r_2$, $1 \leqslant i \leqslant M$, $1 \leqslant k \leqslant N$,

where

$$\delta_z u_{ik} = \frac{u_{i+1k} - u_{ik}}{h}, \quad \delta_{\bar{z}} u_{ik} = \frac{u_{ik} - u_{i-1k}}{h},$$

$$\delta_{z\bar{z}} u_{ik} = \delta_z(\delta_{\bar{z}} u_{ik}) = \frac{u_{i+1k} - 2u_{ik} + u_{i-1k}}{h^2},$$

$$\delta_{\bar{t}} u_{ik} = \frac{u_{ik} - u_{ik-1}}{\tau}, \quad f_{ik}^{(r)} = f(r, z_i, t_k).$$

The boundary conditions (1.1)—(1.4) and the initial condition (1.5) are respectively replaced by the following conditions:

$$u_{ik}(r_1) = \varphi_1(z_i, t_k), \ M_0 + 1 \leqslant i \leqslant M, \ 0 \leqslant k \leqslant N, \ M_0 = \left[\frac{H_0}{h}\right]; \tag{2.1}$$

$$u_{ik}(r_2) = \varphi_2(z_i, t_k), \quad 1 \leqslant i \leqslant M, \quad 0 \leqslant k \leqslant N; \tag{2.2}$$

$$\left.\begin{aligned} \frac{u_{1k}(r) - u_{0k}(r)}{h} &= \psi_1(r, t_k), \\ \frac{u_{M+1k}(r) - u_{Mk}(r)}{h} &= \psi_2(r, t_k), \end{aligned}\right\} \text{ for } r_1 \leqslant r \leqslant r_2, \quad 1 \leqslant k \leqslant N; \tag{2.3}$$

$$\frac{du_{ik}(r_1)}{dr} = \psi_0(z_i, t_k), \quad 1 \leqslant i \leqslant M_0, \quad 1 \leqslant K \leqslant N, \tag{2.4}$$

$$u_{i0}(r) = \varphi_0(r, z_i), \quad 0 \leqslant i \leqslant M+1, \quad r_1 \leqslant r \leqslant r_2. \tag{2.5}$$

The stationary seepage problem is reduced to the following boundary-value problem: in the rectangle $D\{0 < r_1 \leqslant r \leqslant r_2,\ 0 \leqslant z \leqslant H\}$ we seek a function $u=u(r, z)$, satisfying the equation

$$Lu \equiv \frac{\partial^2 u}{\partial r^2} + \frac{1}{r}\frac{\partial u}{\partial r} + \frac{\partial^2 u}{\partial z^2} = f(r, z) \text{ inside } D \tag{3.0}$$

and boundary conditions

$$u|_{r=r_1} = \varphi_1(z), \quad H_0 < z < H \text{ where } 0 \leqslant H_0 \leqslant H; \tag{3.1}$$

$$u|_{r=r_2} = \varphi_2(z), \quad 0 < z < H; \tag{3.2}$$

$$\left.\frac{\partial u}{\partial z}\right|_{z=0} = \psi_1(r), \quad \left.\frac{\partial u}{\partial z}\right|_{z=H} = \psi_2(r), \quad r_1 < r < r_2; \tag{3.3}$$

$$\left.\frac{\partial u}{\partial r}\right|_{r=r_1} = \psi_0(z), \qquad 0 < z < H_0. \tag{3.4}$$

The scheme of the ray method proposed in /1/ takes the following form for problem (3.0)—(3.4):

$$L_h[u_i(r)] \equiv \frac{d^2 u_i(r)}{dr^2} + \frac{1}{r}\frac{du_i(r)}{dr} + \delta_{\bar{z}z}\, u_i(r) = f_i(r), \quad 1 \leqslant i \leqslant M,$$

$$(M+1)h = H; \tag{4.0}$$

$$u_i(r_1) = \varphi_1(z_i), \ M_0 + 1 \leqslant i < M+1, \ M_0 = \left[\frac{H_0}{h}\right]; \tag{4.1}$$

$$u_i(r_2) = \varphi_2(z_i), \quad 0 < i < M+1; \tag{4.2}$$

$$\frac{u_1(r) - u_0(r)}{h} = \psi_1(r), \quad \frac{u_{M+1}(r) - u_M(r)}{h} = \psi_2(r), \quad r_1 \leqslant r \leqslant r_2; \tag{4.3}$$

$$\frac{du_i(r_1)}{dr} = \psi_0(z_i), \quad 0 < i \leqslant M_0. \tag{4.4}$$

In § 1 of the present paper we prove the convergence of the solution of the difference-differential boundary-value problem (2.0)—(2.5) (for $h$ and $\tau$ approaching zero) to the solution of the nonstationary differential boundary-value problem (1.0)—(1.5), which in fact proves the existence of a solution of the latter; we then investigate differential properties of this solution and prove its uniqueness.

In § 2 we give a priori and a posteriori estimates of the error of the ray method for the nonstationary problem.

In § 3 we briefly consider the aspects of § 1 and § 2 in application to stationary problems.

## § 1. CONVERGENCE OF THE RAY METHOD AND EXISTENCE AND UNIQUENESS OF SOLUTION OF THE NONSTATIONARY SEEPAGE PROBLEM (1.0)—(1.5)

1°. We denote by 1) $\Gamma_0$, 2) $\Gamma_1$ and 3) $\Gamma_2$ those parts of the boundary of the domain $Q$ where the functions 1) $\varphi_0$, 2) $\varphi_1$ and $\psi_2$, and 3) $\psi_0$, $\psi_1$, $\varphi_2$, are respectively given, and write $\Gamma = \Gamma_0 + \Gamma_1 + \Gamma_2$. We shall retain these notations for the previously described grid and for the corresponding parts of the boundary. By points of $Q$ we mean the points of $Q$ which do not belong

to $\Gamma$, where $\Gamma$ is the boundary of $Q$. Then problems (1.0)—(1.5) and (2.0)—(2.5) can respectively be written

$$Lu = f \text{ inside } Q, \quad u|_{\Gamma_0} = \varphi_0, \quad u|_{\Gamma_1} = \varphi, \quad \frac{\partial u}{\partial n}\Big|_{\Gamma_2} = \psi, \tag{1}$$

$$L_{h\tau}u_{lk} = f_{lk} \text{ inside } Q, \quad u_{l0} = \varphi_0, \quad u_{lk}|_{\Gamma_1} = \varphi, \frac{\partial u_{lk}}{\partial n}\Big|_{\Gamma_2} = \psi. \tag{2}$$

Boundary conditions (1.1) and (1.4) are assumed, such that there exists a function $\Psi(r, z, t)$, which is continuously differentiable in a closed domain $D$, has continuous fifth derivatives inside $D$, and satisfies the conditions (1.1)—(1.4) on the boundary of $D$ in the classical sense. Any such function will be called five-fold smooth permissible function satisfying the boundary conditions.

*Definition. A solution of problem (1) is a function $u(r, z, t)$ such that:*

*1) $u$ is continuously differentiable inside $Q$ according to the requirements of equation (1.0), and satisfies this equation;*

*2) $u$ satisfies the boundary conditions of problem (1.1) - (1.4) and the initial condition (1.5) in the classical sense;*

*3) $u$ is bounded in $Q$ and has square-summable first derivatives in $Q$, i.e.,*

$$u \in W_2^{(1)}(Q) \,/7/, \tag{3}$$

4) if $\Gamma_\delta$ is the lateral surface of the parallelepiped

$$Q_\delta\{r_1 + \delta \leqslant r \leqslant r_2 - \delta, \quad \delta \leqslant z \leqslant H - \delta, \quad 0 \leqslant z \leqslant T\}, \tag{4}$$

contained in $Q$, and $\Psi(r, z, t)$ is any once continuously differentiable permissible function satisfying the boundary conditions, then for any other such function $\Phi(r, z, t)$ satisfying the corresponding homogeneous boundary conditions we have the limiting relation

$$\lim_{\delta \to 0} \int\int_{\Gamma_\delta} r\Phi \frac{\partial v}{\partial n} d\Gamma_\delta = 0, \tag{5}$$

*where $v = u - \Psi$, and $n$ is the inward normal of $\Gamma_\delta$.*

Observe that if $u$ should be a continuously differentiable function in a closed domain $Q$, requirements 3 and 4 would follow from the other propositions.

In this section we first consider the solution of the difference-differential boundary-value problem (2), and then, using the estimates of the solution $\{u_{lk}(r)\}$ of this problem, and S. N. Bernstein's estimates (on the corresponding parts of the boundary of $Q$) for the derivatives $\{u'_{lk}\}$, $\{u''_{lk}\}$, $\{u'''_{lk}\}$, and for the corresponding difference quotients $\{\delta_z u_{lk}\}$, $\{\delta_{\bar{z}\bar{z}} u_{lk}\}$, $\{\delta_{\bar{z}\bar{z}} u_{lk}\}$, $\{\delta_{\bar{t}} u_{lk}\}$, $\{\delta_{\bar{t}z} u_{lk}\}$, $\{\delta_{\bar{t}} u_{lk}\}$, $\{\delta_{\bar{t}\bar{t}} u_{lk}\}$, $\{\delta_{\bar{z}\bar{z}\bar{z}} u_{lk}\}$, $\{\delta_{\bar{z}\bar{z}\bar{t}} u_{lk}\}$, $\{\delta_z u''_{lk}\}$, $\{\delta_{\bar{t}} u''_{lk}\}$ we prove the following theorem.

*Theorem 1. If the boundary conditions of problem (1) are such that there exists at least one five-fold smooth permissible function $\Psi(r, z, t)$ satisfying these boundary conditions, if the functions*

$$\varphi_0, \quad \frac{\partial^4 \varphi_0}{\partial r^4}, \quad \frac{\partial^4 \varphi_0}{\partial r^2 \partial z^2} \quad \frac{\partial^4 \varphi_0}{\partial z^4}, \tag{6}$$

*and also*

$$f, \quad \frac{\partial^3 f}{\partial r^3}, \quad \frac{\partial^3 f}{\partial z^3}, \quad \frac{\partial^3 f}{\partial t\, \partial z^2}, \quad \frac{\partial^3 f}{\partial t\, \partial r^2}, \quad \frac{\partial^3 f}{\partial z\, \partial r^2}, \tag{7}$$

*are bounded, and if the difference* $\varphi_0(r, z) - \Psi(r, z, 0)$ *in arbitrarily narrow, but fixed strips* $0 \leqslant z \leqslant \gamma$ *and* $H - \gamma \leqslant z \leqslant H$ *is independent of* $z$ *and satisfies the matching conditions*

$$\left.\begin{aligned} &\varphi_0(r_1, z) - \Psi(r_1, z, 0) \equiv 0, \quad \varphi_0(r_2, z) - \Psi(r_2, z, 0) \equiv 0, \\ &\frac{\partial}{\partial r}[\varphi_0(r, z) - \Psi(r, z, 0)]|_{r=r_i} \equiv 0, \quad 0 \leqslant z \leqslant H, \end{aligned}\right\} \tag{8}$$

*then the nonstationary boundary-value problem (1) is uniquely solvable*.*

2°. We now proceed with an investigation of the solution of the difference-differential problem (2).

*Lemma 1 (maximum principle). Let a system of functions* $u_{ik}(r)$ *which are continuous on the closed segment* $0 < r_1 \leqslant r \leqslant r_2$ *and twice differentiable (with respect to* $r$*) at its inner points satisfy everywhere inside* $Q$ *the inequalities* $L_{h\tau}(u_{ik}) \geqslant 0$ $[L_{h\tau}(u_{ik}) \leqslant 0]$. *Then* $\max\limits_{Q} u_{ik}(r)$ $[\min\limits_{Q} u_{ik}(r)]$ *is attained on* $\Gamma$. *If now* $L_{h\tau}(u_{ik}) > 0$ $[L_{h\tau}(u_{ik}) < 0]$ *everywhere inside* $Q$, $\max\limits_{Q} u_{ik}(r)$ $[\min\limits_{Q} u_{ik}(r)]$ *is attained only on* $\Gamma$.

The proof of this lemma is simple, by assuming the opposite.

*Lemma 2. Let a set of functions* $u_{ik}(r)$ *differentiable with respect to* $r$ *on the closed interval* $0 < r_1 \leqslant r \leqslant r_2$ *and twice differentiable with respect to* $r$ *at inner points of this interval satisfy everywhere inside* $Q$ *the condition* $L_{h\tau}(u_{ik}) < 0$, $[L_{h\tau}(u_{ik}) > 0]$; *on the boundary* $\Gamma$ *the boundary conditions (2.1) - (2.5) are satisfied, and* $\psi_0 \leqslant 0, \psi_1 \leqslant 0, \psi_2 \geqslant 0$ $[\psi_0 \geqslant 0, \psi_1 \geqslant 0, \psi_2 \leqslant 0]$. *Then*

$$u_{ik}(r) \geqslant m = \min_{\Gamma_0 + \Gamma_1} \varphi [u_{ik}(r) \leqslant m_0 = \max_{\Gamma_0 + \Gamma_1} \varphi].$$

Proof. Observe that the case $L_{h\tau} u_{ik} > 0$ reduces to $L_{h\tau} u_{ik} < 0$ by substituting $-u_{ik}$ for $u_{ik}$. We can therefore limit the discussion to the case $L_{h\tau} u_{ik} < 0$ only. Then, from Lemma 1, $u_{ik}(r)$ cannot have a minimum inside the domain $Q$. If the minimum is reached on $\Gamma_0 + \Gamma_1$, the lemma is proved. It remains to show the impossibility of a minimum being attained on $\Gamma_2$. Let the minimum occur on the face $r = r_1$ at the point $(r_1, z_{i_0}, t_{k_0}) \in \Gamma_2$. By assumption, $u'_{i_0 k_0}(r_1) = \psi_1(z_{i_0}, t_{k_0}) \leqslant 0$. We define in $Q$ a subdomain $Q'_\delta \{r_1 \leqslant r \leqslant r_1 + \delta, \ i = i_0 - 1, \ i_0, \ i_0 + 1, \ k = k_0, \ k_0 - 1\}$, where $\delta > 0$ is so small that $\delta^2 + \delta < h^2$. We define in $Q'_\delta$ an auxiliary function

$$v_{ik}(r) = \begin{cases} (r - r_1)^2 + (r - r_1), & \text{if} \quad i = i_0, \ k = k_0, \ k_0 - 1, \\ 0, & \text{if} \quad i = i_0 \pm 1, \ k = k_0. \end{cases} \tag{9}$$

By virtue of the choice of $\delta$, we have $L_{h\tau}(v_{ik}) > 0$. Moreover, since $(r_1, z_{i_0}, t_{k_0})$ is a minimum point, $u_{ik}(r) > u_{i_0 k_0}(r_1)$ at all points of $Q'_\delta$, except the points $r = r_1$, where for $i = i_0$, $k = k_0$ we have the equality $u_{ik}(r_1) = u_{i_0 k_0}(r_1)$. Consequently, there exists an $\varepsilon > 0$ such that $u_{ik}(\delta) - u_{i_0 k_0}(r_1) = d > \varepsilon v_{ik}(\delta)$ for $i = i_0$, $k = k_0$, $k_0 - 1$. But then the function

$$w_{ik}(r) = u_{ik}(r) - u_{i_0 k_0}(r_1) - \varepsilon v_{ik}(r)$$

* The existence and the uniqueness of the solution of problem (1) can also be proved with weaker requirements on $f$, $\varphi$, $\Psi$, either by the barrier method, or by passing to closures in appropriate functional classes, but here, for the sake of simplicity, we shall be content with Theorem 1.

is nonnegative on the boundary of $Q'_\delta$. Now as $L_{h\tau} w_{ik} < 0$, we have by Lemma 1 $w_{ik}(r) \geqslant 0$ everywhere inside $Q'_\delta$, and consequently $u_{i_0k_0}(r) - u_{i_0k_0}(r_1) \geqslant \varepsilon v_{i_0k_0}(r)$ for $r_1 \leqslant r \leqslant r_1 + \delta$. We divide the two sides of this inequality by $r - r_1$ where $0 < r - r_1 < \delta$, and pass to the limit as $r \to r_1 + 0$. We then obtain $u'_{i_0k_0}(r_1) \geqslant \varepsilon > 0$, which contradicts the assumption $\psi_0 \leqslant 0$. Hence, $u_{ik}(r)$ cannot have a minimum at any point $(r_1, z_{i_0}, t_{k_0}) \in \Gamma_2$.

If the minimum were attained at a point $(r_0, 0, t_k) \in \Gamma_2$, where by assumption $\psi_1 \leqslant 0$, we would have $\delta_z u_{0k_0}(r_0) \geqslant 0$, and hence $u_{1k_0}(r_0) = u_{0k_0}(r_0)$, i.e., $(r_0, z_1, t_{k_0})$ would also be a minimum point, and should lie on the boundary, i.e., we should have $r_0 = r_1$ or $r_0 = r_2$. If now $(r_0, z_1, t_{k_0}) \in \Gamma_1$, the proof is complete; if however, $(r_0, z_1, t_{k_0}) \in \Gamma_2$, then, according to the preceding, we reach a contradiction. Applying the condition $\psi_2 \geqslant 0$, we analogously discount the possibilities of a minimum at points $(r_0, H, t_{k_0})$. This completes the proof.

*Lemma 3. Let* $|v_{ik}(r)| \leqslant K$ *in* $Q_{\delta\gamma}\{r_1 + \delta \leqslant r \leqslant r_2,\ 0 < \frac{\gamma}{2} \leqslant z_l \leqslant H - \frac{\gamma}{2},\ 0 \leqslant t \leqslant T\}$, *where* $\delta$ *and* $\gamma$ *are sufficiently small positive numbers, and* $K$ *a constant independent of* $h, \tau$. *Let further* $L_{h\tau}(v_{ik})$, $\delta_{\bar{t}} v_{ik}(r_2)$, $\delta_{\bar{z}z} v_{ik}(r_2)$, $v'_{i0}(r)$ *be also uniformly bounded in* $Q_{\delta\gamma}$. *Then, the derivative* $v'_{ik}|_{r=r_2} = v'_{ik}(r_2)$ *is uniformly bounded in* $h, \tau$ *for* $0 < \gamma \leqslant z_l \leqslant H - \gamma$, $0 \leqslant t_k \leqslant T$.

*Lemma 4. Let* $|v_{ik}(r)| \leqslant K$ *in* $Q'_{\delta\gamma}\left\{r_1 + \frac{\delta}{2} \leqslant r \leqslant r_2 - \frac{\delta}{2},\ 0 \leqslant z_l \leqslant H - \gamma,\right.$ $\left.0 \leqslant t_k \leqslant T\right\}$, *where* $\delta$, $\gamma$ *are sufficiently small positive numbers, and the constant* $K$ *is independent of* $h$ *and* $\tau$. *Let further* $L_{h\tau}(v_{ik})$, $\delta_{\bar{t}} v_{0k}(r)$, $v'_{0k}(r)$, $\delta_z v_{i0}(r)$ *be also uniformly bounded in* $h, \tau$ *in* $Q'_{\delta\gamma}$

*Then* $|\delta_z v_{0k}| \leqslant K_1$ *for* $r_1 + \delta \leqslant r \leqslant r_2 - \delta$, $0 \leqslant t_k \leqslant T$, *where* $K_1$ *is independent of* $h, \tau$.

Lemmas 3 and 4 are difference-differential analogs of the lemma in /4/ and are proved analogously to that lemma.

*Lemma 5. Let*

$$M_0 = \sup_Q |f|, \quad m_0 = \sup_{\Gamma_0 + \Gamma_1} |\varphi|, \quad m_1 = \sup_{\Gamma_2} |\psi|.$$

*Then the following estimate holds for the solution of the difference-differential boundary-value problem (2):*

$$|u_{ik}(r)| \leqslant \frac{1}{2}[(r_2 - r_1)^2 - (r - r_1)^2]\left(M_0 + \frac{2m_1}{H - h}\right) + \\ + \frac{m_1}{H - h}\left(z - \frac{H}{2}\right)^2 + m_1(r_2 - r) + m_0. \qquad (10)$$

Proof. The function

$$V^{\pm}_{ik}(r) = \frac{1}{2}[(r_2 - r_1)^2 - (r - r_1)^2]\left(\varepsilon + M_0 + \frac{2m_1}{H - h}\right) + \\ + \frac{m_1}{H - h}\left(z - \frac{H}{2}\right)^2 + m_1(r_2 - r) + m_0 \pm u_{ik}(r), \qquad (10_1)$$

where $\varepsilon > 0$, satisfies the following conditions for $0 < h < \frac{H}{2}$:

$$L_{h\tau} V_{ik}^{\pm} \leqslant -\varepsilon < 0, \quad V_{ik}^{\pm}|_{r_0+r_1} \geqslant 0, \quad \left.\frac{dV_{ik}^{\pm}}{dr}\right|_{r=r_1} \leqslant 0, \quad \delta_z V_{ik}^{\pm}|_{z=0} \leqslant 0, \quad \delta_z V_{ik}^{\pm}|_{z=H} \geqslant 0.$$

Therefore, by Lemma 2, $V_{ik}^{\pm}(r) \geqslant 0$ everywhere in $Q$, i.e.,

$$|u_{ik}(r)| \leqslant \frac{1}{2}[(r_2 - r_1)^2 - (r - r_1)^2]\left(\varepsilon + M_0 + \frac{2m_1}{H-h}\right) +$$

$$+ \frac{m_1}{H-h}\left(z - \frac{H}{2}\right)^2 + m_1(r_2 - r) + m_0.$$

Since the last inequality holds for any $\varepsilon > 0$, and its left-hand side is independent of $\varepsilon$, we can pass to the limit as $\varepsilon \to 0$ and obtain (10).

*Lemma 6. Problem (2) cannot have two different solutions.*

Proof. Let $\bar{u}_{ik}$ and $\bar{\bar{u}}_{ik}$ be two different solutions of problem (2). Then $u_{ik} = \bar{u}_{ik} - \bar{\bar{u}}_{ik}$ is a solution of problem (2) for $f \equiv 0$, $\varphi \equiv 0$, and $\psi \equiv 0$, and, applying estimate (10), we see that $u_{ik} \equiv 0$.

We shall now prove the existence of a solution of the difference-differential boundary-value problem (2) and derive for it an expression in terms of the Bessel functions $I_0(\xi)$ and $K_0(\xi)$. To this end, we write the system of differential equations (2.0) in the following vector-matrix form:

$$\vec{u}_k'' + \frac{1}{r}\vec{u}_k' + \frac{1}{h^2}A\vec{u}_k - \frac{1}{\tau}\vec{u}_k' = \vec{f}_k - \frac{1}{\tau}\vec{u}_{k-1}, \tag{11}$$

where

$$\vec{u}_k(r) = \begin{Bmatrix} u_{1k}(r) \\ u_{2k}(r) \\ \vdots \\ u_{M-1k}(r) \\ u_{Mk}(r) \end{Bmatrix}, \qquad \vec{f}_k(r) = \begin{Bmatrix} f_{1k}(r) + \frac{\psi_1(r, t_k)}{h} \\ f_{2k}(r) \\ \vdots \\ f_{M-1k}(r) \\ f_{Mk}(r) - \frac{\psi_2(r, t_k)}{h} \end{Bmatrix},$$

$$A = \begin{Bmatrix} -1 & 1 & 0 & 0 & \cdots & 0 \\ 1 & -2 & 1 & 0 & \cdots & 0 \\ 0 & 1 & -2 & 1 & \cdots & 0 \\ \cdots & \cdots & \cdots & \cdots & \cdots & \cdots \\ 0 & \cdots & 1 & -2 & 1 & \\ 0 & \cdots & 0 & 1 & -1 & \end{Bmatrix}.$$

The boundary conditions (2.3) have not been taken into consideration. If the solution of problem (2) at the $(k-1)$-th time section is known, then to find it on the $k$-th section it suffices to solve equation (11) with boundary conditions (2.1), (2.2), and (2.4). By using an orthogonal matrix $B = \| b_{is} \|$,

$$b_{is} = \begin{cases} (-1)^{i+s}\sqrt{\frac{2}{M}}\sin\left(i - \frac{1}{2}\right)\frac{\pi s}{M}, & 1 \leqslant i \leqslant M,\ s \neq M, \\ (-1)^{i+s}\sqrt{\frac{1}{M}}, & 1 \leqslant i \leqslant M,\ s = M, \end{cases}$$

the matrix $A$ is diagonalized to $\Lambda = B'AB$, with diagonal elements $-\lambda_s$, where $\lambda_s = 4\cos^2\frac{\pi s}{2M}$, $1 \leqslant s \leqslant M$, /1, 5, 6/.

After this transformation, equation (11) is rewritten

$$BB'\vec{u}_k'' + \frac{1}{r}BB'\vec{u}_k' + \frac{1}{h^2}B\Lambda B'\vec{u}_k - \frac{1}{\tau}BB'\vec{u}_k = \vec{f}_k - \frac{1}{\tau}\vec{u}_{k-1}.$$

Pre-multiplying this vector equation by $B' = B^{-1}$ and setting $\vec{V}_k = B'\vec{u}_k$, we obtain the following equation for the vector $\vec{V}_k$:

$$\vec{V}_k'' + \frac{1}{r}\vec{V}_k' + \frac{1}{h^2}\Lambda\vec{V}_k - \frac{1}{\tau}\vec{V}_k = \\ = B'\vec{f}_k - \frac{1}{\tau}\vec{V}_{k-1} = \vec{G}_k, \qquad (11_1)$$

which is equivalent to the following uncoupled system of ordinary differential equations:

$$v_{sk}'' + \frac{1}{r}v_{sk} - \left(\frac{\lambda_s}{h^2} + \frac{1}{\tau}\right)v_{sk} = g_{sk}. \qquad (11_2)$$

The general solution of this equation has the form

$$v_{sk}(r) = A_{sk}\bar{w}_{sk}(r) + B_{sk}\bar{\bar{w}}_{sk}(r) + z_{sk}(r),$$

where $z_{sk}(r)$ is a particular solution of the inhomogeneous equation $(11_2)$, $\bar{w}_{sk}(r)$ and $\bar{\bar{w}}_{sk}(r)$ are the fundamental system of solutions of the corresponding homogeneous equation $(11_2)$, and $A_{sk}$ and $B_{sk}$ are arbitrary constants. As a fundamental system, we can choose the Bessel functions $I_0(\xi)$ and $K_0(\xi)$, setting $\bar{w}_{sk}(r) = I_0(\alpha_s r)$, $\bar{\bar{w}}_{sk}(r) = K_0(\alpha_s r)$, where

$$\alpha_s = \sqrt{\frac{\lambda_s}{h^2} + \frac{1}{\tau}}$$

The general solution of equation (11) then takes the form $\vec{u}_k = B\vec{V}_k$, where

$$u_{ik}(r) = \sum_{s=1}^{M-1}(-1)^{i+s}\sqrt{\frac{2}{M}}\sin\left(i - \frac{1}{2}\right)\frac{\pi s}{M} \times \\ \times [A_{sk}I_0(\alpha_s r) + B_{sk}K_0(\alpha_s r) + z_{sk}(r)] + \\ + \frac{(-1)^{M+1}}{\sqrt{M}}[A_{Mk}I_0(\alpha_M r) + B_{Mk}K_0(\alpha_M r) + z_{Mk}(r)]. \qquad (12)$$

To find $A_{sk}$, $B_{sk}$, we solve the system of $2M$ linear algebraic equations in $2M$ unknowns, obtained from conditions (2.1), (2.2), and (2.4). The determinant of this system does not vanish (this follows from the unique solvability of problem (2)). We have thus proved the existence of a solution of problem (2) and expressed it in terms of known functions $I_0(\xi)$ and $K_0(\xi)$. Hence it follows that if $f, \varphi, \psi \in C^{(n)}$, the solution of problem (2) $u_{ik}(r)$ belongs to $\in C^{(n+2)}$.

3°. To prove the existence of a solution of the boundary-value problem (1) by the ray method, it suffices to prove the compactness of the family of functions $\{u_{ik}(r)\}$ and of the family of derivatives and difference quotients with respect to $r$ and $z$ up to the third order inclusive and with respect to up to the second order inclusive in the corresponding subdomains of the parallelepiped $Q$, inwards, or adjoining appropriate parts of the boundary.

This can be achieved by applying difference analogs of S. N. Bernstein's estimates /8, 4, 9/.

Seeing that a five-fold smooth permissible function $\Psi(r, z, t)$ satisfying the boundary conditions of the problem exists, and passing now to a new unknown function $v=u-\Psi$, where $u$ is the required solution of problem (1), we obtain for $v$ a boundary-value problem (1) with homogeneous boundary conditions; $v$ also satisfies the initial condition $v|_{t=0}=\varphi_0-\Psi|_{t=0}$, which will be called the modified initial condition; for $v_{ik}$ we correspondingly obtain a difference-differential boundary-value problem (2), also with homogeneous boundary conditions and $v_{i0}=\varphi_0(r, z_i)-\Psi_{i0}(r)$. This substitution of variables simplifies further manipulations; we shall assume it to have been carried out.

To derive the difference analogs of Bernstein's estimates, it is convenient to apply the identities

$$\delta_z(U_{ik}V_{ik})=(\delta_z U_{ik})V_{i+1k}+U_{ik}(\delta_z V_{ik}), \tag{13}$$

$$\delta_{\bar{z}}(U_{ik}V_{ik})=(\delta_{\bar{z}}U_{ik})V_{ik}-U_{i-1k}(\delta_{\bar{z}}V_{ik}), \tag{14}$$

$$L_{h\tau}(U_{ik}V_{ik})=U_{ik}L_{h\tau}(V_{ik})+V_{ik}L_{h\tau}(U_{ik})+2U'_{ik}V'_{ik}+$$
$$+(\delta_z U_{ik})\cdot(\delta_z V_{ik})+(\delta_{\bar{z}}U_{ik})(\delta_{\bar{z}}V_{ik})+\tau(\delta_{\bar{t}}U_{ik})\cdot(\delta_{\bar{t}}V_{ik}). \tag{15}$$

From estimate (10) we have

$$|v_{ik}(r)|\leqslant K, \tag{10*}$$

where $K$ is a constant independent of $h, \tau$. If the estimate (10*) applies to some function $U_{ik}(r)$, we shall express this fact by the equality $U_{ik}(r)=O(1)$. We thus have $v_{ik}(r)=O(1)$. We now proceed with difference analogs of Bernstein's estimates. First consider the estimates in the parallelepiped

$$Q_{1\delta}\{r_1+\delta\leqslant r\leqslant r_2-\delta,\ 0\leqslant z_i\leqslant H,\ 0\leqslant t_k\leqslant T\},$$

where $\delta$ is a positive number satisfying the inequality $0<\delta<\frac{r_2-r_1}{2}$.

To estimate $v'_{ik}(r)$ in $Q_{1\delta}$ we take the function

$$z_{ik}(r)=(v'_{ik})^2R^2(r)+c_1v_{ik}^2+c_2r^2 \text{ in } Q_{1\alpha}, \text{ where } 0<\alpha<\delta,$$

$c_1$ and $c_2$ are some positive constants, and $R(r)=(r-r_1-\alpha)(r_2-\alpha-r)$. It is easily seen that $L_{h\tau}z_{ik}>0$ for sufficiently large $c_1$ and $c_2$ everywhere inside $Q_{1\alpha}$. Hence, by Lemma 1, the maximum of $z_{ik}(r)$ in $Q_{1\alpha}$ is reached only on the boundary of $Q_{1\alpha}$. Since $\delta_z z_{0k}\equiv\delta_z z_{Mk}\equiv 0$, then, by Lemma 2, the maximum of $z_{ik}(r)$ can be attained only for $k=0$, either for $r=r_1+\alpha$ or $r=r_2-\alpha$. But from condition (6), and also by virtue of the conditions $v_{ik}(r)=O(1)$, $R(r_1+\alpha)=R(r_2-\alpha)=0$ we have $z_{ik}(r)=0$ on these parts of the boundary of $Q_{1\alpha}$. Hence, $z_{ik}(r)=0(1)$ everywhere in $Q_{1\alpha}$. Therefore,

$$|v'_{ik}(r)|\leqslant\frac{O(1)}{R(r)}=O(1)$$

in any subdomain $Q_{1\delta}$, $0<\alpha<\delta$.

Analogous estimates are obtained for $v'_{ik}(r)$ in $Q_{1\delta}$. To prove that $\delta_z v_{ik}(r)$ is bounded in $Q_{1\delta}$, consider the function $z_{ik}(r)=(\delta_z v_{ik})^2R^2(r)+c_1(v_{ik})^2+c_2r^2$. It is easily seen that $L_{h\tau}(z_{ik})>0$ in $Q_{1\alpha}(0<\alpha<\delta)$ for sufficient large (positive) $c_1$ and $c_2$. By Lemma 1, $z_{ik}$ has a maximum on the boundary of $Q_{1\alpha}$. On the other

hand from the equalities $\delta_z v_{0k} \equiv \delta_z v_{Mk} \equiv 0$ and from the conditions of Theorem 1 we have $z_{ik}(r) = O(1)$ in $Q_{1\alpha}$. Hence

$$|\delta_z v_{ik}| \leqslant \frac{O(1)}{R(r)} = O(1) \text{ in } Q_{1\delta} \text{ for } 0 < \alpha < \delta.$$

A similar estimate is obtained for $\delta_z v_{ik}$ in $Q_{1\delta}$. To estimate $\delta_z v_{ik}$ we consider the function

$$z_{ik}(r) = (\delta_z v_{ik}')^2 R^2(r, z, t) + c_1 [(\delta_z v_{ik}')^2 + (\delta_z v_{i-1,k}')^2 + (\delta_z v_{i+1k}')^2 + (\delta_z v_{ik-1}')^2] + c_2 r^2,$$

where

$$R(r, z, t) = \left(r - r_1 - \frac{\delta}{2}\right)\left(r_2 - \frac{\delta}{2} - r\right) \times \left(z - \frac{\gamma}{2}\right)\left(H - \frac{\gamma}{2} - z\right)\left(t - \frac{\beta}{2}\right),$$

and, as before, find that

$$\delta_z v_{ik}' = O(1) \text{ in } Q_{\beta\gamma\delta}\{r_1 + \delta \leqslant r \leqslant r_2 - \delta, \quad \gamma \leqslant z \leqslant H - \gamma, \quad \beta \leqslant t \leqslant T\},$$

where $\beta$, $\gamma$, $\delta$ are arbitrarily small positive numbers.

The uniform boundedness of $\delta_{\bar{t}} v_{ik}(r)$ in the entire domain is proved as follows. The function $\delta_{\bar{t}} v_{ik}$ satisfies the equality $L_{h^2}(\delta_{\bar{t}} v_{ik}) = \delta_{\bar{t}} f_{ik}$, $2 \leqslant k \leqslant N$. In order that this equality be meaningful for $k = 1$, we extend the definition of $v_{ik}$ for $k = -1$, stipulating

$$\frac{d^2 \varphi_0(r, z_i)}{dr^2} + \frac{1}{r} \cdot \frac{d\varphi_0(r, z_i)}{dr} + \delta_{z\bar{z}} \varphi_0(r, z_i) - \frac{\varphi_0(r, z_i) - v_{i,-1}(r)}{\tau} = f_{i0}(r), \tag{16}$$

where $1 \leqslant i \leqslant M$; $v_{0,-1}(r) = v_{1,-1}(r)$, $v_{M+1,-1}(r) = v_{M,-1}(r)$. From (16) and (6), we have

$$\delta_{\bar{\tau}} v_{i0}(r) = \frac{\varphi_0(r, z_i) - v_{i,-1}(r)}{\tau} = O(1).$$

Further, $\delta_{\bar{t}} v_{ik}(r)$ satisfies the boundary conditions

$$\delta_{\bar{t}} v_{ik}|_{\Gamma_1} = 0, \quad \frac{d}{dn}(\delta_{\bar{t}} v_{ik})\Big|_{\Gamma_2} = 0.$$

Hence the estimate (10) holds for $\delta_{\bar{t}} v_{ik}$, where $m_0 = m_1 = 0$, and $M_0$ is replaced with $M_1 = \max_Q \left|\frac{\partial f}{\partial t}\right| + 1$, taking $\tau$ sufficiently small.

If $v_{ik}$ is replaced everywhere by $\delta_{\bar{t}} v_{ik}$ and the conditions of Theorem 1 are taken into consideration, it can easily be shown that $\delta_{\bar{t}} v_{ik}'$, $\delta_{\bar{t}} v_{ik}''$, $\delta_{\bar{t}z} v_{ik}$, $\delta_{\bar{t}z} v_{ik}'$ are bounded in $Q_{1\delta}$. From equation (2.0) and from previous estimates follows the boundedness of $\delta_{z\bar{z}} v_{ik}$, $\delta_{z\bar{z}} v_{ik}'$, $\delta_{z\bar{z}z} v_{ik}$ in $Q_{1\delta}$. To estimate $\delta_{z\bar{z}\bar{t}} v_{ik}$ we apply Lemma 4, substituting $\delta_{z\bar{z}\bar{t}} v_{ik}$ for $v_{ik}$. It is easily verified that all the requirements of the lemma are satisfied under this substitution, and thus

$$\delta_{z\bar{z}\bar{t}} v_{1k}(r) = O(1), \quad \delta_{z\bar{z}\bar{t}} v_{Mk}(r) = O(1)$$

for $r_1 + \delta \leqslant r \leqslant r_2 - \delta$, $1 \leqslant k \leqslant N$.

But then, using the function

$$z_{ik}(r) = (\delta_{z\bar{z}\bar{t}} v_{ik})^2 R^2(r) + c_1 (\delta_{z\bar{t}} v_{ik})^2 + c_2 r^2$$

and Bernstein's estimate, we find that $\delta_{\bar{z}z\bar{t}}v_{ik}(r) = O(1)$ in $Q_{1\delta}$. From equation (2.0) then follows that $\delta_{\bar{t}\bar{t}}v_{ik}(r)=O(1)$ in $Q_{1\delta}$.

We have thus obtained the necessary estimates in all subdomains of type $Q_{1\delta}$.

The estimates of all these quantities are analogously obtained in subdomains of the form $Q_{2\delta\gamma}\{r_1 \leqslant r \leqslant r_1+\delta,\ 0<\gamma\leqslant z\leqslant H_0-\gamma,\ 0\leqslant t\leqslant T\}$, adjoining $\Gamma_2$ for $r=r_1$. To estimate $v'_{ik}(r)$, we take the function $z_{ik}(r) = (v_{ik})^2R^2(r, z) + + c_1[v^2_{i+1k}+v^2_{ik}+v^2_{i-1k}] + c_2r^2$, where $R(r, z) = (r-z_1-\delta)(z-\gamma)(H_0-\gamma-z)$, and form Bernstein's estimate. We similarly estimate $\delta_z v_{ik}$ in $Q_{2\delta\gamma}$. To estimate $\delta_z v_{ik}$ we take the function

$$z_{ik}(r) = (\delta_z v_{ik})^2 R^2(z) + c_1[v^2_{i+1k}+v^2_{ik}+v^2_{i-1k}] + c_2(r-r_1)^2,$$
$$R(z) = (z-\gamma)(H_0-\gamma-z).$$

The estimate of $\delta_{z\bar{z}}v_{ik}$ is similarly obtained, and the boundedness of $v'_{ik}$ in $Q_{2\delta\gamma}$ follows from (2.0). Estimates are thus obtained for derivatives and difference quotients of second order for the case of compact $v'_{ik}$ in $Q_{2\delta\gamma}$.

In domains of type $Q_{3\delta\gamma}\{r_2-\delta\leqslant r\leqslant r_2,\ 0<\gamma\leqslant z\leqslant H-\gamma, 0\leqslant t_k\leqslant T\}$ it is sufficient to estimate $\delta_z v_{ik}$ and $v'_{ik}$, since $\delta_{\bar{t}}v_{ik}$ has been estimated in all of $Q$. To prove the boundedness of $\delta_z v_{ik}$ we consider the function

$$z_{ik}(r) = (\delta_z v_{ik})^2 R^2(r, z) + c_1(v^2_{i+1k}+v^2_{ik}+v^2_{i-1k}) + c_2r^2,$$

where $R(r, z) = (r_2-\delta-r)(z-\gamma)(H-\gamma-z)$. The family $\{v'_{jk}\}$ should first be estimated on the boundary $r=r_2$ using Lemma 3, and then estimated inside $Q_{3\delta\gamma}$ according to Bernstein.

$v'_{ik}$ and $\delta_z v_{ik}$ are analogously estimated in regions of type

$$Q_{4\delta\gamma}\{r_1\leqslant r\leqslant r_1+\delta,\ H_0+\gamma\leqslant z\leqslant H-\gamma,\ 0\leqslant t\leqslant T\}.$$

4°. We can now prove existence and uniqueness of the solution of problem (1). From the estimates in 3° we see that $v_{ik}(r)$ are compact, in the sense of uniform convergence, in any subdomain of the form $Q_\varepsilon = D_\varepsilon\times[0, T]$, where $D_\varepsilon$ is a closed subdomain obtained from the rectangle $D$ by removing an $\varepsilon$-neighborhood of the point $(r_1, H_0, 0)$, and also of the corner points. The families $v'_{ik}(r)$, $\delta_z v_{ik}$ are compact in $\bar{Q}_\varepsilon = \bar{D}_\varepsilon\times[0, T]$, where $\bar{D}_\varepsilon$ is obtained from $D$ by removing $\varepsilon$-strips adjoining a part of the boundary $\Gamma_1$. The families $\delta_{\bar{t}}v_{ik}$ $v'_{ik}$, $\delta_{z\bar{z}}v_{ik}$ are compact in $\bar{Q}_\varepsilon = \bar{D}_\varepsilon\times[\beta, T]$, where $\bar{D}_\varepsilon$ is any truly interior subdomain of $D$, and $\beta>0$ is any arbitrarily small number. Therefore, from the family $v_{ik}(r)$ depending on $h$ and $\tau$ we can pick out a subsequence $v^s_{ik}(r)$ such that for $|h_s|+|\tau_s|\to 0$ it and its derivatives and difference quotients entering equation (2.0) converge uniformly in their compactness regions. As in /10/, we can prove that the limiting function $v(r, z, t)$ satisfies equation (1.0) inside $Q$, and also the initial and the homogeneous boundary conditions (1.1)—(1.4) and the modified initial condition (1.5), in the classical sense. Clearly, the function $u=v+\Psi$ meets requirements 1 and 2 of the definition of the solution $u$ of the initial problem (1) with inhomogeneous boundary conditions.

We shall prove that the limiting function $v(r, z, t)$ not only satisfies requirements 1 and 2, but also requirements 3 and 4 of the definition of the solution of problem (1). We first consider requirement 3. Boundedness of $v$ and $\frac{\partial v}{\partial t}$ in $Q$ follows from uniform boundedness (in $Q$) of $v_{ik}$ and $\delta_{\bar{t}}v_{ik}$, respectively. Therefore, to prove the inclusion $V\in W_2^1(Q)$, it suffices to establish the inequality

$$E^{Q}(v, v) = \int_0^T dt \int_0^H dz \int_{r_1}^{r_2} r\left[\left(\frac{\partial v}{\partial r}\right)^2 + \left(\frac{\partial v}{\partial z}\right)^2\right] dr < +\infty. \tag{17}$$

Multiplying (2.0) by $h\tau r\Phi$, where $\Phi = \Phi(r, z, t)$ is a sufficiently smooth function, integrating and summing over the $Q$ grid, we obtain

$$h\tau \sum_{k=1}^{N} \sum_{i=1}^{M} \int_{r_1}^{r_2} \{(rv'_{ik})'\Phi_{ik} + r(\delta_{z\bar{z}} v_{ik})\Phi_{ik} - r(\delta_{\bar{t}} v_{ik})\Phi_{ik} - rf_{ik}\Phi_{ik}\} dr \equiv 0.$$

Integrating and summing by parts the first and the second terms of this sum, we obtain

$$h\tau \sum_{k=1}^{N} \sum_{i=1}^{M} \int_{r_1}^{r_2} r[v'_{ik}\Phi'_{ik} + (\delta_z v_{ik})\cdot(\delta_z \Phi_{ik} + (\delta_{\bar{t}} v_{ik} + f_{ik})\Phi_{ik}]dr =$$
$$= \tau \sum_{k=1}^{N} \left\{h \sum_{i=1}^{M} (rv'_{ik}\Phi_{ik})\Big|_{r_1}^{r_2} + \int_{r_1}^{r_2} [(\delta_z v_{Mk})\Phi_{M+1k} - (\delta_z v_{0k})\Phi_{1k}]\, dr\right\}. \tag{18}$$

If we set $\Phi_{ik} = v_{ik} - w_{ik}$, where $w(r, z, t)$ is any once continuously differentiable function satisfying the homogeneous boundary conditions (1.1)—(1.4), and $w_{ik}(r)$ its values on the nodal lines, the right-hand side of equation (18) vanishes by virtue of the boundary conditions for $v_{ik}$ and $\Phi_{ik}$, and (18) can be written.

$$h\tau \sum_{k=1}^{N} \sum_{i=1}^{M} \int_{r_1}^{r_2} r[(v'_{ik})^2 + (\delta_z v_{ik})^2]\, dr =$$
$$= h\tau \sum_{k=1}^{N} \sum_{i=1}^{M} \int_{r_1}^{r_2} r[v'_{ik}\cdot w'_{ik} + (\delta_z v_{ik})\cdot(\delta_z w_{ik}) -$$
$$- (\delta_t v_{ik} + f_{ik})(v_{ik} - w_{ik})]\, dr.$$

Applying the inequality $ab \leqslant \varepsilon a^2 + \frac{b^2}{\varepsilon}$ to the terms on the right-hand side, and seeing that $v_{ik}$, $w_{ik}$, $\delta_t$, $v_{ik}$, $f_{ik}$, are bounded, we obtain, after transferring the remaining terms to the left-hand side, that for a sufficiently small $\varepsilon > 0$

$$E^{Q}_{h\tau}(v_{ik}, v_{ik}) = h\tau \sum_{k=1}^{N} \sum_{i=1}^{M} \int_{r_1}^{r_2} r[(v'_{ik})^2 + (\delta_z v_{ik})^2]\, dr \leqslant C < +\infty, \tag{19}$$

where the constant $C$ is independent of $h$ and $\tau$.

If summation and integration in the left-hand side of (19) is extended not over $Q$, but over a closed parallelepiped $Q^*_\delta\{r_1 + \delta \leqslant r \leqslant r_2 - \delta,\ \delta \leqslant z \leqslant H - \delta,\ \delta \leqslant t \leqslant T\}$, lying inside $Q$, the inequality is a fortiori satisfied with the previous constant $C$ in the right-hand side. Passing to the limit for $|h_s| + |\tau_s| \to 0$ and seeing that $\frac{\partial v}{\partial r}$ and $\frac{\partial v}{\partial z}$ are continuous in $Q_\delta$ and

$$(v^{(s)}_{ik})' \rightrightarrows \frac{\partial v}{\partial r}, \qquad \delta_z v^s_{ik} \rightrightarrows \frac{\partial v'}{\partial z} \text{ in } Q_\delta,$$

we obtain

$$E^{Q^*_\delta}(v, v) = \iiint_{Q^*_\delta} r\left[\left(\frac{\partial v}{\partial r}\right)^2 + \left(\frac{\partial v}{\partial z}\right)^2\right] dQ \leqslant C. \tag{19$_1$}$$

Since the constant on the right-hand side of (19) is independent of $\delta$, we pass to the limit $\delta \to 0$ and obtain

$$E^Q(v, v) = \iiint_Q r\left[\left(\frac{\partial v}{\partial r}\right)^2 + \left(\frac{\partial v}{\partial z}\right)^2\right] dQ \leqslant C, \tag{20}$$

which concludes the proof of the inclusion $v \in W_2^{(1)}(Q)$. Hence it follows that the function $u = v + \Psi$ also belongs to $W_2^1(Q)$.

It now remains to prove that $u$ satisfies requirement 4 in the definition of the solution of problem (1). It is clear enough to show that for the function $v$

$$\lim_{\delta \to 0} \iint_{\Gamma_\delta} r\Phi \frac{\partial v}{\partial n} d\Gamma_\delta = 0 \tag{21}$$

for any once continuously differentiable permissible function $\Phi$ satisfying the homogeneous conditions (1.1)—(1.4).

From Green's formula and equation (1.0) we have

$$D^{Q_\delta}(v, \Phi) \equiv \iiint_{Q_\delta} r\left[\frac{\partial v}{\partial r} \cdot \frac{\partial \Phi}{\partial r} + \frac{\partial v}{\partial z} \frac{\partial \Phi}{\partial z} + \right.$$

$$\left. + \frac{\partial v}{\partial t} \Phi + \bar{f}\Phi\right] dQ = \iint_{\Gamma_\delta} r\Phi \frac{\partial v}{\partial n} d\Gamma_\delta, \tag{22}$$

where $\bar{f} = f - L\Psi$. In view of the inclusion $v \in W_2^1(Q)$ and the limitations imposed on $f$ and $\Phi$, the integral

$$D^Q(v, \Phi) = \iiint_Q r\left[\frac{\partial v}{\partial r} \cdot \frac{\partial \Phi}{\partial r} + \frac{\partial v}{\partial z} \cdot \frac{\partial \Phi}{\partial z} + \right.$$

$$\left. + \frac{\partial v}{\partial t} \Phi + \bar{f}\Phi\right] dQ \tag{23}$$

exists and

$$\lim_{\delta \to 0} D^{Q_\delta}(v, \Phi) = D^Q(v, \Phi). \tag{24}$$

Therefore relationship (21) for any continuously differentiable function $\Phi$ satisfying the homogeneous conditions (1.1)—(1.4) is equivalent to

$$D^Q(v, \Phi) = 0, \tag{25}$$

or alternatively

$$\lim_{\delta \to 0} D^{Q_\delta}(v, \Phi) = 0.$$

Designating the left-hand side of (18) by $D^Q_{h\tau}(v_{ik}, \Phi_{ik})$, we find that, by the conditions for $v_{ik}$ and $\Phi$,

$$D^Q_{h\tau}(v_{ik}, \Phi_{ik}) \equiv h\tau \sum_{k=1}^{N} \sum_{i=1}^{M} \int_{r_1}^{r_2} r\left[ v'_{ik} \Phi'_{ik} + \delta_z v_{ik} \delta_z \Phi_{ik} + (\delta_{\bar{t}}\, v_{ik} + \right.$$

$$\left. + \bar{f}_{ik}) \Phi_{ik} \right] dr = 0. \tag{25*}$$

In this equality, however, we cannot directly pass to the limit for $|h_s| + |\tau_s| \to 0$; this direct transition to the limit is admissible for the last term only; it gives

$$\lim_{|h_s|+|\tau_s|\to 0} h\tau \sum_{k=1}^{N}\sum_{i=1}^{M}\int_{r_1}^{r_2} r\,(\delta_{\bar{i}}\, v_{ik} + \bar{f}_{ik})\,\Phi_{ik}\,dr =$$

$$= \iiint_{Q} r\left[\frac{\partial v}{\partial t} + \bar{f}\right]\Phi\,dQ. \tag{26}$$

The behavior of the expression

$$E^{Q}_{h\tau}(v_{ik}, \Phi_{ik}) = h\tau \sum_{k=1}^{N}\sum_{i=1}^{M}\int_{r_1}^{r_2} r\,[v'_{ik}\,\Phi'_{ik} + (\delta_z v_{ik})\cdot(\delta_z \Phi_{ik})]\,dr \tag{27}$$

at the limit requires further study. Let $G_\delta$ be the boundary domain left after removing the parallelepiped $Q_\delta$ from $Q$; we retain the same notations for the corresponding grid domains. Then $E^{Q}(v, \Phi)$ and $E^{Q}_{\tau h}(v_{ik}, \Phi_{ik})$ are representable in the form

$$E^{Q}(v, \Phi) = E^{Q_\delta}(v, \Phi) + E^{G_\delta}(v, \Phi), \quad E^{Q}_{h\tau}(v_{ik}, \Phi_{ik}) = E^{Q_\delta}_{h\tau}(v_{ik}, \Phi_{ik}) +$$

$$+ E^{G_\delta}_{h\tau}(v_{ik}, \Phi_{ik}). \tag{28}$$

Applying the Cauchy-Bunyakovskii [Cauchy-Schwarz] inequality to the sums and integrals, we easily obtain

$$|E^{G_\delta}_{h\tau}(v_{ik}, \Phi_{ik})| \leqslant \sqrt{E^{G_\delta}_{h\tau}(v_{ik}, v_{ik})}\cdot\sqrt{E^{G_\delta}_{h\tau}(\Phi_{ik}, \Phi_{ik})}.$$

Therefore, from (19),

$$|E^{G_\delta}_{h\tau}(v_{ik}, \Phi_{ik})| \leqslant \sqrt{C}\cdot\sqrt{E^{G_\delta}_{h\tau}(\Phi_{ik}, \Phi_{ik})},$$

and hence, $\Phi$ being bounded in $Q$, we obtain for sufficiently small $\delta > 0$

$$|E^{G_\delta}_{h\tau}(v_{ik}, \Phi_{ik})| < \varepsilon \tag{29}$$

uniformly in $h$ and $\tau$. Analogously we find that for sufficiently small $\delta > 0$

$$|E^{G_\delta}(v_{ik}, \Phi_{ik})| < \varepsilon. \tag{30}$$

Applying (28) and (29) and (30), we obtain

$$|E^{Q}_{h\tau}(v_{ik}, \Phi_{ik}) - E^{Q}(v, \Phi)| \leqslant 2\varepsilon + |E^{Q_\delta}_{h\tau}(v_{ik}, \Phi_{ik}) - E^{Q_\delta}(v, \Phi)|$$

for sufficiently small $\delta > 0$ uniformly in $h$ and $\tau$. But for any fixed $\delta > 0$

$$\lim_{|h_s|+|\tau_s|\to 0.} E^{Q_\delta}_{h\tau}(v_{ik}, \Phi_{ik}) = E^{Q_\delta}(v, \Phi).$$

Hence, for sufficiently small $|h_s| + |\tau_s|$ we have

$$|E^{Q}_{h\tau}(v_{ik}, \Phi_{ik}) - E^{Q}(v, \Phi)| < 3\varepsilon. \tag{31}$$

That is,

$$\lim_{|h_s|+|\tau_s|\to 0.} E^{Q}_{h\tau}(v_{ik}, \Phi_{ik}) = E^{Q}(v, \Phi). \tag{32}$$

Therefore, passing to the limit in (25*) as $|h_s| + |\tau_s| \to 0$, we obtain (25). Hence, relationship (21) for the function $v$ is satisfied for any once continuously differentiable permissible function $\Phi$ satisfying the homogeneous conditions (1.1)—(1.4). Hence clearly follows requirement 4

for the solution of problem (1) concerning the function $u=v+\Psi$. This completes the proof of the existence of the solution.

We now prove the uniqueness of this solution. Let $\bar{u}$ and $\bar{\bar{u}}$ be any two solutions of this problem. Then the function $U=\bar{u}-\bar{\bar{u}}$ is a solution of the corresponding homogeneous problem with $f\equiv 0$, $\varphi\equiv 0$ and $\psi\equiv 0$. The relation (23) therefore takes the form

$$D^Q(U,\Phi)\equiv\iiint_Q r\left[\frac{\partial U}{\partial r}\frac{\partial\Phi}{\partial r}+\frac{\partial U}{\partial z}\frac{\partial\Phi}{\partial z}+\frac{\partial U}{\partial t}\Phi\right]dQ=0 \tag{33}$$

for any continuously differentiable permissible function $\Phi$ satisfying (1.1)—(1.4). Since $U$ belongs to the closure of the set of all these functions in the metric $W_2^1(Q)$, $U$ can be substituted for $\Phi$ in (33), which gives

$$D^Q(U,U)=\iiint_Q r\left[\left(\frac{\partial U}{\partial r}\right)^2+\left(\frac{\partial U}{\partial z}\right)^2+\frac{\partial U}{\partial t}U\right]dQ=0. \tag{34}$$

Integrating over $t$ and applying the initial condition $U(r, z, 0)\equiv 0$, we obtain

$$D^Q(U,U)\equiv\iiint_Q r\left[\left(\frac{\partial U}{\partial r}\right)^2+\left(\frac{\partial U}{\partial z}\right)^2\right]dQ+$$
$$+\iint_D rU^2(r,z,T)\,dD=0.$$

Hence, $U(r, z, T)\equiv 0$, with the possible exception of corner points and the point $(r_1, H_0, T)$. Since the upper limit $T$ of integration over $t$ can be chosen arbitrarily, we have $U(r, z, t)\equiv 0$ everywhere in $Q$, with the possible exception of the vertical sides of the parallelepiped $Q$ and the vertical segment $[r_1, H_0, 0\leqslant t\leqslant T]$. This proves the uniqueness of the solution of the boundary-value problem (1).

From the proof of the uniqueness of the solution of (1) it follows that not only the subsequence $v_{ik}^s(r)$, corresponding to the sequence of spacings $h_s$, $\tau_s$, approaching zero, converges to the solution $v$, but that $v_{ik}(r)$ converges to the solution $v$ for any arbitrary approach of $h$, $\tau$ to zero.

## § 2. ESTIMATING THE ERROR OF THE RAY METHOD FOR THE NONSTATIONARY PROBLEM (1)

1°. A priori estimate. Let $u(r, z, t)$ be the solution of problem (1) having bounded derivatives $\frac{\partial^4 u}{\partial z^4}$ and $\frac{\partial^2 u}{\partial t^2}$ in the parallelepiped $Q$. Let

$$M_s=\sup_Q\left|\frac{\partial^s u}{\partial z^s}\right|,\quad N_s=\sup_Q\left|\frac{\partial^s u}{\partial t^s}\right|. \tag{35}$$

Let $u_{ik}(r)$ be the solution of problem (2). We estimate the error of the ray method

$$v_{ik}(r)=u(r, z_i, t_k)-u_{ik}(r). \tag{36}$$

Applying the Taylor expansion, we obtain

$$\delta_{z\bar{z}}u(r, z_i, t_k)=\frac{\partial^2 u(r, z_i, t_k)}{\partial z^2}+\frac{h^2}{12}R_z, \tag{37}$$

where

$$R_z = \frac{1}{2}\left[\frac{\partial^4 u(r, \overline{z}, t_k)}{\partial z^4} + \frac{\partial^4 u(r, \overline{\overline{z}}, t_k)}{\partial z^4}\right],$$

$\overline{z}$, $\overline{\overline{z}}$ lie on the segment $[z_i - h, z_i + h]$, and

$$\delta_{\overline{t}}\, u(r, z_i, t_k) = \frac{\partial u(r, z_i, t_k)}{\partial t} - \frac{\tau}{2} R_{\overline{t}},$$

where

$$R_t = \frac{\partial^2 u(r, z_i, \overline{t})}{\partial t^2}, \quad t_k - \tau \leqslant \overline{t} \leqslant t_k. \tag{38}$$

Therefore

$$L_{h\tau}(v_{ik}) = \frac{h^2}{12} R_z + \frac{\tau}{2} R_t \text{ inside } Q. \tag{39}$$

On the boundary $\Gamma$ the function $v_{ik}$ satisfies the conditions

$$v_{ik}(r_1) = 0, \quad M_0 + 1 \leqslant i \leqslant M, \quad 0 \leqslant k \leqslant N; \tag{40}$$

$$v_{ik}(r_2) = 0, \quad 1 \leqslant i \leqslant M, \quad 0 \leqslant k \leqslant N; \tag{41}$$

$$\delta_z v_{0k}(r) = \frac{h}{2} \cdot \frac{\partial^2 u(r, \theta_1 h, t_k)}{\partial z^2},$$

$$\delta_z v_{Mk}(r) = -\frac{h}{2} \frac{\partial^2 u(r, H - \theta_2 h, t_k)}{\partial z^2} \tag{42}$$

$$\text{for } r_1 \leqslant r \leqslant r_2, \quad 1 \leqslant k \leqslant N;$$

$$\frac{dv_{ik}(r_1)}{dr} = 0, \quad 1 \leqslant i \leqslant M_0, \quad 1 \leqslant k \leqslant N; \tag{43}$$

$$v_{i0}(r) \equiv 0. \tag{44}$$

Applying the estimate (10) to the solution of boundary-value problem (38)—(43), and using (35), (37), (38), we see that everywhere in $Q$

$$|v_{ik}(r)| \leqslant \frac{1}{2}[(r_2 - r_1)^2 - (r - r_1)^2]\left(\frac{M_4 h^2}{12} + \frac{N_2 \tau}{2} + \frac{M_3 h}{H - h}\right) + \\ + \frac{M_2 h}{2(H - h)}\left(z_i - \frac{H}{2}\right)^2. \tag{45}$$

If we use a mesh of straight lines displaced by $\frac{h}{2}$ along the $z$-axis /11/, then, by improving the approximation of the boundary conditions on the faces $z=0$ and $z=H$, we obtain the estimate

$$|v_{ik}(r)| \leqslant O(h^2 + \tau). \tag{46}$$

2°. A posteriori estimates. S.A. Gerschgorin's estimates (45), (46) have the disadvantage that they contain maxima of the absolute values of derivatives of the unknown solution. Of considerable value are other estimates which are expressed in terms of the previously found solution and known quantities, i.e., the so-called a posteriori estimates. These estimates were derived by D. F. Davidenko /13/ for the solution of the Dirichlet problem for the Laplace and Poisson equations. Analogous estimates can be derived for the nonstationary problem (1) in the case of a perfect borehole, when $H_0 = 0$ and $u|_{r=r_i} = \varphi_i(z, t)$, $0 \leqslant z \leqslant H$, $0 \leqslant t \leqslant T$, $i = 1.2$ is known for $r = r_i$. We shall assume that the solution of this problem, whose

existence has been proved in §1, is such that the initial and the boundary conditions are satisfied also at the corner points of $Q$. We shall further require two theorems, proved in /14/ and /15/, which we restate here in application to problem (1) with $H_0=0$.

*Theorem of L. Nirenberg. Let the continuous solution $u$ of equation (1.0) reach its minimum at some interior point $P'(r', z', t') \in Q$, and let $f \leqslant 0$ everywhere in $Q$. Then $u \equiv u(r', z', t') \equiv \text{const}$ everywhere in $Q$ for $t \leqslant t'$.*

*Theorem of R. Vyborny. Let $u(r, z, t)$ be a continuous solution of problem (1) for $H_0=0$ which reaches its minimum in $Q$ at the point $P'(r', z', t') \in \Gamma_2$. Then at this point $\frac{\partial u}{\partial z}\Big|_{z=0} > 0$ if $P'$ belongs to the face $z=0$, and $\frac{\partial u}{\partial z}\Big|_{z=H} < 0$ if $P'$ belongs to the face $z=H$.*

Suppose that an interpolatory function $u_h(r, z, t)$ has been somehow constructed, which coincides with the solution $u_{ik}(r)$ of problem (2) for $H_0 = 0$ on the nodal lines, is continuous, its derivatives which enter equation (1.0) are bound in $Q$, satisfies the same conditions on $\Gamma_2$ as the solution $u(r, z, t)$ of problem (1) for $H_0 = 0$, and on $\Gamma_0 + \Gamma_1$ takes the value $u_h|_{\Gamma_0+\Gamma_1} = \varphi^*(s)$. Then the following estimate holds:

$$|u(r, z, t) - u_h(r, z, t)| \leqslant Eg_0(r, t) + \varepsilon_0, \tag{47}$$

where

$$g_0(r, t) = \min\{g(r); t\}, \quad g(r) = \frac{r_2^2 - r^2}{4} + \frac{r_2^2 - r_1^2}{4 \ln \frac{r_2}{r_1}} \ln \frac{r}{r_2},$$

$$E = \sup_Q |f - Lu_h|, \quad \varepsilon_0 = \sup_{\Gamma_0+\Gamma_1} |\varphi(s) - \varphi^*(s)|.$$

In particular, if $\varphi^* \equiv \varphi$, we should set $\varepsilon_0 = 0$ in (47). Indeed, consider the auxiliary functions

$$V^{\pm}(r, z, t) = Eg(r) + \varepsilon_0 \pm (u - u_h),$$

which satisfy the following inequalities:

$$LV^{\pm} = \pm f \mp Lu_h - E \leqslant 0,$$

$$V^{\pm}|_{\Gamma_0+\Gamma_1} = \pm\varphi \mp \varphi^* + \varepsilon_0 + Eg(r)_{\Gamma_1} \geqslant 0.$$

From R. Vyborny's theorem it follows that $\min_Q V^{\pm}$ cannot be reached on the faces $z=0$, $z=H$. Hence, $\min_Q V^{\pm}$ is attained either on $\Gamma_0 + \Gamma_1$, or inside $Q$. If $\min_Q V^{\pm}$ is reached inside $Q$, then from Nirenberg's theorem, seeing that $LV^{\pm} \leqslant 0$, we infer that the minimum is reached for $t=0$. Thus $\min_Q V^{\pm}$ is invariably attained on $\Gamma_0 + \Gamma_1$, where the function $V^{\pm}$ is nonnegative. Therefore, everywhere in $Q$ $V^{\pm} \geqslant 0$, which is equivalent to the inequality

$$|u - u_h| \leqslant Eg(r) + \varepsilon_0. \tag{48}$$

Now consider the auxiliary functions

$$V^{\pm}(r, z, t) = Et + \varepsilon_0 \pm (u - u_h).$$

Reiterating the preceding arguments, we obtain the inequality

$$|u-u_h| \leqslant Et + \varepsilon_0, \tag{49}$$

which together with (48) gives the estimate (47).

Remark 1. If we have found a function $\tilde{u}_h(r, z, t)$ which on the inner nodal lines differs from $u_{ik}(r)$, we may use the estimate

$$|u-\tilde{u}_h| \leqslant \max_Q |u-u_h| + \max_Q |u_h-\tilde{u}_h|, \tag{50}$$

where $u_h(r, z, t)$ is the interpolative function coinciding with $u_{ik}(r)$ on the nodal lines. The first term on the right-hand side of (50) is estimated by the preceding inequalities, and the second term is known at least on the nodal lines. $|Lu_h|$ can be estimated using the theorem of V. S. Ryaben'kii (/16/, p. 158), which gives estimates of arbitrary interpolative functions $u_h$ in terms of difference quotients of corresponding orders of a function defined at grid points.

Remark 2. The estimates (47), (50) have a certain advantage over Gerschgorin's estimates (45), (46): they do not require knowledge of the maximum of the absolute values of the derivatives of the required solution $u(r, z, t)$ and are expressed in terms of the previously found solution and known quantities. They can be used in estimating the accuracy of the approximate solution of problem (2) not only in conjunction with the ray method, but also with other methods, e.g., the difference method.

The main difficulty involved in the application of the a posteriori estimates is the construction of the interpolative function $u_h(r, z, t)$. Here we may use interpolation Hermite polynomials, trigonometric polynomials, etc. /11/.

## § 3. CASE OF STATIONARY SEEPAGE

In this section we briefly apply the analysis of §§ 1, 2 to nonstationary seepage. As in § 1, we shall consider the boundary conditions (3.1)—(3.4) to be such that a function $\Psi(r, z)$ exists, which is continuously differentiable in a closed domain $D$, has continuous fifth derivatives inside $D$, and satisfies the boundary conditions (3.1)—(3.4) in the classical sense. Any such function will be called five-fold smooth permissible function satisfying the boundary conditions of the problem.

*Definition. A solution of problem (3.0) - (3.4) is a function $u$ such that:*

*1) $u$ is continuously differentiable inside $Q$, in accordance with equation (3.0), and satisfies this equation;*

*2) $u$ satisfies the boundary conditions of problem (3.1) - (3.4) in the classical sense;*

*3) $u$ is bounded in $Q$ and $u \in W_2^1(Q)$;*

*4) if $\Gamma_\delta$ is the boundary of subdomain $D_\delta\{r_1+\delta \leqslant r \leqslant r_2-\delta, \delta \leqslant z \leqslant H-\delta\}$, and $\Psi(r, z)$ is a once continuously differentiable permissible function satisfying the boundary conditions of the problem, then*

$$\lim_{\delta \to 0} \int_{\Gamma_\delta} r\Phi \frac{\partial v}{\partial n} d\Gamma_\delta = 0,$$

*where* $v=u-\Psi$, $n$ *is the normal to* $\Gamma_\delta$, *and* $\Phi$ *any once continuously differentiable permissible function satisfying the homogeneous boundary conditions*

$$\Phi|_{\Gamma_1}\equiv 0,\quad \left.\frac{\partial\Phi}{\partial n}\right|_{\Gamma_2}\equiv 0.$$

As in § 1, stationary analogs of Lemmas 1 and 2 on the maximum principle and of Lemmas 5 and 6, leading to the existence and uniqueness of solution, apply to problem (4.0)—(4.4). According to Ya. I. Alikhashin, the general solution has the form

$$u_i(r)=\sum_{s=1}^{M-1}(-1)^{i+s}\sqrt{\frac{2}{M}}\sin\left(i-\frac{1}{2}\right)\frac{\pi s}{M}\times$$
$$\times\left[A_sI_0(\alpha_s r)+B_sK_0(\alpha_s r)+z_s(r)\right]+$$
$$+\frac{(-1)^{M+1}}{\sqrt{M}}\left[A_M\ln\frac{r}{r_2}+B_M+Z_M(r_1)\right],$$

where $\alpha_s=\frac{2}{h}\cos\frac{\pi s}{M}$, and $I_0(\xi), K_0(\xi)$ are Bessel functions; $A_s$, $B_s$ are determined from the system of algebraic equations obtained from the requirement that conditions (4.1), (4.2), (4.3) be satisfied.

Using S. N. Bernstein's estimate, as in § 1, we prove the following theorem.

*Theorem 2. If the functions* $f(r,z)$, $\frac{\partial^3 f}{\partial r^3}$, $\frac{\partial^3 f}{\partial z^3}$, $\frac{\partial^3 f}{\partial z\,\partial r^2}$ *are bounded in* $D$, *problem (3.0) - (3.4) is uniquely solvable.*

As for nonstationary seepage, we can obtain both the Gerschgorin and Davidenko estimates. In the case of simplest approximation of the derivative $\frac{\partial u}{\partial z}$ on the sides $z=0$ and $z=H$, as in (4.3), we reach by considerations of § 2 the estimate

$$|u(r,z_i)-u_i(r)|\leqslant\frac{1}{2}[(r_2-r_1)^2-(r-r_1)^2]\times$$
$$\times\left(\frac{M_4h^2}{12}+\frac{M_2h}{H-h}\right)+\frac{M_3h}{2(H-h)}\left(z_i-\frac{H}{2}\right)^2,$$

where $M_s=\sup_D\left|\frac{\partial^s u}{\partial z^s}\right|$, $0\leqslant s\leqslant 4$, and if the derivatives $\frac{\partial u}{\partial z}$ for $z=0$ and $z=H$ are approximated with a half-mesh-spacing shift /11/, we have the better estimate

$$|u(r,z_i)-u_i(r)|\leqslant O(h^3).$$

Davidenko's a posteriori estimate for a perfect borehole ($H_0=0$) has in this case the form

$$|u-u_h|\leqslant Eg(r)+\varepsilon_0,$$

where

$$g(r)=\frac{r_2^2-r^2}{4}+\frac{r_2^2-r_1^2}{\ln\frac{r_1}{r_2}}\ln\frac{r}{r_2},$$

$$E=\sup_D|f-Lu_h|,\quad \varepsilon_0=\sup_{\Gamma_1}|\varphi(s)-\varphi^*(s)|.$$

The proof of these estimates in the stationary case follows §2 in its entirety, with the theorems of E. Hopf and G. Giraud /17, 18/ substituted for the theorems of I. Nirenberg and R. Vyborny.

The existence and uniqueness of the generalized solution for the stationary problem in a more general case were previously considered in /19/.

Theorem 2 can easily be extended to line schemes in cases *Aa, Ab, Ab′, Ac, Ba, Bb, Bb′, Bc, B′a, B′b, B′b′, B′c, Ca, Cb, Cb′* of /20/.

BIBLIOGRAPHY


1. ALIKHASHKIN, Ya. I. Reshenie zadachi o nesovershennoi skvazhine metodom pryamykh (Solution of the the Problem of Imperfect Borehole by the Ray Method). — Vychislitel'naya matematika, No. 1. 1957.
2. ROTHE, E. Über Wärmeleitungsgleichung mit nichtkonstanten Koeffizienten im räumlichen Falle. — Math. Ann. 104: 340-354. 1940.
3. TIKHONOV, A.N. Ob uravnenii teploprovodnosti dlya neskol'kikh peremennykh (On the Heat Equation in Several Variables). — Byulleten' MGU, sektsiya AI, No. 9. 1938.
4. VENTTSEL', T.D. Pervaya kraevaya zadacha i zadacha Koshi dlya kvazilineinogo parabolicheskogo uravneniya so mnogimi prostranstvennymi peremennymi (First Boundary-Value Problem and Cauchy Problem for the Quasilinear Parabolic Equation in Many Space Variables). — Matematicheskii sbornik, Vol. 41, No. 4. 1957.
5. SLOBODYANSKII, M.G. a) Sposob priblizhennogo integrirovaniya uravnenii s chastnymi proizvodnymi i ego primenenie k zadacham teorii uprugosti (A Method of Approximate Integration of Partial Differential Equations and Its Application to Problems of Elasticity Theory). — PMM, Vol. 3, No. 1. 1939. b) Prostranstvennye zadachi teorii uprugosti dlya prizmaticheskikh tel (Three-Dimensional Problems of Elasticity Theory for Prismatic Bodies). — Uchenye zapiski MGU, No. 39 (mekhanika). 1940.
6. FADDEEVA, V.N. Metod pryamykh v primenenii k nekotorym kraevym zadacham (Ray Method Applied to Some Boundary-Value Problems). — Trudy Matematicheskogo Instituta im. V.A. Steklova, Vol. 28. 1949.
7. SOBOLEV, S.L. Nekotorye primeneniya funktsional'nogo analiza v matematicheskoi fizike (Some Applications of Functional Analysis in Mathematical Physics). —LGU. 1950.
8. BERNSTEIN, S.N. Ogranichenie modulei posledovatel'nosti proizvodnykh reshenii uravnenii parabolicheskogo tipa (Bounds of Absolute Values of the Sequence of Derivatives of Solutions of Parabolic Equations). — DAN SSSR, Vol. 18, No. 7. 1938.
9. KARMANOV, V.G. O sushchestvovanii reshenii nekotorykh kraevykh zadach dlya uravnenii smeshannogo tipa (On the Solvability of Some Boundary-Value Problems for Mixed Equations). — Izvestiya AN SSSR, seriya matematicheskaya, Vol. 22, No. 1. 1958.
10. PETROVSKII, I.G. Lektsii ob uravneniyakh s chastnymi proizvodnymi (Lectures on Partial Differential Equations). — Fizmatgiz, Moskva. 1962.
11. BEREZIN, I.S. and N.P. ZHIDKOV. Metody vychislenii (Numerical Methods), Vol. I and II. — — Fizmatgiz, Moskva. 1959.
12. GERSCHGORIN,S. Fehlerabschätzung für des Differenzenverfahren zur Lösung partieller Differenzialgleichungen. — ZAMM, Vol. 10, No. 4. 1930.
13. DAVIDENKO, D.F. Thesis. — MGU. 1960.
14. NIRENBERG, L.A. Strong Maximum Principle for Parabolic Equations. — Comm. on Pure and Appl. Math., Vol. 6, No. 2. 1953.
15. VYBORNY, R. O svoistvakh reshenii nekotorykh kraevykh zadach dlya uravnenii parabolicheskogo tipa (On Properties of Solutions of Some Boundary-Value Problems for Parabolic Equations). —DAN SSSR, Vol. 117, No. 4. .1957.
16. RYABEN'KII, V.S. and FILIPPOV, A.F. Ob ustoichivosti raznostnykh uravnenii (On the Stability of Difference Equations). — Gostekhizdat, Moskva. 1956.
17. MIRANDA, C. Equazioni Differentiali Parziali di tipo Ellitico. — Springer (Berlin). 1956.
18. OLEINIK, O.A. O svoistvakh reshenii nekotorykh kraevykh zadach dlya uravnenii ellipticheskogo tipa (On Properties of Solutions of Some Boundary-Value Problems for Elliptic Equations). — Matematicheskii sbornik, Vol. 30, No. 3. 1952.

19. EIDUS, D.M. Smeshannaya zadacha dlya uravnenii 2-go poryadka ellipticheskogo tipa (Mixed Problem for Second Order Elliptic Equations). — Thesis, LGU. 1950.
20. NEMCHINOV, S.V. O reshenii metodom setok kraevykh zadach dlya uravnenii v chastnykh proizvodnykh 2-go poryadka ellipticheskogo tipa (Difference Solutions of Boundary-Value Problems for Second Order Elliptic Partial Differential Equations). — Zhurnal Vychislitel'noi Matematiki i Matematicheskoi Fiziki, Vol. 2, No. 3. 1962.

## EXPLANATORY LIST OF ABBREVIATED NAMES OF USSR INSTITUTIONS AND PERIODICALS APPEARING IN THIS BOOK

| Abbreviation | Full name (transliterated) | Translation |
|---|---|---|
| AN SSSR | Akademiya Nauk SSSR | Academy of Sciences of the USSR |
| DAN SSSR | Doklady Akademii Nauk SSSR | Reports of the Academy of Sciences of the USSR |
| GITTL | Gosudarstvennoe Izdatel'stvo Tekhnicheskoi i Teoreticheskoi Literatury | State Publishing House of Technical and Theoretical Literature |
| LGU | Leningradskii Gosudarstvennyi Universitet | Leningrad State University |
| MGU | Moskovskii Gosudarstvennyi Universitet | Moscow State University |
| NII | Nauchno-Issledovatel'skii Institut | Scientific Research Institute |
| PMM | Prikladnaya Matematika i Mekhanika | Applied Mathematics and Mechanics |
| UMN | Uspekhi Matematicheskikh Nauk | Advances in Mathematical Sciences |
| VTs | Vychislitel'nyi Tsentr | Computational Center |